

**University of Alberta**

Deactivation studies of noble metal catalysts for lean methane combustion

by

Georgeta Mihaela Istratescu

A thesis submitted to the Faculty of Graduate Studies and Research  
in partial fulfillment of the requirements for the degree of

Master of Science

in

Chemical Engineering

Department of Chemical and Materials Engineering

© Georgeta Mihaela Istratescu

Spring 2014

Edmonton, Alberta

Permission is hereby granted to the University of Alberta Libraries to reproduce single copies of this thesis and to lend or sell such copies for private, scholarly or scientific research purposes only. Where the thesis is converted to, or otherwise made available in digital form, the University of Alberta will advise potential users of the thesis of these terms.

The author reserves all other publication and other rights in association with the copyright in the thesis and, except as herein before provided, neither the thesis nor any substantial portion thereof may be printed or otherwise reproduced in any material form whatsoever without the author's prior written permission.

## **Dedication**

I would like to dedicate this work to my daughter, family and dear friends. Maria, your smile and love always made my day. I always feel blessed to have you in my life. Mom and Dad, you always gave me love and support to reach my dreams. Thank you for your encouragements. My dear friends thank you for your patience and support. I am fortunate to have you in my life. Reuben, thank you for your love and support.

## Abstract

Green House Gases (GHG) contribution to global warming has led to extensive research into reduction of emission of the GHG. Transportation, as a main contributor to GHG, faces a major challenge in researching and developing of new technologies with the aim of reducing the carbon foot print. The use of alternative fuels with lower harmful emissions became obvious as a result of emission control regulations and climate change. Natural gas engines gained popularity due to their ability to burn the fuel almost completely, which recommends them as an environmentally friendly alternative to fossil fuels engines. However, the incomplete combustion of methane in natural gas engines will release methane and carbon monoxide into the atmosphere. The fugitive methane emission problem can be tackled by the development of performant catalytic converters. A better understanding of catalytic converters for natural gas engines can be obtained by research of activity and stability of catalytic converters with different formulations.

This project reports on catalytic activity and stability of three sets of catalyst. The first set, palladium only catalysts provided by 15, 80 and 150 g/ft<sup>3</sup> loading, were designed for methane combustion but not necessarily for lean burn engines. The second set studied were 2 catalysts: Pt and Pt-Pd (4:1) catalyst, with a loading of 95 g/ft<sup>3</sup>. Their mainly intend was the use as diesel oxidation catalysts. The third set of catalytic converters was designed for use for lean burn gas engines. The catalysts studied were Pt-Pd (1:5) with a loading of 150 g/ft<sup>3</sup>, Pd 122 (122 g/ft<sup>3</sup>), Pd Rh (117.15:2.85) (loading 120 g/ft<sup>3</sup>) and PtPdRh (19:73:2.85) with a loading of 94.85 g/ft<sup>3</sup>. The influence of different pretreatments on the catalyst activity (i.e. de-greening temperature, reduction process) were studied through ignition-extinction experiments. The stability of the catalyst was investigated through thermal ageing experiments. The effect of water on the catalytic activity was investigated through hydrothermal ageing experiments. The exploratory experiments resulted in the development of two testing sequences for the

evaluation of activity and performance of the catalysts: variable temperature thermal ageing test and variable temperature hydrothermal ageing test.

Chemisorption method (CO chemisorption) was used to investigate the changes that take place in a catalyst as a result of different treatments. Temperature programmed reduction (TPR) was used to characterize Pt, Pd 80 and Pt-Pd (4:1) catalysts. Thermal electron microscopy (TEM) was used to investigate the changes in the size of catalyst particles as a result of thermal and hydrothermal ageing of the samples: Pt, Pd 122, Pd 150, Pt-Pd (4:1), Pt-Pd (1:5), PdRh, PtPdRh.

## **Acknowledgment**

I take this opportunity to express my deepest appreciation to my supervisor, Dr. Robert Hayes, for all his help, guidance and patience during my graduate studies and research. His knowledge, enthusiasm and optimism provided me with the useful tools in planning and developing of this research project.

I also thank to Dr. Sieghard E. Wanke for his enthusiasm, professionalism and precious advice which helped me to better understand catalysts and catalytic combustion. His valuable and constructive suggestions during this research project are highly appreciated.

I wish to express my deepest thanks to Dr. Natalia Semagina for her contribution to this project. Her invaluable advice, help and guidance with characterizing and testing of the catalysts are very much appreciated. Her generous support and encouragement are especially appreciated.

I would like to offer my special thanks to Walter Boddez, Les Dean and Richard Cooper for their help in developing and running the experimental set-up. Their willingness to give their time and advice is so generously appreciated.

I wish to acknowledge the help of Long Wu, whose personality and criticism motivated me to improve the experimental set-up. His initial work in building up the reaction system is appreciated.

I am very thankful to Natural Science and Engineering Research of Canada as well as Alberta Innovates for funding of my graduate study and research.

I wish to offer my special thanks to Umicore AG of Germany and Westport Innovates of Canada for their generous supply of catalysts used in this research project.

Lastly, I wish to thank to my friends and family for their support and encouragement throughout my study.

## Table of Contents

1. Introduction	1
1.1. Background	1
1.2. Why natural gas engines?	2
1.3. Why catalytic converters?	3
1.4. Scope of work	4
1.5. Structure of the thesis	5
2. Literature review	6
2.1 Fossil fuels	6
2.2. Greenhouse gas effect	7
2.3. History of methane and catalytic combustion	9
2.3.1. Methane	9
2.3.2. Catalysts and Catalytic reactions	10
2.4. Catalytic Converters	12
2.5. Activity and deactivation of noble metal catalysts	20
2.5.1. Activity of noble metal catalysts	21
2.5.2. Stability of noble metal catalysts	23
2.6. Catalytic converter formulation	29
2.6.1. Rare earth and metal oxides combustion catalysts	29
2.6.2. Noble metal supported catalysts	30

2.7. Characteristics of noble metal supported catalysts	31
2.7.1. Pd catalyst	31
2.7.2. Pt catalyst	31
2.7.3. PtPd bimetallic catalyst	32
2.7.4. PdRh bimetallic catalyst	32
3 Experiments and procedures	34
3.1. Experimental set-up and materials	34
3.2. Experiment design	38
3.2.1. Catalytic activity evaluation of the supported catalyst	39
3.2.2. Catalytic stability evaluation of the supported catalyst	40
3.3. Catalyst characterisation methods	42
4 Experimental results and analysis	45
4.1. Exploratory tests	45
4.1.1. Reactor	46
4.1.2. Cordierite	46
4.1.3. Alumina	48
4.2. Activity experiments	49
4.2.1. Pt-Pd (4:1) bimetallic catalyst	49
4.2.2. Pt catalyst	55
4.2.3. Pd catalyst	58
4.2.4. CO chemisorption and Temperature Programed Reduction	62

4.3. Thermal ageing	64
4.3.1. Pt catalyst	65
4.3.2. Pd catalyst	67
4.3.3. Bimetallic Pt-Pd (4:1) catalyst	71
4.4. Variable temperature thermal ageing test (thermal ageing 650 C)	75
4.4.1. Pt catalyst	76
4.4.2. Pd 150 catalyst	78
4.4.3. Pt-Pd (4:1) catalyst	85
4.4.4. Pt-Pd (1:5) catalysts	87
4.5. Hydrothermal ageing	96
4.5.1. Constant temperature thermal ageing test	96
4.5.1.1. Pt catalyst	96
4.5.1.2. Pt-Pd (4:1) catalyst	98
4.6. Variable temperature hydrothermal ageing test (hydrothermal ageing 650 C)	102
4.6.1. Pt catalyst	102
4.6.2. Pd 150 catalyst	104
4.6.3. Pt-Pd (4:1) catalyst	109
4.6.4. Pt-Pd (1:5) catalyst	114
4.7. Three way catalytic converters	123

4.7.1. Variable temperature thermal ageing test (VTTAT) (thermal ageing 550 C)	123
4.7.1.1. Pd 150 catalyst	124
4.7.1.2. Pd 122 catalyst	126
4.7.1.3. PdRh catalyst	128
4.7.1.4. PtPdRh catalyst	133
4.7.1.5. PtPd (1:5) catalyst	135
4.7.2. Variable temperature hydrothermal ageing test (VTHTAT) (hydrothermal ageing 550 C)	145
4.7.2.1. Pd 150 catalyst	146
4.7.2.2. Pd 122 catalyst	147
4.7.2.3. PdRh catalyst	149
4.7.2.4. PtPdRh catalyst	152
4.7.2.5. Pt-Pd (1:5) catalyst	154
4.8. De-greening temperature effect on the catalytic activity	168
4.8.1. Pd 150 catalyst	169
4.8.2. Pt-Pd (1:5) catalyst	174
4.9. Hydrogen effect on the catalytic activity	189
4.9.1. Pd 80 catalyst	189
4.9.2. Pd 150 catalyst	192
4.9.3. PdRh catalyst	193

4.9.4. PtPdRh catalyst	195
4.9.5. Pd 122 catalyst	196
4.10. The influence of catalyst loading on the activity and stability of the catalyst	202
5 Summary of experimental results and future work	205
5.1.1. General behaviour of the catalysts	205
5.1.2. Diesel oxidation catalysts: Pd 80, Pd 150, Pt, Pt-Pd (4:1), Pt-Pd (1:5) catalysts	205
5.1.3. Three way catalytic converters: Pd 150, Pd 122, Pt-Pd (1:5), Pd Rh, PtPdRh	206
5.2. Further work	208
5.2.1. Gas constituents	208
5.2.2. Characterisation of the catalysts	208
5.2.3. Study and development of different catalyst formulations	209
References	210
Appendix A. Summary of experiments	224

## List of tables

Table 4.1	CO chemisorption test for Pd catalyst	62
Table 4.2	The initial and final conversion of methane at 500 °C and 400 °C	66
Table 4.3	The changes in methane conversion over Pd catalyst	69
Table 4.4	Methane conversion of Pt, Pt-Pd (4:1), Pd 150 and Pt-Pd (1:5) catalysts	120
Table 4.5	Methane conversion over Pt, Pt-Pd (4:1), Pd 150 and Pt-Pd (1:5) catalysts after VTHTA test	122
Table 4.6	Summary of T100 and T50 of the light off curve of methane combustion of Pt, Pd 150, Pt-Pd (4:1) and Pt-Pd (1:5) catalysts before VTHTAT, after VTHTAT and in presence of water	123

## List of figures

2.1	Catalytic combustion as a function of temperature, adapted from Manna, A. M. (2006)	21
3.1	Diagram of the reactor system	34
3.2	Lab view of program	36
3.3	Monolith samples	37
3.4	Catalyst samples	37
4.1	Ignition-extinction curve of methane conversion in absence of supported catalyst	46
4.2	Ignition-extinction curves of methane conversion over cordierite	47
4.3	Variable temperature thermal ageing test of methane conversion of cordierite	48
4.4	Ignition-extinction curves of methane conversion over alumina	49
4.5	An ignition-extinction cycle of methane conversion of Pt-Pd (4:1) catalyst	50
4.6	Extinction curve of methane conversion over Pt-Pd (4:1) catalyst	51
4.7	Extinction curve of methane conversion over Pt-Pd (4:1) catalyst	51
4.8	Extinction curve of methane conversion over Pt-Pd (4:1) catalyst	52
4.9	Extinction curves of methane conversion over Pt-Pd (4:1) catalyst	53
4.10	Extinction curves of methane conversion over Pt-Pd (4:1) catalyst	54
4.11	Extinction curve of methane conversion over Pt-Pd (4:1) catalyst	55
4.12	Ignition-extinction curve of methane conversion over Pt catalyst	56
4.13	Ignition-extinction curves for Pt-Pd (4:1) (MI-028) and Pt (MI-058) catalysts	57
4.14	Extinction curves of methane combustion over Pt catalyst	57
4.15	Ignition-extinction curves of methane conversion over Pd catalyst	58
4.16	Ignition-extinction curves of methane combustion over Pt-Pd (4:1) (MI-028), Pt (MI-058) and Pd (MI-066) catalysts	59

4.17	Extinction curves of methane combustion over Pd 80 catalyst	60
4.18	Extinction curves of methane conversion over Pt-Pd (4:1) (MI-003), Pt (MI-061) and Pd 80 (MI-067) catalysts	61
4.19	TPR results of Pt, Pd and Pt-Pd (4:1) catalysts	63
4.20	Ignition-extinction for methane conversion over Pt catalyst (MI-058)	65
4.21	4.21. Thermal stability of Pt catalyst at 500°C (MI-073) and 400°C (MI-074)	66
4.22	Ignition-extinction curve of methane conversion over Pd catalyst (MI-106)	67
4.28	Constant temperature thermal ageing test of methane conversion over Pd catalyst	68
4.24	Ignition-extinction curves of methane conversion over Pt-Pd (4:1) catalyst (MI-133)	71
4.25	Ignition-extinction curves of methane conversion over Pt-Pd (4:1) catalyst	72
4.26	Constant temperature thermal ageing at 400°C of Pt-Pd (4:1) catalyst	73
4.27	Constant temperature thermal ageing at 400°C of Pt-Pd (4:1) catalyst (MI-147)	74
4.28	Constant temperature thermal ageing of Pt-Pd (4:1) catalyst at 400°C	74
4.29	Ignition-extinction curves of methane conversion of Pt catalyst	76
4.30	Variable temperature thermal ageing test of methane conversion over Pt catalyst (MI-200)	77
4.31	Ignition-extinction curves of methane conversion over Pd 150 catalyst: before VTTAT (MI-254), after VTTAT (MI-256) and in presence of water (MI-257)	78
4.32	Variable temperature thermal ageing test of methane conversion of Pd 150 catalyst	79
4.33	Ignition-extinction curves of methane conversion of Pd 150 catalyst: before VTTAT (MI-258) and after VTTAT (MI-260)	81
4.34	Variable temperature thermal ageing test of methane conversion of Pd 150 catalyst (MI-259)	81
4.35	Comparison of varied temperature thermal ageing tests of methane conversion over Pd 150 catalyst: MI-255 vs. MI-259	82
4.36	Ignition-extinction curve for methane conversion for Pd 150 catalyst: before VTTAT (MI-268) and after VTTAT (MI-270)	83
4.37	Variable temperature thermal ageing test of methane conversion over Pd 150 catalyst (MI-269)	84

4.38	Variable temperature thermal ageing test of methane conversion of Pd 150 catalyst at 350°C (MI-255) and 450°C (MI-269)	85
4.39	Ignition-extinction curve of methane conversion of Pt-Pd (4:1) catalyst	86
4.40	Variable temperature thermal ageing test (VTTAT) of methane conversion of Pt-Pd (4:1) catalyst (MI-212)	87
4.41	Ignition-extinction curve of methane conversion of Pt-Pd (1:5) catalyst: before VTTAT (MI-221), after VTTAT (MI-223) and in the presence of water (MI-224)	88
4.42	Variable temperature thermal ageing test of methane conversion of Pt-Pd (1:5) catalyst (MI-222)	89
4.43	Ignition-extinction curves of methane conversion of Pt-Pd (1:5) catalyst: before VTTAT (MI-232) and after VTTAT (MI-234)	90
4.44	Variable temperature thermal ageing test for methane conversion over Pt-Pd (1:5) catalyst (MI-233)	91
4.45	Variable temperature thermal ageing test at 350°C (MI-233) vs 300°C (MI-222)	91
4.46	Ignition-extinction curves for Pt (MI-199), Pd 150 (MI-254), Pt-Pd (4:1) (MI-211) and Pt-Pd (1:5) (MI-221) catalysts	92
4.47	Ignition-extinction of methane conversion after variable temperature thermal ageing test for Pt (MI-201), Pd 150 (MI-256), Pt-Pd (4:1) (MI-213) and Pt-Pd (1:5) (MI-223) catalysts	93
4.48	Variable temperature thermal ageing test at 350 C of methane conversion of Pd 150 (MI-259) and Pt-Pd (1:5) (MI-233) catalyst	94
4.49	Variable temperature thermal ageing test for Pd 150 and Pt-Pd (4:1) catalyst	95
4.50	Ignition-extinction curve of methane conversion of Pt catalyst	97
4.51	Constant temperature hydrothermal ageing of Pt catalyst	98
4.52	Ignition-extinction curves for methane conversion for Pt-Pd (4:1) catalyst	99
4.53	Constant temperature hydrothermal ageing test of methane conversion at 550°C, for Pt-Pd (4:1) catalyst	99
4.54	Ignition-extinction curves of methane conversion over Pt-Pd (4:1) catalyst before (MI-173) CTTAT, after (MI-177) CTTAT and in the presence of water (MI-178)	100
4.55	Comparison of constant temperature hydrothermal ageing test results for Pt and Pt-Pd (4:1) catalysts at 550°C	101

4.56	Ignition-extinction curves of methane combustion of Pt catalyst before (MI-274), after (MI-276) VTHTAT and in the presence of water (MI-277)	103
4.57	Variable temperature hydrothermal ageing test of methane combustion of Pt catalyst (MI-275)	103
4.58	TEM images of Pt catalyst before (left) and after (right) hydrothermal ageing	104
4.59	Ignition-extinction curves of methane conversion over Pd 150 catalyst, before (MI-261) and after (MI-263) variable temperature hydrothermal ageing test	105
4.60	Variable temperature hydrothermal ageing test of methane conversion of Pd 150 catalyst (MI-262)	106
4.61	Ignition-extinction curve of methane conversion of Pd 150 catalyst: before (MI-278), after (MI280) VTHTAT and in the presence of water (MI-281)	107
4.62	Variable temperature thermal ageing test of methane conversion of Pd 150 catalyst (MI-279)	108
4.63	Variable temperature hydrothermal ageing test at 350°C (MI-262) and 450°C (MI-279) of methane conversion of Pd 150 catalyst	109
4.64	Ignition-extinction curves of methane conversion of Pt-Pd (4:1) catalyst: before VTHTAT (MI-239) and after VTHTAT (MI-241) and in the presence of water (MI-242)	110
4.65	TEM images of Pt-Pd (4:1) catalyst before hydrothermal ageing test	111
4.66	TEM images of Pt-Pd (4:1) catalyst after the hydrothermal ageing test	111
4.67	Variable temperature hydrothermal ageing test of methane conversion of Pt-Pd (4:1) catalyst (MI-240)	112
4.68	Ignition-extinction curves of methane conversion after variable temperature hydrothermal ageing test of Pt (MI-276), Pd (MI-280) and Pt-Pd (4:1) (MI-241) catalysts	113
4.69	Ignition-extinction curves of methane conversion in presence of water of Pt (MI-277), Pd 150 (MI-281) and Pt-Pd (4:1) (MI-242) catalysts	114
4.70	Ignition-extinction curves of methane conversion of Pt-Pd (1:5) catalyst: before VTHTAT (MI-228), after VTHTAT (MI-230) and in the presence of water (MI-231)	115
4.71	Variable temperature thermal ageing test of methane conversion of Pt-Pd (1:5) catalyst (MI-229)	116
4.72	TEM images of Pt-Pd (1:5) catalyst before and after hydrothermal ageing test	117
4.73	Ignition-extinction curves of methane conversion of Pt-Pd (1:5) catalyst: before (MI-244) and after (MI-246) HTA, and in the presence of water (MI-247)	118

4.74	Variable temperature hydrothermal ageing test of methane combustion over Pt-Pd (1:5) catalyst (MI-245)	119
4.75	Ignition-extinction curves of methane conversion of Pt, Pd 150, Pt-Pd (4:1) and Pt-Pd (1:5) catalysts	120
4.76	Ignition-extinction curves of methane conversion of Pt, Pd 150, Pt-Pd (4:1) and Pt-Pd (1:5) catalysts, after VHTTA test	121
4.77	Ignition-extinction curves of methane conversion in presence of water, of Pt, Pd 150, Pt-Pd (4:1) and Pt-Pd (1:5) catalysts	122
4.78	Ignition-extinction curves of methane conversion of Pd 150 catalyst: before (MI-374) and after (MI-376) thermal ageing test, and in the presence of water (MI-377)	123
4.79	Variable temperature thermal ageing test for methane conversion over Pd 150 catalyst	126
4.80	Ignition-extinction curve of methane conversion of Pd 122 catalyst: before (MI-362) and after (MI-364) thermal ageing, and in the presence of water (MI-365)	127
4.81	Variable temperature thermal ageing test for methane conversion over Pd 122 catalyst (MI-363)	128
4.82	Ignition-extinction curve of methane conversion of PdRh catalyst: before (MI-344) and after (MI-347) thermal ageing test, and in the presence of water (MI-348)	129
4.83	Variable temperature thermal ageing test of methane conversion of PdRh catalyst (MI-346)	130
4.84	Ignition-extinction curves of methane conversion of PdRh catalyst: before thermal ageing (MI-349), after (MI-351) thermal ageing, and in the presence of water (MI-352)	131
4.85	Variable temperature thermal ageing test of methane conversion of PdRh catalyst (MI-350)	132
4.86	Comparison of VTTA 350 (MI-346) and VTTA 450 (MI-350) tests of methane conversion of PdRh catalyst	133
4.87	Ignition-extinction curves of methane conversion of PtPdRh catalyst: before (MI-323) and after (MI-328) thermal ageing, and in the presence of water (MI-329)	134
4.88	Variable temperature thermal ageing test of methane conversion of PtPdRh catalyst (MI-327)	135
4.89	Ignition-extinction curves of methane conversion in presence of Pt-Pd (1:5) catalyst: before (MI-286) and after (MI-290) thermal ageing test	136
4.90	Variable temperature thermal ageing test of methane conversion of Pt-Pd (1:5) catalyst (MI-289)	137
4.91	Ignition-extinction curves of methane conversion of Pd 122 (MI-362) and PdRh (MI-349) catalysts	138

4.92	Variable temperature thermal ageing test of methane conversion of Pd 122 (MI-363) and PdRh (MI-350) catalysts	139
4.93	Ignition-extinction curves of methane conversion of Pd 122 (MI-364) and PdRh (MI-351) after VTTA test	139
4.94	Ignition-extinction curves of methane conversion of PdRh (MI-349) and PtPdRh (MI-323) catalysts	140
4.95	VTTAT for methane conversion over PdRh (MI-350) and PtPdRh catalysts (MI-327)	141
4.96	Ignition-extinction curves of methane conversion after VTTAT, of PdRh (MI-351) and PtPdRh (MI-328)	142
4.97	Ignition-extinction of methane conversion in presence of water of PdRh (MI-352) and PtPdRh (MI-329) catalysts	143
4.98	Ignition-extinction curves for methane conversion over Pd 150 (MI-374) and Pt-Pd (1:5) (MI-286) catalysts	143
4.99	Variable temperature thermal ageing test for Pd 150 (MI-375) and Pt-Pd (1:5) (MI-289) catalysts	144
4.100	Ignition-extinction curves of methane conversion of Pd 150 (MI-376) and Pt-Pd (1:5) (MI-290) catalysts	145
4.101	Ignition-extinction curves of methane conversion of Pd 150 catalyst (MI-339)	146
4.102	Variable temperature hydrothermal ageing test of methane conversion of Pd 150 catalyst (MI-341)	147
4.103	Ignition-extinction curves for methane conversion over Pd 122 catalyst: before (MI-357) and after (MI-359) VTHTAT, and in the presence of water (MI-360)	148
4.104	Variable temperature hydrothermal ageing test of methane conversion of Pd 122 catalyst (MI-358)	149
4.105	Ignition-extinction curve for methane conversion over PdRh catalyst: before (MI-370) and after (MI-372) thermal ageing and in the presence of water (MI-373)	150
4.106	Variable temperature hydrothermal ageing test of methane conversion of PdRh catalyst (MI-371)	151
4.107	Ignition-extinction curve of methane conversion over PtPdRh catalyst (MI-319)	152
4.108	Variable temperature hydrothermal ageing test of methane conversion of PtPdRh catalyst (MI-320)	154
4.109	Ignition-extinction curves of methane conversion over Pt-Pd (1:5) catalyst: before (MI-301) and after (MI-304) hydrothermal ageing test	154
4.110	Variable temperature thermal ageing test of methane conversion over Pt-Pd (1:5) catalyst (MI-302)	156
4.111	Ignition-extinction curves for methane conversion over Pd 122 (MI-357) and Pd 150 (MI-339) catalysts	157

4.112	Variable temperature hydrothermal ageing test for methane conversion over Pd 122 (MI-341) and Pd 150 (MI-358) catalysts	158
4.113	Ignition-extinction curves for methane conversion over Pd 122 (MI-359) and Pd 150 (MI-342) catalysts, after VTHTA test	159
4.114	Ignition-extinction curves for methane conversion for Pd 122 (MI-357) and PdRh (MI-370) catalysts	160
4.115	Variable temperature hydrothermal ageing test for methane conversion over Pd 122 (MI-358) and PdRh (MI-371) catalysts	161
4.116	Ignition-extinction curves of methane conversion after hydrothermal ageing, for Pd 122 (MI-359) and PdRh (MI-372) catalysts	161
4.117	Ignition-extinction curves of methane conversion in presence of water, of PdRh (MI-373) and Pd 122 (MI-360) catalyst	162
4.118	Ignition-extinction curves of methane conversion of PdRh (MI-370) and PtPdRh (MI-319) catalysts	163
4.119	Variable temperature hydrothermal ageing test of methane conversion of PdRh (MI-371) and PtPdRh (MI-320) catalysts	164
4.120	Ignition-extinction curves of methane conversion over PtPdRh (MI-321) and PdRh (MI-372) catalysts, after VTHTA test	165
4.121	Ignition-extinction curves of methane conversion in the presence of water for PtPdRh (MI-322) and PdRh (MI-373) catalysts	165
4.122	Ignition-extinction curves of methane conversion for Pt-Pd (1:5) (MI-301) and Pd 150 (MI-339) catalysts	166
4.123	Variable temperature thermal ageing test of methane conversion for Pt-Pd (1:5) (MI-303) and Pd 150 (MI-341) catalysts	167
4.124	Ignition-extinction curves of methane deactivation after VTHTA test, of Pd 150 (MI-342) and Pt-Pd (1:5) (MI-304) catalysts	168
4.125	Ignition-extinction curves of methane conversion over Pd 150 catalyst de-greened at 650°C (MI-258) and 550°C (MI-374)	169
4.126	Variable temperature thermal ageing test of methane conversion over Pd 150 catalyst, de-greened at 650°C (MI-259) and 550°C (MI-375)	170
4.127	Ignition-extinction curves of methane conversion for Pd 150 catalyst de-greened at 650°C (MI-260) and 550 °C (MI-376)	170

4.128	Ignition-extinction curve of methane conversion after VTHTA test, of Pd 150 catalyst de-greened at 650°C (MI-278) and 550°C (MI-339)	171
4.129	Variable temperature thermal ageing test of methane conversion over Pd 150 catalyst de-greened at 650°C (MI-279) and 550°C (MI-341)	172
4.130	Ignition-extinction curves of methane conversion after VTHTA test for Pd 150 catalyst de-greened at 650°C (MI-280) and 550°C (MI-342)	173
4.131	Ignition-extinction curves of methane conversion over Pt-Pd (1:5) catalyst de-greened at 650°C (MI-232) and 550°C (MI-286)	174
4.132	Variable temperature thermal ageing test of methane conversion of Pt-Pd (1:5) catalyst de-greened at 650°C (MI-233) and 550°C (MI-289)	175
4.133	Ignition-extinction curves of methane conversion of Pt-Pd (1:5) catalyst de-greened at 650°C (MI-234) and 550°C (MI-290), after VTHTA test	176
4.134	Ignition-extinction curves of methane conversion over Pt-Pd (1:5) catalyst de-greened at 650°C (MI-228) and 550°C (MI-295)	177
4.135	Variable temperature thermal ageing test of methane conversion over Pt-Pd (1:5) catalyst, de-greened at 650°C (MI-229) and 550°C (MI-296)	178
4.136	Ignition-extinction curve of methane conversion after VTHTA test, over Pt-Pd (1:5) catalyst de-greened at 650°C (MI-230) and 550°C (MI-297)	179
4.137	Ignition-extinction curves of methane conversion over Pt-Pd (1:5) catalyst de-greened at 650°C (MI-244) and 550°C (MI-301)	180
4.138	Variable temperature hydrothermal ageing test of methane conversion over Pt-Pd (1:5) catalyst de-greened at 650°C (MI-245) and 550°C (MI-303)	180
4.139	Ignition-extinction curves of methane conversion after VTHTA test for Pt-Pd (1:5) catalyst de-greened at 650°C (MI-246) and 550°C (MI-304)	181
4.140	Variable temperature hydrothermal ageing test of methane conversion over Pt-Pd (1:5) catalyst (MI-310)	182
4.141	Variable temperature hydrothermal ageing test of methane conversion over Pt-Pd (1:5) catalyst de-greened at 550°C (MI-310) and 650°C (MI-245)	183
4.142	Variable temperature hydrothermal ageing test of methane conversion over Pt-Pd (1:5) de-greened at 600°C (MI-312)	184

4.143	Variable temperature hydrothermal ageing test of methane conversion over Pt-Pd (1:5) catalyst de-greened at 550°C (MI-310) and 600°C (MI-312)	185
4.144	Variable temperature thermal ageing test of methane conversion of Pt-Pd (1:5) catalyst de-greened at 650°C (MI-245) and 600°C (MI-312)	185
4.145	Variable temperature hydrothermal ageing of Pt-Pd (1:5) catalyst, de-greened at 550°C (MI-331)	186
4.146	Variable temperature hydrothermal ageing of methane conversion of Pt-Pd (1:5) catalyst de-greened at 550°C (MI-302 vs MI-331)	186
4.147	Variable temperature hydrothermal ageing of methane conversion of Pt-Pd (1:5) catalyst de-greened at 600°C (MI-336)	187
4.148	Variable temperature hydrothermal ageing test of methane conversion of Pt-Pd (1:5) catalyst de-greened at 600°C (MI-312 vs MI-336)	188
4.149	Ignition-extinction curves of methane conversion of Pd 80 catalyst before (MI-089) and after (MI-098) thermal ageing	190
4.150	Ignition-extinction curves of methane conversion of Pd 80 catalyst before (MI-106) and (MI-111) after thermal ageing	190
4.151	Ignition-extinction curves of methane conversion of Pd 80 catalyst after the thermal ageing experiments (MI-111) and after the sample was reduced (MI-112)	191
4.152	Ignition-extinction curves of methane conversion over Pd 80 catalyst: MI-106 fresh and reduced sample, MI-112 thermally aged and reduced sample	192
4.153	Ignition-extinction curves of methane conversion of Pd 150 catalyst: MI-339 fresh and reduced sample; MI-340 thermally aged and non-reduced sample	193
4.154	Ignition-extinction curves of methane conversion of PdRh catalyst: MI-315 fresh and reduced sample; MI-316 thermally aged sample	194
4.155	Ignition-extinction curves of methane conversion of PdRh catalyst: MI-344 fresh and reduced sample; MI-345 thermally aged sample	194
4.156	Ignition-extinction curves of methane conversion of PtPdRh catalyst: MI-323 fresh and reduced sample; MI-324 thermally aged sample	195
4.157	Ignition-extinction curves of methane conversion over PtPdRh catalyst: MI-325 the third ignition-extinction cycle; MI-326 the forth ignition-extinction cycle	196

4.158	Ignition-extinction curves of methane conversion of Pd 122 catalyst: MI-379 fresh and reduced sample; MI-380 thermally aged sample	197
4.159	Ignition-extinction curves of methane conversion of Pd 122 reduced sample: MI-379 vs MI-381	198
4.160	Ignition-extinction curves of methane conversion of Pd 122 catalyst: MI-380 thermally aged sample; MI-381 reduced sample	198
4.161	Ignition-extinction curves of methane conversion of Pd 122 catalyst: MI-381 reduced sample; MI-382 thermally aged sample	199
4.162	Ignition-extinction curves of methane conversion of Pd 122 catalyst: MI-383 de-greened sample, non-reduced	200
4.163	Ignition-extinction curves of methane conversion over Pd 122 catalyst: MI-379 de-greened and reduced sample; MI-383 just de-greened sample	200
4.164	Ignition-extinction curves of methane conversion of Pd 122 catalyst: MI-383 just de-greened sample; MI-384 used sample	201
4.165	Ignition-extinction curves of methane conversion over Pd 122 (MI-357) and Pd 150 (MI-339) catalysts	202
4.166	Variable temperature hydrothermal ageing test of methane conversion over Pd 122 (MI-358) and Pd 150 (MI-341)	203
4.167	Ignition-extinction curves of methane conversion over Pd 122 (MI-359) and Pd 150 (MI-342) catalysts, after VTHTA test	204

## List of acronyms

CTTAT	Constant temperature thermal ageing test
CTHTAT	Constant temperature hydrothermal ageing test
GC	Gas chromatograph
GHG	Greenhouse Gas
GWP	Global warming potential
I-E	Ignition and extinction curves
LSA	Low surface area
ppm	Parts per million
SS	Stainless steel
TC	Thermocouple
TEM	Transmission electron microscopy
TGA	Thermo gravimetric Analysis
UK	United Kingdom
USA	United States of America
VOC	Volatile organic compound
VTTAT	Variable temperature thermal ageing test
VTHTAT	Variable temperature hydrothermal ageing test
XPS	X-ray photoelectron spectroscopy

# Chapter 1. Introduction

## 1.1 Background

Climate change due to global warming is a major concern for environmentalists and humans. The rise in temperature could have devastating environmental results like record heat, drought, storms, and change in the hydrologic cycle with impact on the ocean warming, rising sea levels and the risk of flooding.

Over the past century, the average increase of the Earth's surface temperature was 0.8 °C, with the biggest contribution in the last three decades. The main contributor to the global warming is the release of the heat-trapping greenhouse gases into the atmosphere (National Research Council, 2011). The Intergovernmental Panel on Climate Change (IPCC) predicts a 0.2 °C warming per decade for the next two decades. It also predicts that the climate warming during the 21 century will be larger than for the previous century, even if the greenhouse gas emissions will be kept at the same level as for the 20<sup>th</sup> century (Solomon, et al, 2007).

The climate change is not the only concern regarding the consequences of air pollution. Air pollution is accountable also for the adverse effects on human health. The Great Smog of 1952 (London, UK) lasted for 4 days (December 05 to December 09) and resulted in many human and animal casualties. The medical reports estimated that 12,000 people died prematurely and 100,000 became ill. It has been reported that animals died asphyxiated by smog (UK Weather Forecast, n.d.). As a consequence, a series of laws and regulations were implemented to reduce air pollution and to avoid such situations. The Clean Air Act came into effect in England in 1956.

Another example of air pollution effect on human health is the smog events of Los Angeles city (USA). Due to its location, Los Angeles has a history of smog

events, dating back to 1943 (LA weekly, 2005). The release of medical reports prompted the authorities to investigate the cause of smog formation. Arie Jan Haagen-Smit, the father of air pollution control, linked Southern California's smog problem to automobile exhaust (Haagen-Smit, 1954). Haagen-Smit developed a method to determine the intensity of the smog (the rubber test). He also identified that the main precursors of the smog (unburned hydrocarbons, ozone, and nitrogen oxides) were coming from automobile and industrial fuel combustion (Haagen-Smit, 1952). As a result, The Clean Air Act of 1955 was the first regulation passed by the Congress of US to control air pollution and to protect the human (Sunggyu, 1997). SO<sub>x</sub> and NO<sub>x</sub> emitted by fuel industry were the first air pollutants regulated under the Clean Air Act. These regulations set the limits of pollutant discharges. In the United States, the Environmental Protection Agency (EPA) was empowered to establish air quality standards. EPA is also responsible for the implementation of Clean Air Act by controlling the air pollution emissions. However, The Clean Air Act regulations are used as the minimum requirements in air pollution control.

## **1.2. Why natural gas engines?**

Fossil fuels, as one of the most important source of energy, have a profound impact on human life. It is estimated that 75 % of the CO<sub>2</sub> produced in the last 20 years came from burning fossil fuels. The photosynthesis process of the plants can absorb just 2.9 billion metric tons of carbon dioxide produced each year. It is estimated that 3.2 billion metric tons remain un-processes and are added annually to the atmosphere, which results in continuous accumulation in the atmosphere of the greenhouse gases (US Department of Energy, 2004).

The formation of smog was connected to the automobile exhaust by studies of Arie Haagen-Smith (Haagen-Smit, 1954) and it is nowadays recognized that transportation is the main contributor to air pollution (Government of Canada, 2012).

These results highlight the importance of using cleaner sources of energy as well as the developing of new technologies that will decrease the emission of harmful components into the atmosphere.

The use of natural gas instead of alternative fossil fuels brings the advantages of a cleaner and more efficient source of energy: natural gas burns almost completely and the release of energy per unit of CO<sub>2</sub> produced is higher compared with other fuels. Considering the contribution of gasoline and diesel vehicles to air pollution, the development of natural gas engines was forthcoming.

The use of natural gas for engine operating equipment dates back to the 1800's. It is worth mentioning that the first natural gas engine, although not for vehicles, was developed by Philippe Lebon d'Humbersin in 1801 (ThinkQuest team, 2000). Samuel Brown built the first motor vehicle in 1823. Jean Joseph Etienne Lenoir in 1860 built a double working engine (Washington Gas Light Co, 2013). However, the contribution of Nikolaus August Otto and Eugen Langen in 1867, paved the way of the development of natural gas engines. In 1869 they founded "NA Otto and Cie" a gas engine factory, where engineers like Wilhelm Maybach and Gottlieb Daimler found success.

With time, natural gas engines became more and more attractive due to the intrinsic knock resistance of natural gas as a fuel, as well as lower emissions associated with burning of natural gas. The first natural gas vehicle hit the roads of Po River Valley (Italy) in 1930 (Sperling et al., 2009). Nowadays, there are 15 million natural gas vehicles worldwide.

### **1.3. Why catalytic converters?**

Air pollution refers to changes in natural characteristics of the atmosphere due to releases of toxic compounds or particulate matter into the atmosphere. It was recognized that hydrocarbons, ozone, and nitrogen oxides from automobile exhaust and industrial fuel combustion are the primary precursors of smog

formation (Haagen-Smit, 1954), as well as acid rains. Smog has a negative impact on the environment and human health. Allergies, asthma, lung cancer, heart diseases, were all connected with smog and air pollution. Smog also reduces the amount of sunlight to the ground, with direct impact on plant photosynthesis process. An improper photosynthesis weakens the plants and their ability to fight diseases. Acid precipitations affect lake ecosystems, damages plants and trees leaves and roots with direct impact on photosynthesis process.

Unburned fuel from automobile engines results in the release of air pollutants into the atmosphere. Therefore, an after treatment system is desirable in order to limit the air pollutants. Catalytic converters were found to be the solution to this problem. However, development of highly efficiency catalytic converters was not an easy task. High activity in pollutant conversion and stability over time are the main properties desired in a catalytic converter.

The development of catalytic convertors for natural gas vehicle (NGV) is still considered to be a major challenge. First of all, methane is the least reactive hydrocarbon and therefore the most difficult to activate. In addition, the temperature of exhaust gases from NGV is relatively low (typically between 300°C and 500°C). A further difficulty is that NGV exhaust gases contain relatively low concentrations of unburned methane (between 500 and 5000 ppm) and large amounts of water vapor.

#### **1.4. Scope of work**

The purpose of this work was to investigate the performance of a series of platinum group metal (PGM) oxidation catalysts as candidates for exhaust after-treatment system for natural gas engine vehicles.

Different catalysts formulations of the Pt only, Pd only, bimetallic Pt-Pd (4:1), Pt-Pd (1:5), Pd Rh and three metallic Pt Pd Rh monolith catalysts were studied for the oxidation reaction of lean concentration methane-air mixture. The changes

with time of catalytic activity due to methane, water and temperature exposure were studied.

## **1.5. Structure of this thesis**

This thesis consists of five chapters.

Chapter 1 presents the sources and problems of methane emissions. The study and development of catalytic converters is introduced as a major motivation of this project.

Chapter 2 presents catalytic combustion as a potential solution in mitigation of fugitive methane emissions.

Chapter 3 describes the procedures, set-up and materials used in experiments. It also describes the methods used in catalysts characterization.

Chapter 4 presents literature review, results and discussions of the experiments.

Four topics are covered in this chapter:

- the sintering process of metal particles,
- performance and stability of catalytic converters
- re-dispersion process of the metal particles,
- hydrogen effect on the catalytic activity of Pd and Pt-Pd catalysts

Chapter 5 presents the summary of research and the prospective directions of future research

## Chapter 2 Literature review

### 2.1 Fossil fuel

The use of fossil fuels as a source of energy dates back in history.

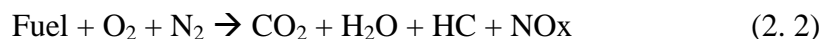
One of the first mentions about the fossil fuels was of Plutarch, a Greek historian (around year 100 A.D.) (US Department of Energy, 2013). The “external fires” were a result of natural gas seeping through cracks which were probably flared up by lightning strikes.

Asphalt, a derivative of petroleum, was used as an adhesive and waterproof material in construction and ship sealing as well as in preserving the mummies from ancient Egypt.

The use of fossil fuels increased in the modern era, which resulted in an increase in air pollution and greenhouse gases. Natural gas comes as an alternative to petroleum products. The high release of energy per unit of carbon dioxide produced, due to its low C/H ratio, makes methane a desirable fuel. The complete combustion of fuel can be represented by the overall reaction:



A complete combustion takes place when the fuel and oxygen combine stoichiometric. In the real-world complete combustion is not achieved (US Environmental Protection Agency, (n.d.)). If not enough oxygen is available, carbon monoxide (CO), nitrogen oxides (NO<sub>x</sub>) and unburned hydrocarbons are also formed.



The CO generation decreases with the increase of combustion temperature. The NO<sub>x</sub> generation decreases with the decrease of combustion temperature.

## 2.2. Greenhouse gas effect

In the energy balance of the Earth-atmosphere system, the Earth is absorbing some of the energy emitted by the sun (Sunggyu, 1997). Therefore, to maintain the energy balance, the Earth is re-emitting a small fraction of energy that it absorbs from the sun. However this happens at a different radiation wavelength (IR radiation) compared with the wavelength of the radiation emitted by sun (UV, Visible and near-IR wavelength) due to the difference in temperatures of the Earth and Sun. The atmosphere (ozone and water vapor) absorbs 23% of the incoming solar radiation in the UV, Visible and near-IR wavelength.

Greenhouse gas constituents are inefficient absorbers of solar radiation but are strong absorbers of IR radiation. Based on their local temperature, the absorbed long wave radiation is re-emitted some in the space, and some downwards to Earth. The increase in greenhouse gas concentration results in an increase of the trapping effect of long wave radiation, which results in warming up of the Earth surface.

The main contributors to greenhouse gas effects are carbon dioxide (CO<sub>2</sub>), nitrogen oxides (NO<sub>x</sub>), methane (CH<sub>4</sub>) and water vapor (H<sub>2</sub>O).

**Carbon monoxide (CO):** Is a product of incomplete combustion of fuel that takes place when the carbon is partially oxidised. Carbon monoxide is dangerous to humans by forming carboxyhemoglobin, therefore affecting the capacity of the blood to carry oxygen. Carbon monoxide is odorless, colorless and tasteless, with a density similar to the air. The incomplete combustion of fuel can be a result of poor fuel-air mixing, insufficient oxygen availability or low combustion temperature.

**Carbon dioxide (CO<sub>2</sub>):** During the combustion process the majority of the fuel is converted to carbon dioxide. However, combustion of natural gas generates less CO<sub>2</sub> than combustion of coal and heavier hydrocarbons (Sunggyu, 1997). Carbon dioxide is colorless. It is odorless at low concentrations, and it has an acidic odor at higher concentrations. With a life time of 50 to 200 years, and a global

warming potential over all time period, carbon dioxide is considered a contributor to the greenhouse gases (US Environmental Protection Agency, 2013).

**Volatile Organic Compounds (VOC):** The incomplete combustion of fossil fuel also results in releasing into the atmosphere of volatile organic compounds. Hydrocarbons like paraffin, olefins, cycloparaffin and partially oxidised hydrocarbons are of special interest due to their health effect (Goldsmith et al., 1959, Henderson, 1922).

**Nitrogen Oxides (NO<sub>x</sub>):** The composition of atmosphere that surrounds us is ~78% nitrogen, 21% oxygen and 1% other gases. Therefore, at high temperatures and pressure, the nitrogen will react with oxygen forming nitrogen oxides. In the homogeneous combustion nitrogen monoxide (NO) is the species that is usually formed. Nitrogen dioxide can be formed by the reaction of nitrogen monoxide and oxygen. Nitrous oxide (N<sub>2</sub>O) is formed by heterogeneous reactions, i.e. catalytic converters, selective catalytic reduction units (Hayes et al., 1997). Nitrogen oxides NO<sub>x</sub>, formed during the combustion reaction are considered to be important air pollutants, due to its contribution to global warming as well as acid rains and fog mist.

**Water Vapor (H<sub>2</sub>O):** Water vapor is a good absorber of radiation (i.e. clouds) and in consequence an important contributor to greenhouse gas.

An important increase of water vapor into the atmosphere is given by the water evaporated from land and sea. It is well known that the increase in temperature brings an increase of water vapor into the atmosphere. As a consequence, the warming effect of the climate change results in more water to be adsorbed into the atmosphere (Hansen, 2008). It is worth mentioning that the life time of water in atmosphere is very short (days).

**Methane (CH<sub>4</sub>):** In 1976 the potential of methane as a greenhouse gas was assessed by Wei-Chyung Wang from NASA GISS (Schmidt, 2006). It was observed that methane has the capacity of trapping some infrared radiation frequencies emitted from the Earth's surface. By analyzing the gas bubbles

trapped in the Greenland and Arctic ice, it could be observed that the concentration of CO<sub>2</sub> and CH<sub>4</sub> increased rapidly since middle 1800 when the industry boomed. It also was demonstrated that methane not just contributes to the amount of greenhouse gas but also, the increase in atmosphere temperature contributes to an accelerated increase of methane in atmosphere.

Due to its efficiency in trapping radiation, the global warming potential of methane is higher comparative with CO<sub>2</sub>. It was calculated that for a 100-year period, the global warming potential of methane is 23 times higher than of CO<sub>2</sub>. This makes it the least desirable greenhouse gas emission in the atmosphere.

## **2.3 History of Methane and Catalytic Combustion**

### *2.3.1 Methane*

The first mention of methane as marsh gas was in a letter of Benjamin Franklin included in Joseph Priestley book “Experiments and observations on different kinds of airs”, in 1774 (Priestley, 1774). In his letter, Benjamin Franklin, an American scientist, inventor, civic activist and diplomat, narrates about some surface water phenomenon. Benjamin heard that a sudden flame will catch and spread on the water when a lighted candle was prompted near the water surface.

Dr. Samuel Finley, the fifth president of The College of New Jersey, witnessed the phenomenon and sent a letter to Royal Society of London, in 1765. In his letter, Dr. Samuel Finley describes how marsh gas from a local mill was set on fire by an employee, and that the experiment was reproduced a couple of times with the same result. Unfortunately the letter and the results were not published in the “Transitions” as the phenomenon could not be explained (Priestley, 1774).

Alessandro Volta, an Italian physicist known mainly for pioneering work in electricity, finds about the marsh gas experiments from New Jersey (the flammable air), and in 1777 discovers the “flammable gas” at Lake Maggiore. In

1778 Alessandro Volta succeeds to isolate methane, while studying the chemistry of gases (Liu et al., 2012).

In the early 1800s, Sir Humphry Davy and Michael Faraday, English chemists and inventors, investigated methane hydrate while they are in Italy (Knight, 1992).

From what we know nowadays, methane,  $\text{CH}_4$ , the simplest of the alkanes, it's a very stable compound. Methane stability is due to the equivalences of all four C-H bonds, as described by Sir Humphry Davy in 1817 (Knight, 1992). Due to its structure, methane reactions are difficult to control.

Methane is the main component of natural gas, is colorless and odorless. It is flammable only at concentrations of 5-15% in air. Methane produces more heat per mass unit compared with other hydrocarbons which makes it an ideal candidate in heating processes.

### *2.3.2 Catalysts and Catalytic Reactions*

The first work in catalysis is attributed to Sir Humphry Davy. Sir Humphry Davy was known mainly for his work in alkali and alkaline earth metals (Knight, 1992). However, due to his recognition as a great chemist of his time, Sir Humphry Davy was asked in 1814 by Dr. Robert Gray, Rector and Chairman of the Society for Preventing Accidents in Coal Mines, to develop safety lamps for coal mining. Fugitive methane was a big problem in coal mine explorations. It caused casualties due to the use of candles as sources of light, which was causing explosions (i.e. in the Felling Colliery coal mine explosion 92 men were killed). Davy was familiar with methane and air mixture. Him and Michael Faraday previously studied mixtures of methane and air. Sir Humphry Davy found that a fine platinum wire glowed red hot when it was heated and put in explosive mixture of methane and air. Davy also noticed that a flammable mixture of oxygen and coal gas became inflammable after it was in prolonged contact with a

heated platinum wire. This phenomenon was later defined as heterogeneous catalysts. He observed a similar behavior for palladium, but not for copper, silver, gold, iron or zinc. This special property of platinum to glow in presence of methane air mixture was exploited by Davy in his safety lamp. As soon as the methane air mixture was present, the wire was ignited and became white hot when the concentration reached the flammability limit.

It is nowadays considered that Humphry Davy paved the way for research in heterogeneous catalytic oxidation. His work in platinum and palladium as catalysts was continued by Edmund Davy, Michael Faraday, Johann Dobereiner, Pierre Dulong, Louise Thenard and many others. Edmund Davy, Sir Humphry Davy's cousin, showed that the surface area of a catalyst plays an important role in the catalytic activity. An increase in surface area of platinum lowers the combustion temperature of a mixture of oxygen and hydrogen (Hunt, 1979).

Nowadays it is known that the role of the catalyst is to lower the activation energy, consequently increasing the rate of reaction, without being itself consumed in the reaction or undergoing any permanent chemical change (Hayes et al., 1997). A catalytic reaction can be homogeneous (takes place between reactants in the same phase i.e.  $\text{NaI (aq)}$  for the decomposition reaction of  $\text{H}_2\text{O}_2$ ) or heterogeneous (takes place between reactants in different phases, i.e.  $\text{Au}$  for decomposition of  $\text{N}_2\text{O}$ ).

In the heterogeneous catalysis the reaction takes place at the catalyst surface and in consequence the transport phenomenon becomes very important for the overall process. With the increase of temperature, the mass transfer to the catalytic sites becomes important. The rate of reaction depends on mass transfer coefficients as well as kinetic rate parameters.

## 2.4 Catalytic Converters

The interest in catalytic converters for automobiles came after research studies showed the impact of air pollution on human health and environment (i.e. Great smog of London 1952, Los Angeles smog of 1955).

As was previously mentioned, Arie Jan Haagen-Smit linked Southern California's smog to automobile exhaust (Haagen-Smit, 1954). As a result of his research, the automobile industry decided to install positive crankcase ventilation devices as the first emission control system, in 1961 (Zhang, (n.d.), Haagen-Smit, 1958, Haagen-Smit, 1961, Haagen-Smit, 1962, Haagen-Smit, 1973). James Bonner (Bonner, 1977), in his tribute to Arie Jan Haagen-Smit mentioned that, as a Chairman of Air Resources Board in California (USA), Arie shut down Volkswagen sales in California for a week, when they failed their compliance with the California Regulation Certificate.

The first catalytic converter for automobile car exhaust after treatment was patented by Eugene J. Houdry in 1956. Houdry founded Oxy-Catalyst to develop catalysts for controlling odors and fumes exhausted from industrial processes and vehicles (Houdry et al., 1958). The first catalytic converter was designed to reduce the amount of unburned hydrocarbons and carbon monoxide in automobile exhausts (Houdry, 1956). The catalytic structure consisted of a porcelain shaped support that was thermally resistant to temperatures up to 2000 F. Active alumina was deposited as a thin film on the external surface of the catalytically inert porcelain structure. The alumina thin film was impregnated with platinum which together with alumina was catalyzing the oxidation reactions. Unfortunately the tetraethyl lead present in gasoline at that time was poisoning the catalyst which made Houdry's catalytic converter unsuccessful.

More and more studies highlighted the impact of air pollution on environment and human health and as a consequence Governments around the world imposed lower limits of emission of pollutants from car exhaust and industry. The Auto

industry responded by more research in developing new solutions to emission control technology (US Environmental Protection Agency, 1994).

One of the first steps taken by US Environmental Protection Agency, which was approved in 1973. The new regulation imposed a restriction of the lead content in all grades of gasoline produced (US Environmental Protection Agency, 1973). This significant step opened a new era in research and development of catalytic converters for car exhaust. Engelhard Corporation, with the research of John J. Mooney and Carl D. Keith, played an important role in developing more durable catalytic converters.

Following the new regulations of removing lead from the gasoline process, the first production of catalytic converters was possible in 1973. As a consequence, catalytic converters were widely introduced on production automobiles in 1975 model year in USA market (Zhang, (n.d.)). The oxidation catalysts or diesel oxidation catalysts were able to handle just hydrocarbon and carbon monoxide. The three-way catalyst developed by John J. Mooney and Carl D. Keith from Engelhard Corporation uses a single catalyst bed to convert hydrocarbon, carbon monoxide and nitrogen oxides into less harmful products (Zhang, (n.d.)). Since then different catalytic formulations and catalyst designs were developed.

A catalytic converter for automobile exhaust after treatment consists mainly of substrate, washcoat and the noble metal catalyst (Zhang, (n.d.)). The substrate can be a pellet or a honeycomb structure that provides a high surface-to-volume ratio and an even flow distribution of the exhaust across the bed. The monolith of the honeycomb structure can have specific size of the wall and channels and various shapes of the channels, i.e. square, hexagonal, sinusoidal (Hayes, 1997). The washcoat is often a mixture of alumina and silica and has the role to increase the surface area of the substrate; other metal oxides can be added to alumina, i.e. BaO which results in suppression of surface area decrease at high temperatures. The catalyst is generally a noble metal: platinum, palladium and/or rhodium; the addition of catalyst promoters can reduce the tendency of a catalyst to sinter, or can enhance the oxidation activity of a catalyst (Hayes, 1997).

The first catalytic converter used for automobile exhaust treatment was a pellet-type catalyst developed by General Motor and was a base-metal catalyst without noble metals (Church, 2006). One or two beds of pellet coated catalyst were fitted into a catalyst container surrounded by thermal isolation (Davis Recycling Inc., 2007, Patel et al. 2012). In a fixed bed pellet catalyst, the gas flows through the channels between the pellets and the catalytic reaction takes place in the porous structure of the pellets (Hayes, 1997). The big disadvantage of the pellet bed catalysts is given by the attrition of the catalyst which creates pressure drops and voids in the bed, which enables the bypassing of the exhaust gases.

Ford Motor Corporation and 3M obtained ceramic honeycomb structures by dipping paper into ceramic slurries and then shaped them (Church, 2006). Corning Glass Works developed an extruded honeycomb substrate. W. R. Grace developed and honeycomb structure out of clay like material.

The first catalysts tested for catalytic converters were monel metal, copper nickel alloy, vanadium pent oxide, ruthenium a.s.o. Johnson Matthey developed a rhodium promoted platinum catalyst. Platinum and palladium mixture catalyst were the most used catalyst in the middle of 1970s.

The first oxidation catalyst systems used air pumps to supply the necessary oxygen. A recirculation of the exhaust gas lowered the combustion temperature and resulted in better control of NO<sub>x</sub>.

Cerium was found to play an important role in the catalyst formulation: promotes the water shift gas reaction, acts as an oxygen storage component, stabilizes the surface area of alumina and acts as a promoter for platinum group metals.

The extruded die process for honeycomb ceramic monolith was patented by Rodney Bagley in 1974 (Bagley, 1974).

In 1977 John J. Mooney and Carl D. Keith working together with Engelhard's engineers team developed a honeycomb ceramic structure with tiny passages, which were coated with a mixture of rare earth oxides, multivalent base-metal

oxides and Pt and Rh noble metals (Mooney, (n.d.)). The catalyst was a three way catalyst developed to simultaneously oxidize hydrocarbons and carbon monoxide as well as to reduce the NO<sub>x</sub>. The catalyst was working efficiently at stoichiometric mixtures of air-fuel ratio. The catalyst also showed durability and hydro-thermally stability. The honeycomb structure offered the advantage of limited attrition and pressure drop in the catalyst and lighter weight. The disadvantage of honeycomb structure was given by less favorable mass transfer rates of reactants (Hayes et al. 1997).

John J. Mooney and Carl D. Keith received many awards for their contribution in controlling the emissions of toxic components from automobile exhaust (US Patent and Trademark Office, 2012).

There are several variations of catalytic converters used. A two-way converter is usually a diesel oxidation converter which reduced hydrocarbon and carbon monoxide emissions by oxidizing them to carbon dioxide and water.

A diesel oxidation catalyst is usually platinum or palladium based, as well as bimetallic Pt-Pd catalyst. The role of the catalytic converter is to oxidize unburned hydrocarbons and carbon monoxide to less harmful carbon dioxide (Zhang, (n. d.)).

Two techniques are used to reduce NO<sub>x</sub> emissions from a diesel engine:

- NO<sub>x</sub> traps
- selective catalytic reduction (SCR)

The NO<sub>x</sub> trap developed by Renault captures and stores the emitted NO<sub>x</sub> from the diesel engines. The NO<sub>2</sub> is trapped by the BaO as a Ba(NO<sub>3</sub>)<sub>2</sub>, after NO<sub>x</sub> was oxidized to NO<sub>2</sub> by platinum. The NO<sub>x</sub> trap is regenerated when the stored NO<sub>x</sub> is purged off with air and converted to nitrogen and neutral gases. Additional sensors for oxygen and heat are installed on the tailpipe as well as intake manifold and contribute to managing the NO<sub>x</sub> trap and the combustion modes (Renault.com, (n. d.)).

Selective catalytic reduction (SCR) is a system responsible for injecting a reducing agent (i.e. urea) into the exhaust stream which converts nitrogen oxides to nitrogen, water and carbon dioxide, the reaction taking place in an oxidizing atmosphere (Ayoub et al., 2011, Van Helder et al., 2004, Diesel Technology Forum: What is SCR?).

To meet the environmental requirements for particulate matter emission, diesel engine automobiles are equipped with diesel particulate filters (DPF) which traps the particulate matter from diesel exhaust. The filters can be single-use which has to be replaced and disposed once they are full of particulate matter, or reusable filters which uses a regeneration filter process as part of engine programming, which heats the filters to soot combustion temperature (Corning Incorporated Technologies, (n.d.)).

A three-way catalytic converter oxidizes burned hydrocarbons and carbon monoxide to carbon dioxide and water as well as reduces nitrogen oxides to nitrogen and oxygen. In a three-way catalytic converter, platinum and palladium oxidize the un-burned hydrocarbons and carbon monoxide, while rhodium reduces the nitrogen oxides.

Invented by John J. Mooney, the three way catalytic converter had a big impact on decreasing air pollution due to transportation. The three-way catalytic converter was first used on automobiles in the 1970's.

High catalytic activity and durability of the catalyst over time were some of the issues addressed by many researchers.

Ball Douglas et al, developed a new technology of precious metal addition (PMA) for Pd/Rh catalysts in order to minimize the negative interactions between washcoat components (Ball et al. 2006). In conventional design strategies, Pd and Rh were separated in washcoat layers in order to avoid alloy formation. This design avoided the negative effects on NO<sub>x</sub> performance. Pt/Rh, Pd/Rh and Pt/Pd/Rh catalytic converters were developed by designing washcoat components highly effective for all three noble metals Pt, Pd and Rh. The common strategies

in the design of TWC catalysts are pre-impregnation, PGMs' chemical fixation on selective supports and washcoat layering. The alumina and oxygen storage components were optimized for each platinum group metal specific layer. For oxygen storage (OS) properties,  $\text{CeO}_2$  and  $\text{ZrO}_2$  and other metal oxides can be used. Adding Zr to  $\text{CeO}_2$  lattice resulted in both stabilization of the  $\text{CeO}_2$  and access to bulk oxygen. The increase of Zr content in  $\text{CeO}_2$  lattice brought an increase in both oxygen release and thermal stability properties. The availability and reactivity of OS materials toward the release of oxygen was increased by using new materials with stable cubic crystal structure for Zr, which also decreased the temperature where Ce was 100% reduced. It was observed that a loss of catalytic performance results by Pd and Rh alloying under reducing conditions. However, due to selective enrichment of the alloy surface with Pd, the Rh function and consequently the  $\text{NO}_x$  performance were diminished. This had a positive impact on the catalytic activity of the new developed catalytic converters.

Eckhoff from Umicore (Eckhoff, 2006) designed a new set up of the catalyst for high performance engines. They obtained an early operation as well as a fast heat up of the catalyst by placing the double brick catalyst closer to manifold in a close-coupled (CC) position. This arrangement allows a decrease of the cold start emissions due to a faster warm up of the second brick. However, the design proposed by Eckhoff requires higher temperatures stable catalysts due to higher operating temperatures.

Another solution to remove the hydrocarbon automobile emissions in the start-up phase is given by Kanazawa Takaaki et al. from Toyota Motor Corporation and Yamamoto Shinji et al. from Nissan Motor Corporation (Kanazawa et al., 2006). The Toyota Corporation research team studied the use of a hydrocarbon adsorbent zeolite for adsorption of carbon 2 and above as a pre-treatment for the automobile exhaust before entering the catalytic converter. The system is operated by a valve that closes the direct access to the catalyst in the start-up phase of the engine. After the catalyst reaches the activation temperature, the valve opens to allow the car exhaust to be treated on the catalyst. Alumina and zeolite impregnated systems

were studied and the results were compared. The results showed that in Ag impregnated zeolite with a pore size of 0.1 nm the hydrocarbons were easily adsorbed. However, it was found that in the presence of water, the aluminium content plays a negative role in hydrocarbon adsorption. Ag impregnate ZSM5 and ferrierite also showed high thermal stability.

The Nissan Corporation research team (Yamamoto et al. 2006) developed an in-line hydrocarbon adsorbent system which incorporates an adsorbent substrate into the existing catalytic converter. The adsorbent proposed by Yamamoto et al. will therefore have the ability to regenerate by allowing at higher temperatures the adsorbed hydrocarbon species to desorb and react with the catalyst (i.e. the activation temperature of the catalyst).

Tanaka from Daihatsu Motor (Tanaka et al., 2006) designed a perovskite-type oxide catalytic converter able to self-regenerate the precious metals. In previous studies Tanaka et al. reported a high activity Pd perovskite type catalyst. The disadvantage of this type of catalyst was that in reducing atmosphere the Pd perovskite catalyst segregated. However it was observed that perovskite crystals were formed again and showed high activity when the catalyst was exposed to oxidizing atmosphere.

Schmidt from DaimlerChrysler AG reported the development of a new Pt-Rh catalyst which shows similar catalytic activity and ageing stability with Pd-Rh corresponding three-way catalyst (Schmidt, 2006). The catalytic converter developed by Schmidt consisted of a two separated washcoat layers tailored to the catalytic function of Pt and Rh respectively which improved the metal-support interactions. This resulted in a reduction of the sintering behavior of the catalyst.

Brisley developed an advanced Pt-Rh catalyst which was exposed and treated the same way as the current Pt-Rh catalyst as well as advanced Pd-Rh catalyst (Brisley, 2006). The results showed the same performance and thermal stability for advanced Pt-Rh catalyst and advanced Pd-Rh catalysts. However, the

advanced Pt-Rh catalyst showed a better light off performance compared with current Pt-Rh catalyst and Pd-Rh catalyst.

Another catalytic converter set-up is suggested by Votsmeier (Votsmeier, 2006) consisting of a small start catalyst with relatively small volume and high noble metal loading for a rapid light off, and a larger volume underfloor catalyst with high space velocity and low precious metal loading for NO<sub>x</sub> removal. The stability and durability of a catalytic converter is improved by using specific dopant in the washcoat, as well as by using noble metal deposition techniques. A decrease of a noble metal loading can be realized by optimization of position and geometry of catalyst. Results from computer simulation concluded that the oxygen storage capacity of the underfloor catalyst plays an important role in the catalyst performance and that only a relatively small volume of the start-up catalyst contributes to the light off performance of the catalyst.

Punkte from Engelhard Technologies developed a Pt, Pd, Rh tri-metallic three-way catalyst (Punkte et al., 2006). The washcoat deposition used was separate layers for Pd and Rh, with Rh present in the top layer. This will avoid interactions and alloy formation between Pd and Rh with the aim of preserving NO<sub>x</sub> efficiency of the three way catalytic converter. Pt was added to the top layer. A series of catalytic converters were prepared with different loading of three noble metals. From the experimental results it was observed that Pd makes the greatest contribution and the increase in Pd loading has a positive effect on the light off performance. The contribution of Pt catalyst to CO and NO<sub>x</sub> conversion increases with the increases of both Pt and Pd loading.

Liu, and Dettling from Engelhard Corporation (Liu et al., 2006) describe the inconvenience of Pd Rh alloy formation when the noble catalysts are prepared in the same washcoat. However when engineered washcoat are used, a very high performing Pd-Rh catalytic converter is obtained. The design of the catalytic converter has to take in consideration the tendency of Rh catalyst to interact with the support at elevated temperatures (above 850 °C). It was showed that the

increase of Pd catalyst loading has a positive impact on the conversion of hydrocarbon and nitrogen oxides.

Metal supported catalysts are seen as a new generation for close-coupled catalysts (Bruck et al., 2006) due mainly to their very good mechanical durability, their ability to reduce the cold start emissions by shortening the heating-up time, as well as reduction of pressure loss in high load operation system.

The high number of published papers regarding three-way catalyst improvements as well as advantages of different catalyst set-up suggests the importance of decreasing air pollution due to transportation. It is worth mentioning the effort put in by different car maker companies as well as oil producer companies that address the problem of a more performant catalysts (Schleyer et al., 2006).

## **2.5 Activity and deactivation of noble metal catalysts**

### *2.5.1 Activity of noble metal catalysts*

In the heterogeneous catalysis the reaction takes place at the catalyst surface which makes the transport phenomenon very important for the overall process (Hayes et al., 1997).

The overall catalytic process is given by:

- the transport of the reactants from the bulk fluid to the surface of the catalyst; the mass transfer to the catalytic sites becomes important with the increase of temperature
- diffusion of the reactants into the structure pore
- chemical reaction on the catalytic sites
- diffusion of the products to the external surface of the catalyst
- the transport of products from the surface of the catalyst in the bulk fluid

The overall rate of reaction in a catalytic combustor, the kinetics of reaction and the transport processes intra and interphase, as well as their combined effects play important roles

In the catalytic combustion the start of combustion is given by the increase of the temperature of the reaction mixture (point A), which depends on both the catalyst and the reactants (Wan Abu Baker et al., 2010, Manna, 2006, Lee et al., 1995). At this point the intrinsic surface reaction is the rate limiting step. An additional increase in the temperature will result in an exponential increase in the rate of the chemical reaction (point B). When the heat of reaction is higher than the heat provided, the gas phase reactions are initiated (point C). A further increase in temperature will result in a point where the homogeneous reactions become important (point D). Figure 1 presents the general pattern of catalytic combustion.

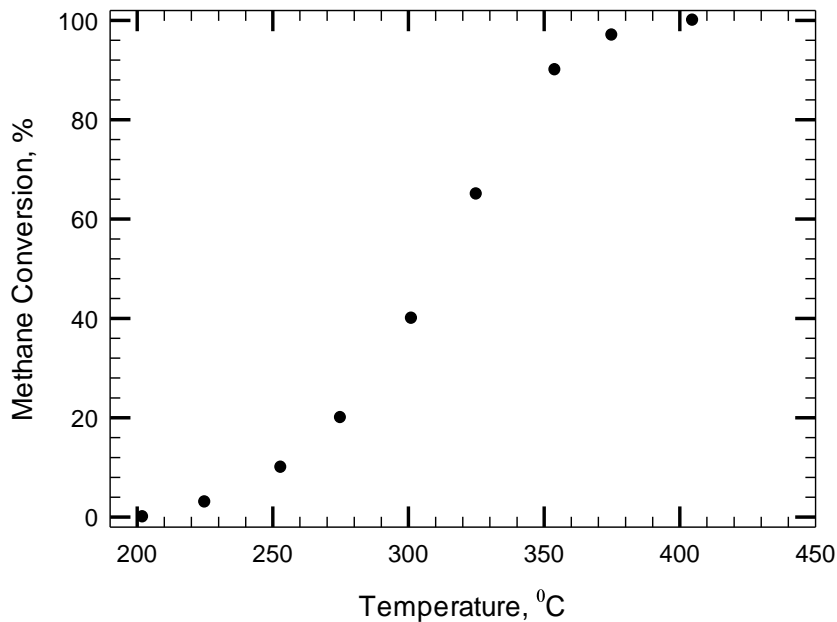


Figure 2.1. Catalytic combustion as a function of temperature, adapted from Manna, A. M. (2006)

One of the most important parameters for the evaluation of catalyst performance is the light off temperature. The light off temperature and the efficiency of conversion of a catalytic converter depends on the monolith's properties as well as temperature, flow velocity and composition of the reactants (Windman et al. 2002). The light off temperature is defined as the inlet temperature where the conversion rate of the reactants reaches a specific percent of conversion. T50 is the light off temperature where a 50% of the reactants are converted.

### *2.5.2 Stability of noble metal catalysts*

Stability of a catalyst is given by the ability of a catalyst to maintain its initial catalytic activity. The changes in catalytic activity occur due to changes in the structure or by poisoning or fooling of the active sites of the catalyst. The changes in structure of the catalyst are mainly due to the sintering of the catalyst as a consequence of temperature, reactants and atmosphere exposure.

While poisoning and fooling of a catalyst can be avoided by removing the responsible elements from the fuel, sintering of particles structure asks for better understanding of the phenomenon that can take place inside the particles.

The high volume of available research data related with sintering of catalytic converters highlights the importance of the sintering process in the development of catalytic converters with superior performance and reliability. The influence of temperature, atmosphere and time exposure were the main studied factors contributing to sintering of catalytic converters, as well as developing models that predicted the performance and reliability of a catalytic converter.

For a better understanding of the process and the factors that influence the sintering of catalytic converters, a short literature review is presented below.

*a) The influence of temperature*

Baird studied the effect of pre-treatment at various temperatures and pressure on the sintering effect of Pt black particles (Baird et al., 1973a). The catalysts were pre-treated in air at varied temperatures, followed by He and H<sub>2</sub> treatment. An increase in particles size was observed with the increase of treatment temperature up to 400°C. Baird suggests that the welding process that initiates the particles growth is due to the contact between clean metal particles as a result of surface cleaning of particles by hydrogen. This process is inhibited by the presence of carbonaceous or other species (oxygen) present at the surface of the particles.

Dadyburjor proposed two models for the splitting phenomenon of Pt crystallites in sintering of platinum particles (Dadyburjor, 1979). In the models proposed by Dadyburjor, it was assumed that cracks are formed in the crystallites in order to relieve the stress of lattice mismatch due to the difference in lattice parameter of PtO and pure metal. It was concluded that the imperfections present in the crystallite structure contributed to the splitting of the metal crystallites.

Flynn in his study on platinum particle sintering in oxygen atmosphere (Flynn et al., 1975) concluded that significant sintering of particles takes place at temperatures above 550 °C (the range of particles size was between 5 and 27 nm); below 550 °C the sintering of Pt particles was reduced (the range of particles size was the same as the untreated sample, between 1 and 5 nm). From the electron micrographs results it was also concluded that above 600°C the number of particles was decreased due to significantly increase in Pt particles size.

Wanke reviewed the results of numerous research data related to sintering of metal particles and analyzed mechanistic models that would explain the sintering process (Wanke et al., 1975). Wanke defines the sintering process as, changes in the metal particle distribution as a consequence of the processes that takes place in the catalyst due to temperature increase and interaction with the atmosphere present. The literature review concludes that temperature, time and atmosphere are the main factors accountable for the rate of sintering of metal crystallite.

Different metal size crystallites were obtained by thermal ageing of the particles at different temperatures and time exposures. The changes in dispersion of supported metal catalyst were assessed by chemisorption of carbon monoxide. In order to explain the sintering process, Wanke analyzes in detail the changes in the dispersion of the crystallite as an atomic migration model of the crystallite.

Fiedorow and Wanke (1976) studied the sintering of five Pt/Al<sub>2</sub>O<sub>3</sub> catalysts with different metal loading (0.5 to 4.0 wt% Pt) (Fiedorow et al., 1976). Samples were treated at different temperatures in the presence of oxygen. It was observed that for all catalyst treated at temperatures below 600°C, the dispersion increases with a maximum of two to three times the initial dispersion. A very important observation was that re-dispersion occurred for the sintered catalyst after a subsequent treatment at 550°C in oxygen atmosphere.

#### *b) The influence of atmosphere*

Baird studied the effect of pre-treatment in different atmospheres on the sintering of Pt particles, i.e. hydrogen, helium, air and ethylene (Baird et al., 1973a). They concluded that hydrogen plays an important role in sintering of platinum particles while air, helium and ethylene play smaller roles.

Manninger studied the sintering process of black Pt in different atmospheres (Manninger, 1984). It was observed that sintering of Pt crystallites in hydrogen takes place at temperatures as low as 150 °C. It was concluded that the starting temperature of the sintering process is determined by the energy barrier of the Pt atoms migration on the surface. It was assumed that the hydrogen adsorbed on the surface combines with Pt atoms and forms a surface layer of quasi-liquid Pt-H which contributes to the migration process of Pt atoms. In oxidizing atmosphere it was observed that the mobility of platinum atoms was much lower due to much stronger bond of the Pt-O surface layer compared with Pt-H.

Fiedorow studied the sintering of five Pt/Al<sub>2</sub>O<sub>3</sub> catalysts (Fiedorow et al., 1976). It was observed that in the presence of oxygen atmosphere the dispersion of the

particles increased for all samples. However, when samples were treated in presence of hydrogen, no increase in dispersion of Pt particles was observed.

Wanke found that at elevated temperatures, sintering of platinum particles is more pronounced in oxygen containing atmospheres compared with inert or hydrogen atmospheres (Wanke et al., 1975). They found that the loss in dispersion as a function of atmosphere increases in the order: vacuum > nitrogen/hydrogen > oxygen.

Flynn studied the effect of atmosphere on the sintering process of platinum catalyst. To analyze the process of metal particles sintering Flynn recorded the electron micrograph of the same area of the catalyst before treatment and after different treatments (Flynn et al., 1975). The study took into consideration the movement of the metal particles due to loss of water from the substrate. From the electron micrograph results it was concluded that Pt was atomically dispersed for the unreduced catalyst. However, during the reduction process some agglomerations of Pt particles occurred at 300 °C. It was observed that after thermal treatment in helium at 500 °C, the small Pt particles are replaced by larger particles as a result of agglomeration. An interesting observation was that a freezing of the agglomeration process of metal particles took place when the samples were cooled fast as compared to when the samples were cooled slowly.

### *c) The influence of metal particle size*

Wanke studied the sintering process of a platinum supported catalyst and found a disagreement with the crystallite migration model (Wanke et al., 1975). It was observed that Pt particles continued to sinter even after the size of Pt particles exceeded the size of the support particles.

Flynn studied the influence of particle size distribution on sintering process (Flynn et al., 1975). An untreated sample and a mixture of untreated and pre-sintered sample were sintered in the same conditions. It was found that sintering in catalysts with wide size distribution (mixed particle sample) is faster compared

with narrow size distribution (untreated sample) for oxidizing atmosphere and temperatures above 600 °C.

*d) The influence of time exposure*

Flynn studied the influence of time exposure on the sintering process of noble metals (Flynn et al., 1975). Flynn found that for hydrogen atmosphere, for temperatures below 400 °C, the particles increase in size with the increase of time exposure.

Fiedorow studied the influence of time exposure on the sintering process of the Pt catalyst (Fiedorow et al., 1976). Samples were treated for different times and at different temperatures (up to 700 °C) in the presence of oxygen. It was observed that for temperatures below 550 °C the change in dispersion for all samples did not depend on the period of treatment. For treatment at temperatures above 550 °C, the dispersion is decreasing with the increase of time treatment. However, no significant changes in dispersion of Pt as a function of time were observed when samples were treated in presence of hydrogen.

*e) The influence of metal loading*

Flynn in his study of sintering process of platinum based catalyst (Flynn et al., 1975) observed that loading of the catalyst plays an important role in the sintering process. He found that, for the same thermal treatment at 550°C, samples with higher loading (4 % Pt) shows an increase in particle size, while samples with lower loading (2 % Pt) showed no significant change in particle size.

Fiedorow and Wanke studied the sintering of Pt/Al<sub>2</sub>O<sub>3</sub> catalysts with different metal loading (0.5 to 4.0 wt % Pt) (Fiedorow et al., 1976). It was concluded the sintering of metal particles is a function of the metal loading, i.e. the higher the metal loading, the stronger the sintering process as well as the increase in the particle size.

*f) The influence of catalyst-support interaction*

With more and more available research data in the sintering process of catalytic converters, it became obvious that the interaction between catalyst and support plays an important role in the sintering process. In catalytic converters, the support of the catalyst has two objectives: to provide a large exposed surface for the active metal as well as to impede the agglomeration of the active metal by physically separating them (Wanke et al., 1975). From experimental studies it was concluded that strong interactions between the support and the catalyst particles slows down the sintering process therefore improving the stability of the catalytic converter.

Fiedorow studied the correlation between changes in support surface area and the Pt dispersion (Fiedorow et al., 1976). The results showed that the decrease in surface area with the increase of temperature does not contribute to the decrease in platinum dispersion. Fiedorow concluded that platinum crystallite growth is responsible for the decrease in Pt dispersion. He also concluded that the loss in support area due to 700 °C treatment is partially responsible for the lower re-dispersion of the catalyst after subsequent treatment at 550 °C.

*g) Re-dispersion of the catalyst*

Studying the sintering process of metal particles, different researchers observed that for specific temperatures and atmosphere, a re-dispersion of metallic particles takes place, which gives an increase in catalytic activity of the catalytic converter.

Baird, in his study about the influence of atmosphere and temperature pre-treatment on the sintering process of Pt black particles, observed an increase in particle size for temperatures below 400°C (Baird et al., 1973). For temperatures above 400 °C (up to 500 °C), a decrease in particle size was observed.

In his study on the sintering process of Pt supported catalyst as a function of temperature, Fiedorow observed that in an oxygen atmosphere for temperature

above 400 °C, a re-dispersion of the particles takes place (Fiedorow et al., 1976). The re-dispersion was observed even for samples pre-sintered at higher temperatures (700 °C). However, the process of re-dispersion of the samples pre-sintered at high temperatures was less significant due to sintered support.

In his detailed review about the influence of atmosphere and temperature on the sintering process of metal crystallites, Wanke concluded that for specific temperature range, sintering in oxidizing atmosphere requires higher activation energies than in reducing atmosphere (Wanke et al., 1975). As a result a re-dispersion of sintered metallic particles will take place in that temperature range. This seems to be true for an oxidizing atmosphere and temperatures between 450°C and 600°C, when an increase in oxygen and hydrogen up take was observed (Flynn et al., 1975). Outside of this temperature range, a loss of dispersion of metal particles was observed (Lietz et al., 1983).

Ruckenstein studied and developed a model for the re-dispersion process of the Pt sintered crystallites supported on alumina (Ruckenstein et al., 1977). In the model it was taken into account the dependence of diffusion, migration and coalescence of crystallites on the metal loading, allowing the model to interpret sintering and splitting in distinctive manner. Using the model it was concluded that migration and coalescence are controlled by the diffusion process.

#### *h) Influence of water*

Baird studied the influence of water on the sintering process of Pt black particles (Baird et al., 1973). He found that water promotes the sintering process if the surface of particles is not covered by hydrogen.

## 2.6 Catalytic converter formulation

The activity and stability of a catalytic converter depends on the type and combination of the catalyst used in the assembly (Chauhan, 2010). Metal oxides and noble metals are used predominantly in catalytic converters. The early research of catalytic converters focused on metal based catalysts. However, these catalysts proved high sensitivity to poisoning and thermal deactivation. At low temperatures, the catalytic activity of metal based catalysts was found to be inferior to the noble metal catalysts (Anderson et al., 1961).

The combustion catalyst can be supported or un-supported. Supported catalysts offer a higher exposure of the active sites. The supported catalysts also showed a higher thermal stability compared with their un-supported counterparts due to better heat transfer ability. However, in supported catalyst the support can be involved in the oxidation reaction due to their ability to store oxygen.

An ideal supported catalyst should show low ignition temperatures, high activity and high resistance to poisoning and thermal deactivation. In catalytic converters for vehicle a low ignition temperatures is desired due to a better control of the emissions during the start-up process. A low ignition temperature also brings the benefits of a decrease in the formation of nitrogen oxides.

### *2.6.1. Rare earth and metal oxides combustion catalysts*

Different formulations of combustion catalysts were developed during time. It was found that oxides of Co, Fe, Mn, Cr, Ni and Cu offer potential as combustion catalysts (Hayes et al., 1997). Choudhary studied a few rare earth oxides and found that  $\text{CeO}_2$  show the lower activity in methane conversion compared with  $\text{Eu}_2\text{O}_3$ ,  $\text{Yb}_2\text{O}_3$ ,  $\text{La}_2\text{O}_3$  and  $\text{Sm}_2\text{O}_3$  (Choudhary et al., 1992). All of them indicated a low activity in the conversion of methane. However, the rare earth oxides proved better use as dopants to increase the catalytic activity of metal oxides. Haruta showed that gold dispersed on reducible metal oxides shows high activity in CO

and hydrocarbons oxidation at low temperatures (Haruta et al., 1994). Choudhary, studied the activity of magnesium oxide doped with rare earth oxides (La, Eu, Yb, Sm, Nd) (Choudhary et al., 1997). He found that the selectivity and catalytic activity of MgO are increased in the presence of promoters (i.e. rare earth oxides).

Perovskite type catalyst earned their place in the catalytic combustors due to their high activity and thermal resistance in hydrocarbon combustion. Their general structure,  $ABO_3$  allows different combinations of metal oxides with face centre cubic structure (FCC). Generally, A is the rare earth element responsible for the thermal stability, while B is a transition metal responsible for the catalytic activity of perovskite catalyst. Perovskite-type catalysts have been suggested in methane combustion.

#### *2.6.2. Noble metal supported catalysts*

Noble metal catalyst earned their top position in catalytic combustion due to their higher activity compared with metal oxides. The most used formulations are Pt and Pd supported catalysts. Platinum group metals show high activity in methane combustion.

During the high temperature ageing, changes in the chemical states of precious metals and washcoat materials can occur, with direct impact on the thermal stability of a catalyst (Lassi, 2004). Ageing atmosphere has an influence on the sintering process of the active metals and can either accelerate or inhibit phase transitions of the active metal.

Designing noble metal catalytic converters is not an easy task. For noble metal catalysts, there are a few factors that must be kept in mind: the activity, stability to water or poisoning deactivation of the catalyst, the phase change as a function of temperature and the interaction with the support.

## 2.7 Characteristics of noble metal supported catalysts

Noble metal catalyst won their place in catalytic converters due to their high activity. Pt, Pd and Rh show high activity in methane conversion. Other noble metals showed lower stability, they oxidize easily and are more expensive, which made Pt, Pd and Rh to be the most used noble metals in the catalytic conversion of methane.

### 2.7.1. Pd catalyst

Palladium oxide, as the most active catalyst in methane combustion, is recommended for ignition of methane for temperatures below 750 °C. For temperatures above 750 °C, sintering of metal particles takes place as well as the reduction of palladium oxide to less active metallic catalyst. By reducing the active surface area, the sintered particles show less activity compared with un-sintered particles.

The activity of Pd O catalyst as a function of particle size was studied by many researchers (Van Giezen, 1997). It has been demonstrated that for catalyst pre-treated in He or H<sub>2</sub>, the activity of PdO catalyst increased with the increase in particle size (Hicks et al., 1990).

Lassi studied the thermodynamic equilibrium calculations of the oxidation-reduction behavior of palladium and found that phase stability in Pd/PdO system changes as a function of temperature and oxygen partial pressure (Lassi, 2004). Pd metallic phase increases with the increase of temperature and decrease of oxygen partial pressure.

### 2.7.2. Pt catalyst

Pt catalyst shows lower activity in methane conversion compared with Pd catalyst. However, Pt catalyst shows higher resistance to sintering due to thermal

ageing (Hurtado et al., 2004), higher resistance to water deactivation (Gelin et al., 2004) and higher resistance to sulphur poisoning (Meeyoo et al., 1998), compared with Pd catalyst. The active phase for Pt catalyst is considered to be Pt metallic.

The activity of Pt catalyst as a function of particle size was also studied (Hicks et al., 1990). It has been demonstrated that the activity of Pt catalyst increases with the increase in particle size.

### *2.7.3. PtPd bimetallic catalyst*

Pd catalyst shows high activity in methane combustion but low resistance to water and sulphur deactivation. On the other hand, Pt catalyst shows low activity in methane combustion but high resistance to water and sulphur deactivation. Therefore it is expected that a Pt-Pd bimetallic catalyst will combine their monometallic properties and create a catalyst with higher performance in methane combustion. To obtain the desirable properties, the bimetallic catalyst must be properly tailored. The electronic effects as well as the presence of mixed sites are just two of the factors that have to be taken into account. Persson studied different Pd bimetallic catalysts with Rh, Ni, Pt, Ir, Co, Cu, Au and Ag (Persson et al., 2005). However, it was found that Pd and Pt formed an alloy and that the Pd-Pt bimetallic catalyst was the most promising by showing high activity and stability in methane combustion.

### *2.7.4. PdRh catalyst*

Lassi studied the PdRh bimetallic catalyst for catalytic converters (Lassi, 2004). Lassi found that thermal treatment under the reducing and oxidizing atmosphere strongly affected the catalyst stability. However, the catalytic activity remained higher in the presence of reducing ageing atmosphere. The activity and thermal stability of a catalyst were affected by changes in the chemical states of palladium and rhodium. It was found that thermal deactivation of the aged catalysts is due to the collapse in surface area and the sintering of the Rh metal particles. It was

assumed that the decrease in catalytic activity was due to the active metal particles encapsulated in the sintered washcoat. The stabilization studies of supported rhodium oxide showed bulk rhodium oxide phases, thermodynamically stable between 500-1050°C. For the samples aged below 650°C in presence of air, a highly dispersed rhodium oxide was formed. However, for ageing temperatures above 650°C large particles of  $\text{Rh}_2\text{O}_3$  together with smaller particles of  $\text{RhO}_2$  are observed. The observed low thermal stability and catalytic activity of rhodium under oxidizing conditions has been attributed to the interaction of Rh with the alumina support and the diffusion of rhodium into the bulk of alumina at high temperatures.

Persson in his study on bimetallic catalysts concluded that despite a high activity of methane conversion, PdRh bimetallic catalyst does not show a stable activity (Persson et al., 2005).

## Chapter 3. Experiments and procedures

The main objective of this project was to study the activity and deactivation patterns for a series of catalysts to determine their potential as possible candidates for use in car exhaust treatment of natural gas vehicles. These activity and deactivation studies were performed in a micro-reactor system and used ground samples of commercial catalysts.

This chapter describes the experimental apparatus used, the catalysts studied, and the experimental protocols developed.

### 3.1. Experimental set-up and materials

The experimental set-up used for methane combustion experiments consisted of a micro-reactor, furnace, thermocouples and temperature controller, flow meters, gas and water supplies, see Figure 3.1.

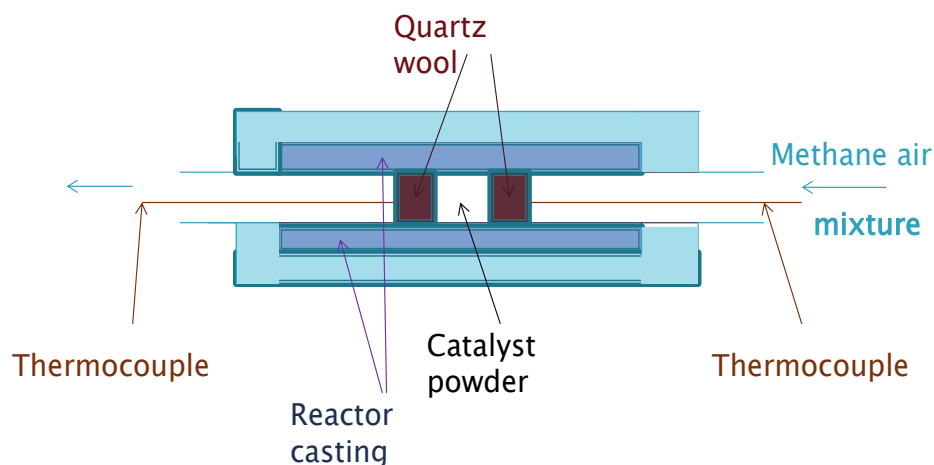


Figure 3.1. Diagram of the reactor system

The micro-reactor consisted of an inner tube (3/8" diameter made out of 316 stainless steel) and an outer sleeve (7/8" diameter made out of 316 stainless steel) to provide a constant temperature along the wall of the reactor. Three

thermocouples (K-type from Omega) were used for monitoring the temperature in the reaction system. Thermocouples T1 and T2 were placed in the inner tube of the reactor (before and after the catalyst sample), while the thermocouple T3 was placed in the outer sleeve.

The composition of the reactor exhaust was analyzed by a gas chromatograph (GC HP-7890-A type from Agilent Technologies Incorporation). The GC analysing column was 19095 P-Q4. The carrier gas was helium (Ultra high purity 5.0 from Praxair) with a flow rate of 11cc/min.

Methane and air flow rates were controlled by flow meters in separate lines (line 1 for extra dry air controlled by a Matheson Modular DYNA-blender model 8250 and line 2 for methane in nitrogen mixture controlled by a MKS Type 1479). The gases were mixed together before they entered the reactor.

For experiments with water, water was added to the reactor by a syringe pump (KDS100L). The feed lines were heated to evaporate the water.

Jeol JEM-2100 Transmission Electron Microscope with GIF filter was used for samples characterisation. The test produces high-resolution two dimensional images of the samples at nano-scale level. TEM is a powerful tool that can assess changes in particle size as result of sintering process.

Micromeritics RS 232 Chemisorption Analyzer was used for active surface and particle size determination of the samples. This test is important because it can highlight the changes in the catalytic activity as a result of temperature and atmosphere exposure.

The experimental conditions as well as the temperature controller, GC and water syringe pump system were controlled by LabView software connected to an Opto-22 system. The LabView acquired and recorded both the experimental conditions and results in excel files. The Labview program developed for controlling the tests is presented in Figure 3.2.



Figure 3.2. Labview program

Catalyst samples in the form of washcoated 400 CPSI square channel monoliths were obtained from Umicore AG, Hanau, Germany. Eight catalysts were used in the investigation, consisting of various combinations of precious metals. The catalysts were:

**Platinum only:** The precious metal loading was 95 g/ft<sup>3</sup> of Pt (0.635% Pt).

**Palladium only:** Three catalysts with palladium only with loadings of 80 g/ft<sup>3</sup> (0.54% Pd), 150 g/ft<sup>3</sup> (1% Pd) and 122 g/ft<sup>3</sup> (0.82% Pd). The samples of 80 g/ft<sup>3</sup> and 150 were older technology, whilst the 122 g/ft<sup>3</sup> sample was very recent.

**Platinum and palladium bimetallic catalysts:** One sample was mostly platinum, with a total loading of 95 g/ft<sup>3</sup> with a 4:1 ratio by mass of platinum to palladium (0.508 % Pt, 0.127 % Pd). The second sample contained a total loading of 150 g/ft<sup>3</sup> with a mass ratio of 1 part platinum to 5 parts palladium (0.16% Pt, 0.835% Pd).

**Palladium and rhodium bi-metallic catalyst:** The PGM loading was 122 g/ft<sup>3</sup> with a mass ratio of 41 parts of Pd to one part of Rh (0.8% Pd, 0.02% Rh).

**Platinum, palladium and rhodium tri-metallic catalyst:** The PGM loading was  $95 \text{ g/ft}^3$  with a mass ratio of 20 parts Pt, 77 parts Pd and 3 parts of Rh (0.13% Pt, 0.49% Pd, 0.02% Rh).

The precious metal loading is based on volume of monolith, and these loading levels are typical for lean burn automotive applications. The percent of precious metal loading was calculated using the standard information of monolith and samples: 12% washcoat, 6.5 wall thickness and bulk density of cordierite  $\rho_{\text{bulk cord}}=528.3 \text{ kg/m}^3$ . A picture of the monolith samples provided by Umicore is shown in Figure 3.3. The monoliths were crushed, ground, and screened to form particles in the range of 300-400 microns. Pictures of the crushed samples are shown in Figure 3.4.

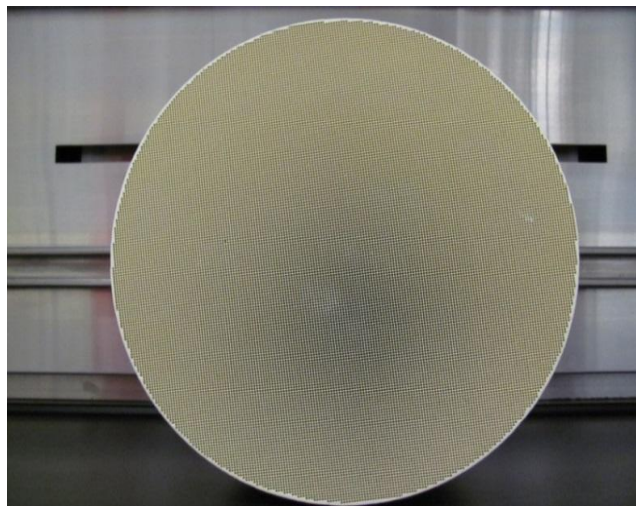


Figure 3.3 Monolith sample



Figure 3.4. Catalyst samples (left to right): cordierite, Pt, Pd 80, Pd 150, PtPd (4:1), PtPd(1:5), Pd 122, PdRh, PtPdRh

### **3.2. Experiment design**

The experiment design was validated after exploratory tests to find the proper approach to test the catalysts. The reactor system set up assured a very good reproducibility and repeatability of experiments, as it will be seen later.

#### **Sample preparation**

The monolith cores were ground and screened to particle size of 200-400  $\mu\text{m}$ . 0.5 g of sample (which includes substrate material) was used in the experiments. The sample was placed in the inner tube of the reactor, delimited by layers of quartz wool to prevent the catalyst powder from leaving the reactor.

#### **Pre-treatment of the catalyst**

##### *De-greening of the catalyst*

The 95 g/ft<sup>3</sup> samples were aged in air at 650°C for 16 hours by the provider company prior to receipt. The remainder were provided without any pre-treatment and were de-greened at either at 650°C or 550°C, depending on the experiments. The de-greening of the supported catalyst was performed to obtain a more stable structure as well as to remove the volatiles from the synthesis process.

##### *Reduction of the catalyst*

To have the same base line in the experiments, all of the catalyst samples were reduced following the same procedure: hydrogen was fed to reactor (40-50 cc/min); then the temperature of the reactor was raised at 500°C and kept at 500°C for 30 minutes; then the hydrogen flow was cut off and nitrogen was fed to reactor; the reactor was slowly brought to room temperature under nitrogen flow (50 cc/min); then nitrogen flow was cut off and air was fed to reactor overnight (50 cc/min).

## Testing of the catalyst

### *Air-methane composition*

For all experiments, the flow rate of air was  $225 \pm 1.5$  ml/min, while the flow rate of methane balanced in nitrogen was adjusted to obtain concentrations of 4100 or 4700 ppm.

For hydrothermal experiments, water was added to obtain a 5% water concentration in the feed stream (mole basis).

### *3.2.1. Catalytic activity evaluation*

Ignition-extinction cycles were used to assess the catalytic activity.

#### *Ignition*

The ignition (light-off) curves were obtained by passing an air-methane mixture over the catalysts while increasing the temperature in the reactor. The set point temperature was determined for all the catalysts after preliminary tests. The increase in temperature was performed in a 50 degree stepwise fashion, until 100% of methane conversion was obtained. The ignition curves were followed by extinction curves, which were obtained by decreasing the temperatures in the same 50 degree stepwise fashion, until a very low conversion of methane was obtained (close to zero).

#### *Extinction*

After 100% conversion of air-methane mixture was obtained the temperature was decreased to the start point in steps with a 50 degree increment; at each step, three to four GC injections were performed.

### 3.2.2. Catalytic stability evaluation

Four tests were developed to assess the stability of the catalysts:

#### *Constant temperature thermal ageing test (CTTAT)*

The process of thermal ageing of a catalyst is used to assess the ability of a catalyst to maintain its initial activity over time. A sintering process of metal and support particles, as well as volatilization of metal particles can take place during the thermal ageing process. The sintering process of a catalyst and the factors that can influence it are described in the literature review (Chapter 2).

The stability of the catalysts was evaluated by exposing the catalyst to reactants at constant temperature. The reactor was heated up to the desired temperature in the presence of nitrogen flowing through the reactor. At the desired temperature, the nitrogen was cut off and reactants were added to the reactor. The reactor was kept at constant temperature for several hours.

#### *Constant temperature hydrothermal ageing test (CTHTAT)*

The process of thermal ageing of a catalyst is used to assess the ability of a catalyst to maintain its initial activity over time, in presence of water. Similar like for thermal ageing process, a sintering process of metal and support particles, can take place during the thermal ageing process.

The stability of the catalysts was evaluated by exposing the catalyst to reactants and water at constant temperature. The reactor was heated up to the desired temperature in the presence of nitrogen flowing through the reactor. At the desired temperature, the nitrogen was cut off and reactants were added to reactor. 5% vol. water was added to the gas stream, after the activity was measured in the absence of water. The reactor was kept at constant temperature for several hours.

#### *Variable temperature thermal ageing test (VTTAT)*

Depending on the initial activity of the catalyst, the catalyst was cycled between two temperatures. The higher temperature was either 650°C (Pt, Pt-Pd (4:1), Pt-Pd

(1:5), Pd 150 catalysts) or 550°C (Pd 150, Pt-Pd (1:5), Pd 122, PdRh, PtPdRh). The lower temperature was chosen from the light off curve of the activity test and was the temperature for which the sintering effect of the thermal ageing treatment was determined. The reactor was heated up to the higher temperature in the presence of reactants flowing through reactor (CH<sub>4</sub> 4100±50 ppm, total flow rate 235±10 cc/min). The reactor was kept at the higher temperature for one hour (i.e. 4 GC injections), then the temperature was decreased and kept for one hour at the lower temperature of the test (4 GC injections). The catalyst was cycled for 8 times between the two temperatures. Then the reactor was kept at the lower temperature for 5 hours. In some of the experiments 5% vol. water was added to the reactant stream for another 5 hours. After the water was cut off, the reactor was kept at constant temperature for another 5 hours.

#### *Variable temperature hydrothermal ageing test (VTHTAT)*

Similar to the VTTA test, the catalyst was cycled between two temperatures. The higher temperature was either 650°C (Pt, Pt-Pd (4:1), Pt-Pd (1:5), Pd 150 catalysts) or 550°C (Pd 150, Pt-Pd (1:5), Pd 122, PdRh, PtPdRh). The lower temperature was chosen from the light off curve of the activity test and was the temperature for which the sintering effect of the hydrothermal ageing treatment was determined. The lower temperature was chosen from the light off curve of the activity test. The reactor was heated up to the higher temperature in the presence of reactants flowing through reactor (CH<sub>4</sub> 4100±50 ppm, total flow rate 235±10 cc/min). The reactor was kept at the higher temperature for one hour (4 GC injections), then water was added to the reactant stream (5% vol.). The reactor was kept at the higher temperature in presence of water for one hour (4 GC injections) then the temperature was decreased and kept for one hour at the lower temperature of the test (4 GC injections). After 8 cycles, the reactor was kept at constant temperature for 10 hours, at the lowest temperature of the cycle. After the water was cut off, the reactor was kept at constant temperature for another 5 hours.

### **3.3. Catalyst characterization methods**

CO Chemisorption and Temperature Programmed Reduction tests were performed to characterize Pd 80, Pt-Pd (4:1) and Pd catalysts.

To understand the changes that take place in the catalysts during the thermal and hydrothermal treatments, the samples were characterized by Transmission Electron Microscopy (TEM).

#### *Carbon monoxide (CO) Chemisorption*

Carbon monoxide chemisorption is a very useful tool in quantitative evaluation of surface active sites where the chemical reaction will take place. CO chemisorption is mainly used in catalysis for metal dispersion and metal surface area measurements. From the way CO is chemisorbed on the particle surface (linear, bridge or twin type) one can determine the dispersion of a metal, i.e. linear type conformation will adsorb on one metal particle (Pt catalyst), bridge conformation will adsorb on two metal particles (Pd catalyst) while in twin conformation 2 CO molecules are adsorbed on one metal atom (Rh catalyst).

First the sample is pre-treated in presence of oxygen or hydrogen, followed by pulse CO admission. CO interacts easily with transitional metal particle due to its electron donor properties. The CO chemisorption results allow us to determine the surface active area as well as the size of the metal particles.

#### *Temperature Programmed Reduction (TPR)*

Temperature programmed methods study the temperature-dependence of specific adsorption and desorption processes of solid samples in specific gas atmosphere. The technique provides a fingerprint of the reduction profiles of solid samples (Jones. et al, 1986, Niemantsverdriet (2007).

The catalyst is placed in a U shape glass tube which is placed in a reactor heated at a rate of 0.1 to 10 C per minute, controlled by a processor. Reducing gas is flowing over the catalyst bed. The hydrogen content before and after the reaction is analyzed by a TCD. The change in hydrogen concentration outlines the gas consumption of the catalyst.

### **Monometallic supported catalysts**

Characterization by TPR method of monometallic supported catalysts provides useful information on the reduction conditions of the catalyst.

Supported catalysts may exhibit different reduction patterns compared with the unsupported catalysts (Jones et al., 1986). When there is no interaction between the support and active metal, the reduction pattern reduces in a similar manner with unsupported active metal. When there is an interaction between the support and active metal, the reduction pattern may result in an identifiable metal support compound. Depending on the nature of the interaction between metal and support, the reduction process may be hindered or promoted for supported metal catalysts (i.e.  $\text{SiO}_2$ ,  $\gamma\text{-Al}_2\text{O}_3$ ).

The TPR provides an insight into the reduction processes mechanism which plays an important role in designing the optimum work conditions of the catalyst. The phases present in supported catalysts as well as the degree of reduction can be identified using TPR patterns.

### **Bimetallic catalysts**

The TPR curves are a very useful tool for bimetallic catalysts characterization, giving the information of the contact between the two metals. When a TPR pattern of a stoichiometric bimetallic catalyst shows a big peak in the area of one of the monometallic reduction temperature, it provides evidence regarding that metal's ability to act as a catalyst in the reduction of the second metal. The presence of a single peak in a TPR spectrum of a bimetallic catalyst gives evidence of the intrinsic bimetallicity of the two metals.

TPR proved to be a useful tool in establishing of the condition of the active metal, interactions between active metal and the support, characterization of catalysts (i.e. hydroprocessing catalysts or noble metal electrocatalysts) (Jones et al., 1986).

### *Transmission Electron Microscopy*

Transmission Electron Microscopy (TEM) is a microscopy method which provides images of a specimen at nano-scale level. TEM uses transmitted and scattered electrons of a primary beam which passes through a sample (Niemantsverdriet, 2007). Parallel rays of the electron beam are produced by a condenser. The rays then penetrates the sample and a two dimensional image of the sample is obtained as a function of density and thickness of the samples.

TEM is used in science, nanotechnology, catalysis and metallurgy, as well as medicine and biology.

## Chapter 4. Experimental results and analysis

This chapter presents the experimental results obtained during the study. The results can be divided into a number of areas, which are:

- 1- Study of the effect of thermal and hydrothermal ageing on the activity of Pt, Pd 122, Pd 150, Pt-Pd (4:1), Pt-Pd (1:5), Pd Rh, PtPdRh catalysts
- 2- Study of the sintering and re-dispersion process of metal particles.
- 3- Study of the pre-treatment effect on catalytic activity of Pd 80 and Pd 122 catalyst.
- 4- Study of the effect of metal loading on the catalytic activity for Pd 122 and Pd 150 catalysts
- 5- Characterization of the catalysts (i.e. CO chemisorption, TEM)

### 4.1. Exploratory tests

At the beginning of the study, experiments were performed to assess the catalyst performance. The exploratory tests included thermal and hydrothermal ageing experiments for Pt 95, Pd 80 and bimetallic Pt-Pd 95 (4:1) catalysts.

The activity and stability of the catalysts were evaluated from experimental results. T50, the temperature of the light off curve where 50% of reactants were converted to products, was used to evaluate the activity of the catalyst. The stability of the catalysts was determined as the changes in reactant conversion over time. Prior to presenting any activity study of the catalysts, the activity of reactor, cordierite and alumina are presented.

#### 4.1.1. Reactor

An ignition-extinction cycle of methane conversion was performed for the empty reactor. This test was performed to provide information about reactions taking place in absence of supported catalyst (blank). The results are presented in figure 4.1. It can be observed that for experimental conditions, the conversion of methane starts around 400°C and a 13% conversion of methane was obtained at 550 °C.

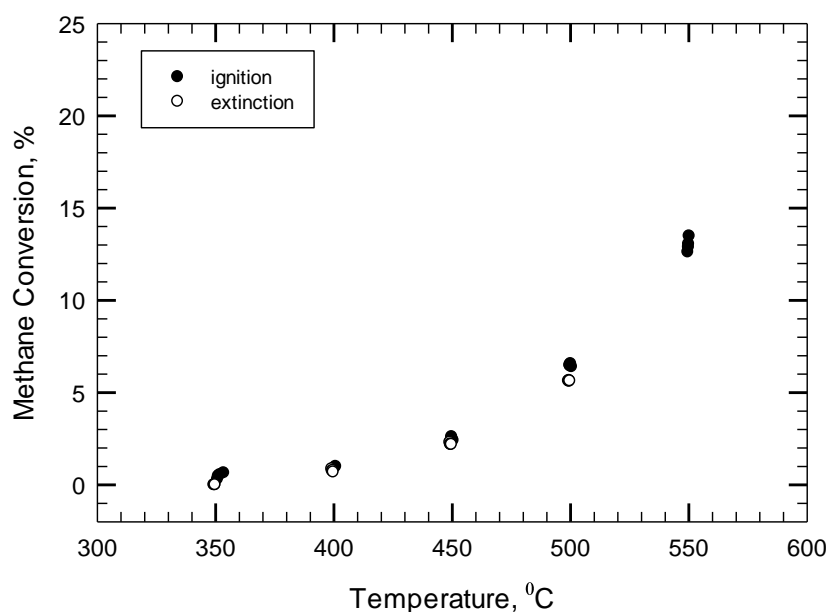


Figure 4.1. Ignition-extinction curve of methane conversion in absence of supported catalyst (MI-314) (CH<sub>4</sub> 4100±50 ppm, total flow rate 235 cc/min)

#### 4.1.2. Cordierite

The contribution to the conversion of methane of the support material, without additives and promoters, was investigated. A variable temperature thermal ageing sequence was performed for cordierite (as described in Chapter 3): the cordierite sample was first de-greened at 650°C in presence of air and then reduced at 500°C in presence of hydrogen; then an ignition-extinction cycle was performed,

followed by an thermal ageing experiment; another ignition-extinction cycle was performed to assess the changes in the catalytic activity due to thermal ageing.

Figure 4.2 compares the experimental results of methane conversion before (MI-307) and after (MI-309) variable temperature thermal ageing test. A decrease in catalytic activity can be observed as a result of thermal ageing.

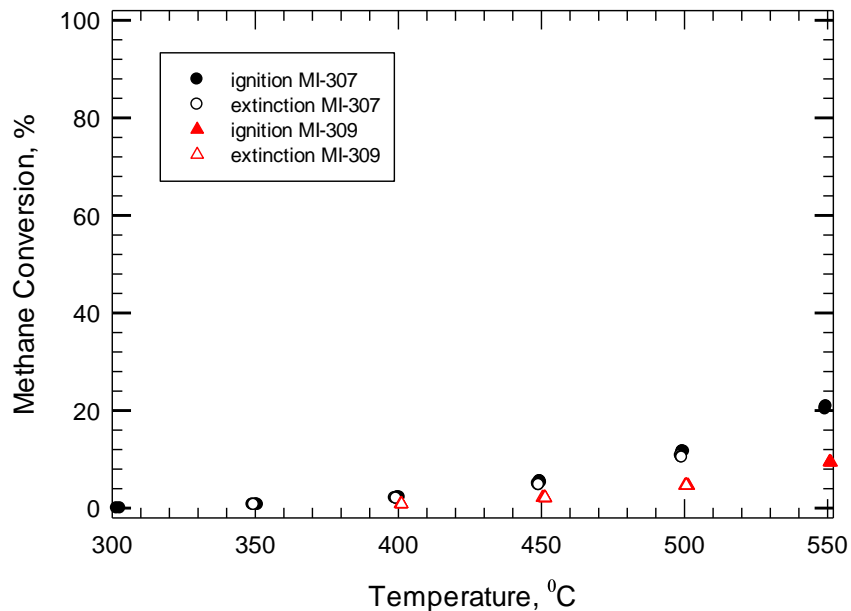


Figure 4.2. Ignition-extinction curves of methane conversion over cordierite (MI-307) (CH<sub>4</sub> 4100±50 ppm, total flow rate 235 cc/min)

Figure 4.3 presents the experimental results of variable temperature thermal ageing test. The sample was thermally aged at 550°C and the changes in catalytic activity were monitored for the 500°C intervals. The activity of the first 500°C interval was around 10% conversion of methane. After 25 hours the activity decreased to 8% conversion. When water was switched on the activity decreased to almost zero. A slight recovery in activity can be observed after the water was switched off.

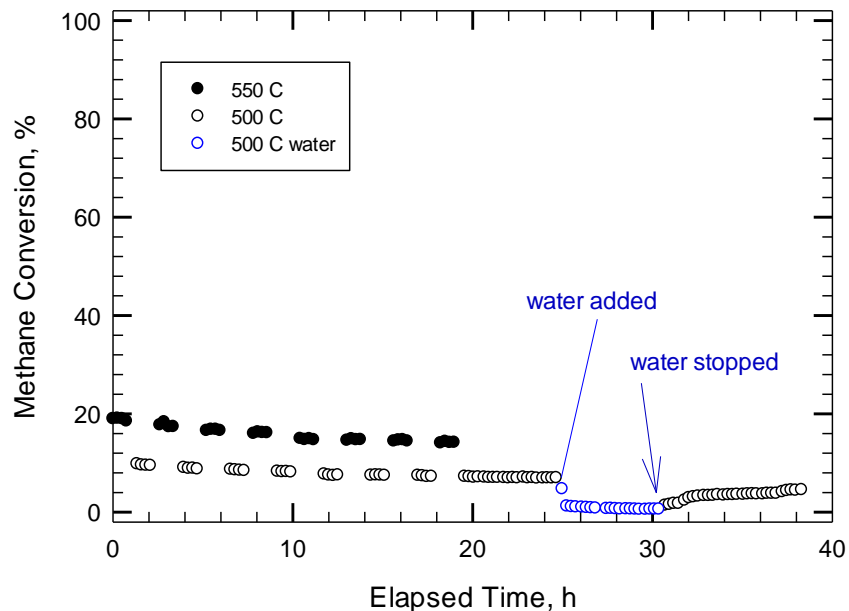


Figure 4.3. Variable temperature thermal ageing test of methane conversion of cordierite (MI-308) (CH<sub>4</sub> 4100±50 ppm, total flow rate 235 cc/min)

#### 4.1.3. Alumina

The alumina sample was first de-greened at 650°C in presence of air and then reduced at 500°C in presence of hydrogen.

Figure 4.4 compares the results of a series of ignition-extinction curves of methane conversion in presence of alumina: MI-225, MI-226 and MI-227. The ignition-extinction curves form a small negative hysteresis for the first 2 ignition-extinction cycles. 100% conversion of methane was obtained at 650°C for the first ignition-extinction cycle and at 750°C for the second and third ignition-extinction cycle. The changes in the catalytic activity of alumina can be observed from the changes in the conversion of methane for the same temperatures, i.e. 100% conversion of methane was obtained for the MI-225 test, 78% conversion of methane for the MI-226 and just 10% conversion of methane for the MI-227.

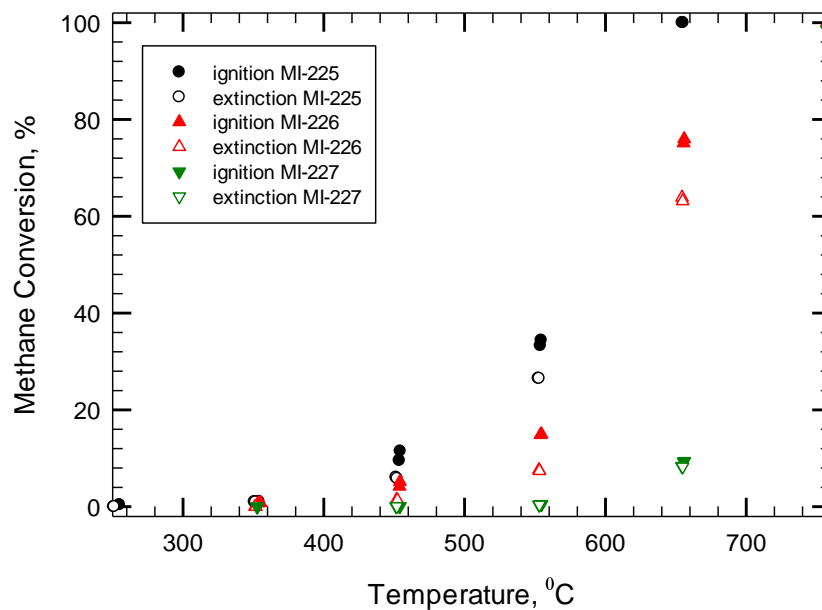


Figure 4.4. Ignition-extinction curves of methane conversion over alumina (MI-225) (CH<sub>4</sub> 4100±50 ppm, total flow rate 235 cc/min)

## 4.2. Activity experiments

### 4.2.1. Pt-Pd (4:1) bimetallic catalyst

The catalytic activity and stability of the catalyst were assessed by investigative experiments.

An ignition-extinction cycle for Pt-Pd (4:1) catalyst is presented in figure 4.5. From this figure it can be seen that the ignition follows a normal ignition pattern: the conversion is zero at low temperatures and increases with the increase of temperature. Similar for extinction, the conversion decreases with the decrease of temperature.

It is interesting to observe that for Pt-Pd (4:1) catalyst, the ignition-extinction curves form a hysteresis loop, with extinction being more active than the ignition (positive hysteresis). T50 of the light off curve was 475°C. (T50=475°C)

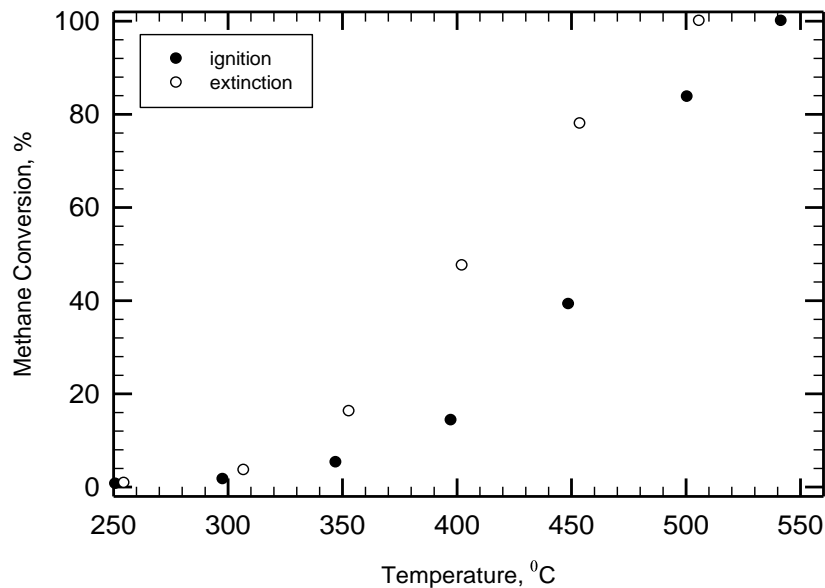


Figure 4.5. An ignition-extinction cycle of methane conversion of Pt-Pd (4:1) catalyst (MI-028) (CH<sub>4</sub> 4700±50 ppm, total flow rate 235 cc/min)

When extinction experiments were performed separate from ignition experiments, different behaviours were observed. According with figure 4.5, it was expected that 100% conversion of methane would be obtained at 500°C, 550°C and 600°C. However, different conversions of methane were obtained depending on the temperature the reactants were added during the heating up process of the reactor. For example, when the reactants were added to the reactor at room temperature, the conversion of methane was 100% at 600°C and 550°C, and 88% at 500°C (figure 4.6). However, a conversion of methane lower than 100% was obtained when reactants were added to the reactor at 600°C (~81% of methane conversion at 600°C, 60% at 550°C and ~43% at 500°C) (figure 4.7).

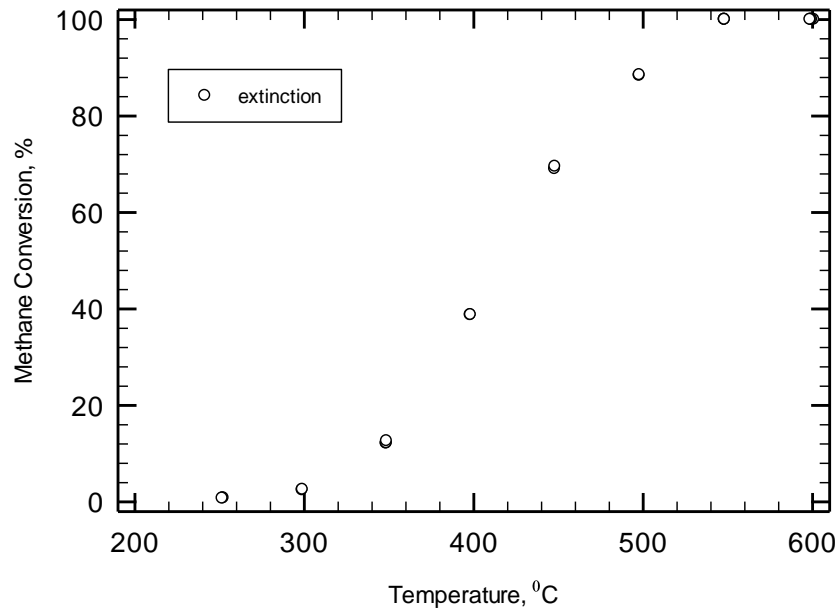


Figure 4.6. Extinction curve of methane conversion over Pt-Pd (4:1) catalyst; the reactants were added at 25°C (CH<sub>4</sub> concentration 4700±50 ppm, total flow rate 235 cc/min)

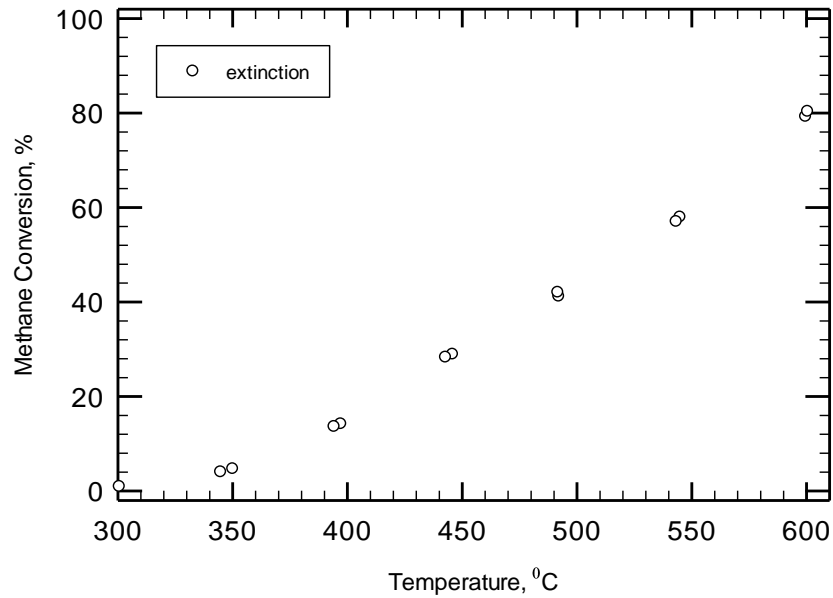


Figure 4.7. Extinction curve of methane conversion over Pt-Pd (4:1) catalyst; the reactants were added at 600°C (MI-002) (CH<sub>4</sub> concentration 4700±50 ppm, total flow rate 35 cc/min)

When the reactor was heated up to 600°C in the presence of air, and the reactants were added at 600°C, 100% conversion of methane was obtained at 600°C (figure 4.8). It can be observed that the extinction curve follows very close the experimental results of reactants added at room temperature. Considering the lean methane concentration is an oxidizing atmosphere (CH<sub>4</sub> concentration 4700±50 ppm) the results suggest that oxygen plays an important role in methane combustion over Pt-Pd (4:1) bimetallic catalyst. The test was repeated and similar results were obtained.

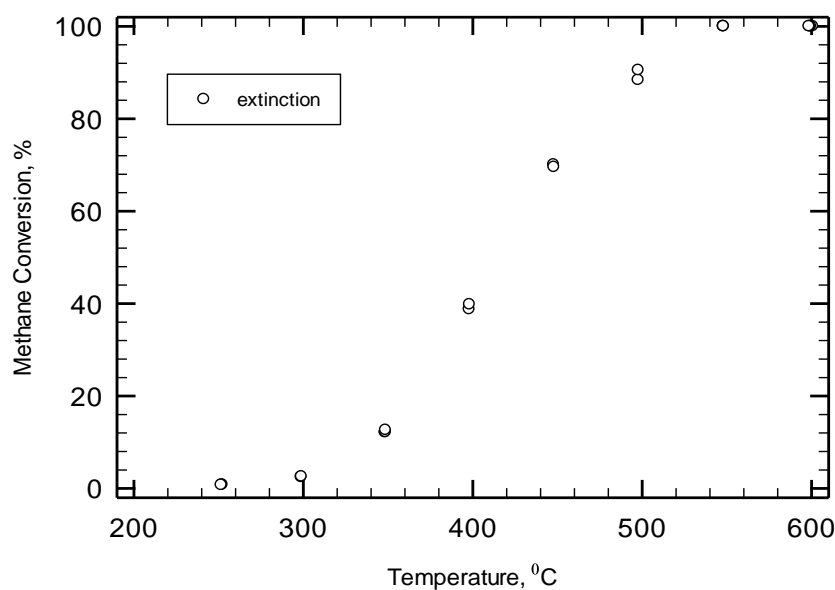


Figure 4.8. Extinction curve of methane conversion over Pt-Pd (4:1) catalyst; the reactor was heated up to 600°C in presence of air and reactants were added at 600°C (MI-043) (CH<sub>4</sub> 4700±50 ppm, total flow rate 235 cc/min)

To investigate the role of temperature and oxidizing atmosphere in methane conversion over Pt-Pd (4:1) catalyst, two sets of experiments were designed.

In the first set, the effect of oxygen atmosphere at room temperature was investigated. One sample was exposed overnight to an oxidizing atmosphere at room temperature. The extinction curve was obtained by heating up the reactor

without air flowing through reactor (MI-039). Another sample was exposed overnight and heated up in the presence of a non-oxidizing atmosphere (MI-030). Figure 4.9 compares the experimental results of the two tests (MI-039 and MI-030).

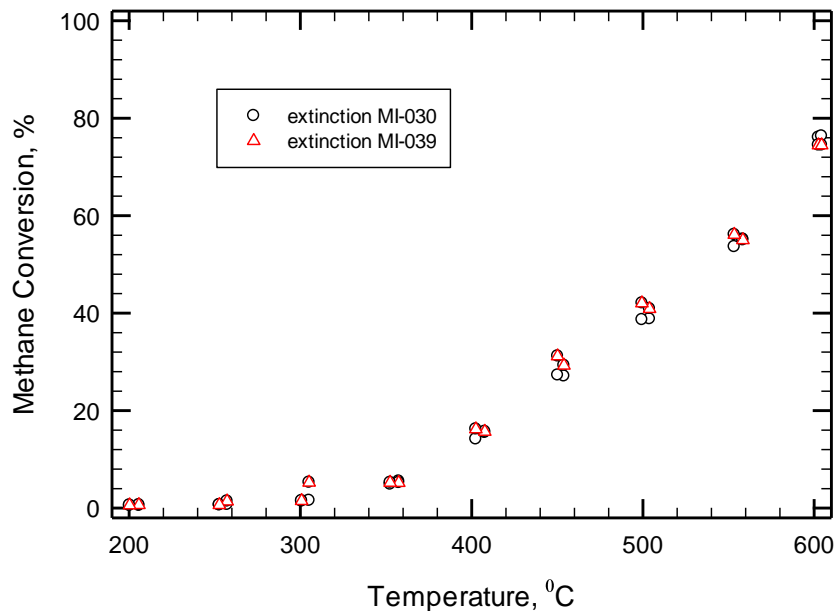


Figure 4.9. Extinction curves of methane conversion over Pt-Pd (4:1) catalyst (MI-030 vs MI-039) (CH<sub>4</sub> 4700±50 ppm, total flow rate 235 cc/min)

From figure 4.9 it can be seen that the results of both experiments are close, which suggest that oxidizing atmosphere plays an important role in the conversion of methane of Pt-Pd (4:1) catalyst, at higher temperatures.

A second set of experiments was designed to investigate the effect of oxidizing atmosphere above room temperature. This time the reactants were added to the reactor at specific temperatures (200°C, 300°C, 350°C, 400°C and 500°C). The summary of these experimental results is shown in figure 4.10.

From figure 4.10 it can be observed that 100% conversion of methane was obtained when reactants were added at temperatures below 400°C and that the

results are very similar. When the reactants were added to the reactor at 500°C, 100% methane conversion was obtained just at 600°C. When reactants were added to the reactor at 600°C, a conversion lower than 100% was obtained (~80%).

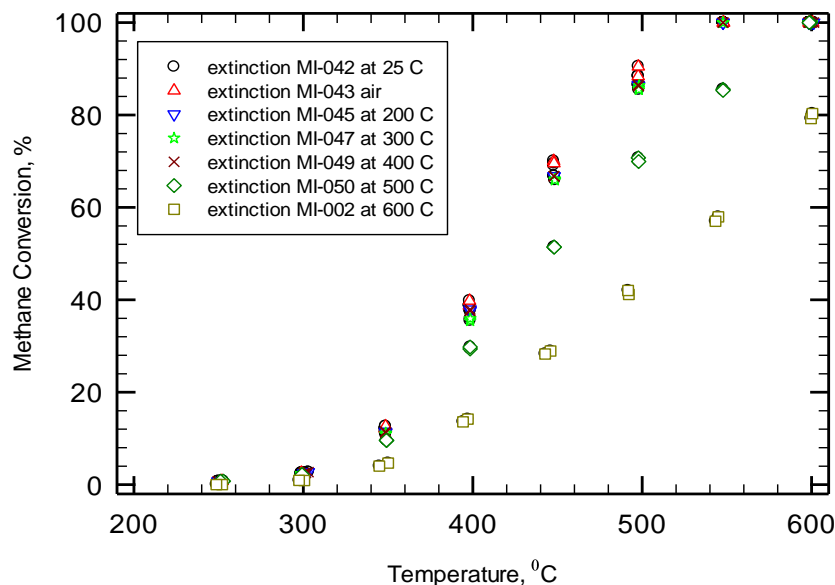


Figure 4.10. Extinction curves of methane conversion over Pt-Pd (4:1) catalyst (MI-042 the reactants were added at room temperature; MI-043 the reactor was heated up to 600°C in the presence of air and the reactants were added at 600 C; MI-045 the reactants were added at 200°C; MI-047 the reactants were added at 300°C; MI-049 the reactants were added at 400°C; MI-050 the reactants were added at 500°C; MI-002 the reactants were added at 600°C) (CH<sub>4</sub> 4700 ppm, total flow rate 235 cc/min)

The test and conditions were repeated and very close results were obtained. Figure 4.11 compares the experimental results for the case of reactants added at 600°C.

From the experimental results it can be concluded that for Pt-Pd (4:1) catalyst, the presence of an oxidizing atmosphere (air-methane mixture) during the heating up process has a positive impact on methane conversion.

Similar tests were performed for Pt and Pd catalysts to determine if similar behaviour is observed.

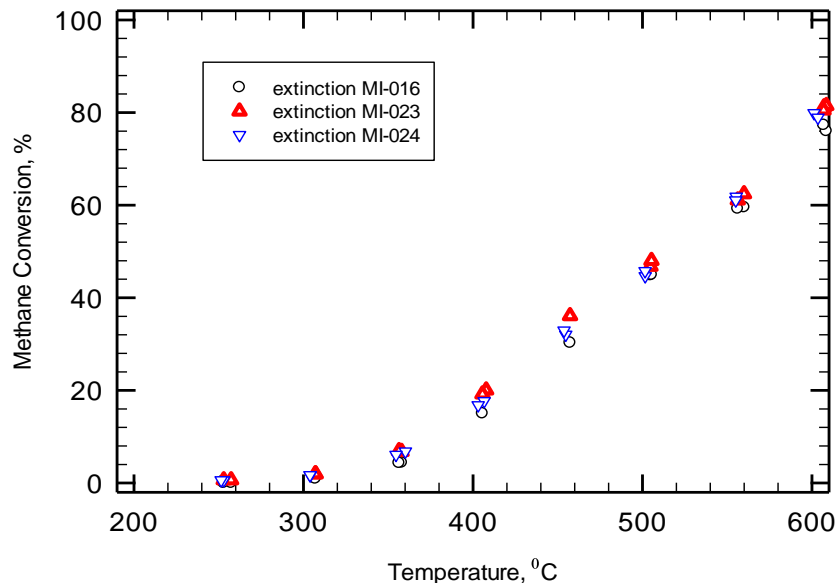


Figure 4.11. Extinction curve of methane conversion over Pt-Pd (4:1) catalyst; the reactants were added at 600°C (MI-016, MI-023, MI-024) (CH<sub>4</sub> 4700±50 ppm, total flow rate 235 cc/min)

#### 4.2.2. Pt catalyst

The ignition (light-off) curves were obtained following the same protocol as for Pt-Pd (4:1) catalyst (see above).

An ignition-extinction cycle for Pt catalyst is presented in figure 4.12. From this figure it can be seen that the ignition curve follows a normal ignition pattern: the conversion is zero at low temperatures and increases with the increase of temperature. Similar for extinction, the conversion decreases with the decrease of temperature.

From figure 4.12 a small hysteresis loop can be observed. For Pt catalyst however, the extinction curve shows a lower activity than the ignition curve (negative hysteresis), which is opposite of Pt-Pd (4:1) catalyst.

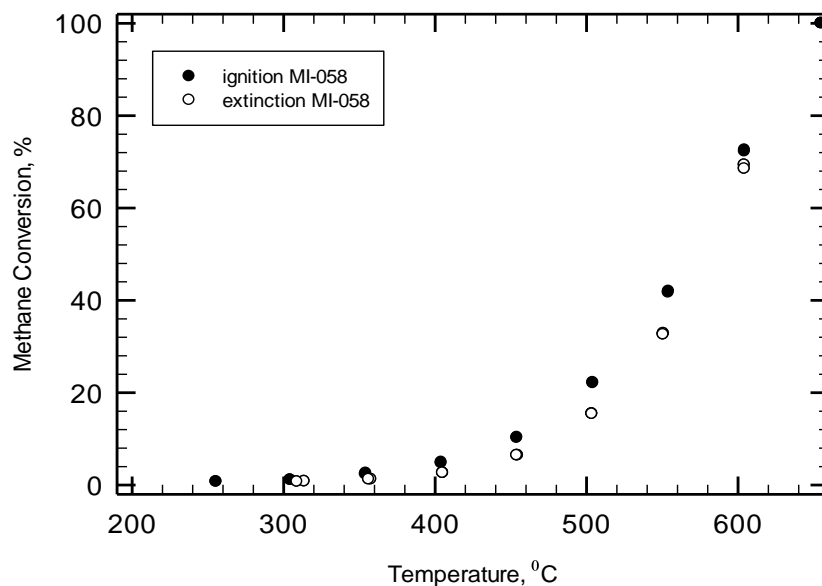


Figure 4.12. Ignition-extinction curve of methane conversion over Pt catalyst (CH<sub>4</sub> 4700±50 ppm, total flow rate 235 cc/min)

A complete conversion of methane was obtained at 650°C, a higher temperature than for bimetallic Pt-Pd (4:1) catalyst (100% conversion at 550°C). T<sub>50</sub> for Pt catalyst is 575°C.

In figure 4.13, the ignition-extinction curves of Pt-Pd (4:1) and Pt catalyst are compared. From the experimental results it can be concluded that a small amount of Pd added to Pt catalyst decreases T<sub>50</sub> from 575°C to 475°C.

Several tests were performed on Pt catalyst, following the previous protocol: reactants were added to room temperature (MI-059), reactants were added to 650°C (MI-060) and reactants were added at 600°C (MI-061). Figure 4.14 shows the comparison of these results.

From figure 4.14 it can be concluded that the presence of non-oxidizing atmosphere at high temperatures does not play an important role in conversion of methane over Pt catalyst.

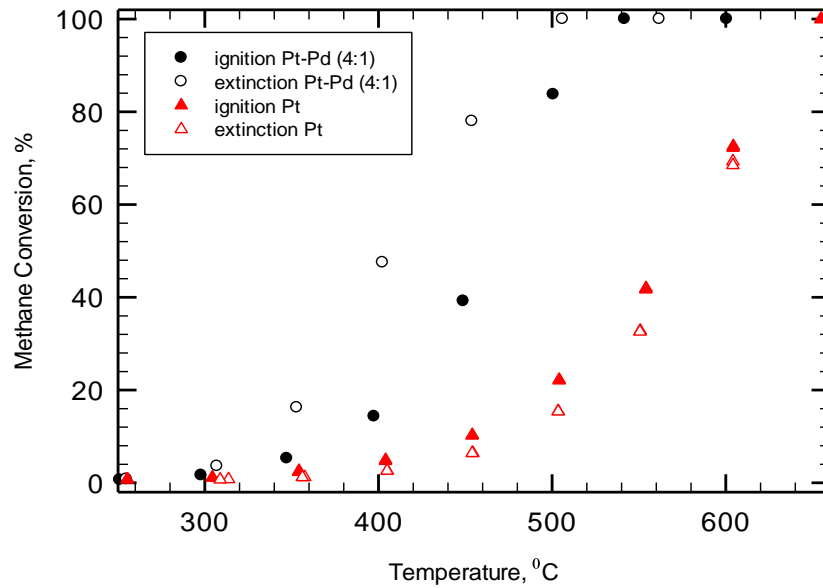


Figure 4.13. Ignition-extinction curves for Pt-Pd (4:1) (MI-028) and Pt (MI-058) catalysts (CH<sub>4</sub> 4700±50 ppm, total flow rate 235 cc/min)

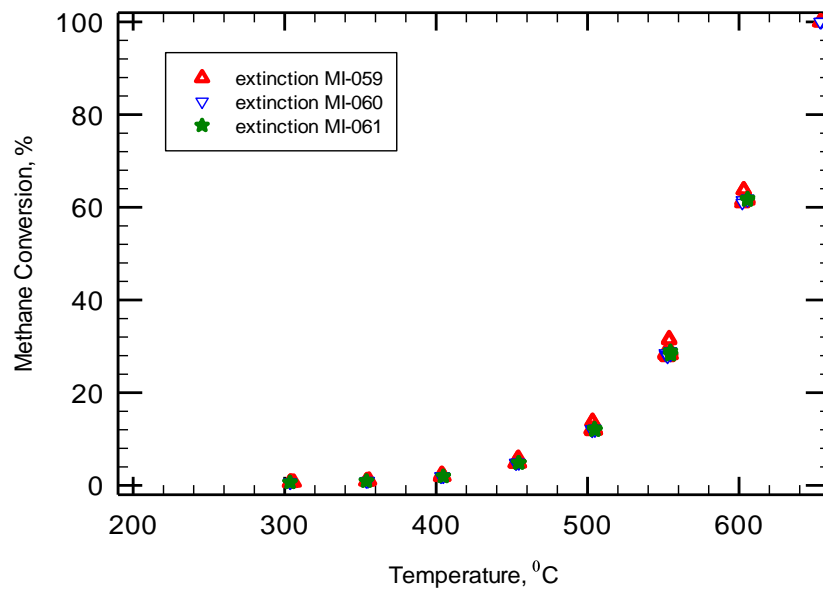


Figure 4.14. Extinction curves of methane combustion over Pt catalyst; reactants were added at room temperature (MI-059); reactants were added at 650°C (MI-060); reactants were added at 600°C (MI-061) (CH<sub>4</sub> 4700±50 ppm, total flow rate 235 cc/min)

### 4.2.3. Pd catalyst

The ignition (light-off) curves were obtained following the same protocol as for Pt-Pd (4:1) catalyst [see Pt-Pd (4:1) catalyst].

Figure 4.15 presents the ignition-extinction cycle for Pd catalyst. From this figure it can be observed that a hysteresis loop is present, with ignition more active than extinction (negative hysteresis). T50 of the light off curve is 310°C which is lower compared with Pt-Pd (4:1) catalyst ( $T_{50} = 475^{\circ}\text{C}$ ).

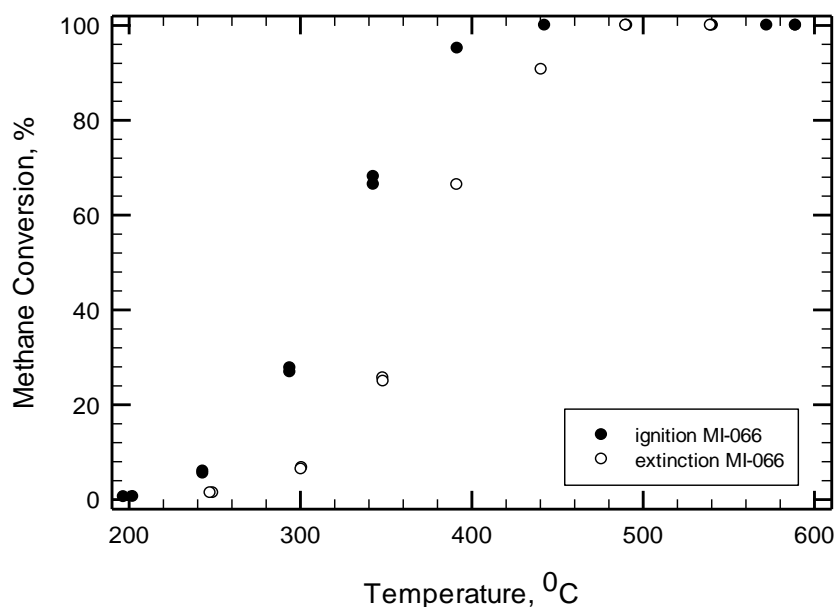


Figure 4.15. Ignition-extinction curves of methane conversion over Pd catalyst ( $\text{CH}_4$  4700±50 ppm, total flow rate 235 cc/min)

A comparison of the ignition-extinction curves of methane combustion over Pt-Pd (4:1), Pt and Pd catalysts is presented in figure 4.16. It can be observed that Pd catalyst shows the highest activity of methane conversion. However, the predominantly Pt catalyst (Pt-Pd (4:1)) shows an activity intermediate to Pd and Pt catalyst.

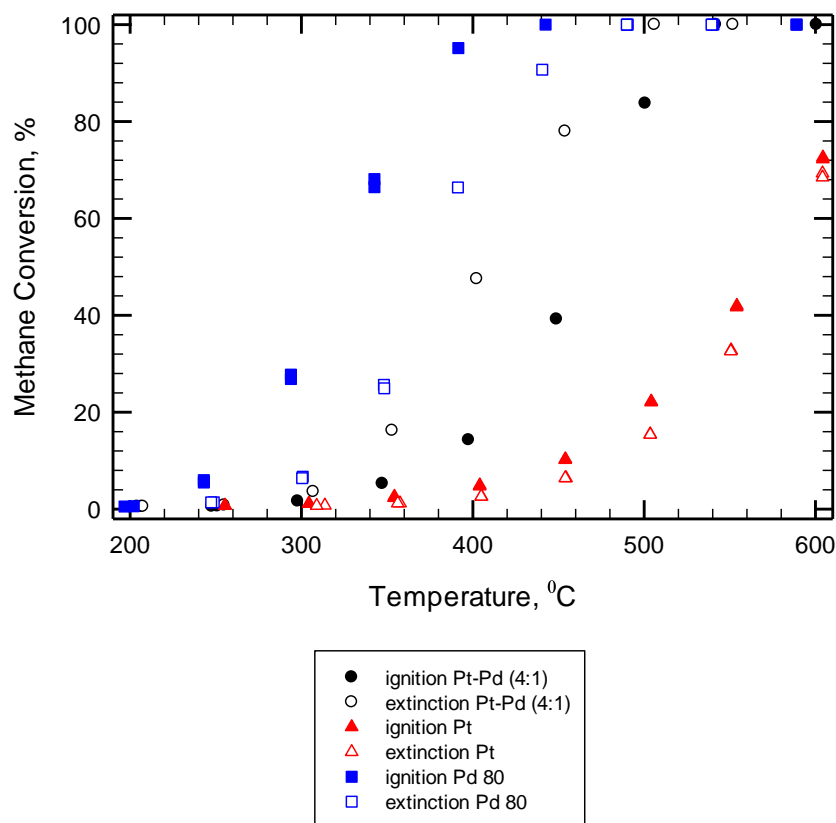


Figure 4.16. Ignition-extinction curves of methane combustion over Pt-Pd (4:1) (MI-028), Pt (MI-058) and Pd (MI-066) catalysts (CH<sub>4</sub> 4700±50 ppm, total flow rate 235 cc/min)

To determine the influence of temperature and oxidizing atmosphere on the extinction curves, the same protocol was followed as described above (reactants were added at different temperatures of the catalyst; see Pt-Pd (4:1) catalyst). The summary of results is presented in figure 4.17. From the experimental results it can be concluded that the presence of an oxidizing atmosphere in the heating up process of the catalyst, does not play an important role in the conversion of methane over Pd 80 catalyst.

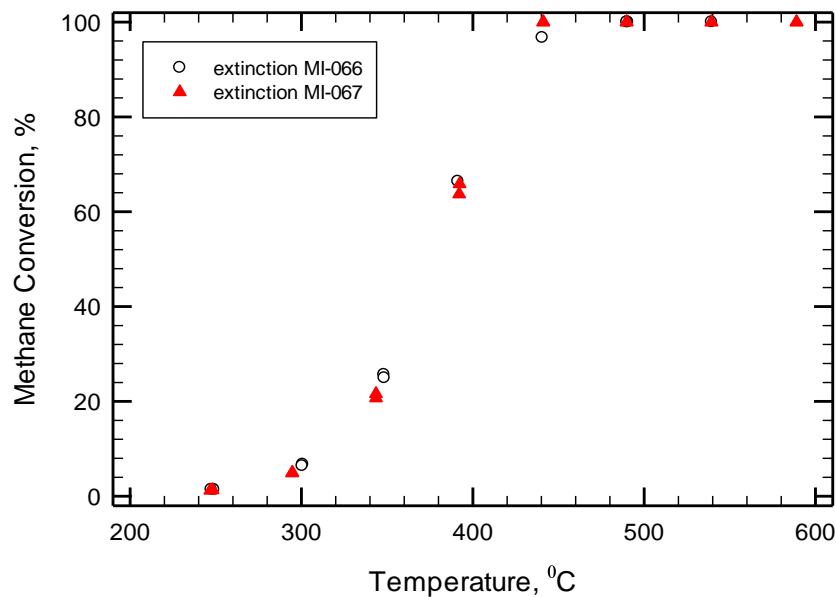


Figure 4.17. Extinction curves of methane combustion over Pd 80 catalyst; MI-066 reactants were added at room temperature; MI-067 reactants were added at 600°C

Figure 4.18 presents a summary of the experimental results of methane conversion of Pt-Pd (4:1), Pt and Pd catalysts, heated up in the presence of non-oxidizing atmosphere. As we previously mentioned, the bimetallic Pt-Pd (4:1) catalyst is the only one that shows a dependence of methane conversion on the temperature and atmosphere. However, for Pd catalyst due to its high activity of methane conversion, this effect can be hidden.

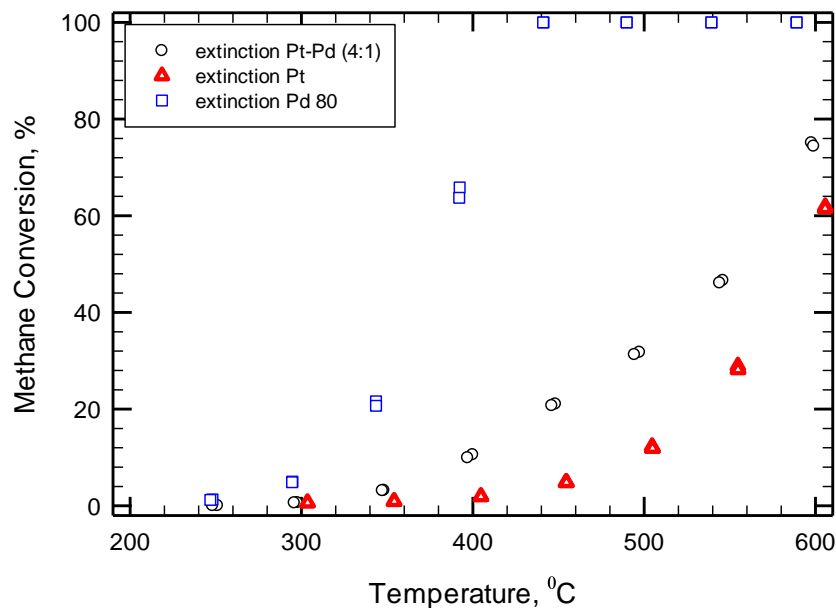


Figure 4.18. Extinction curves of methane conversion over Pt-Pd (4:1) (MI-003), Pt (MI-061) and Pd 80 (MI-067) catalysts; reactant were added at 600°C (CH<sub>4</sub> 4700±50 ppm, total flow rate 235 cc/min)

## Conclusions

Pt and Pd 80 catalyst showed a negative hysteresis, while bimetallic Pt-Pd (4:1) catalyst showed a positive hysteresis

Pd only showed the highest activity in methane conversion, Pt catalyst showed the lowest conversion and Pt-Pd (4:1) catalyst showed intermediate conversion

The dependence of catalytic activity on the temperature and atmosphere present in the reactor was clearly observed just for Pt-Pd (4:1) catalyst.

#### 4.2.4. CO Chemisorption and Temperature programmed reduction

##### *CO chemisorption*

To further investigate the dependence of catalytic activity of Pt-Pd (4:1) catalyst on the temperature and atmosphere, an investigatory CO chemisorption test was designed to closely follow the experimental conditions of the catalyst testing.

The catalyst was aged at 650°C for 16 hours in the presence of oxygen, followed by the reduction process and a CO chemisorption test (CO chem 1). Then the sample was heated to 600°C in the presence of oxygen followed by cooling down process to room temperature, in the presence of oxygen. After that the catalyst was heated up to 600°C and cooled to room temperature in the presence of inert gas (He). A reduction process was performed, followed by a CO chemisorption test (CO chem. 2). The experimental results are presented in Table 4.1.

Table 4.1. CO chemisorption test for Pd catalyst

Sample ID	Mass, g	CO Chem 1, micromol/g catalyst	CO Chem 2, micromol/g catalyst
Pd	0.2090	6.0	6.6
Pt	3.1080	1.0	0.8
Pt-Pd (4:1)	1.0100	2.3	2.3

A slight increase in particle size can be observed for the Pd catalyst exposed to inert atmosphere. For Pt catalyst, slight decrease in particle size can be observed, while for Pt-Pd (4:1) catalyst there is no change in particle size.

From CO chemisorption results it was concluded that heating the catalysts in oxygen or inert gas does not change the nanoparticles size (the change in particle size is not significant). This result is extremely important for the Pt-Pd (4:1)

catalyst as it concludes that the decrease in activity as a function of temperature and atmosphere is not due to the sintering process of the catalyst particles.

The increase in the particles size of Pd catalyst during the reduction process is assumed to be due to the high capacity of hydrogen adsorption characteristic of Pd catalyst. It was demonstrated that the adsorption of hydrogen results in a change in lattice for Pd catalyst (Maeland, A. et al., 1966).

### *Temperature programmed reduction*

The TPR test was used to characterize the Pt, Pd 80 and Pt-Pd (4:1) catalysts. The catalysts were reduced by flowing hydrogen and the changes in the concentration of hydrogen as a function of temperature, was recorded downstream of the reactor.

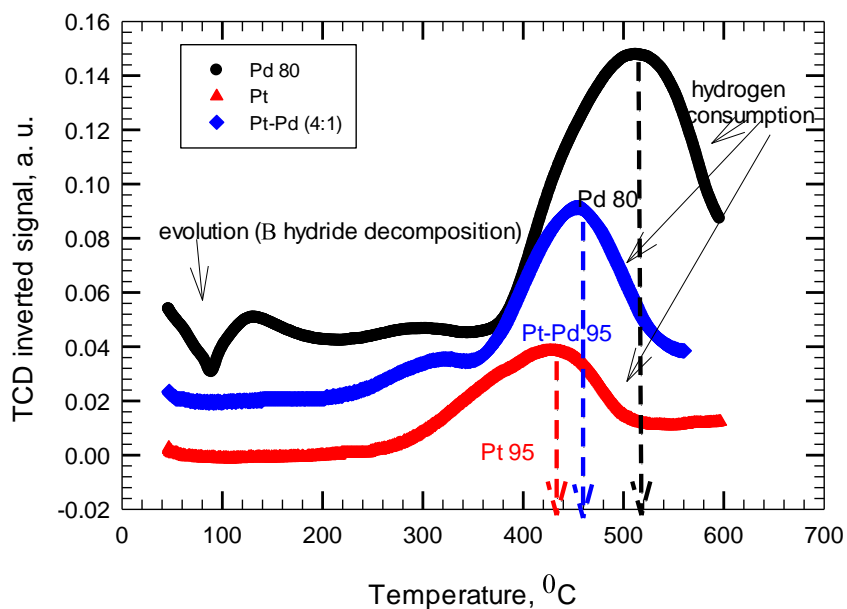


Figure 4.19. TPR results of Pt, Pd and Pt-Pd (4:1) catalysts

Figure 4.19 presents the summary of TPR results of Pt, Pd and Pt-Pd (4:1) catalysts. The profile for Pt-Pd (4:1) catalyst differs from that of either Pt or Pd catalysts, as the reduction took place at temperatures between the monometallic species (Pt and Pd). This result suggests that in bimetallic catalyst Pt and Pd are in intimate contact (i.e. alloy), and that Pt catalyses the reduction of Pd catalyst.

## **Conclusions**

From CO chemisorption results it was concluded that the change in particle size as a result of heating up the reactor in presence of oxygen or inert gas is insignificant and is not responsible for the decrease in activity as a function of temperature and atmosphere present.

From the TPR result was concluded that Pt-Pd (4:1) catalyst is an alloy rather than mixture of Pt and Pd catalysts.

## **4.3. Thermal ageing**

Thermal ageing test was performed to evaluate the changes in activity of a supported catalyst in presence of reactants and temperature.

Each sample was de-greened by exposure to air at 650°C for 16 hours. The de-greened process was followed by the reduction of the catalyst by exposure to hydrogen at 500°C for 30 minutes.

An ignition-extinction test was performed to assess the activity of the catalyst.

Exploratory tests for evaluation of thermal stability of Pt, and Pd catalysts were performed at constant temperatures, in presence of reactants (CH<sub>4</sub> 4700±50 or 4100±50 ppm, total flow rate 235 cc/min).

#### 4.3.1. Pt catalyst

The catalytic activity was determined from the ignition-extinction curves, as well as T50 of the light-off curve. The stability of the catalyst was evaluated from the changes in reactant conversion over time, in presence of Pt catalyst.

An ignition-extinction curve for Pt catalyst is presented in figure 4.20. 100% conversion of methane was obtained at 650°C. The presence of a small negative hysteresis can be observed (ignition more active than extinction). T50 of the light off curve was 575°C.

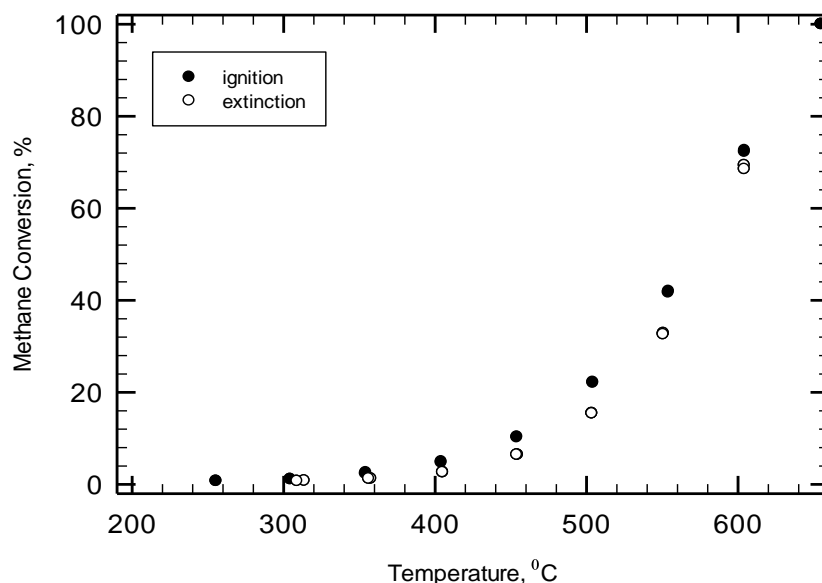


Figure 4.20. Ignition-extinction for methane conversion over Pt catalyst (MI-058) (CH<sub>4</sub> 4700±50 ppm, total flow rate 235 cc/min)

The stability of Pt catalyst was evaluated by exposing the catalyst to reactants at 500°C and 400°C (CH<sub>4</sub> 4700±50 ppm). The reactor was heated up to the desired temperature in the presence of nitrogen flowing through the reactor. At the desired temperature, the nitrogen was cut off and reactants were added to the reactor. The reactor was kept at the desired temperature for 7 hours. The summary of results is presented in figure 4.21.

It can be observed that the change in methane conversion at 500°C was very small (initial conversion of methane was 11.22% and the final conversion, after 7 hours, was 9.25%). Therefore, it was assumed that for 500°C, the temperature and the reactants do not affect the activity of Pt catalyst.

The change in methane conversion at 400°C was negligible (initial conversion of methane was 2.29 and the final conversion was 1.78%). Therefore, it was assumed that for 400°C the temperature and the reactants do not affect the activity of Pt catalyst.

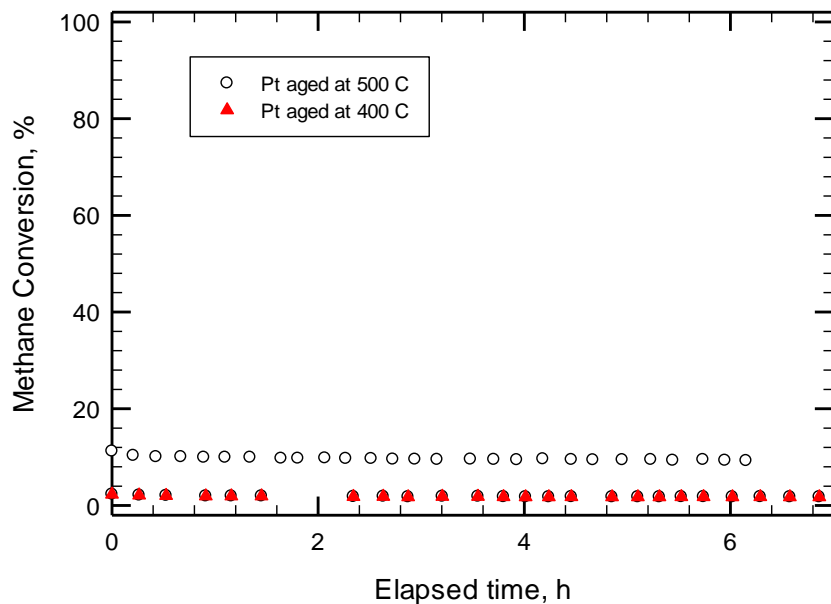


Figure 4.21. Thermal stability of Pt catalyst at 500°C (MI-073) and 400°C (MI-074) (CH<sub>4</sub> 4700±50 ppm, total flow rate 235 cc/min)

A summary of results is presented in Table 4.2.

Table 4.2. The initial and final conversion of methane at 500 °C and 400 °C

Temp, °C	X <sub>initial</sub> , %	X <sub>final</sub> , %
500	11.22	9.25
400	2.29	1.78

The slight decrease in methane conversion for Pt catalyst after 7 hours exposure at 500°C and 400°C can be explained by Mars-Van Krevelen mechanism. As it is known, Pt catalyst is not very active in the conversion of methane ( $T_{50}=575^{\circ}\text{C}$ ). As a result, the water formed during the reaction is not very attracted by the active sites of the catalyst, and in consequence does not block them. Also, above 450°C it is expected that the hydroxyl groups eventually adsorbed, are removed as means of reaction with methane.

#### 4.3.2. Pd catalyst

As in the case of Pt catalyst described above, the catalytic activity of Pd catalyst was determined from the ignition-extinction curves as well as  $T_{50}$  for the light-off curve. The stability of the catalysts was determined as the changes in reactant conversion over time, in presence of Pd catalyst.

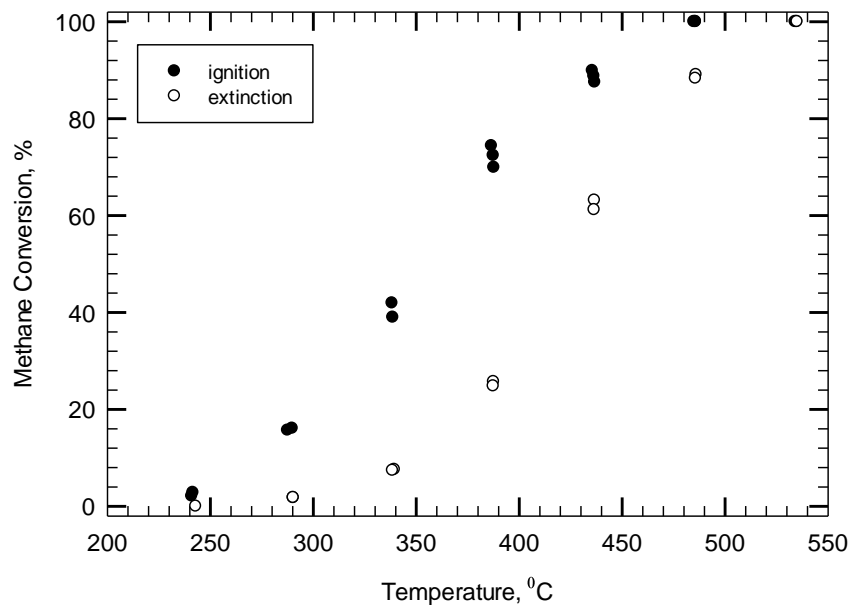


Figure 4.22. Ignition-extinction curve for methane conversion over Pd catalyst (MI-106) ( $\text{CH}_4$  4700±50 ppm, total flow rate 235 cc/min)

Figure 4.22 presents the ignition-extinction curves of methane conversion over Pd catalyst. The presence of a wide negative hysteresis loop can be observed. T50 was 350°C.

Thermal stability of Pd catalyst was evaluated similar as for Pt catalyst: the reactor was heated to the desired temperature, in the presence of a non-oxidizing atmosphere flowing through the reactor. At the desired temperature, the nitrogen was cut off and the reactants were added to the reactor. The reactor was kept at a constant temperature for up to 20 hours.

Thermal stability for Pd catalyst was evaluated at 500°C, 450°C, 400°C and 350°C. A summary of the experimental results is presented in figure 4.23.

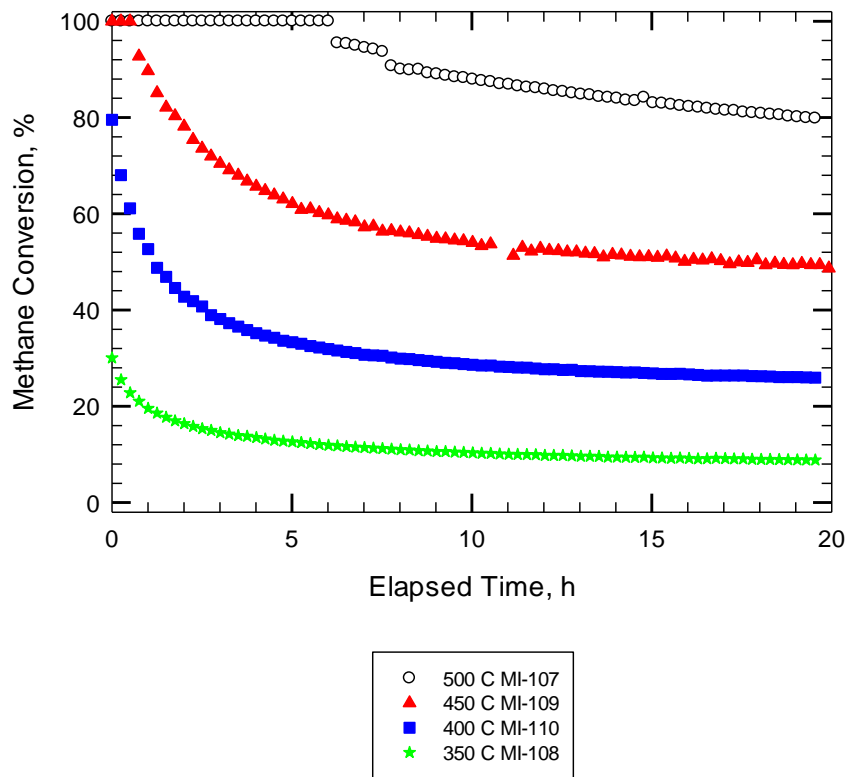


Figure 4.28. Constant temperature thermal ageing test of methane conversion over Pd catalyst (CH<sub>4</sub> 4700±50 ppm, total flow rate 235 cc/min)

The experimental results of initial and final conversion of methane, as a function of temperature are presented in table 4.3. The strong decrease in methane conversion for Pd catalyst, over time can be observed from figure 4.23 and table 3 results.

Table 4.3. The changes in methane conversion over Pd catalyst

T, °C	$\chi_{\text{initial}}$ , %	$X_{7\text{ h}}$ , %	$X_{20\text{ h}}$ , %
500	100	94.5	79.83
450	100	57.22	48.76
400	79.53	3069	25.95
350	30.06	11.42	8.83

It can be observed that the conversion of methane increases with the increase in temperature. As a result, more water is formed during the reaction at higher temperatures, i.e. more water will be formed at 500°C compared with 350°C. When we compare the decrease in methane conversion after 20 hours, it can be observed that for 400°C and 450°C, the decrease in methane conversion is similar (around 50%), after 20 hours exposure to reactants (CH<sub>4</sub> 4700±50 ppm). For 500°C and 350°C the decrease in methane conversion is around 20%. This can be explained by Mars-Van Krevelen mechanism for methane oxidation of highly active catalysts. According with Mars-Van Krevelen mechanism of reaction, water will be preferentially adsorbed on highly active sites of a catalyst. For 450°C and below, the hydroxyl groups will be adsorbed and block the highly active sites of Pd catalyst. In methane conversion, temperatures higher than 450°C are required in order to remove the adsorbed hydroxyl groups. This can explain the big drop in methane conversion for 400°C and 450°C. However, at 350°C, less water is formed during the reaction and in consequence the decrease in methane conversion is smaller. From figure 28 it can also be observed that the time required for obtaining constant conversion, increases with the increase of temperature. This can be assumed to be due to the dependence of water adsorption

on temperature, i.e. at higher temperature it takes longer time to block the active sites of the catalyst.

Zhu G. in his study on the PdO/Pd kinetics as a function of temperature concluded that for methane conversion over Pd catalyst, the reaction mechanism is a function of temperature and the chemical state of Pd catalyst (Zhu et al, 2005). Zhu G. found that at 325°C the adsorbed water is in equilibrium with water vapour and blocks the active sites of the catalyst. He also found that the concentration of adsorbed water decreases with the increase of temperature and at 540°C the deactivation effect of water disappears.

In our study, it is interesting to observe that conversion of methane at 500°C shows a different behaviour compared with 450°C, 400°C and 350°C temperatures: the decrease in methane conversion is almost linear. Also, as it was mentioned before, the decrease in methane conversion is around 20% after 20 hours exposure to reactants, which is lower than for 450°C and 400°C temperatures. Also, for temperatures above 450°C, the hydroxyl groups participate more actively in the reaction of methane combustion and less water will be adsorbed on the surface of the catalyst (Van Giezen 1997).

From the experimental results presented in table 4.2 and 4.3, after 7 hours exposure to reactants, a bigger drop in catalytic activity of methane conversion of Pd catalyst can be observed compared with that of Pt catalyst. For example, the drop in methane conversion for thermal ageing at 500°C is 0.51% for Pt catalyst and 5.5% for Pd catalyst. For thermal ageing at 400°C, the drop in methane conversion is 1.97% for Pt catalyst and 48.76% for Pd catalyst. This can be also explained by the Marc-Van Krevelen mechanism of methane conversion for very active catalytic sites. Due to higher activity in methane combustion of Pd catalyst, it is expected that for temperatures below 450°C, the hydroxyl groups from the water formed during the reaction to be strongly adsorbed on the very active sites of the catalyst and in consequence to block them. On the other hand, Pt catalyst is less active in methane combustion and in consequence, water will not be as much attracted to block the active sites of the catalyst.

#### 4.2.3. Bimetallic Pt-Pd (4:1) catalyst

As in the case of Pt and Pd catalysts described above, the catalytic activity of Pt-Pd (4:1) catalyst was determined from the ignition-extinction curves as well as the T50 of the light-off curve. The stability of the catalysts was determined as the changes in reactant conversion over time. For Pt-Pd (4:1) catalyst the concentration of reactants (CH<sub>4</sub>) was decreased to 4100±50 ppm.

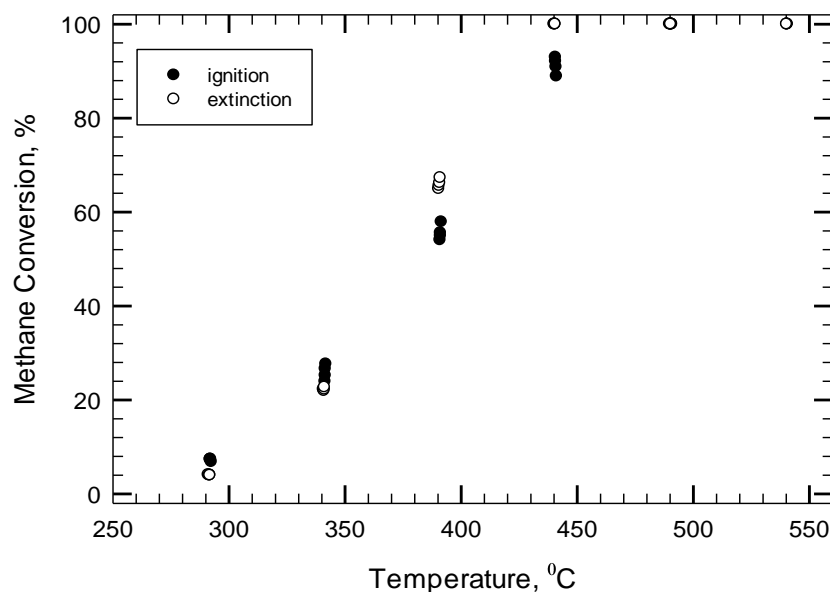


Figure 4.24. Ignition-extinction curves of methane conversion over Pt-Pd (4:1) catalyst (MI-133) (CH<sub>4</sub> 4100±50 ppm, total flow rate 235 cc/min)

The ignition-extinction results of methane conversion (methane concentration 4100±50 ppm) are presented in figure 4.2. A small positive hysteresis can be observed.

From the experimental results it can be concluded that small amounts of Pd added to Pt catalyst, increases the catalytic activity of the catalyst (T<sub>50</sub>=380°C for Pt-Pd (4:1) compared with 575°C for Pt catalyst). It is interesting to observe that the catalysts showed a higher activity for the extinction curve forming a small positive hysteresis loop, for temperatures between 500°C and 350°C.

When the ignition-extinction results of Pt-Pd (4:1) catalyst at  $4100\pm 50$  ppm and  $4700\pm 50$  ppm methane concentration (figure 4.25) are compared, a decrease in the size of the hysteresis loop can be observed. The MI-211 experimental results (CH<sub>4</sub> concentration of  $4100\pm 50$  ppm), shows a shift towards lower temperatures of the hysteresis loops. The change in size and position of the hysteresis loop is assumed to be due to difference in the concentration of methane.

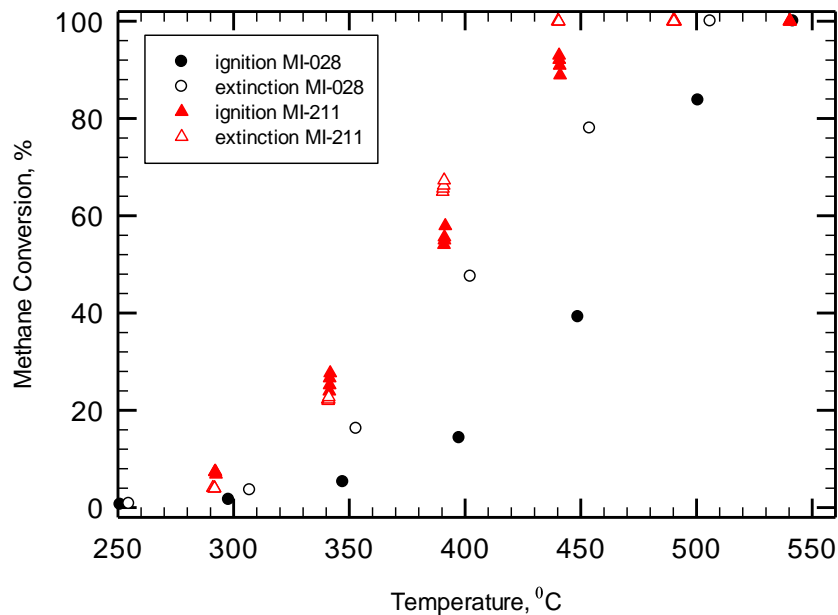


Figure 4.25. Ignition-extinction curves of methane conversion over Pt-Pd (4:1) catalyst; MI-028 CH<sub>4</sub> concentration  $4700\pm 50$  ppm; MI-211 CH<sub>4</sub> concentration  $4100\pm 50$  ppm; (total flow rate 235 cc/min)

Figure 4.26 presents results of the constant temperature thermal ageing test at 400°C. The reactor was first heated up to 440°C and then 2 GC tests were performed; the temperature of the reactor was dropped to 400°C and maintained at constant temperature for 37 hours. The experimental results show a continuous increasing trend of methane conversion.

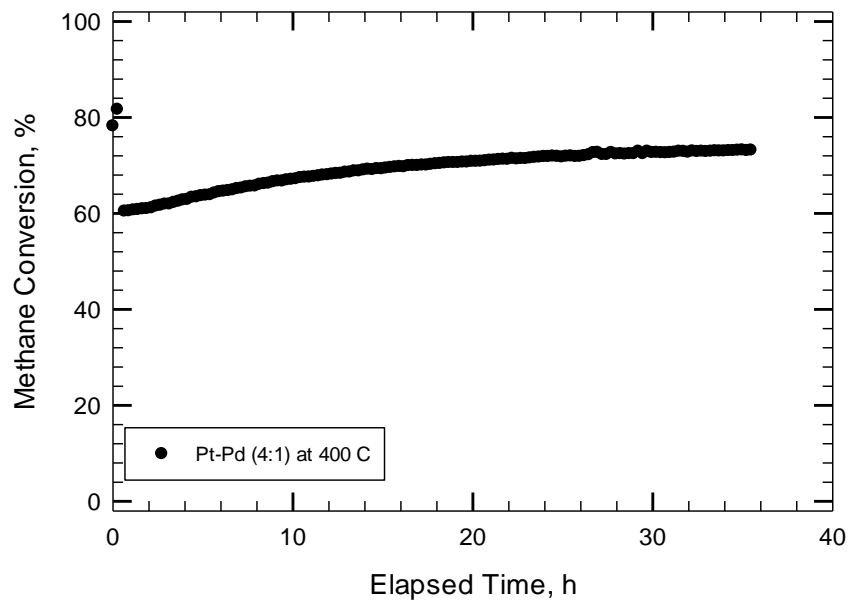


Figure 4.26. Constant temperature thermal ageing at 400°C of Pt-Pd (4:1) catalyst (CH<sub>4</sub> 4100±50 ppm, total flow rate 235 cc/min)

The same CTTAT was performed for a methane concentration of 4700±50 ppm and the results are presented in figure 4.27. It is worth mentioning that no reduction of the catalyst was performed between these tests.

A slight decrease in methane conversion can be observed for 4700±50 ppm methane concentration. However, the first activity point at 440°C is similar for both methane concentrations, which shows a very good thermal stability of the catalyst.

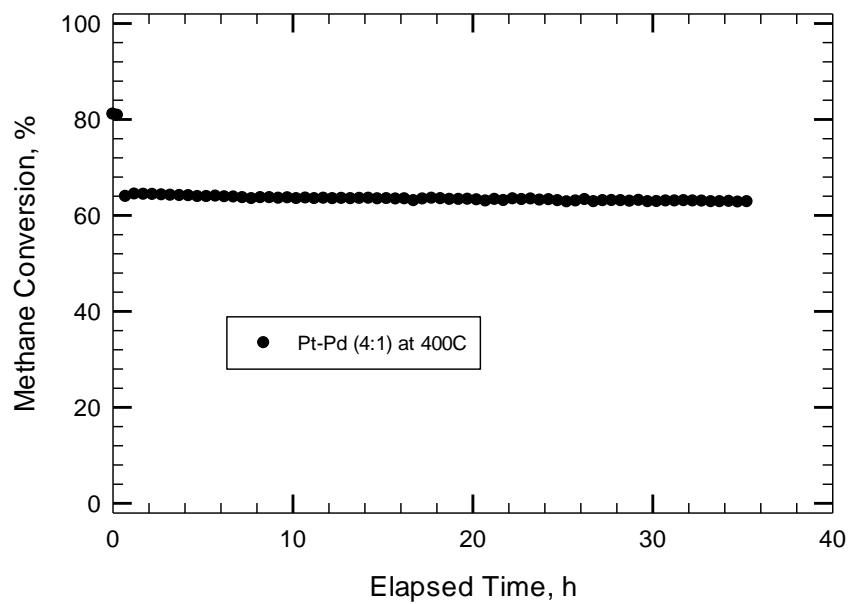


Figure 4.27. Constant temperature thermal ageing at 400°C of Pt-Pd (4:1) catalyst (MI-147) (CH<sub>4</sub> 4700±50 ppm, total flow rate 235 cc/min)

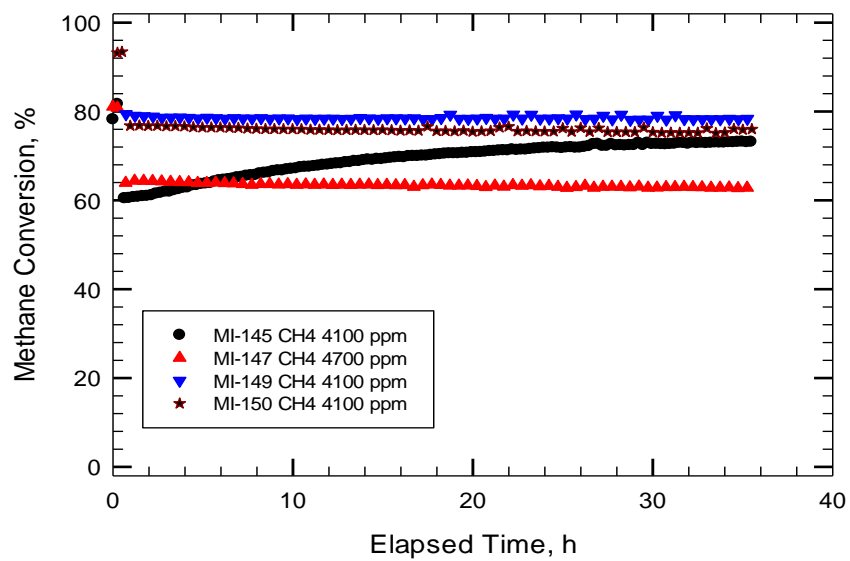


Figure 4.28. Constant temperature thermal ageing of Pt-Pd (4:1) catalyst at 400°C

The same sequence of CTTAT was repeated for the  $4100 \pm 50$  ppm methane concentration, without any reduction of the catalysts between tests. A summary of the experimental results are presented in figure 4.28. It can be observed that for a thermal ageing test of Pt-Pd (4:1) catalyst, 35 hours of thermal treatment is a good approximation (i.e. the results are constant). From the MI-147, MI-149 and MI-150 tests it can be assumed that a small difference in the concentration of methane does not affect the behaviour of the catalyst. However, higher values of methane conversion are obtained for lower methane concentrations.

## **Conclusions**

Different patterns of deactivation as a result of thermal ageing process were observed for Pt, Pd 80 and Pt-Pd 80 catalysts:

- A slight decrease in catalytic activity was observed for Pt catalyst
- A strong decrease in catalytic activity was observed for Pd 80 catalyst
- A slight increase in catalytic activity was observed for Pt-Pd (4:1) catalyst

It was therefore concluded that the addition of Pd to Pt catalyst brings an increase in the performance of the catalyst for the thermal ageing process at constant temperature.

### **4.4. Variable temperature thermal ageing test (VTTAT)**

#### **(thermal ageing $650^\circ\text{C}$ )**

A variable temperature thermal ageing test was developed to thermally age the samples at a high temperature (i.e.  $650^\circ\text{C}$ ) and measure the changes in the catalytic activity at a lower temperature.

All experiments were performed using 4100 ppm methane in extra dry air stream. When water was added to the gas stream, it comprised about 5% by volume of the feed stream.

An ignition-extinction test was performed to assess the activity of the catalyst.

A variable temperature thermal ageing test was performed to monitor the changes in the catalytic activity as a function of thermal treatment.

Another ignition-extinction test was performed to assess the changes in the catalytic activity during the VTTAT. For some sequences, the activity of the catalyst was also assessed in presence of water.

#### 4.4.1. Pt catalyst

Figure 4.29 compares the ignition-extinction results of methane conversion of Pt catalyst before (MI-199) and after (MI-201) the thermal ageing test, as well as in the presence of water (MI-202).

The change in the catalytic activity as a function of thermal ageing and water effect was assessed from the ignition-extinction curves presented in figure 4.29.

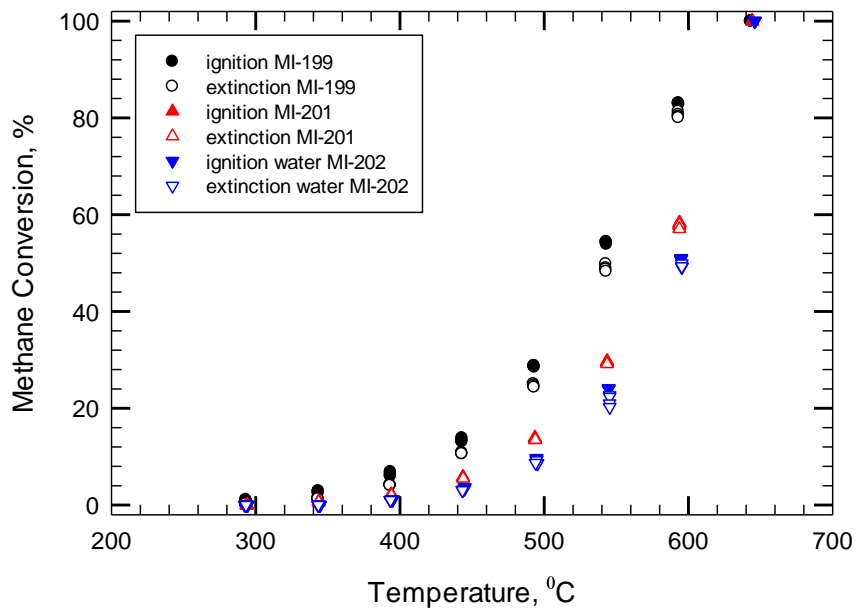


Figure 4.29. Ignition-extinction curves of methane conversion of Pt catalyst (CH<sub>4</sub> 4100±50 ppm; total flow rate 235 cc/min)

The presence of a small negative hysteresis loop can be observed for the initial ignition-extinction cycle. However, after the thermal ageing, no hysteresis loop was observed for the ignition-extinction curves. 100% of methane conversion was obtained at 650°C for all three ignition-extinction cycles.

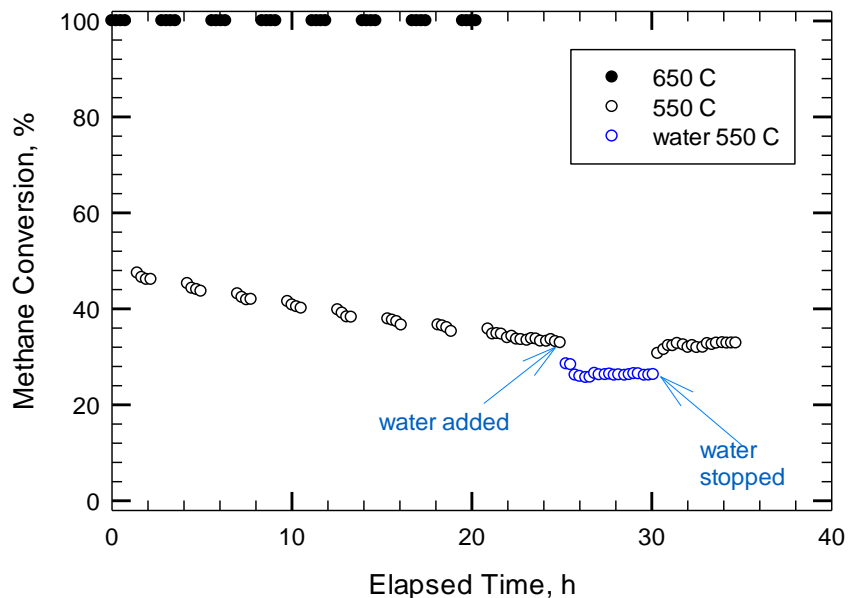


Figure 4.30. Variable temperature thermal ageing test of methane conversion over Pt catalyst (MI-200) (CH<sub>4</sub> 4100±50ppm, 5% vol. water, total flow rate 235 cc/min)

A variable temperature thermal ageing test was performed for Pt catalyst: the sample was thermally aged at 650°C and the changes in catalytic activity were measured at 550°C. From figure 4.30 it can be observed that the initial conversion was about 48% at the beginning of the first 550°C interval. Activity declines during each interval of 550°C. The activity after 20 hours was 37% conversion and decreased to about 34% conversion after 5 hours. When water was added to the reactant stream, the activity dropped to 26%, where it stayed constant for around 5 hours. When the water was switched off the activity returned to 34%.

#### 4.4.2. Pd 150 catalyst

##### Variable temperature thermal ageing test at 350 C

The same sequence of experiments as for Pt catalyst was performed for Pd 150 catalyst: ignition-extinction cycle (MI-254), followed by the variable temperature thermal ageing test (MI-255), an ignition-extinction test to evaluate the changes in catalytic conversion (MI-256), as well as an ignition-extinction cycle in presence of water (MI-257).

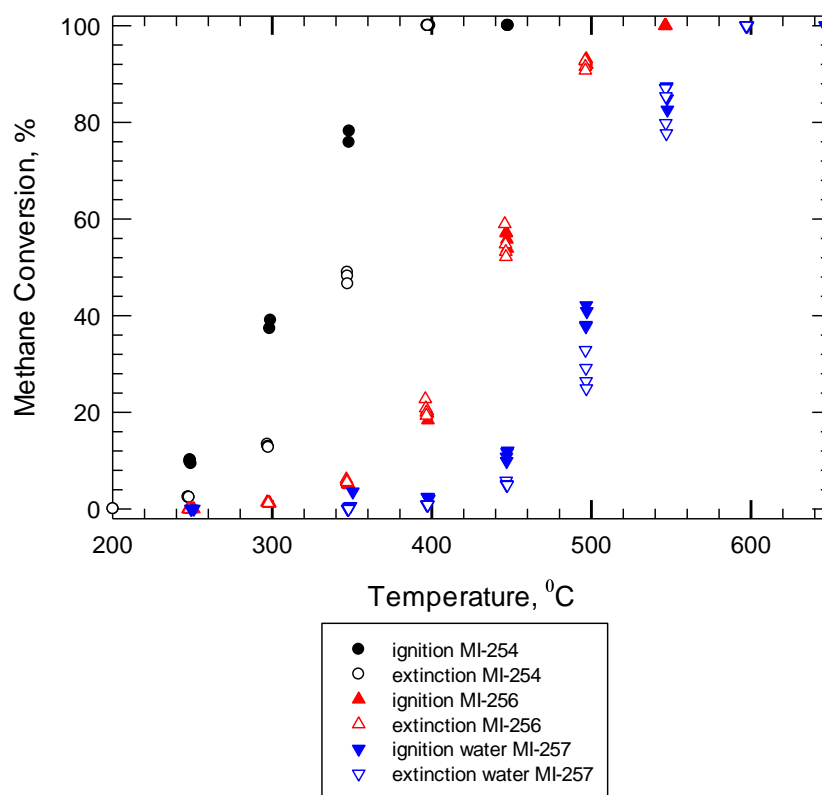


Figure 4.31. Ignition-extinction curves of methane conversion over Pd 150 catalyst: before VTTAT (MI-254), after VTTAT (MI-256) and in presence of water (MI-257) (CH<sub>4</sub> 4100±50 ppm, total flow rate 235 cc/min)

Figure 4.31 compares the ignition-extinction results of methane conversion of Pd 150 catalyst before and after the thermal ageing test, as well as in the presence of water. For the first ignition-extinction cycle (MI-254) a large negative hysteresis loop can be observed and T50 was 315°C. However, after the thermal ageing test, no hysteresis loop was observed. A deactivation, shift toward higher temperatures can be observed for the ignition-extinction curves after the thermal ageing test or as a result of water effect. T50 increases from 315 C (MI-254) to 445°C (MI-256) and 520 C (MI-257) which highlights the decrease in activity as a result of thermal ageing and water effect.

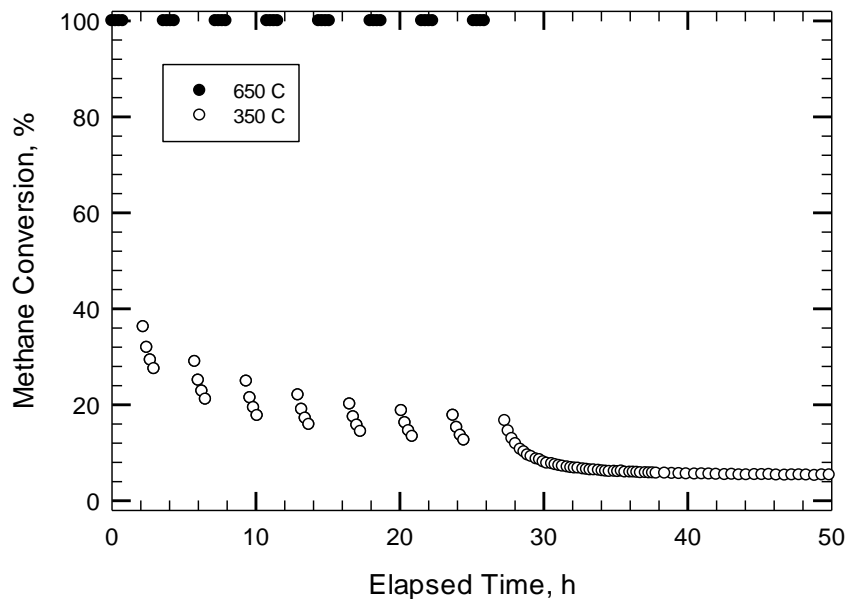


Figure 4.32. Variable temperature thermal ageing test of methane conversion of Pd 150 catalyst (CH<sub>4</sub> 4100±50 ppm, total flow rate 235 cc/min)

Figure 4.32 presents the experimental results of variable temperature thermal ageing test. It can be observed that the activity of the first 350°C interval is about 37% conversion and drops to 26 % conversion. This trend can be observed for each 350°C interval. After 28 hours of thermal ageing, the activity drops to 12% conversion of methane. An interesting observation is that the activity at the

beginning of each 350°C interval is higher than the activity at the end of the previous 350°C interval. After 28 hours of thermal ageing, the temperature was held at 350°C and the activity drops, stabilizing at around 5% conversion.

The decrease in activity of the 350°C intervals can be assumed to be due to the water formed during the reaction which is adsorbed on the active sites of the catalyst (Zhu, G. et al. 2005). Zhu, G. determined the kinetics of methane conversion over Pd catalyst for different temperatures and concluded that for temperatures as low as 325°C the water present in reactor will be adsorbed on the active sites of the catalyst. For higher temperatures (above 540°C) Zhu, G. found that the effect of water on the catalytic activity to disappear.

#### *Variable temperature thermal ageing test at 350 C (water)*

A similar sequence of experiments as previously described was performed for the Pd 150 catalyst, except water was added in the end of varied temperature thermal ageing test: ignition-extinction cycle (MI-258), followed by the variable temperature thermal ageing test (MI-259), an ignition-extinction test to evaluate the changes in catalytic conversion (MI-260).

Figure 4.33 compares the experimental results of ignition-extinction curves before (MI-258) and after (MI-260) thermal ageing test. A small negative hysteresis can be observed for the first ignition-extinction curve and 100% conversion of methane was obtained at 400°C. T50 value for the light off curve was 315°C. However, after the thermal ageing tests, the activity of the catalysts was shifted toward higher temperatures (i.e. the conversion of methane at 400°C before the thermal ageing test was 100 % and after the thermal ageing test was 18 %). 100% conversion of methane was obtained at 550°C. T50 was 425°C.

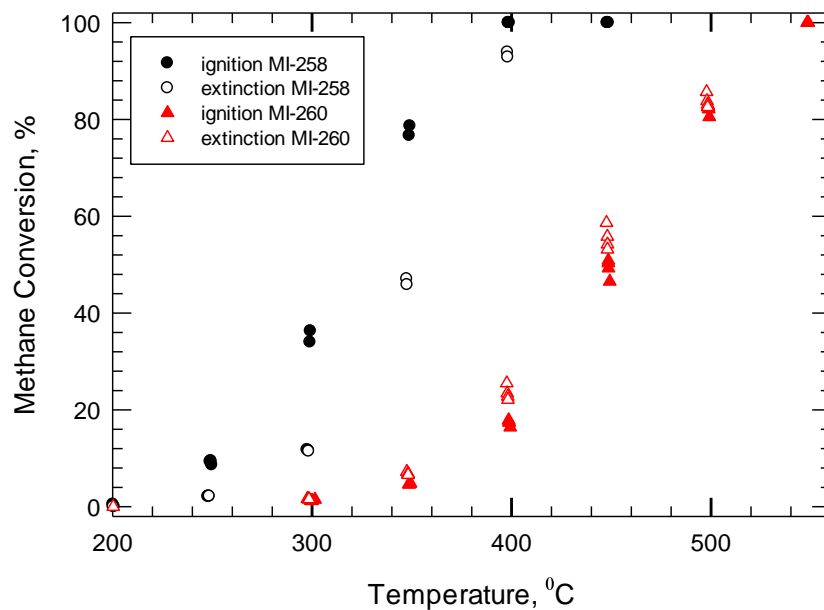


Figure 4.33. Ignition-extinction curves of methane conversion of Pd 150 catalyst: before VTTAT (MI-258) and after VTTAT (MI-260) (CH<sub>4</sub> 4100±50 ppm, total flow rate 235 cc/min)

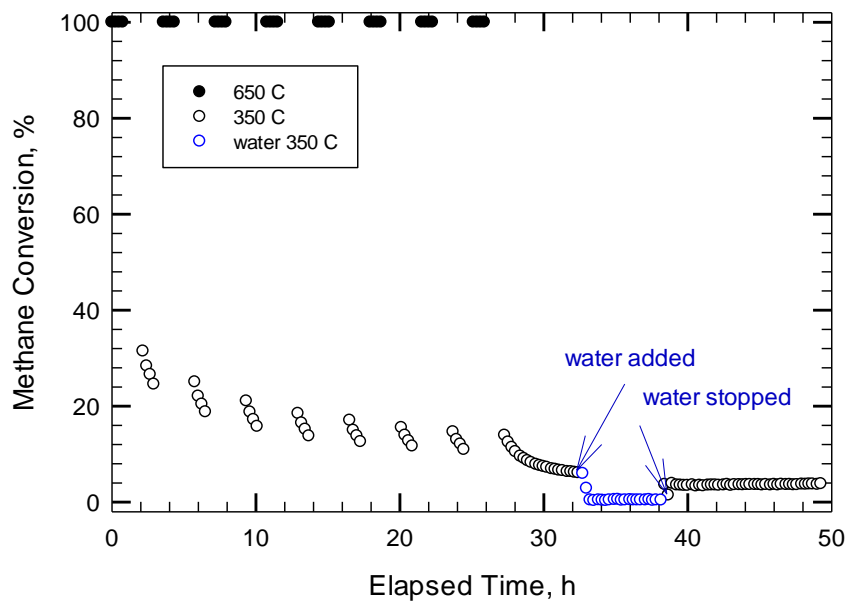


Figure 4.34. Variable temperature thermal ageing test of methane conversion of Pd 150 catalyst (MI-259) (CH<sub>4</sub> 4100±50 ppm, 5% vol water, total flow rate 235 cc/min)

Figure 4.34 presents the experimental results of variable temperature thermal ageing test. It can be observed that the results are very similar with the one performed in the absence of water: the first 350°C activity is about 32% conversion, and falls to 10% conversion after 28 hours of thermal ageing. A similar behavior is observed for the activity of each 350°C interval: the activity in the beginning of the interval is higher than the activity at the end of the previous 350°C interval. When water is added to the system, the activity sharply drops from 7% to almost zero % conversion of methane. When the water is stopped the activity sharply increases to 4% methane conversion. The activity of the catalyst slightly decreases from 4% conversion to 3% conversion, after the water was stopped.

Figure 4.35 presents the comparisons between the two varied temperature thermal ageing tests for Pd 150 catalyst.

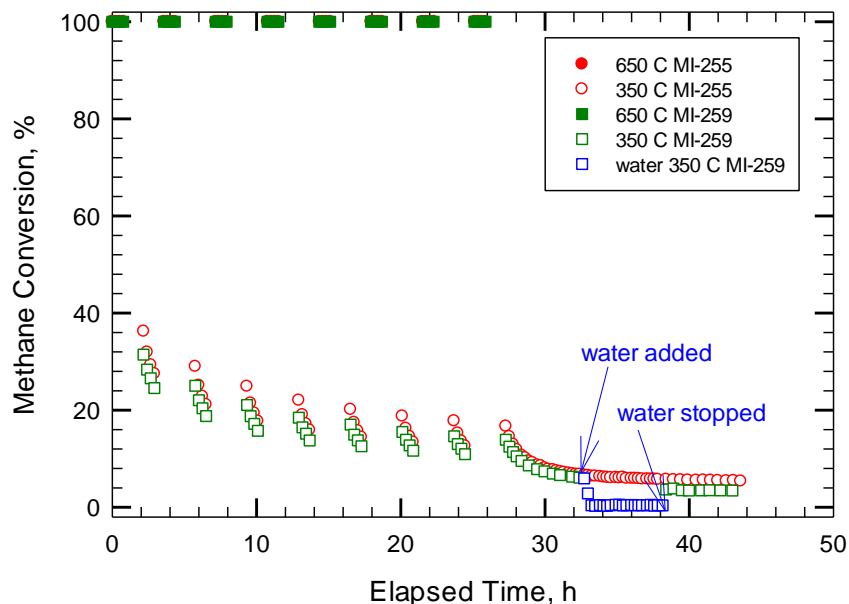


Figure 4.35. Comparison of varied temperature thermal ageing tests of methane conversion over Pd 150 catalyst: MI-255 vs. MI-259 (CH<sub>4</sub> 4100±50ppm, 5% vol. water, total flow rate 235 cc/min)

*Variable temperature thermal ageing test at 450°C*

Due to low results of methane conversion obtained for VTTA test at 350°C, another VTTA test sequence was performed at 450°C, following the same sequence described in the previous experiment: ignition-extinction cycle (MI-268), a variable temperature thermal ageing test (MI-269), an ignition-extinction test to evaluate the changes in catalytic conversion (MI-270).

From figure 4.36 compares the ignition-extinction curves of methane conversion of Pd 150 catalyst before and after the thermal ageing test. It can be observed that for the first ignition-extinction cycle, 100% conversion of methane was obtained at 400°C. The presence of a large negative hysteresis can also be observed. T50 for the light-off curve was 312°C. After the thermal ageing test, 100% conversion of methane was obtained at 550°C and T 50 for the light off curve was 440°C.

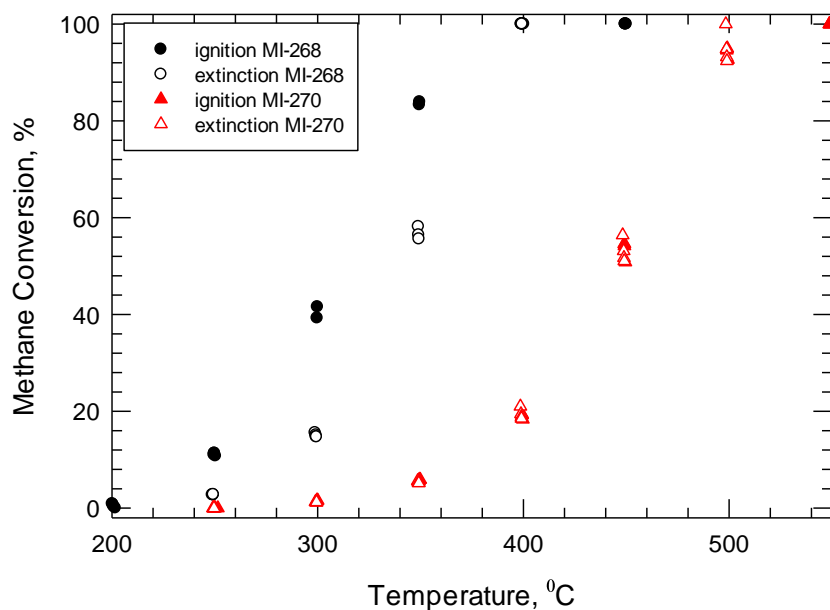


Figure 4.36. Ignition-extinction curve for methane conversion for Pd 150 catalyst: before VTTAT (MI-268) and after VTTAT (MI-270) (CH<sub>4</sub> 4100±50 ppm, total flow rate 235 cc/min)

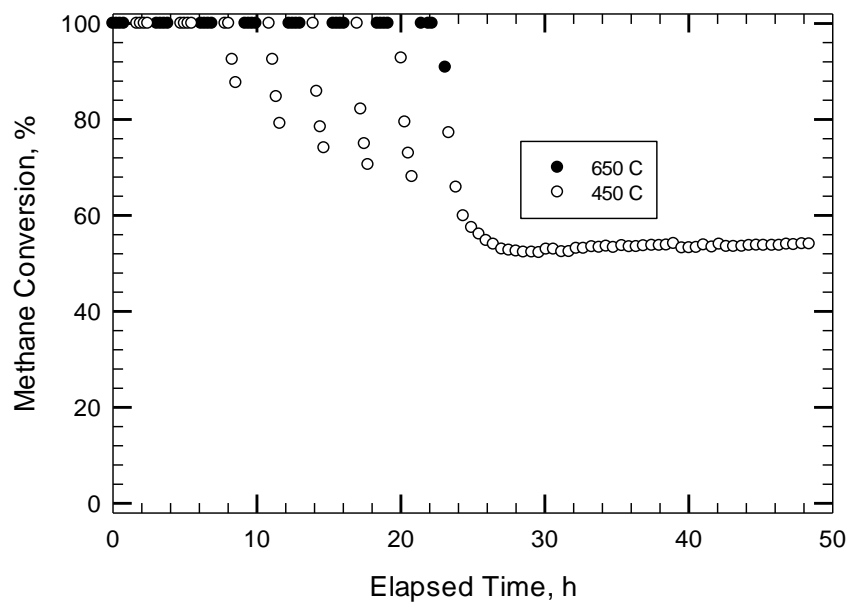


Figure 4.37. Variable temperature thermal ageing test of methane conversion over Pd 150 catalyst (MI-269) (CH<sub>4</sub> 4100±50 ppm, total flow rate 235 cc/min)

Figure 4.37 presents the experimental results of methane conversion of Pd 150 catalyst for the variable temperature thermal ageing test. It can be observed that the conversion of methane of the 450°C intervals follows the same pattern as the 350°C intervals (figure 4.35), i.e. the activity drops during the 450°C interval. However, the drop in activity during 450°C interval is more dramatic than during the thermal ageing of 350°C intervals. As is it expected from the catalytic activity assessment (figure 4.36), the activity at the beginning of the first 450°C is 100%. However, after 8 hours of thermal ageing, the activity at 450°C starts to decrease. As in the previous thermal ageing tests of Pd 150 catalyst, the activity at the beginning of each 450°C interval is higher than the end activity of the previous 450°C interval. After 24 hours of thermal ageing, holding the temperature at 450°C leads to a slight increase in activity from 52 % conversion to around 54% conversion.

For the 450°C drop in activity it can be assumed that the water formed during the reaction is adsorbed and blocks the most active sites of the catalyst. When the temperature is increased to 650°C, the adsorbed water is removed and 100% of methane was obtained. However, during the last interval of 650°C a tendency in activity drop can be observed.

Figure 4.38 compares the experimental results of variable temperature thermal ageing test performed at 350°C and 450°C. A big difference in catalytic activity as a function of temperature can be observed.

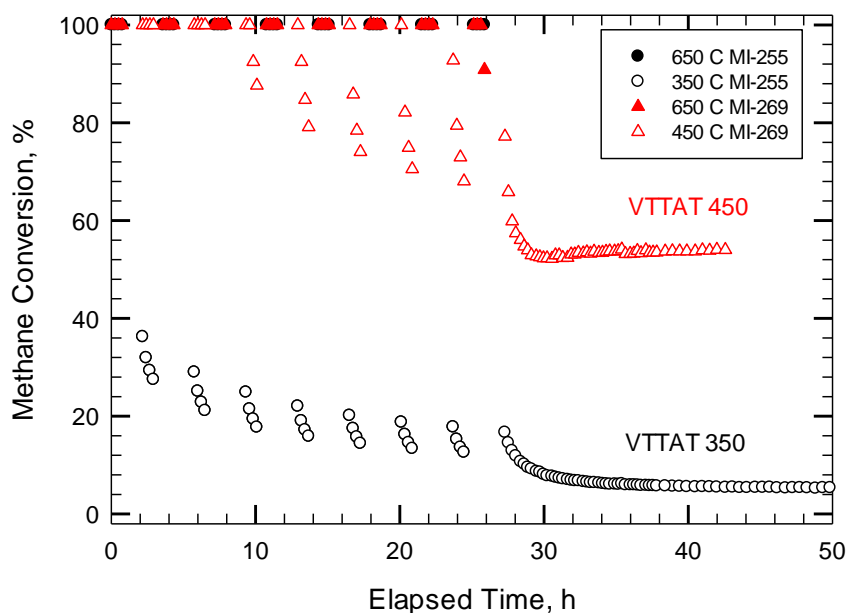


Figure 4.38. Variable temperature thermal ageing test of methane conversion of Pd 150 catalyst at 350°C (MI-255) and 450°C (MI-269) (CH<sub>4</sub> 4100±50 ppm, total flow rate 235 cc/min)

#### 4.4.3. Pt-Pd (4:1) catalyst

The same sequence of experiments as for Pt catalyst was performed for Pt-Pd (4:1) catalyst: ignition-extinction cycle (MI-211), followed by the variable temperature thermal ageing test (MI-212), an ignition-extinction test to evaluate the changes in catalytic conversion (MI-213), as well as an ignition-extinction cycle in presence of water (MI-214).

Figure 4.39 compares the experimental results of ignition-extinction curves before (MI-211) and after (MI-213) thermal ageing as well as in the presence of water (MI-214). A small negative hysteresis loop was formed by the initial ignition-extinction curves, similar with figure 4.24. 100% conversion of methane was obtained at 500°C and T50 was 380°C. The strong effect of water on the catalytic activity of Pt-Pd (4:1) catalyst can be observed by the shift toward higher temperatures of the ignition-extinction curves. The presence of positive hysteresis loops were observed in absence of water, while a negative hysteresis loop was observed in presence of water. In presence of water, 90 % conversion of methane was obtained at 650°C. T50 was 460°C.

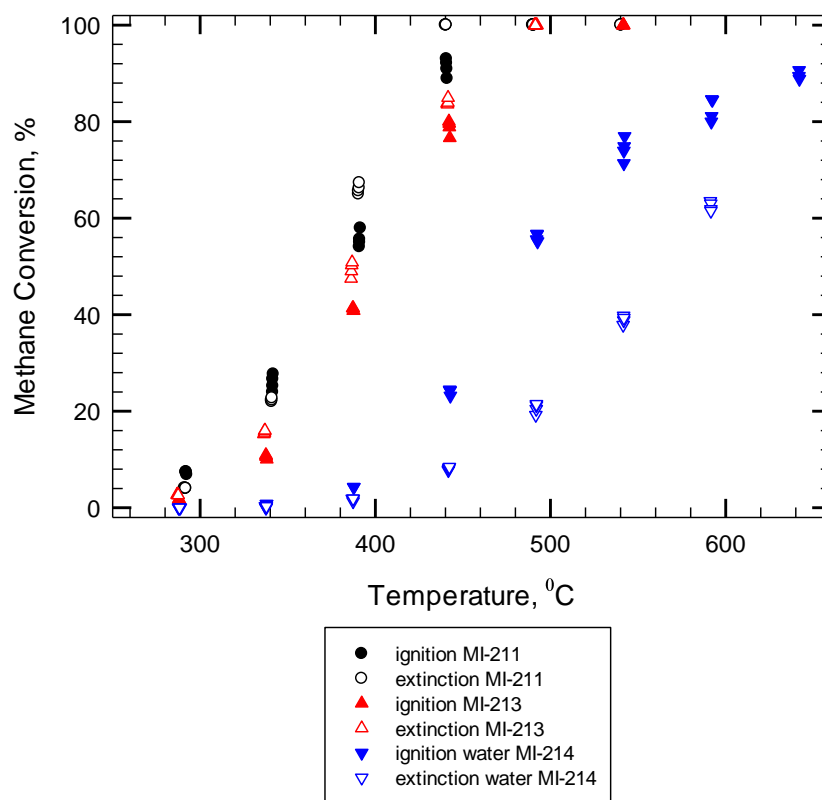


Figure 4.39. Ignition-extinction curve of methane conversion of Pt-Pd (4:1) catalyst: before VTTAT (MI-211), after VTTAT (MI-213) and in presence of water (MI-214) (CH<sub>4</sub> 4100±50 ppm, total flow rate 235 cc/min)

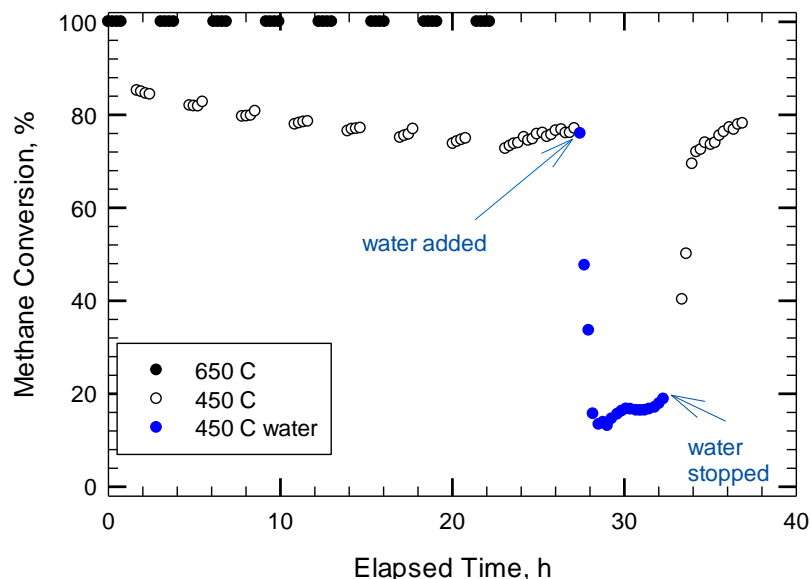


Figure 4.40. Variable temperature thermal ageing test (VTTAT) of methane conversion of Pt-Pd (4:1) catalyst (MI-212) (CH<sub>4</sub> 4100±50 ppm, 5% vol. water, total flow rate 235 cc/min)

The experimental results for VTTA test are presented in figure 4.40. The first activity point at 450°C was about 85%. The activity decreased over the course of the thermal ageing to about 72% after 22 hours. During each 450°C interval, a small increase in activity can be observed. After 22 hours, the catalyst was held at 450°C and the activity increased to about 77%. The activity dropped to 17% conversion in presence of water. The big drop in catalytic activity can be assumed to be due to Pd sensitivity to water deactivation. However after water was switched off, the activity increased to 70% initially, but rose over 5 hours to about 80%.

#### 4.4.4. Pt-Pd (1:5) catalyst

The same sequence of experiments as for Pt catalyst was performed for Pd-Pd (1:5) catalyst: ignition-extinction cycle (MI-221), variable temperature thermal ageing test (MI-222), an ignition-extinction test to evaluate the changes in

catalytic conversion (MI-223), as well as an ignition-extinction cycle in presence of water (MI-224).

Figure 4.41 compares the ignition-extinction curves before (MI-221) and after (MI-223) thermal ageing as well as in the presence of water (MI-224). A small negative hysteresis can be observed for the first ignition-extinction cycle. 100% conversion of methane was obtained at 350°C. T50 was 305°C. A small decrease in catalytic conversion can be observed after thermal ageing (MI-223). This is assumed to be due to the presence of Pt catalyst. 100% of methane conversion was obtained at 400°C and T50 was 355°C. The strong effect of water on the catalytic activity of Pt-Pd (1:5) catalyst can be observed from the decrease in the catalytic activity (MI-224). 100% conversion was obtained at 450°C. T50 was 385°C.

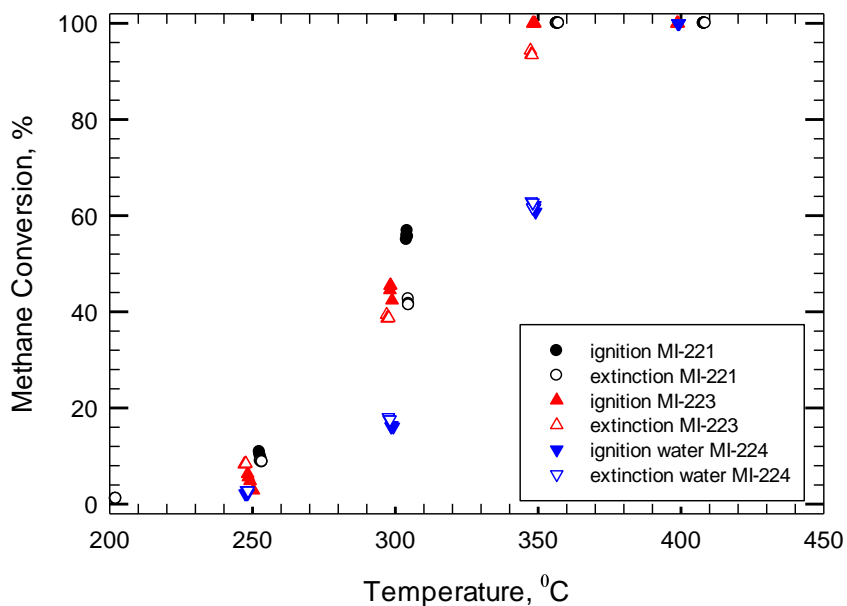


Figure 4.41. Ignition-extinction curve of methane conversion of Pt-Pd (1:5) catalyst: before VTTAT (MI-221), after VTTAT (MI-223) and in the presence of water (MI-224) (CH<sub>4</sub> 4100±50 ppm, 5% mol water, total flow rate 235 cc/min)

From the first ignition-extinction cycle of methane conversion for Pt-Pd (1:5) catalyst, the temperature for measuring the activity for the VTTA test was 300°C. The first activity point at 300°C was about 48% conversion (figure 4.42). Activity drops during each 300°C interval. Similarly as for Pd 150 catalyst, the activity at the beginning of each 300°C interval is higher than the end activity of the previous 300°C interval. This behaviour is assumed to be due to catalyst composition (predominantly Pd). After 26 hours of thermal ageing, the catalyst was held at 300°C and the activity continued a slow decline.

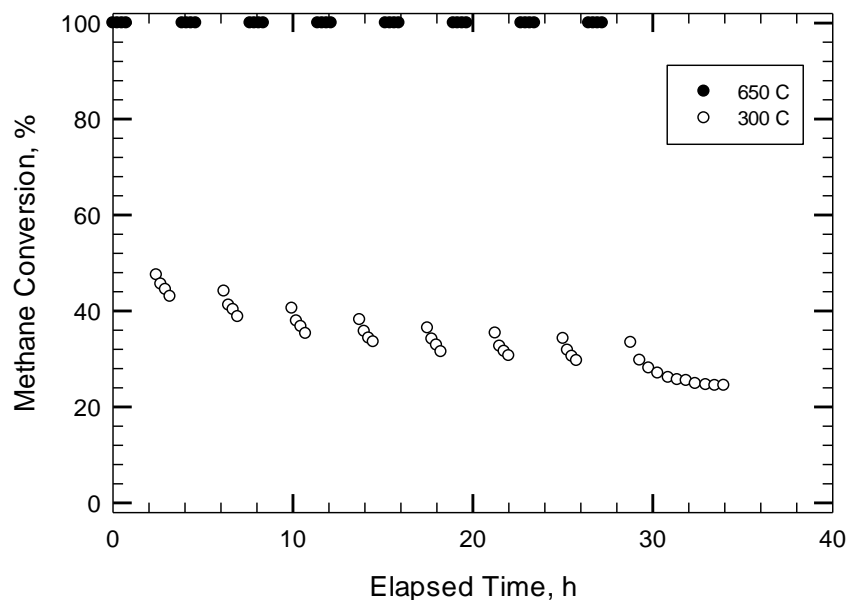


Figure 4.42. Variable temperature thermal ageing test of methane conversion of Pt-Pd (1:5) catalyst (MI-222) (CH<sub>4</sub> 4100±50 ppm, total flow rate 235 cc/min)

#### *Variable temperature thermal ageing 350°C*

The same sequence of experiments as above was performed for thermal ageing at 650°C, with catalytic activity measured at 350°C: ignition-extinction cycle (MI-232), variable temperature thermal ageing test (MI-233), and ignition-extinction test to evaluate the changes in catalytic conversion (MI-234).

A small negative hysteresis can be observed from the first ignition-extinction cycle. 100% conversion of methane was obtained at 350°C. T50 for the light off curve was 305°C. No hysteresis was observed after the thermal ageing. 100% conversion of methane was obtained at 400°C and T50 was 335°C.

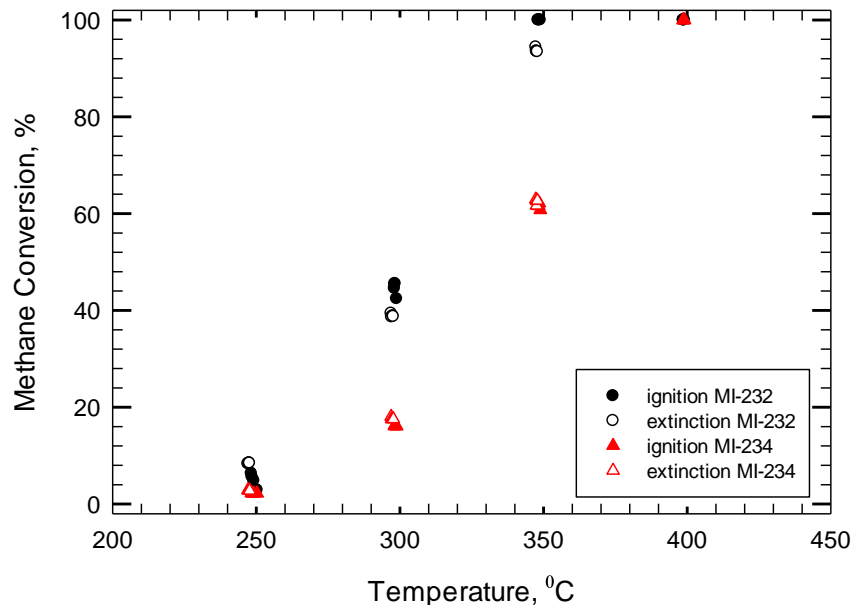


Figure 4.43. Ignition-extinction curves of methane conversion of Pt-Pd (1:5) catalyst: before VTTAT (MI-232) and after VTTAT (MI-234) (CH<sub>4</sub> 4100±50 ppm, total flow rate 235 cc/min)

The variable temperature thermal ageing test at 350°C is presented in figure 4.44 shows a similar behavior as thermal ageing test at 300°C. The activity drops during each 350°C interval. The first activity point at 350°C was about 93% conversion and the activity decreased to 88% conversion. Similar as for Pd 150 catalyst, the activity at the beginning of each 350°C interval is higher than the end activity of the previous 350°C interval. After 26 hours of thermal ageing, the catalyst was held at 350°C and the activity continued a slow decline. After 32 hours 5% vol. of water was added to the gas stream. The activity dropped from 66% conversion to 10% conversion of methane. This is assumed to be due to the

strong effect of water on the Pd. However, after the water was switched off, the activity jumped to 59% conversion and continued slowly to increase.

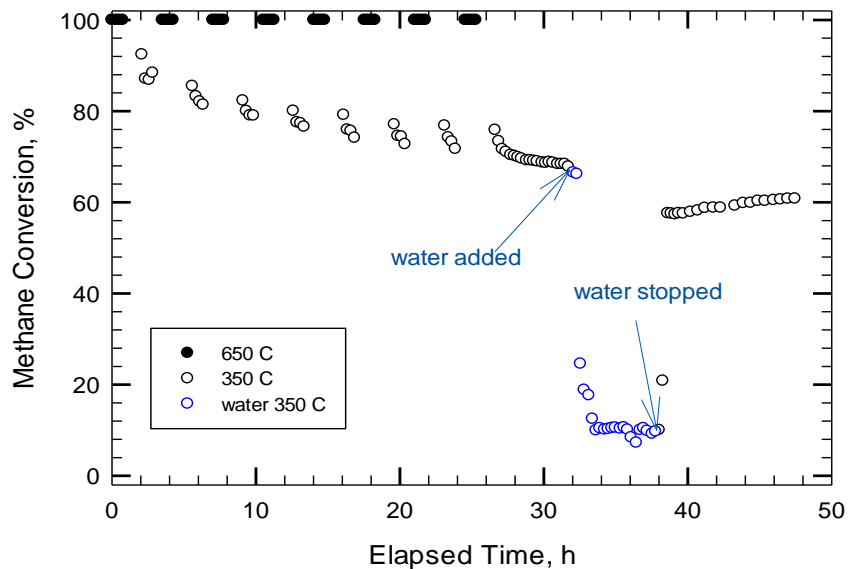


Figure 4.44. Variable temperature thermal ageing test for methane conversion over Pt-Pd (1:5) catalyst (MI-233) (CH<sub>4</sub> 4100±50 ppm, total flow rate 235 cc/min)

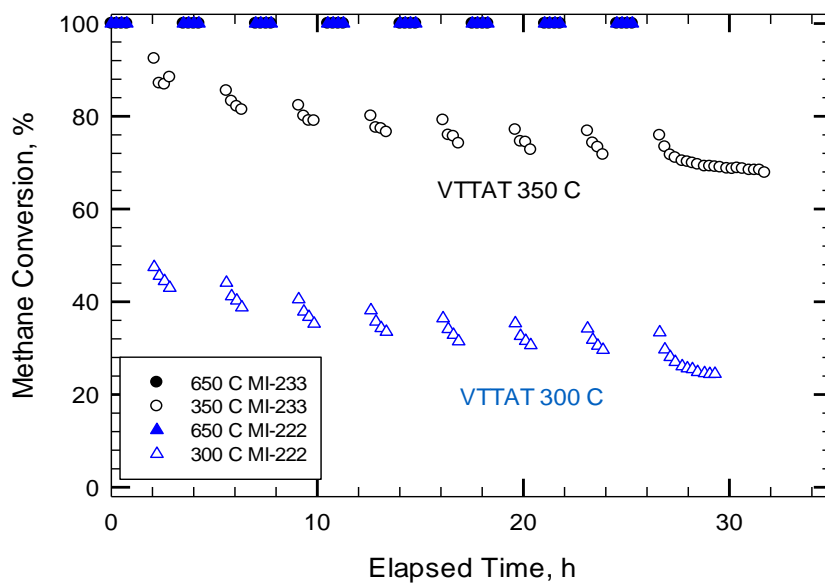


Figure 4.45. Variable temperature thermal ageing test at 350°C (MI-233) vs 300°C (MI-222) (CH<sub>4</sub> 4100±50 ppm, total flow rate 235 cc/min)

Figure 4.45 compares the experimental results of VTТА test at 350°C and at 300°C. It is interesting to observe the difference in catalytic activity as a function of temperature measurement (i.e. 93% conversion of methane was obtained at 350°C compared with 49% conversion, obtained at 300°C), although the behavior is very similar.

## Conclusions

### *Contribution of Pd to the activity of Pt catalyst*

The initial activity of 4 catalysts is compared in figure 4.46: Pt, Pd 150, Pt-Pd (4:1) and Pt-Pd (1:5).

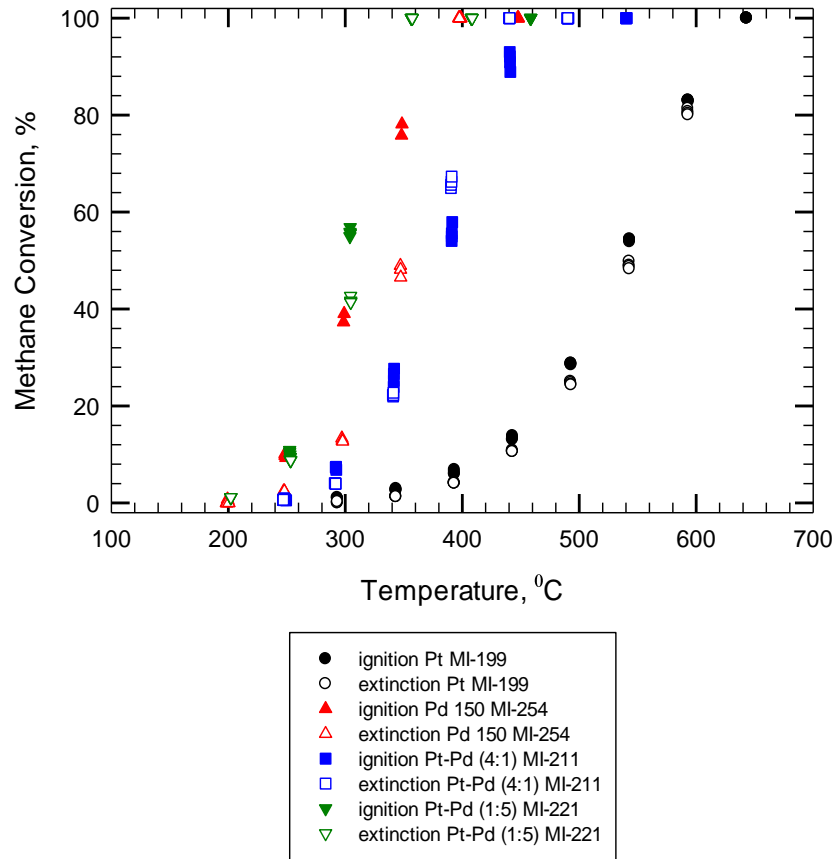


Figure 4.46. Ignition-extinction curves for Pt (MI-199), Pd 150 (MI-254), Pt-Pd (4:1) (MI-211) and Pt-Pd (1:5) (MI-221) catalysts (CH<sub>4</sub> 4100±50 ppm, total flow rate 235 cc/min)

It can be observed that Pd 150 and Pd predominantly catalysts show the highest activity in methane conversion. It can also be observed that all catalysts show a negative hysteresis except the predominantly Pt bimetallic catalyst (Pt-Pd (4:1)).

Figure 4.47 compares the activity of the 4 catalysts after thermal ageing. It can be observed that both bimetallic catalysts Pt-Pd (1:5) and Pt-Pd (4:1) show better resistance to thermal ageing deactivation compared with Pd 150 catalyst. It can be concluded that for methane conversion both Pt-Pd bimetallic catalysts possess good activities and resistance to thermal deactivation.

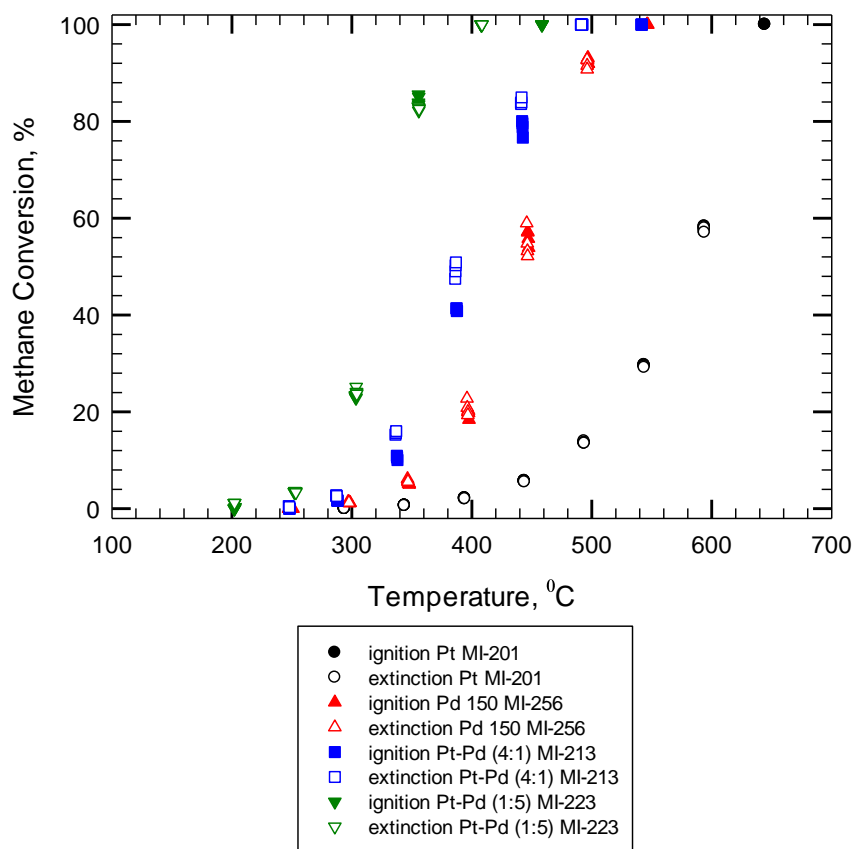


Figure 4.47. Ignition-extinction of methane conversion after variable temperature thermal ageing test for Pt (MI-201), Pd 150 (MI-256), Pt-Pd (4:1) (MI-213) and Pt-Pd (1:5) (MI-223) catalysts (CH<sub>4</sub> 4100±50 ppm, total flow rate 235 cc/min)

### Contribution of Pt catalyst to the stability of bimetallic catalysts

The influence of Pt on the stability of Pd catalyst can be highlighted by comparing the results of variable temperature thermal ageing test. Figure 4.48 compares the results of variable temperature thermal ageing test at 350°C of Pd 150 and Pt-Pd (1:5) catalysts. It can be observed that for the 350°C intervals, the Pt-Pd (1:5) catalysts shows a higher activity compared with Pd 150 catalyst. When water is added to the reactant stream, the bimetallic Pt-Pd (1:5) catalyst shows a better resistance to water deactivation, i.e. 10% conversion of methane for Pt-Pd (1:5) catalyst, compared with zero % conversion of methane for Pd 150 catalyst.

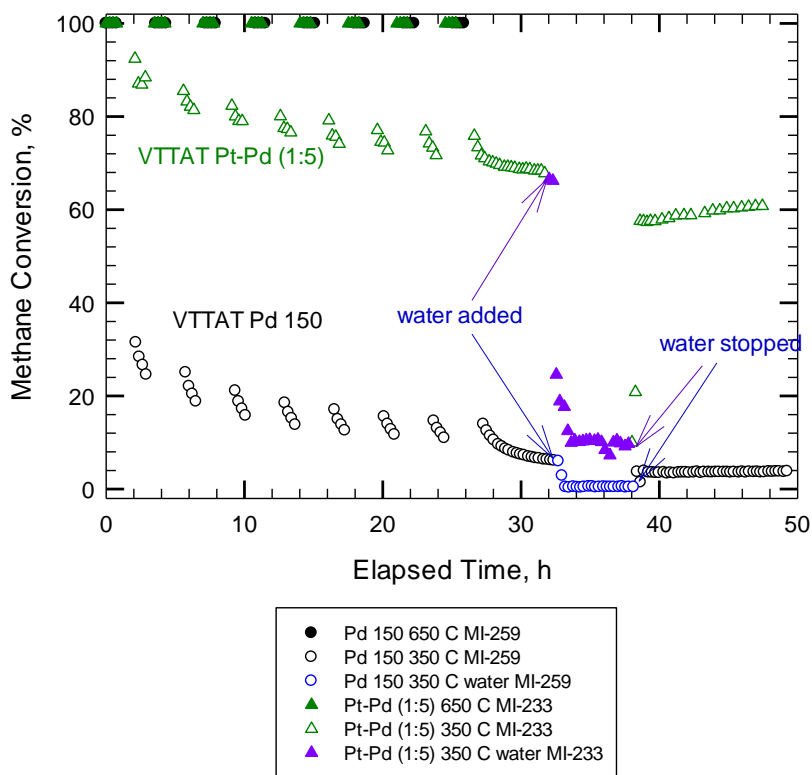


Figure 4.48. Variable temperature thermal ageing test at 350 C of methane conversion of Pd 150 (MI-259) and Pt-Pd (1:5) (MI-233) catalyst (CH<sub>4</sub> 4100±50 ppm, 5% vol. water, total flow rate 235 cc/min)

Figure 4.49 compares the experimental results of variable temperature thermal ageing test at 450°C of Pt-Pd (4:1) and Pd 150 catalysts. It can be observed that the conversion of methane for Pt-Pd (4:1) catalyst is lower for the first 450°C intervals compared with the activity of Pd 150 catalyst. This is assumed to be due to the high presence of Pt catalyst. However, after 10 hours of treatment, the activities of Pd 150 and Pt-Pd (4:1) catalysts become similar and after 15 hours of treatment, the activity of predominantly Pt catalyst becomes higher. This is assumed to be due to the better resistance to water deactivation of predominantly Pt catalyst.

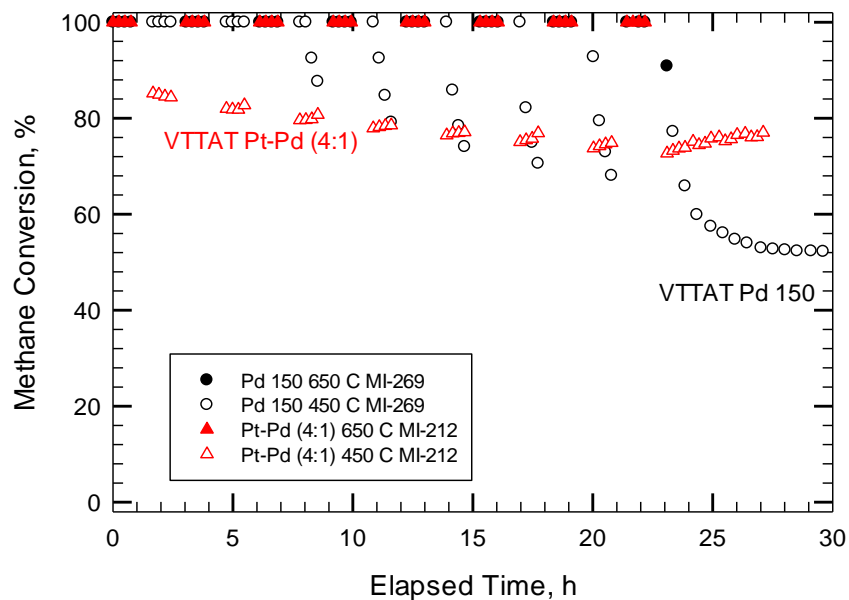


Figure 4.49. Variable temperature thermal ageing test for Pd 150 and Pt-Pd (4:1) catalyst (CH<sub>4</sub> 4100±50 ppm, total flow rate 235 cc/min)

## 4.5. Hydrothermal ageing

The process of hydrothermal ageing of a catalyst is used to assess the ability of a catalyst to maintain its activity over time in presence of wet feed. It is well known that water may accelerate the process of sintering of particles, which contributes to decrease in the catalytic activity of a catalyst (Van Giezen, G. C., 1997).

The first ignition-extinction cycle, used to assess the activity of the catalyst, was always performed in the absence of water.

The evaluation of hydrothermal stability of Pt, Pd and Pt-Pd (4:1) catalysts was performed in presence of reactants and water added to the gas stream, at constant temperatures (constant temperature hydrothermal ageing test) or variable temperature (variable temperature hydrothermal ageing test) (CH<sub>4</sub> 4700±50 ppm, 235 cc/min, water 5% by volume of the feed stream).

### 4.5.1. Constant temperature hydrothermal ageing test (CTHAT)

In the constant temperature hydrothermal test, the reactor was heated up at the desired temperature. After a few tests in absence of water, the water was switched on and the reactor was kept at constant temperature for extended time.

#### 4.5.1.1. Pt catalyst

The catalytic activity was determined from the ignition-extinction curves. The stability of the catalyst was evaluated from the changes in reactant conversion over time.

Figure 4.50 presents the ignition-extinction curves of methane conversion of Pt catalyst (MI-163). 100% conversion of methane was obtained at 650°C. A small negative hysteresis can be observed (ignition more active than extinction). T<sub>50</sub> was 540°C.

Figure 4.51 presents the summary of the experimental results of constant temperature hydrothermal ageing test (CTHTAT).

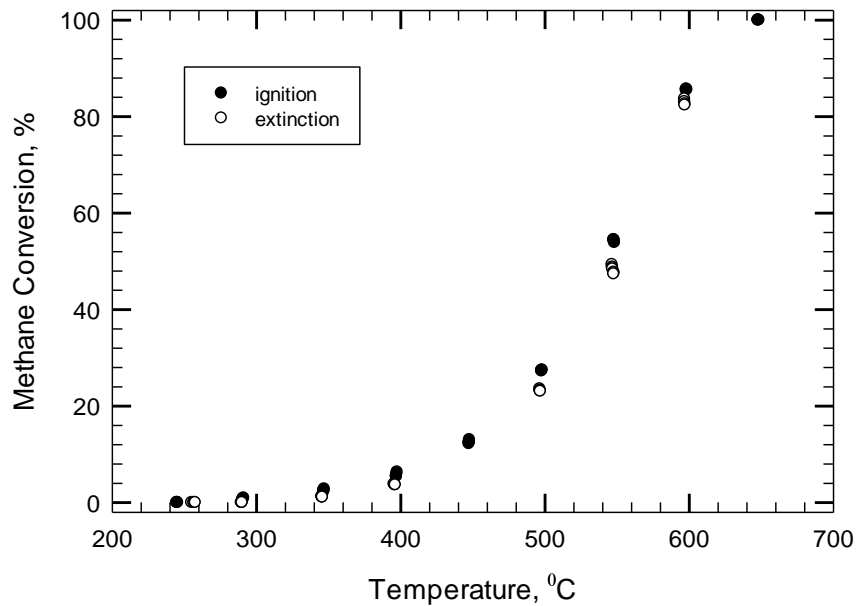


Figure 4.50. Ignition-extinction curve for methane conversion for Pt catalyst (CH<sub>4</sub> 4100 ppm, total flow rate 235 cc/min)

Two important observations can be drawn from figure 4.51:

-The effect of water on the activity of the catalyst decreases as the temperature of the catalysts increase (550°C compared with 650°C). As previously mentioned, for temperature above 450°C the hydroxyl groups from water are more likely to participate in the reaction of methane than to be adsorbed and block the active sites of the catalyst.

-the lower the temperature of reaction, the stronger the effect of water on the catalytic activity (the drop in the conversion of methane is more pronounced), i.e. 600°C compared with 550°C.

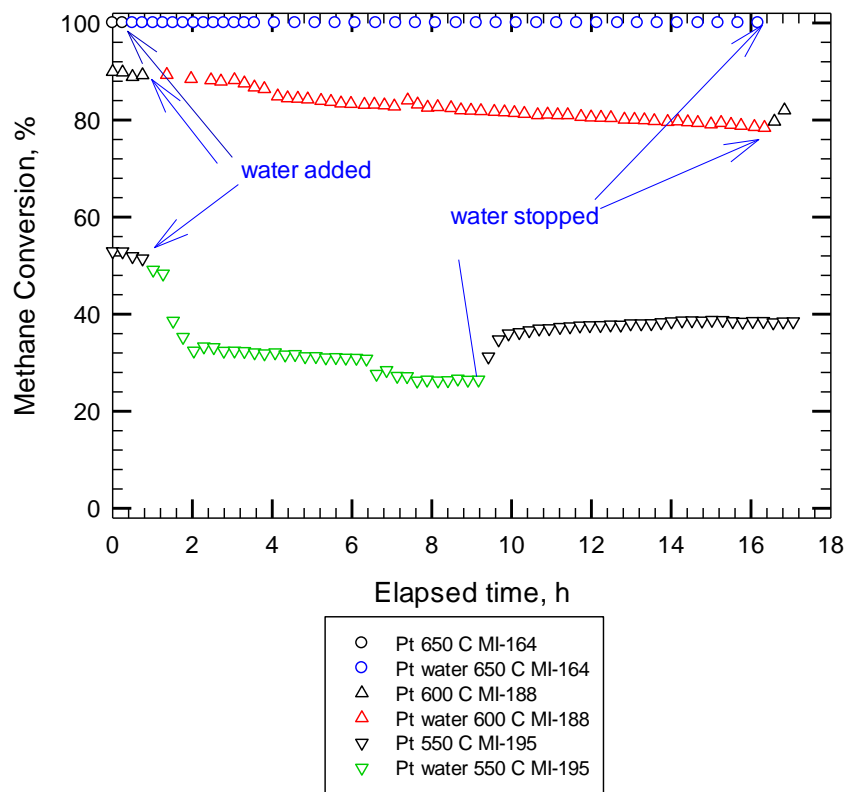


Figure 4.51. Constant temperature hydrothermal ageing of Pt catalyst (CH<sub>4</sub> 4100±50 ppm, 5% vol. water, total flow rate 235 cc/min)

#### 4.5.1.2. Pt-Pd (4:1) catalyst

For Pt-Pd (4:1) catalyst, T<sub>50</sub> value determined from the light off curve was 425°C. 100% conversion of methane was obtained at 550°C. An ignition-extinction curve for Pt-Pd (4:1) catalyst is presented in figure 4.52. The presence of a small positive hysteresis was also observed.

Figure 4.53 presents the experimental results of methane conversion at 550°C. After 4 GC tests, water added to the gas stream. A drop in activity can be observed (60% conversion), which is assumed to be due to the hydroxyl groups blocking the very active sites of Pd catalyst. After water was switched off the activity jumped to 90% conversion of methane and continued to increase.

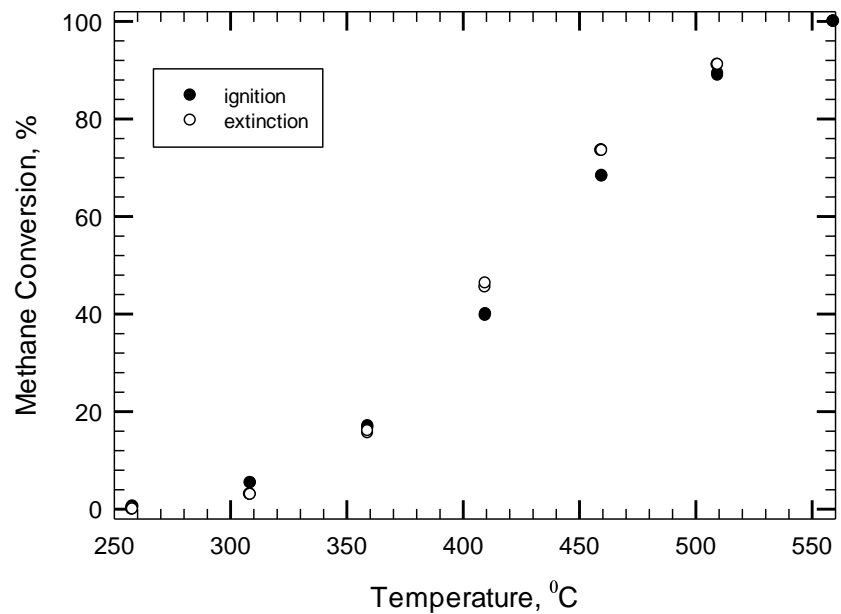


Figure 4.52. Ignition-extinction curves of methane conversion for Pt-Pd (4:1) catalyst (CH<sub>4</sub> 4100±50 ppm, total flow rate 235 cc/min)

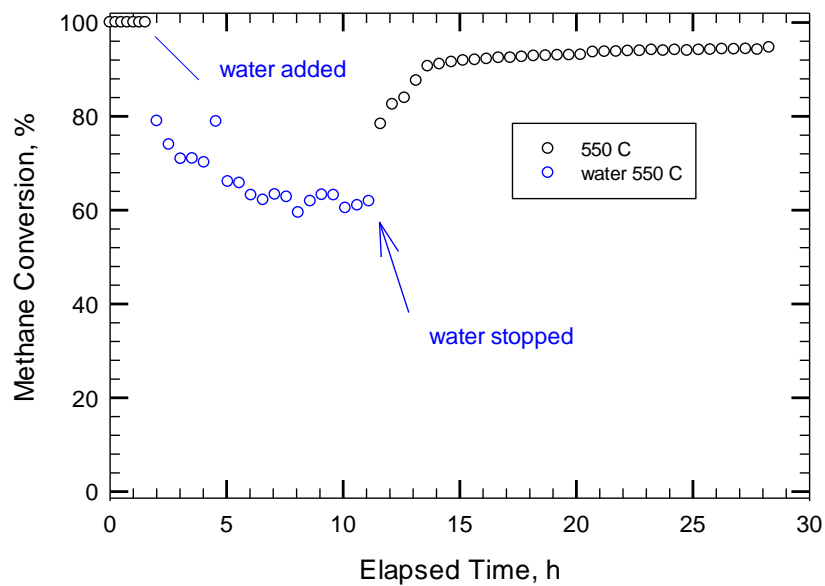


Figure 4.53. Constant temperature hydrothermal ageing test of methane conversion at 550°C, for Pt-Pd (4:1) catalyst (CH<sub>4</sub> 4100±50 ppm, 5% vol. water, total flow rate 235 cc/min)

To determine the change in catalytic activity of Pt-Pd (4:1) catalyst as a result of CTHTA test, and ignition-extinction cycle was performed (MI-177). An ignition-extinction cycle in the presence of water was also performed for Pt-Pd (4:1) catalyst (MI-178) in order to assess the effect of water as a function of temperature. The ignition-extinction cycles are compared in figure 4.54. It can be observed that the ignition-extinction curves before (MI-173) and after (MI-177) the CTHTA test show similar catalytic activity. It was previously observed the stability of Pt-Pd (4:1) to water deactivation. However, the effect of water as a function of temperature can be observed by the shift of the ignition-extinction curves towards higher temperatures, i.e. 100% conversion of methane was obtained at 650°C in presence of water compared with 550°C in absence of water.

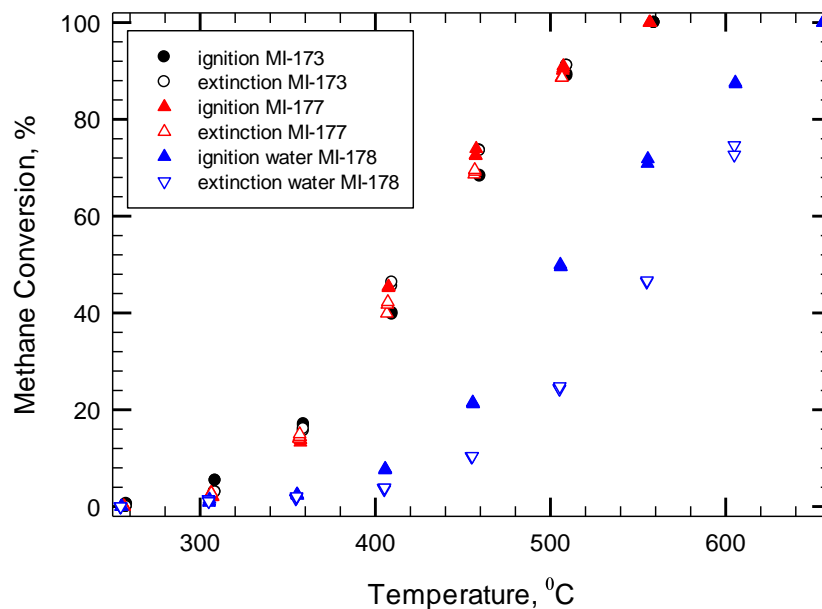


Figure 4.54. Ignition-extinction curves of methane conversion over Pt-Pd (4:1) catalyst before (MI-173), after (MI-177) constant temperature hydrothermal ageing test and in presence of water (MI-178) (CH<sub>4</sub> 4100±50 ppm, total flow rate 235 cc/min)

## Conclusions

The comparison of CHTA tests of Pt and Pt-Pd (4:1) catalysts is presented in figure 4.55. Two important observations can be drawn:

-higher conversion of methane in the presence of water is obtained for Pt-Pd (4:1) (60%) catalyst compared with Pt catalyst (25%)

-the recovery of catalytic activity after the water was switched off is higher for Pt-Pd (4:1) catalyst (93%) compared with Pt catalyst (39%)

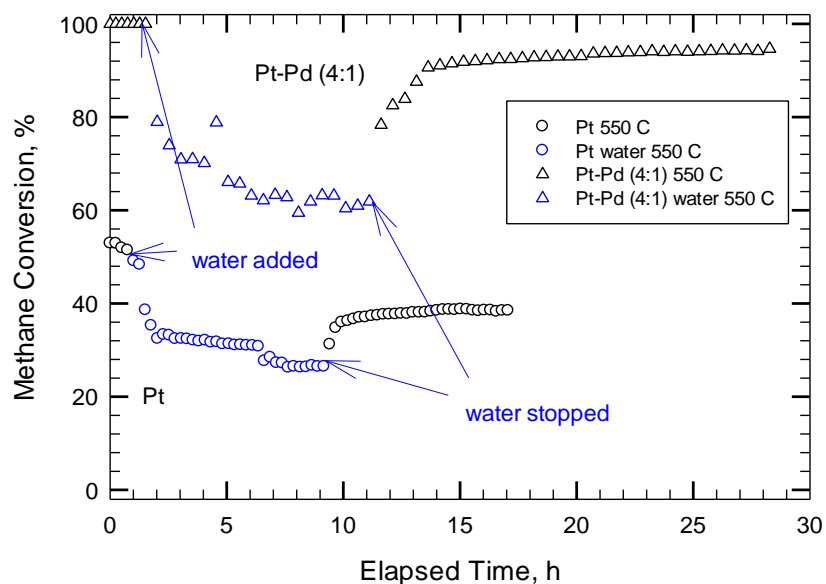


Figure 4.55. Comparison of constant temperature hydrothermal ageing test results for Pt and Pt-Pd (4:1) catalysts at 550°C (CH<sub>4</sub> 4100±50 ppm, 5% vol. water, total flow rate 235 cc/min)

## 4.6. Variable temperature hydrothermal ageing test (VTHTAT)

### (hydrothermal ageing 650 C)

To better evaluate the effect of water on the stability of the catalysts, a variable temperature hydrothermal ageing sequence was performed for Pt, Pt-Pd (4:1), Pt-Pd (1:5) and Pd 150 catalysts.

In the beginning of the sequence, an ignition-extinction test was performed to assess the activity of the catalyst.

A variable temperature thermal ageing test was performed to evaluate the stability of the catalyst with time.

Another ignition-extinction test was performed to assess the changes in the catalytic activity. For some samples, the activity of the catalyst was also assessed in presence of water.

#### 4.6.1. Pt catalyst

A complete sequence of variable temperature thermal ageing test catalyst was performed for Pt catalyst: ignition-extinction (MI-274), variable temperature hydrothermal ageing test (MI-275), ignition-extinction after VTHTAT (figure MI-276), and ignition-extinction in presence of water (MI-277).

Figure 4.56 compares the ignition-extinction curves before (MI-274), after (MI-275) the VTHTAT and in the presence of water (MI-277). The first ignition-extinction curve shows a very small negative hysteresis. 100% conversion of methane was obtained at 650°C. T50 was 540°C. It is interesting to observe that the catalytic activities of Pt catalyst after the VTHTA test and in the presence of water are similar, i.e. 100% conversion of methane was obtained at 650°C and around 20 % conversion of methane was obtained at 550°C for both tests.

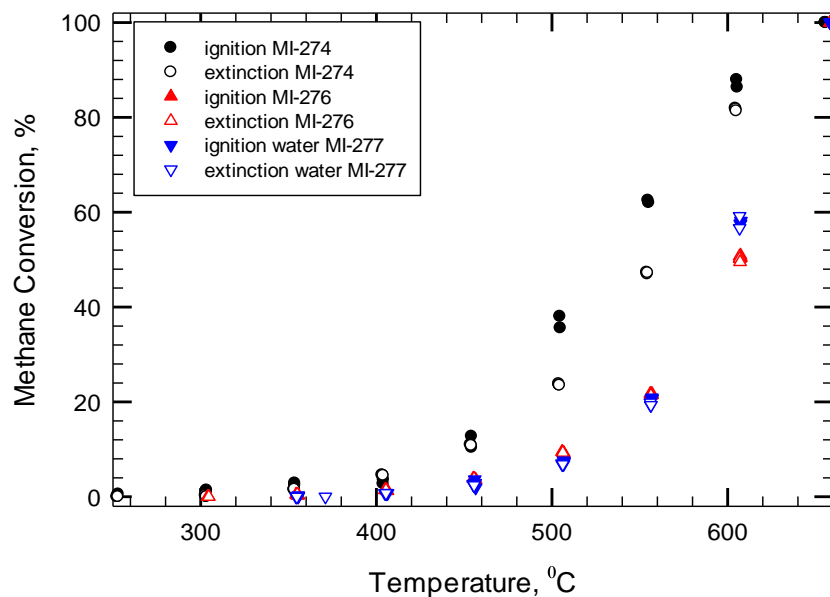


Figure 4.56. Ignition-extinction curves of methane combustion of Pt catalyst before (MI-274), after (MI-276) VTHTAT and in the presence of water (MI-277) (CH<sub>4</sub> 4100±50 ppm, total flow rate 235 cc/min)

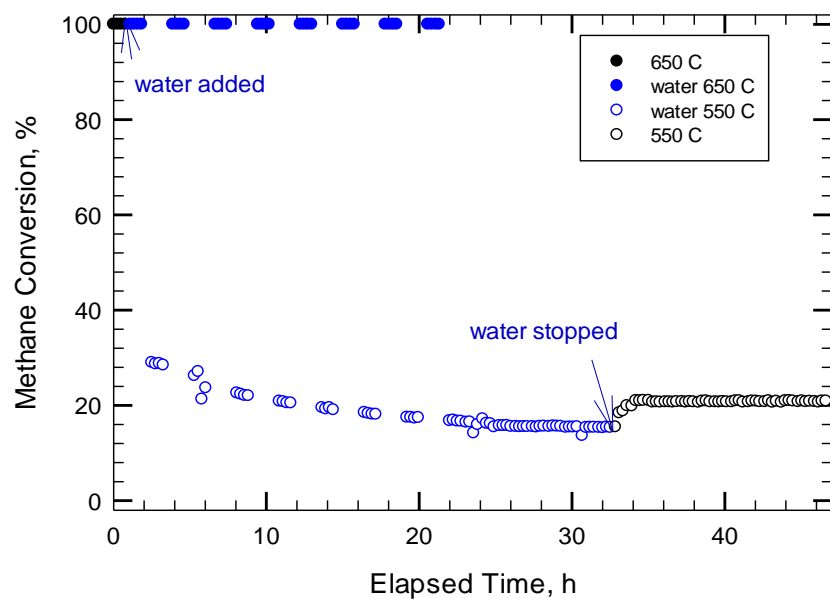


Figure 4.57. Variable temperature hydrothermal ageing test of methane combustion of Pt catalyst (MI-275) (CH<sub>4</sub> 4100±50 ppm, 5% vol. water, total flow rate 235 cc/min)

From the VTHTA test results it can be observed that the first activity point at 550°C was about 32% methane conversion (figure 4.57). After about 25 hours the activity was stabilizing around 18%. When the water was switched off the activity rose to about 22% of methane conversion and stayed constant.

Figure 4.58 presents the TEM image of de-greened (left) and hydrothermally aged (right) samples. An increase in particle size as a result of hydrothermal ageing can be observed and is assumed to be due to the sintering process of particles.

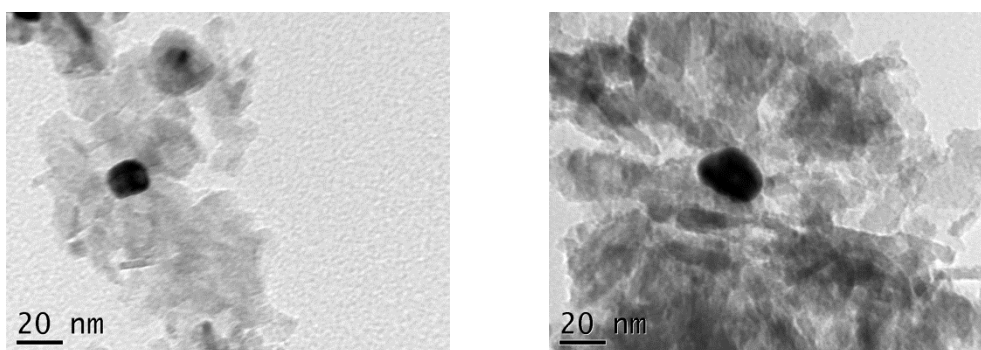


Figure 4.58. TEM images of Pt catalyst before (left) and after (right) hydrothermal ageing

#### 4.6.2. Pd 150 catalyst

##### *Variable temperature hydrothermal ageing at 350°C*

A similar hydrothermal ageing sequence as described above for Pt catalyst was performed for Pd 150 catalyst: ignition-extinction (MI-261), variable temperature hydrothermal ageing test (MI-262), and ignition-extinction (MI-263).

Figure 4.59 compares the experimental results of the ignition-extinction curves before (MI-261) and after (MI-263) the thermal ageing test. From the first ignition-extinction cycle of methane conversion the presence of a large negative hysteresis can be observed. 100% conversion of methane was obtained at 400°C. T50 for the light off curve was 315°C.

The strong effect of hydrothermal ageing is highlighted by the shift of the ignition-extinction curve toward higher temperatures, i.e. 100% conversion was obtained at 550°C compared with 400°C before hydrothermal ageing. T50 of the light off curve was 465°C. However, the activity does not appear to be stable between 350°C and 550°C. The hysteresis loop that can be observed is positive, contrary to the initial hysteresis loop (MI-261 shows a negative hysteresis loop). It can be assumed that this is a result of the water effect during the VTHTA test.

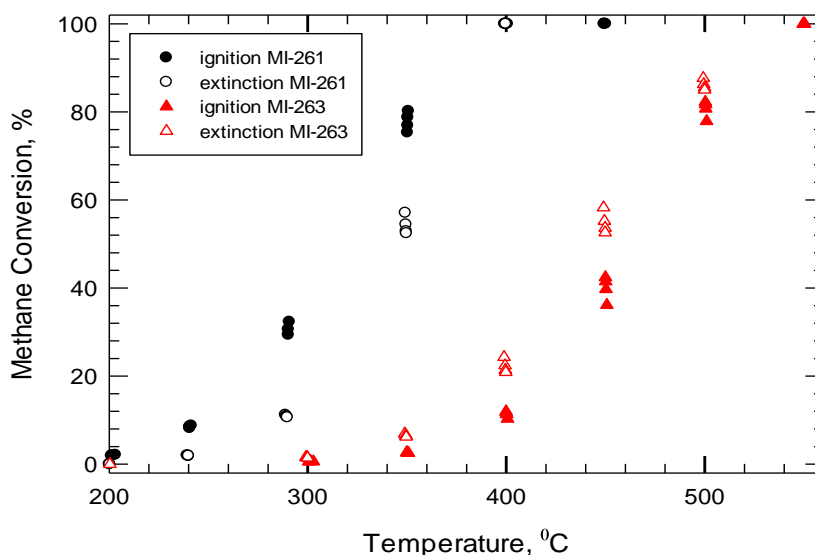


Figure 4.59. Ignition-extinction curves of methane conversion over Pd 150 catalyst, before (MI-261) and after (MI-263) variable temperature hydrothermal ageing test (CH<sub>4</sub> 4100±50 ppm, total flow rate 235 cc/min)

Figure 4.60 presents the experimental results of VTHTA test. It can be observed that the first activity point at 350°C of the VTHTA test was close to zero and remained relatively constant for all 7 intervals, as well as for the 10 hours hydrothermal treatment at 350°C. When water was switched off the activity rose slightly up to 1% conversion of methane.

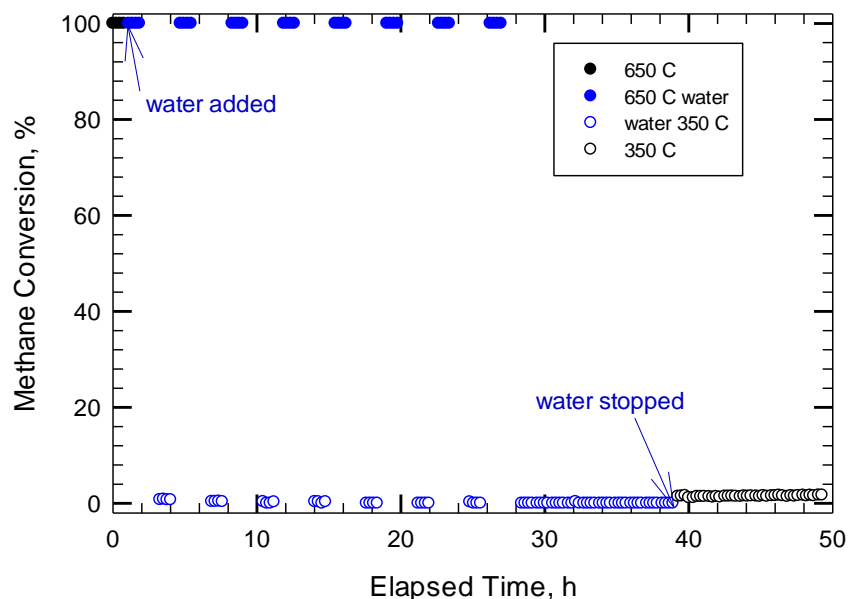


Figure 4.60. Variable temperature hydrothermal ageing test of methane conversion of Pd 150 catalyst (MI-262) (CH<sub>4</sub> 4100±50 ppm, 5% vol. water, total flow rate 235 cc/min)

Due to very low conversion values obtained for the VTHTA test at 350°C, a similar sequence was performed at 450°C.

#### *Variable temperature hydrothermal ageing test at 450°C*

Figure 4.61 compares the ignition-extinction results of a fresh Pd 150 sample (MI-278), after the VTHTAT (MI-280) and in the presence of water (MI-281). The presence of a large negative hysteresis can be observed for the first ignition-extinction cycle (MI-278). 100% conversion of methane was obtained at 400°C. T<sub>50</sub> for the light off curve was 322°C. The effect of VTHTAT on the catalytic activity for the Pd 150 catalyst can be observed from the shift of the ignition-extinction curve toward higher temperatures. 100% conversion of methane was obtained at 500°C and T<sub>50</sub> was 395°C. Similar as for the VTHTAT performed at 350°C, it can be observed that the hysteresis loop is inverted. This effect is assumed to be due to the hydrothermal ageing effect on the catalyst. The effect of

water on the catalytic activity of Pd 150 catalyst can be observed from the MI-21 results. 100% conversion of methane was obtained at 550°C and the activity does not appear to be stable between 350°C and 550°C. T50 for the light off curve is 455°C. It is interesting to observe that for temperatures above 450°C the extinction curve is slightly more active, while for temperatures below 450°C the ignition curve is slightly more active.

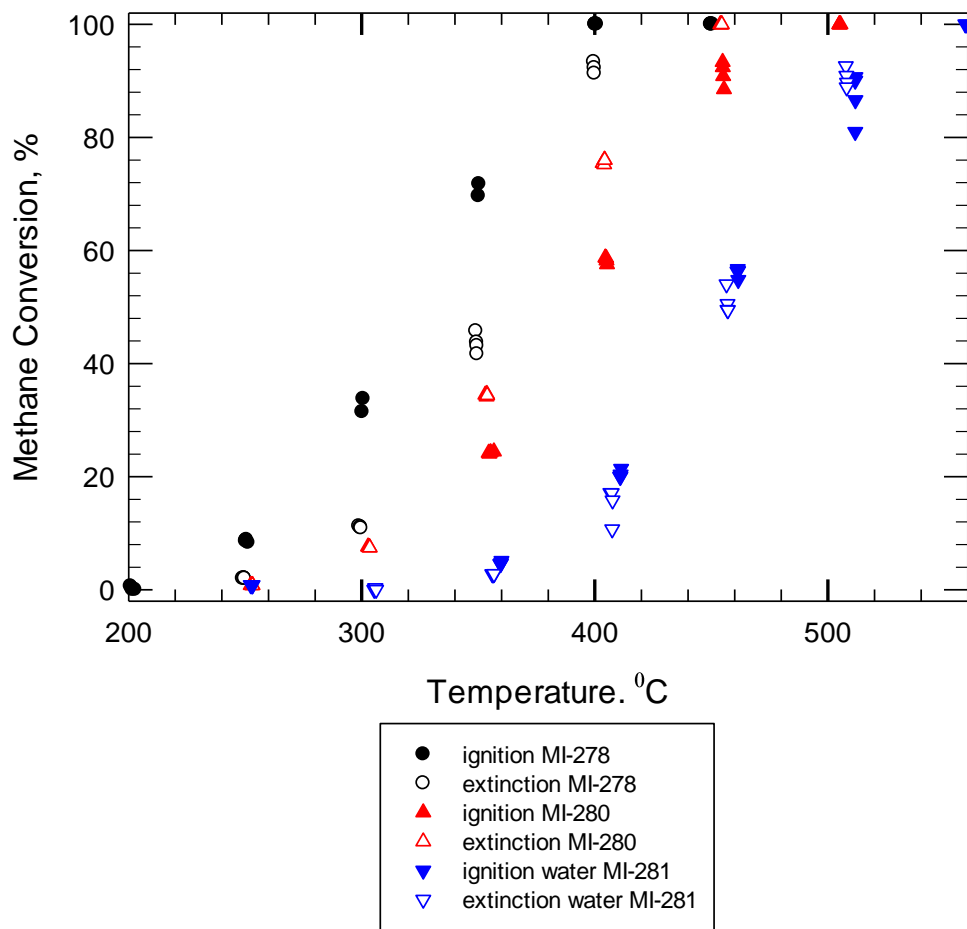


Figure 4.61. Ignition-extinction curve of methane conversion of Pd 150 catalyst: before (MI-278), after (MI280) VTHTAT and in the presence of water (MI-281) (CH<sub>4</sub> 4100±50 ppm, total flow rate 235 cc/min)

The experimental results of variable temperature hydrothermal ageing test are presented in figure 4.62. The first activity point at 450°C was 40%, but fell

rapidly (during first interval) to 16%. Activity continued to fall, and during each 450°C interval the activity was decreasing. However, the activity at the beginning of each 450°C interval is higher than the end activity of the previous 450°C interval. This is consistent with the previous results obtained for Pd 150 catalyst (figure 4.42, and 4.44). After 24 hours of hydrothermal ageing, the temperature was held constant at 450°C, and the activity dropped slightly, to around 4% conversion. When the water was switched off, the activity rose to 44% over 10 hours.

Figure 4.63 compares the experimental results of VTТА test at 350°C (MI-262) and 450°C (MI-279). It is interesting to observe the big increase in activity after the water was switched off for VTHTA test at 450°C compared with the similar test VTHTA test at 350°C.

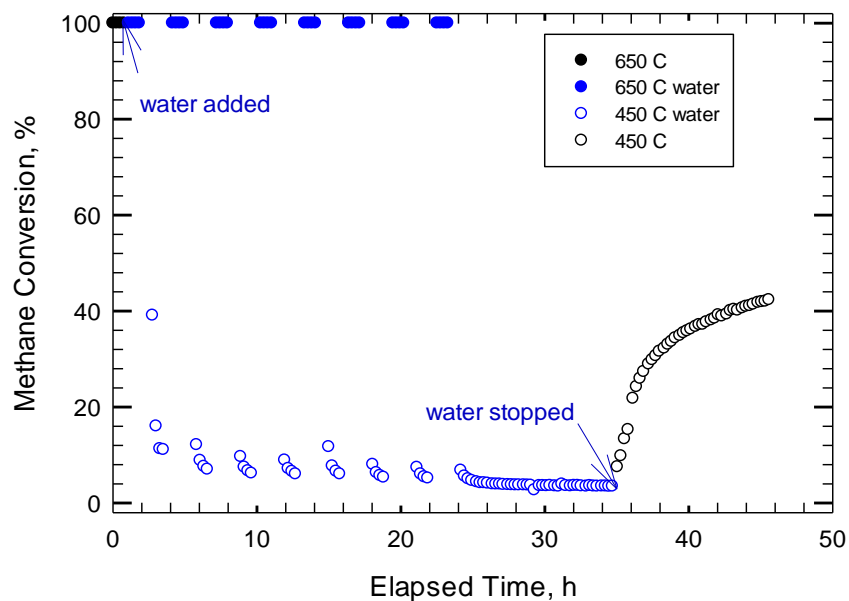


Figure 4.62. Variable temperature thermal ageing test of methane conversion of Pd 150 catalyst (MI-279) (CH<sub>4</sub> 4100±50 ppm, 5% vol. water, total flow rate 235 cc/min)

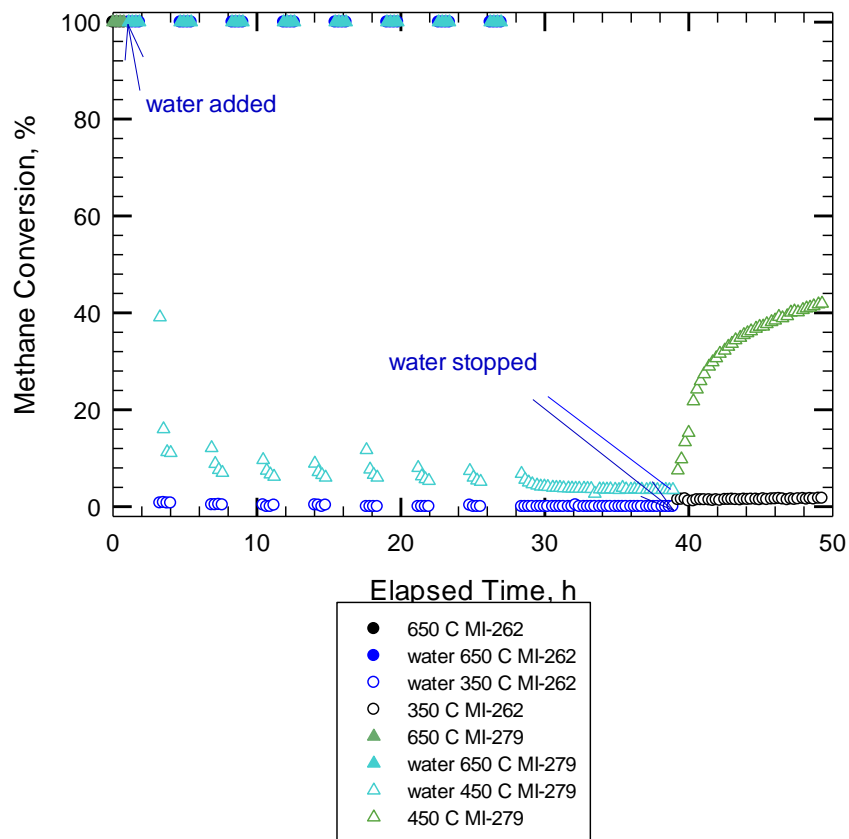


Figure 4.63. Variable temperature hydrothermal ageing test at 350°C (MI-262) and 450°C (MI-279) of methane conversion of Pd 150 catalyst (CH<sub>4</sub> 4100±50 ppm, 5% vol. water, total flow rate 235 cc/min)

As it was previously discussed, this is assumed to be due to the water effect as a function of temperature, i.e. the higher the temperature of reaction, the lower the ability of water to be adsorbed and block the active sites of the catalyst.

#### 4.6.3. Pt-Pd (4:1) catalyst

The same sequence of hydrothermal ageing as described above for Pt catalyst was performed for Pt-Pd (4:1) catalyst: ignition-extinction (MI-239), variable temperature hydrothermal ageing test (MI-240), ignition-extinction (MI-241) and ignition-extinction in the presence of water (MI-242).

From the first ignition-extinction cycle of the Pt-Pd (4:1) catalyst, a small positive hysteresis can be observed. 100% conversion of methane was obtained at 500°C. T50 for the light off curve was 400°C. It can be observed that the effect of hydrothermal ageing on the catalytic activity of Pt-Pd (4:1) catalyst is less pronounced compared with Pd 150 catalyst (figure 4.61). 100% conversion of methane was obtained at 550°C. T50 for the light off curve was 430°C. In the presence of water, the ignition-extinction curves shifts toward higher temperatures. A large negative hysteresis can be observed, opposite to the first ignition-extinction cycle. 100% conversion of methane was obtained at 650°C. T50 for the light off curve was 500°C.

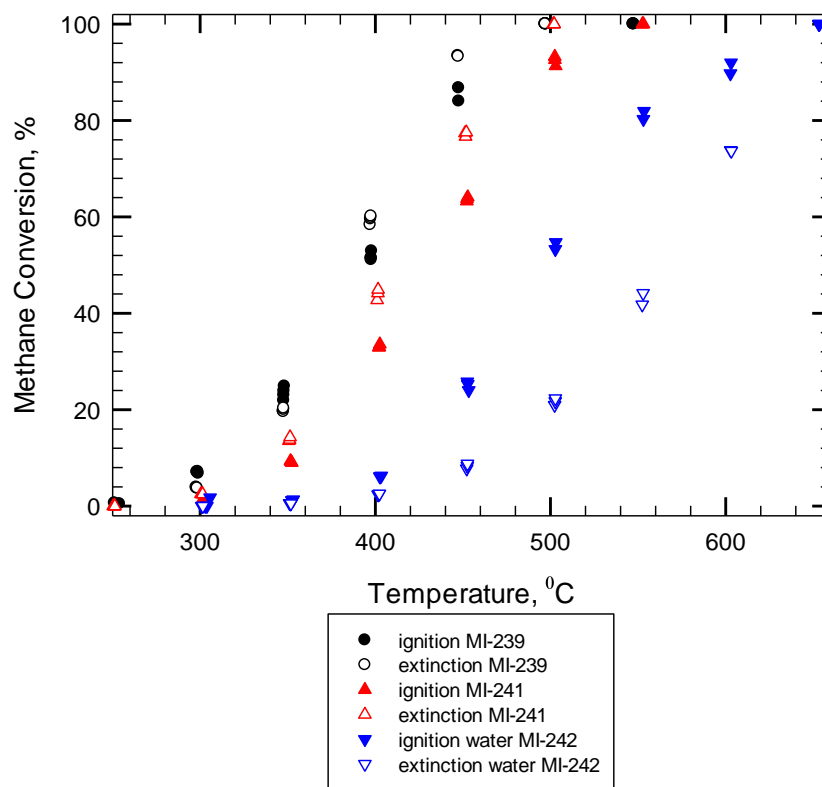


Figure 4.64. Ignition-extinction curves of methane conversion of Pt-Pd (4:1) catalyst: before VTHAT (MI-239) and after VTHAT (MI-241) and in the presence of water (MI-242) (CH<sub>4</sub> 4100±50 ppm, total flow rate 235 cc/min)

The TEM images of Pt-Pd (4:1) catalyst before and after hydrothermal ageing test are presents in figure 4.65 and 4.66 respectively. A slight increase in the particles size can be observed which is assumed to be due to the sintering effect of hydrothermal ageing.

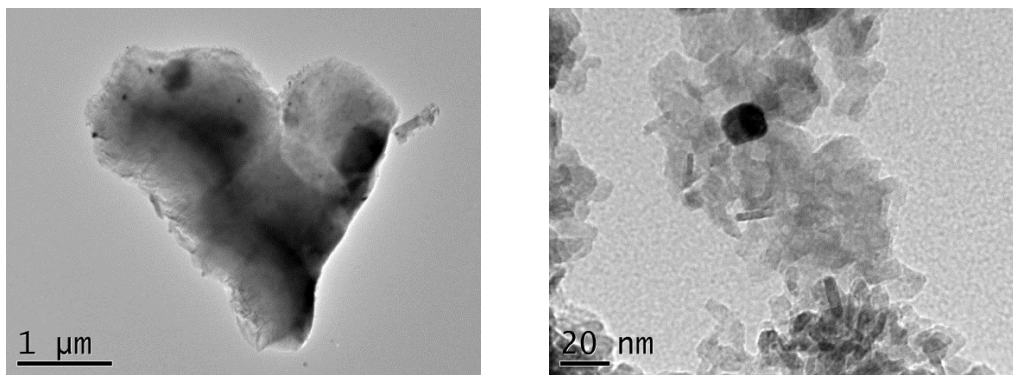


Figure 4.65. TEM images of Pt-Pd (4:1) catalyst before hydrothermal ageing test

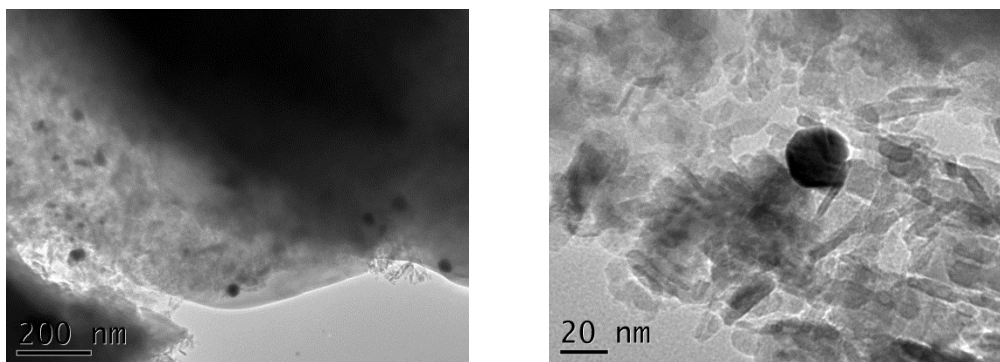


Figure 4.66. TEM images of Pt-Pd (4:1) catalyst after the hydrothermal ageing test

Figure 4.67 presents the experimental results for variable temperature hydrothermal ageing test of the Pt-Pd (4:1) catalyst. The first activity point at 450°C is about 8%. The activity decreases over the course of the hydrothermal ageing to about 4% after 22 hours. During each 450°C interval, a small increase in activity can be observed (similar with the behaviour observed for the varied temperature thermal ageing test of Pt-Pd (4:1) catalyst, figure 4.52). After 22 hours, the reactor was kept at 450°C in presence of water and the activity increased to 12%. When water was switched off, the activity increased to 42% initially, but rose over 15 hours to about 56%.

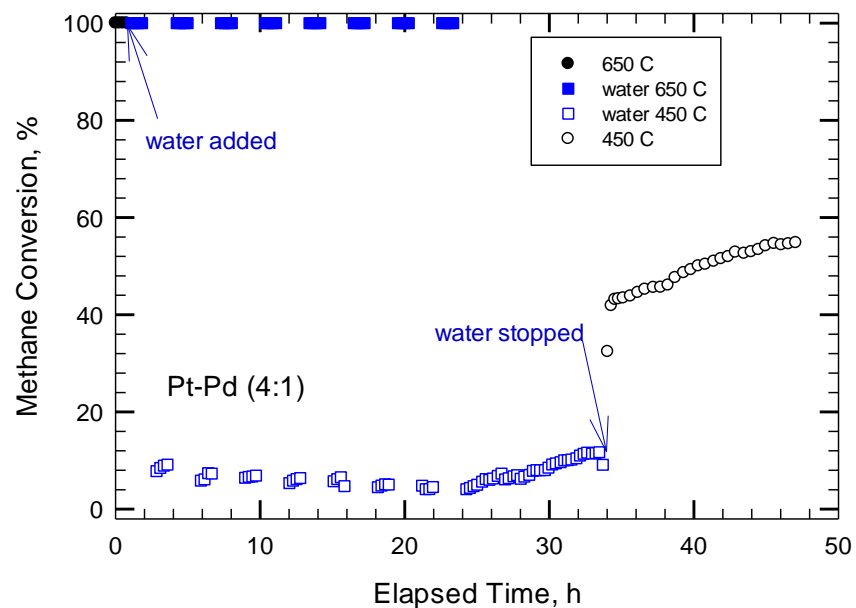


Figure 4.67. Variable temperature hydrothermal ageing test of methane conversion of Pt-Pd (4:1) catalyst (MI-240) (CH<sub>4</sub> 4100±50 ppm, 5% vol. water, total flow rate 235 cc/min)

Figure 4.68 compares the experimental results of methane conversion after variable temperature hydrothermal ageing test of Pt (MI-276, no hysteresis loop), Pd (MI-280, small positive hysteresis loop) and Pt-Pd (4:1) (MI-241 small positive hysteresis loop) catalysts. The small hysteresis loop observed for Pt-Pd (4:1) catalyst can be assumed to be due to the presence of Pd.

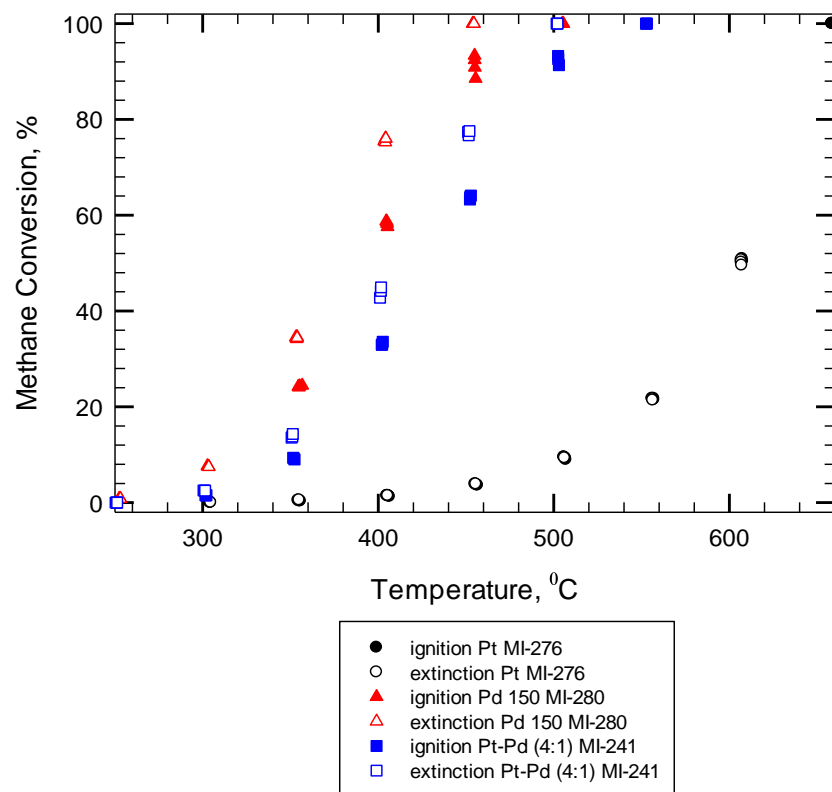


Figure 4.68. Ignition-extinction curves of methane conversion after variable temperature hydrothermal ageing test of Pt (MI-276), Pd (MI-280) and Pt-Pd (4:1) (MI-241) catalysts (CH<sub>4</sub> 4100±50 ppm, total flow rate 235 cc/min)

Figure 4.69 compares the ignition-extinction curves of methane conversion in presence of water of Pt (MI-277), Pd 150 (MI-281) and Pt-Pd (4:1) (MI-242) catalysts. It can be observed that Pd 150 catalyst shows a small positive hysteresis, Pt-Pd (1:4) shows large negative hysteresis, while Pt catalyst shows no hysteresis.

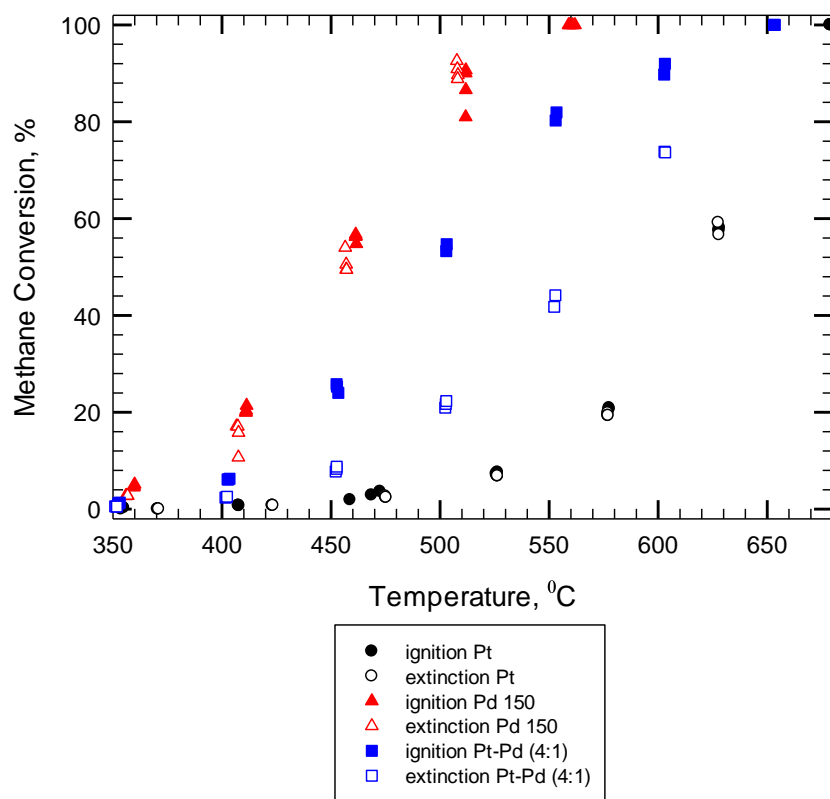


Figure 4.69. Ignition-extinction curves of methane conversion in presence of water of Pt (MI-277), Pd 150 (MI-281) and Pt-Pd (4:1) (MI-242) catalysts (CH<sub>4</sub> 4100±50 ppm, total flow rate 235 cc/min)

#### 4.6.4. Pt-Pd (1:5) catalyst

##### *Variable temperature hydrothermal ageing test at 350°C*

A similar hydrothermal ageing sequence as described above for Pt catalyst was performed for Pt-Pd (1:5) catalyst: ignition-extinction (MI-228), variable temperature hydrothermal ageing test (MI-229), ignition-extinction after the hydrothermal ageing (MI-230) and ignition-extinction in the presence of water (MI-231).

Figure 4.70 compares the ignition-extinction curves before (MI-228) and after (MI-230) the hydrothermal ageing as well as in the presence of water (MI-231). From the first ignition-extinction curves it can be observed that 100% conversion

of methane was obtained at 350°C. T50 for the light off curve was 305°C. The effect of hydrothermal ageing on the catalytic activity can be observed from the shift toward higher temperatures of the ignition-extinction curves. No hysteresis was observed. The activity appears to be unstable between 350°C and 450°C. 100% conversion of methane was obtained at 400°C and T50 for the light off curve was 360°C. No hysteresis was observed for ignition-extinction curves of methane conversion in presence of water. 100% conversion was obtained at 500°C. T50 for the light off curve was 433°C.

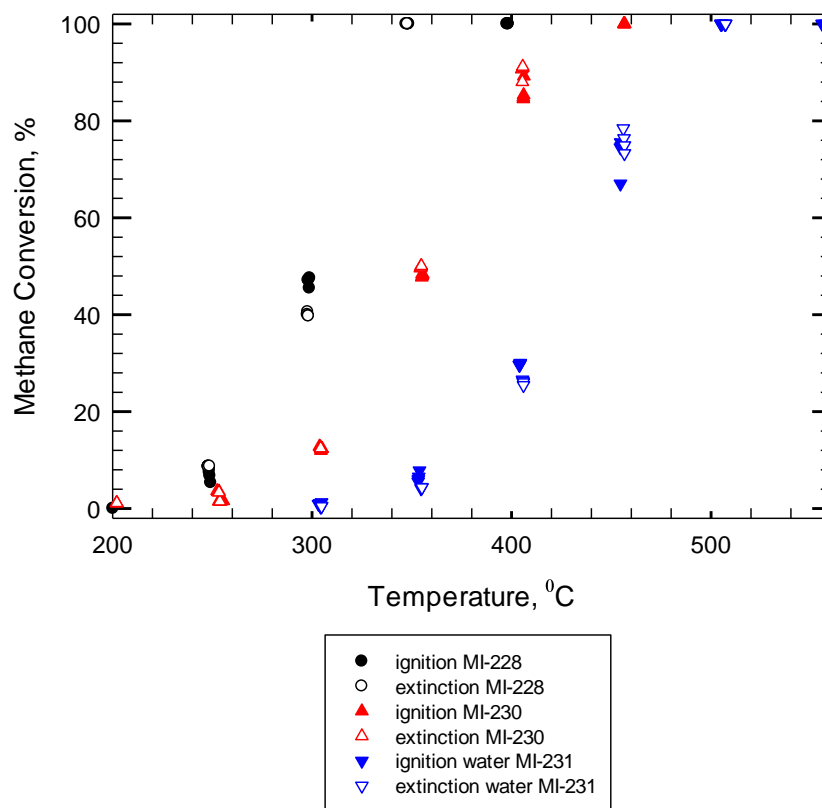


Figure 4.70. Ignition-extinction curves of methane conversion of Pt-Pd (1:5) catalyst: before VTHTAT (MI-228), after VTHTAT (MI-230) and in the presence of water (MI-231) (CH<sub>4</sub> 4100±50 ppm, total flow rate 235 cc/min)

The experimental results for varied temperature hydrothermal ageing test are presented in figure 4.71. It is interesting to note an increase in the catalytic activity for the first interval at 350°C, with the activity point increasing from 15 to 18% conversion. However, all the other 350°C intervals show a very small variation in catalytic activity, except the second 350°C interval which shows a more pronounced decrease in the activity. After 27 hours, the activity of 350°C decreased to about 8% conversion. When the water was switched off, the activity increased quickly to about 40%, and then continued to rise slowly to about 48% conversion.

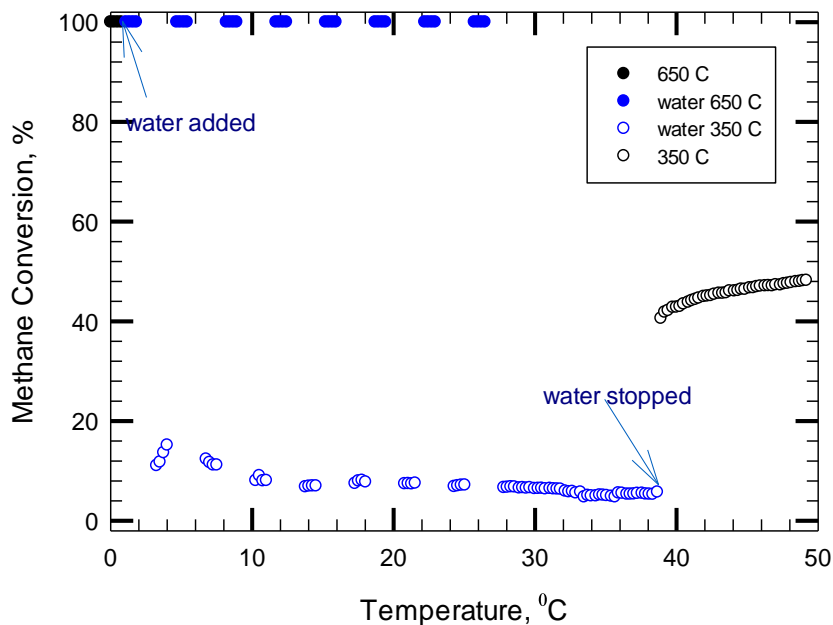


Figure 4.71. Variable temperature thermal ageing test of methane conversion of Pt-Pd (1:5) catalyst (MI-229) (CH<sub>4</sub> 4100±50 ppm, 5% vol. water, total flow rate 235 cc/min)

Figure 4.72 presents the TEM images of Pt-Pd (1:5) catalyst before and after the hydrothermal ageing. An increase in the particle size can be observed as a result of sintering process of the metal particles.

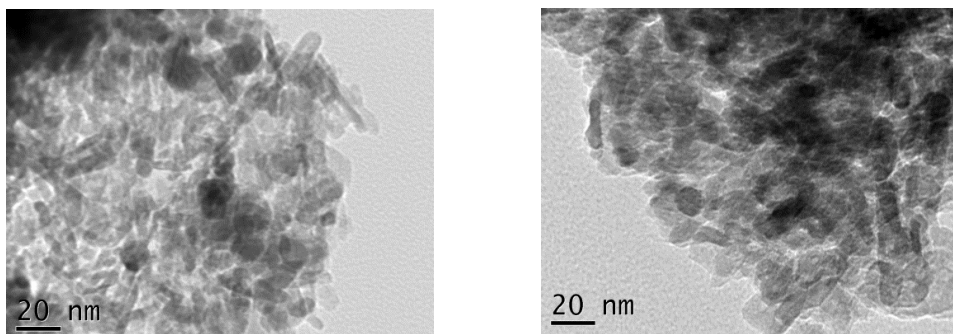


Figure 4.72. TEM images of Pt-Pd (1:5) catalyst before (left) and after (right) hydrothermal ageing test

#### *Variable temperature hydrothermal ageing test at 450°C*

Due to the low methane conversion values during the hydrothermal ageing test at 350°C, the same test was performed at 450°C: ignition-extinction (MI-244), variable temperature hydrothermal ageing test (MI-245), ignition-extinction (MI-246), and ignition-extinction in presence of water (MI-247).

Figure 4.73 compares the ignition-extinction curves of methane conversion over Pt-Pd (1:5) catalyst before (MI-244) and after (MI-246) hydrothermal ageing test as well as in the presence of water (MI-247). A small negative hysteresis can be observed for the first ignition-extinction curves of methane conversion of Pt-Pd (1:5) catalyst. 100% conversion of methane was obtained at 400°C. T50 for the light off curve was 305°C. However, no hysteresis was observed after the hydrothermal ageing test. The effect of hydrothermal ageing on the catalytic activity brings a shift of the ignition-extinction curves of methane conversion towards higher temperatures. 100% conversion of methane was obtained at 450°C. T50 for the light off curve was 360°C (MI-246). The strong effect of water on the catalytic activity can also be observed (MI-247). 100% conversion of methane was obtained at 500°C. T50 for the light off curve was 435°C.

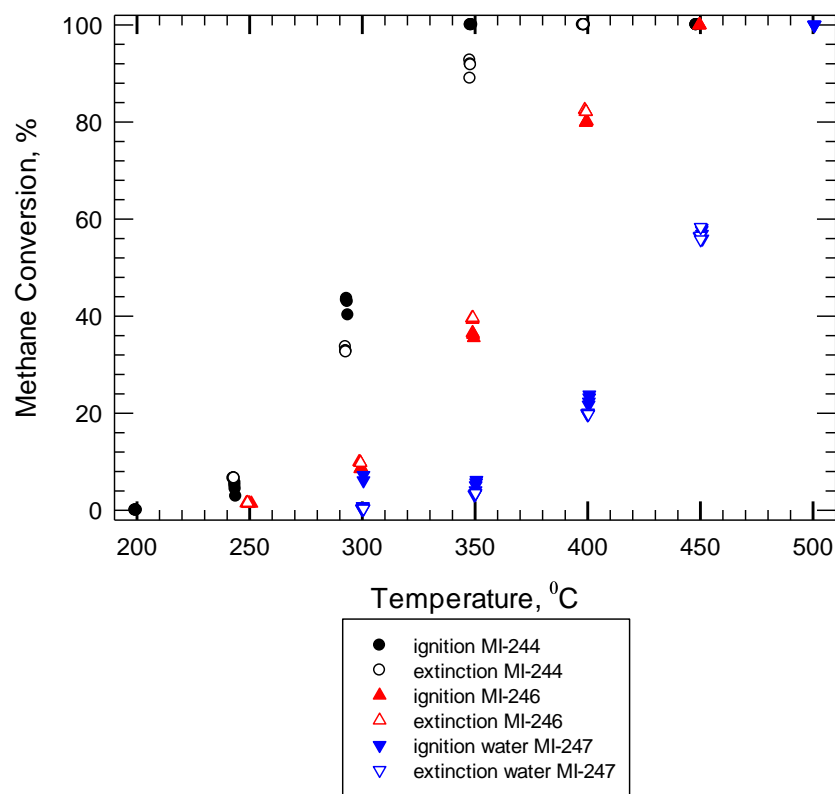


Figure 4.73. Ignition-extinction curves of methane conversion of Pt-Pd (1:5) catalyst: before (MI-244) and after (MI-246) hydrothermal ageing, and in the presence of water (MI-247) (CH<sub>4</sub> 4100±50 ppm, 5% vol. water, total flow rate 235 cc/min)

The experimental results of varied temperature hydrothermal ageing test presented in figure 4.74 show a high resistance to water deactivation of Pt-Pd (1:5). This behaviour is assumed to be due to palladium and hydroxyl interaction as a function of temperature. The first interval at 450°C shows 100% conversion of methane. The decrease in activity due to water deactivation starts with the second interval of 450°C. For all subsequent 450°C a similar pattern with the Pd catalyst was observed: the activity at the beginning of 450°C is higher than the activity at the end of previous 450°C interval. After 35 hours, the activity of 450°C interval decreased to about 48% conversion. When the water was switched off, the activity increased quickly to 100% conversion.

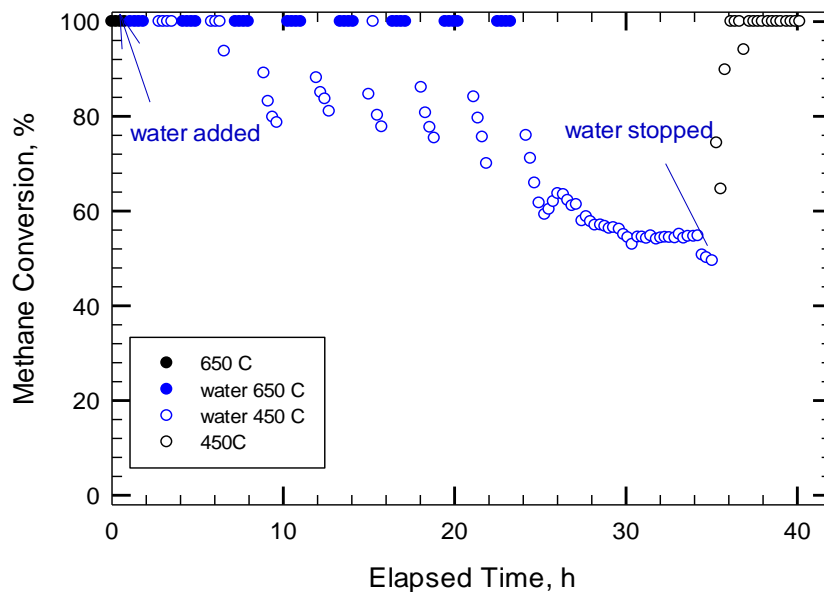


Figure 4.74. Variable temperature hydrothermal ageing test of methane combustion over Pt-Pd (1:5) catalyst (MI-245) (CH<sub>4</sub> 4100±50 ppm, 5% vol water, total flow rate 235 cc/min)

## Conclusions

### *The effect of water deactivation as a function of catalyst formulation*

The effect of water deactivation on the catalytic activity of Pt, Pd 150, Pt-Pd (4:1), Pt-Pd (1:5) was assessed by comparing the ignition-extinction curves before VTHTA test, after VTHTA test and in presence of water.

Figure 4.75 presents the experimental results of catalytic activity of Pt, Pd 150, Pt-Pd (4:1) and Pt-Pd (1:5) catalysts. As it can be expected, the higher activity in methane conversion was shown by Pd and predominantly Pd catalyst (Pt-Pd (1:5)). Pt and predominantly Pt catalyst (Pt-Pd (4:1)) show lower conversion of methane.

Table 4.4 presents the temperatures of the light off curve where 100% conversion (T100) as well as 50% (T50) conversion of methane was obtained.

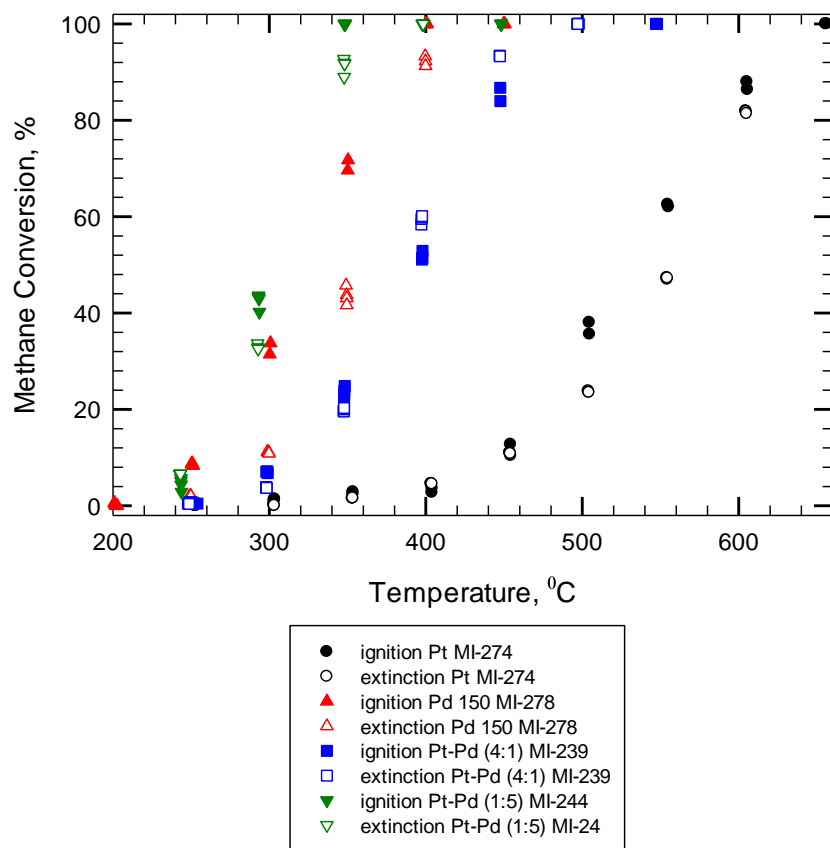


Figure 4.75. Ignition-extinction curves of methane conversion of Pt, Pd 150, Pt-Pd (4:1) and Pt-Pd (1:5) catalysts (CH<sub>4</sub> 4100±50 ppm, total flow rate 235 cc/min)

Table 4.4. Methane conversion of Pt, Pt-Pd (4:1), Pd 150 and Pt-Pd (1:5) catalysts

Sample	T100, °C	T50, °C
Pt	650	540
Pt-Pd (4:1)	500	400
Pd 150	400	322
Pt-Pd (1:5)	400	305

From table 4 it can be observed that lower temperature was necessarily for Pd and predominantly Pd catalyst to obtain complete conversion of methane.

Figure 4.76 presents the catalytic activities of Pt, Pd 150, Pt-Pd (4:1) and Pt-Pd (1:5) catalysts after variable temperature hydrothermal ageing test. A shift to the higher temperatures can be observed for all 4 catalysts. It is interesting to observe that the position of curves related to each other didn't change.

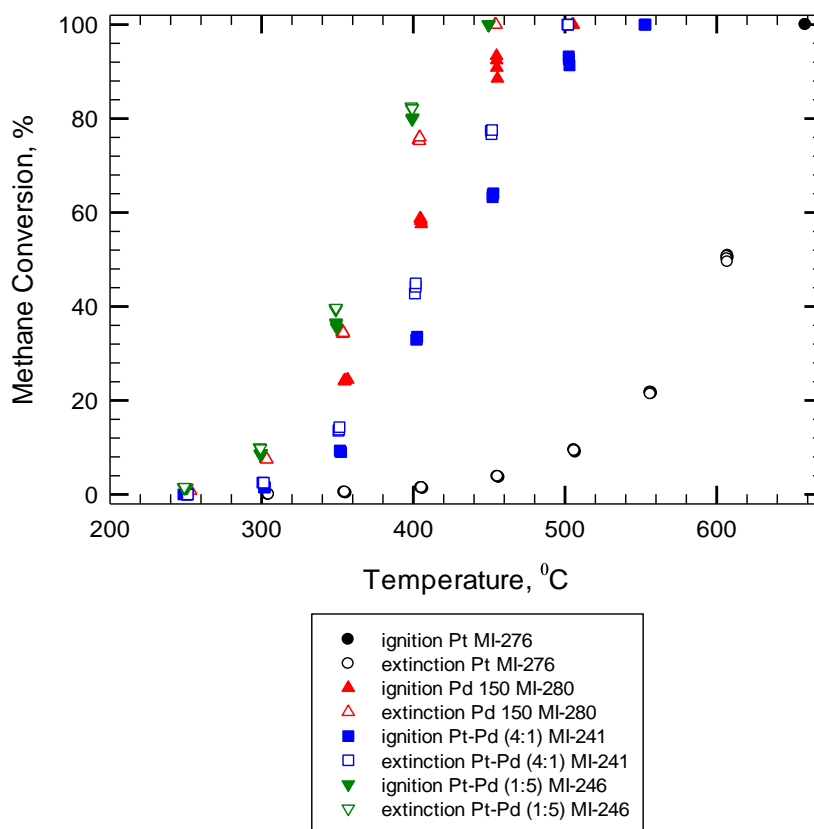


Figure 4.76. Ignition-extinction curves of methane conversion of Pt, Pd 150, Pt-Pd (4:1) and Pt-Pd (1:5) catalysts, after VTHTA test (CH<sub>4</sub> 4100±50 ppm, total flow rate 235 cc/min)

Table 4.5 presents the experimental results of Pt, Pd 150, Pt-Pd (4:1) and Pt-Pd (1:5) catalysts. It can be observed that the temperatures for complete conversion of methane after VTHTA test increases for the Pd formulated catalysts. However, T<sub>50</sub> for the light off curve of methane conversion changes for all catalysts. The changes of catalytic activities of methane conversion in presence of water are presented in figure 4.77.

Table 4.5. Methane conversion over Pt, Pt-Pd (4:1), Pd 150 and Pt-Pd (1:5) catalysts after VTHTA test

Sample	T100, °C	T50, °C
Pt	650	605
Pt-Pd (4:1)	550	430
Pd 150	500	395
Pt-Pd (1:5)	450	360

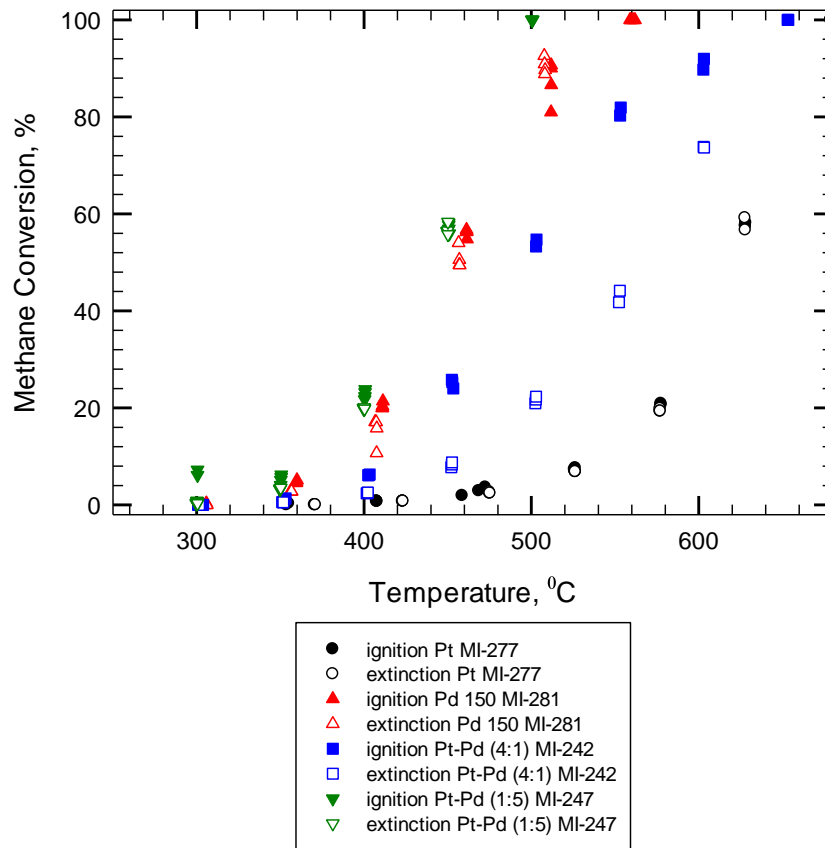


Figure 4.77. Ignition-extinction curves of methane conversion in presence of water, of Pt, Pd 150, Pt-Pd (4:1) and Pt-Pd (1:5) catalysts (CH<sub>4</sub> 4100±50 ppm, 5% vol. water, total flow rate 235 cc/min)

Table 4.6 presents a summary of the T100 and T50 values of methane conversion over Pt, Pd 150, Pt-Pd (4:1) and Pt-Pd (1:5) catalysts. From the experimental results it can be concluded that from all 4 catalysts, Pt-Pd (1:5) presents the best resistance to water deactivation.

Table 4.6. Summary of T100 and T50 of the light off curve of methane combustion of Pt, Pd 15-, Pt-Pd 94:10 and Pt-Pd (1:5) catalysts before VTHTAT, after VTHTAT and in presence of water

Sample	Fresh sample		After VTHTA test		water	
	T100,°C	T50,°C	T100,°C	T50	T100,°C	T50,°C
Pt	650	540	650	605	>650	650
Pt-Pd (4:1)	500	400	550	430	650	500
Pd 150	400	322	500	395	550	455
Pt-Pd (1:5)	400	305	450	360	500	435

## 4.7. Three way catalytic converters

### 4.7.1. Variable temperature thermal ageing test VTTAT, (thermal ageing 550°C)

A similar thermal ageing test was performed for Pd 150, Pd 122, PdRh, PtPdRh and Pt-Pd (1:5) catalyst: the samples were thermally aged at 550°C and the activity was measured at lower temperatures (300°C, 350°C or 450°C).

The samples were prepared as described in Chapter 3: all samples (monolith) were ground to 200-400 micrometer size; the samples were de-greened by exposure to air at 550°C, for 16 hours; the samples were reduced by hydrogen exposure at 500°C, for 30 minutes.

All activity and thermal ageing experiments were performed using 4100 ppm methane in extra dry air stream. When water was added to the gas stream, it comprised about 5% by volume of the feed stream. 0.5 g of sample which includes substrate material was used in the experiments.

An ignition-extinction test was performed to assess the activity of the catalyst.

Thermal ageing was performed at 550°C with activity measurements at lower temperatures, depending on the catalytic activity of each sample.

Another ignition-extinction test was performed to assess the changes in the catalytic activity after the VTTA test. For some sequences, the activity of the catalyst was also assessed in presence of water.

#### 4.7.1.1. Pd 150 catalyst

Figure 4.78 compares the experimental results of ignition-extinction curves of methane conversion of Pd 150catalyst: before thermal ageing (MI-374), after thermal ageing (MI-376) and in the presence of water (MI-377).

For the first ignition-extinction cycle 100% conversion of methane was obtained at 400°C and T50 of the light off curve was 320°C. The presence of a negative hysteresis can be observed (i.e. ignition more active than extinction). A shift of the ignition-extinction curves towards higher temperatures as a result of thermal ageing test can be observed: 100% conversion of methane was obtained at 500°C, and T50 of the light off curve was 420°C. The presence of a positive hysteresis can be observed. In the presence of water, 100% conversion of methane was obtained at 500°C and T50 of the light off curve was 460°C. The presence of a negative hysteresis can be observed.

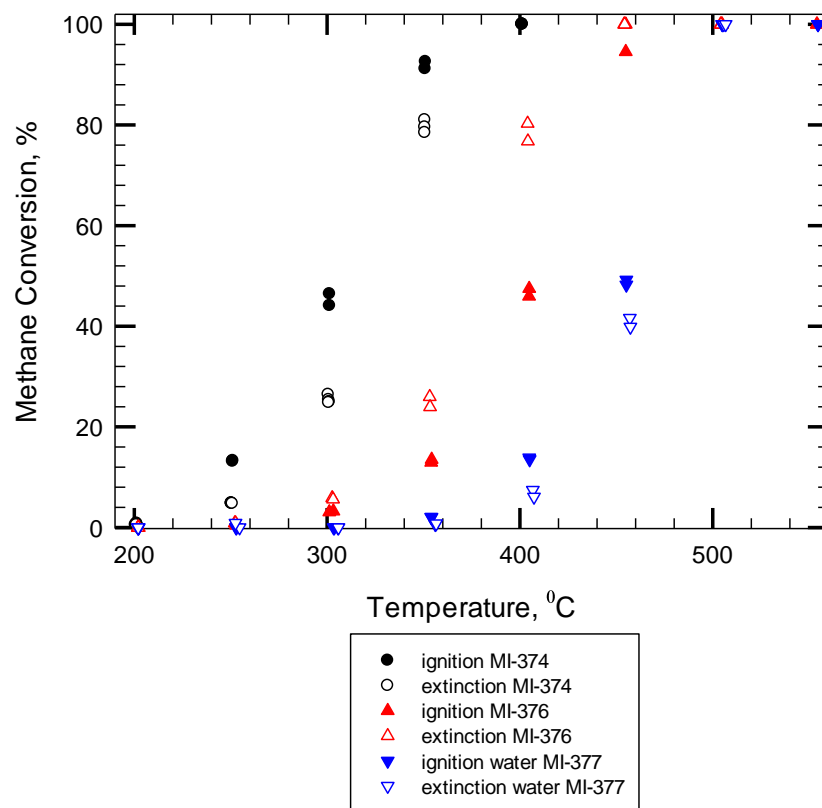


Figure 4.78. Ignition-extinction curves of methane conversion of Pd 150 catalyst: before (MI-374) and after (MI-376) thermal ageing test, and in the presence of water (MI-377) (CH<sub>4</sub> 4100±50 ppm, 5% vol. water, total flow rate 235 cc/min)

The experimental results of VTTA test are presented in figure 4.79. The initial activity for the first 350°C interval was around 74% conversion and it dropped to 59% conversion. The activity drops during each 350°C interval, as previously was seen for Pd 150 catalyst. However, the activity at the beginning of each 350°C interval is higher than the activity at the end of the previous 350°C interval. The activity of the 350°C intervals is decreasing continuously. After 26 hours of thermal ageing, the conversion of methane was around 20% conversion. When water was switched on the activity dropped to nearly 2% conversion, and to 1% after 5 hours of water exposure. When the water was switched off, the conversion of methane increased slightly and after 12 hours was 17%.

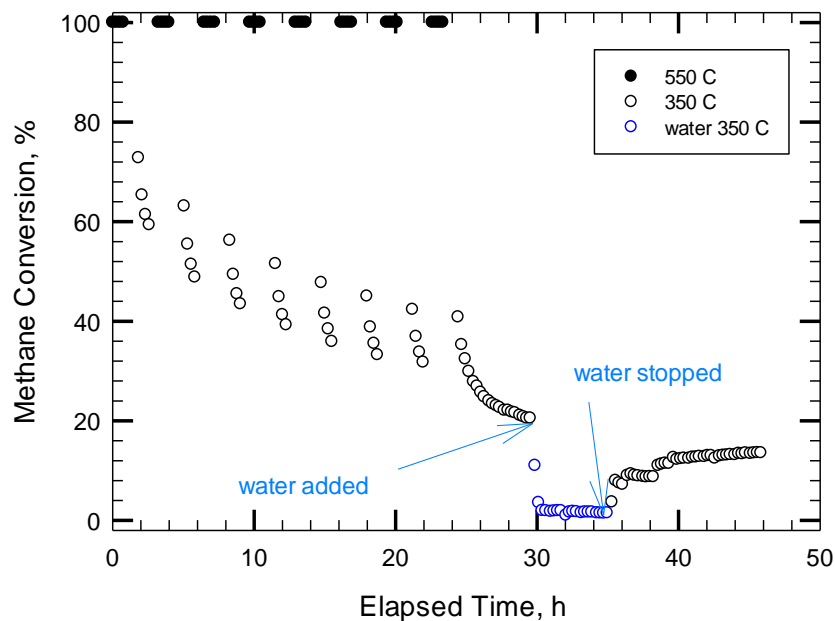


Figure 4.79. Variable temperature thermal ageing test for methane conversion over Pd 150 catalyst (CH<sub>4</sub> 4100±50 ppm, 5% vol. water, total flow rate 235 cc/min)

#### 4.7.1.2. Pd 122 catalyst

The ignition-extinction curves of methane conversion of Pd 122 catalyst, before (MI-362) and after (MI-364) the thermal ageing test as well as in the presence of water (MI-365) are presented in figure 4.80. 100% conversion of methane was obtained at 450°C for the first ignition-extinction cycle. T<sub>50</sub> of the light off curve was 335°C. The presence of a negative hysteresis can be observed (i.e. ignition more active than extinction). However, after the thermal ageing test, the ignition-extinction curves show a positive hysteresis, similar as for Pd 150 catalyst. 100% of methane conversion was obtained at 500°C and T<sub>50</sub> of the light off curve was 435°C. No hysteresis was observed for the ignition-extinction curves in presence of water. 100% conversion of methane was obtained at 550°C. T<sub>50</sub> of the light off curve was 470°C.

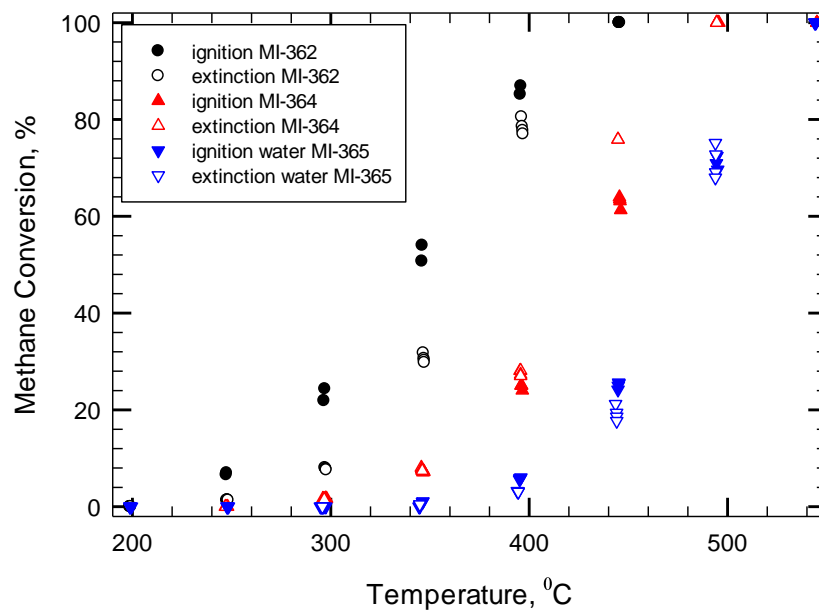


Figure 4.80. Ignition-extinction curve of methane conversion of Pd 122 catalyst: before (MI-362) and after (MI-364) thermal ageing, and in the presence of water (MI-365) (CH<sub>4</sub> 4100±50 ppm, 5% vol. water, total flow rate 235 cc/min)

The experimental results of variable temperature thermal ageing test are presented in figure 4.81. A decrease in catalytic activity can be observed for the fourth 450°C interval and continues for the all subsequent 450°C intervals. As for previously tested Pd catalysts, the activity of the 450°C interval is decreasing continuously. After 26 hours of thermal ageing, the conversion of methane was around 78%. The strong effect of water on the catalytic activity is given by the decrease in activity down to 22% conversion, after 5 hours of water exposure. When the water was switched off, the activity jumped to 41% conversion and continued to increase up to 62% conversion in the next 10 hours.

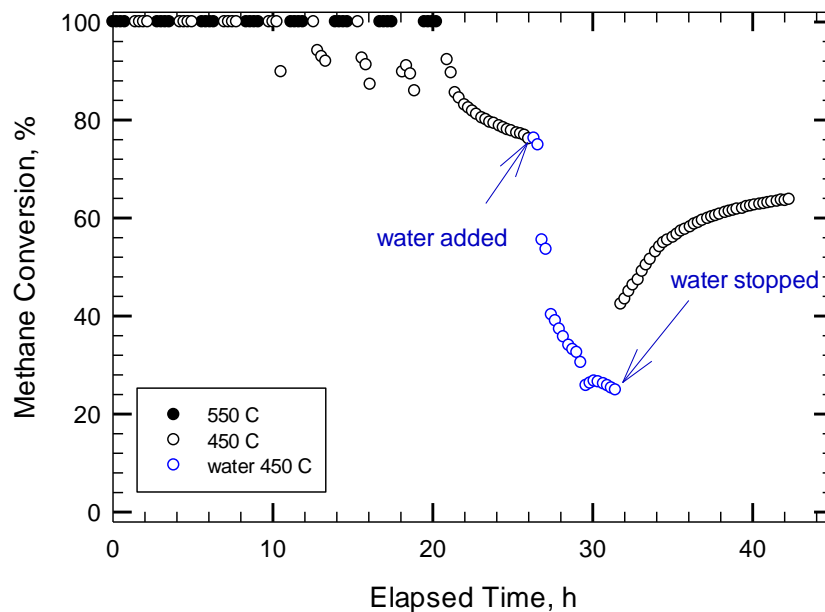


Figure 4.81. Variable temperature thermal ageing test for methane conversion over Pd 122 catalyst (MI-363) (CH<sub>4</sub> 4100±50 ppm, 5% vol. water, total flow rate 235 cc/min)

#### 4.7.1.3. Pd Rh 120 catalyst

##### *Variable temperature thermal ageing test at 350°C*

The same sequence of experiments was performed for PdRh 120 catalyst: ignition-extinction (MI-344), variable temperature thermal ageing test (MI-346), ignition-extinction after VTTAT (MI-347) and ignition-extinction in the presence of water (MI-348).

Figure 4.82 compares the ignition-extinction curves of PdRh 120 catalyst: before (MI-344) and after (MI-347) the thermal ageing test, and in the presence of water (MI-348). For the first ignition-extinction cycle, 100% conversion of methane was obtained at 450°C. The presence of a negative hysteresis can be observed (i.e. ignition more active than extinction). T<sub>50</sub> of the light off curve was 340°C. Thermal ageing process brings a decrease in the catalytic activity of the sample

(MI-347). 100% conversion of methane was obtained at 500°C. T50 of the light off temperature was 475°C. A small positive hysteresis loop can be observed, similar as for Pd 150 catalyst. The strong effect of water on the catalytic activity can be observed from the shift of the ignition-extinction curves toward higher temperatures (MI-348). 100% conversion of methane was obtained at 550°C. T50 of the light off curve was 485°C. The presence of a small negative hysteresis can be observed.

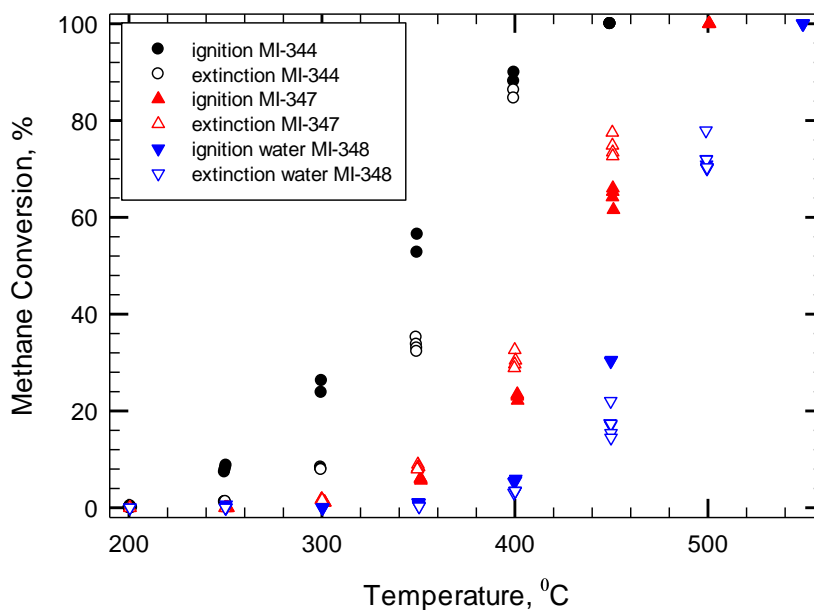


Figure 4.82. Ignition-extinction curve of methane conversion of PdRh catalyst: before (MI-344) and after (MI-347) thermal ageing test, and in the presence of water (MI-348) (CH<sub>4</sub> 4100±50 ppm, 5% vol. water, total flow rate 235 cc/min)

The experimental results of variable temperature thermal ageing test are presented in figure 4.83. The initial activity for the first 350°C interval was around 24% conversion and it dropped to 20% conversion. The activity drops during each 350°C interval, as previously was seen for Pd and predominantly Pd catalysts. Similarly with Pd catalyst, the activity at the beginning of each 350°C interval is higher than the activity at the end of the previous 350°C interval. As for

previously tested Pd catalysts, the activity of the 350°C intervals is decreasing continuously. After 26 hours of thermal ageing, the conversion of methane was around 14% conversion. When water was switched on the activity dropped to nearly zero % conversion. When the water was switched off, the activity increased to 13% conversion in 3 hours and stayed relatively constant for another 7 hours.

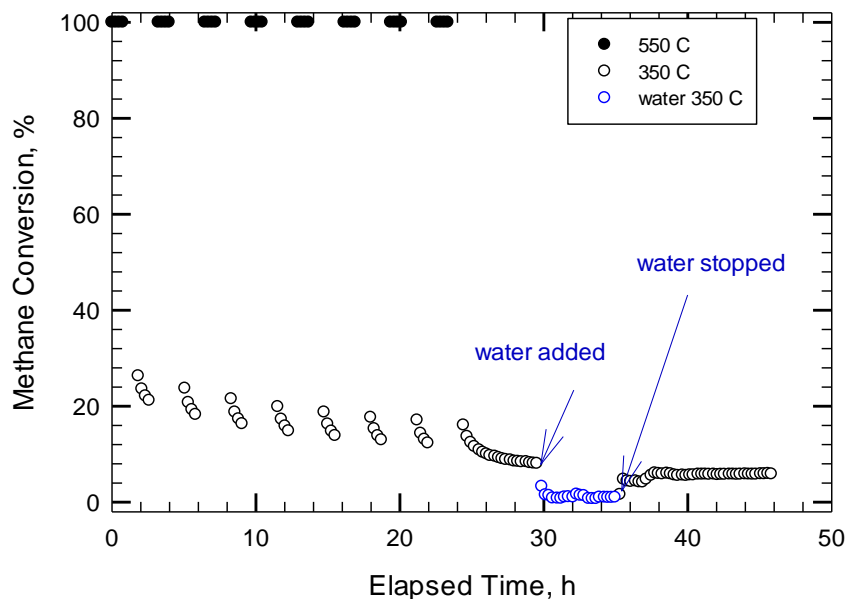


Figure 4.83. Variable temperature thermal ageing test of methane conversion of PdRh catalyst (MI-346) (CH<sub>4</sub> 4100±50 ppm, 5% vol. water, total flow rate 235 cc/min)

#### *Variable temperature thermal ageing test at 450°C*

Due to the low values obtained for PdRh catalyst for methane conversion during VTTA test, another VTTA test was performed at 450°C.

Figure 4.84 compares the ignition-extinction curves of methane conversion before (MI-349) and after the thermal ageing tests (MI-351), as well as in the presence of water (MI-352). The presence of a negative hysteresis was observed for the first ignition-extinction cycle (MI-349). The activity does not appear to be stable.

100% conversion of methane was obtained at 450°C. T50 of the light off curve was 340°C. After the thermal ageing test, a very small positive hysteresis can be observed (MI-351). 100% conversion of methane was obtained at 500°C. T50 of the light off curve was 425°C. However, the activity does not appear to be stable. The presence of a small positive hysteresis can be observed for the ignition-extinction cycle in the presence of water. 100% conversion of methane was obtained at 550°C. T50 of the light off curve was 485°C. However, the activity does not appear to be stable.

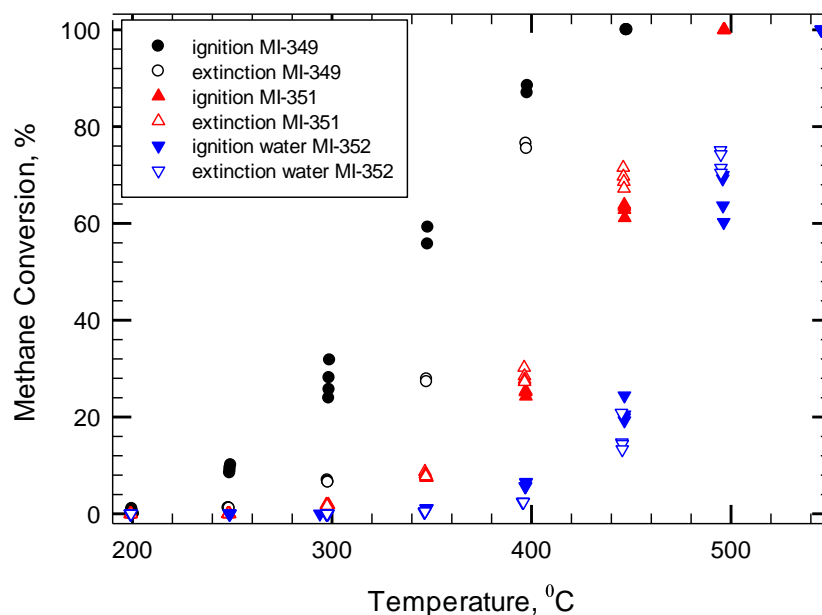


Figure 4.84. Ignition-extinction curves of methane conversion of PdRh catalyst: before thermal ageing (MI-349), after (MI-351) thermal ageing, and in the presence of water (MI-352) (CH<sub>4</sub> 4100±50 ppm, 5% vol. water, total flow rate 235 cc/min)

The experimental results of the variable temperature thermal ageing test are presented in figure 4.85. A decrease in catalytic activity can be observed for the sixth 450°C interval. Starting with the sixth 450°C interval, the activity drops during each 450°C interval, as previously was seen for Pd catalysts. The activity at the beginning of each 450°C interval is higher than the activity at the end of the

previous 450°C interval. The activity of the 450°C intervals is decreasing continuously. After 26 hours of thermal ageing, the conversion of methane was around 78% conversion. When water was switched on, the activity dropped to nearly 43% conversion and decreases continuously for the 5 hours of water treatment, down to 19% conversion. When the water was switched off, the activity jumped to 40% conversion and continued to increase up to 62% in the next 10 hours.

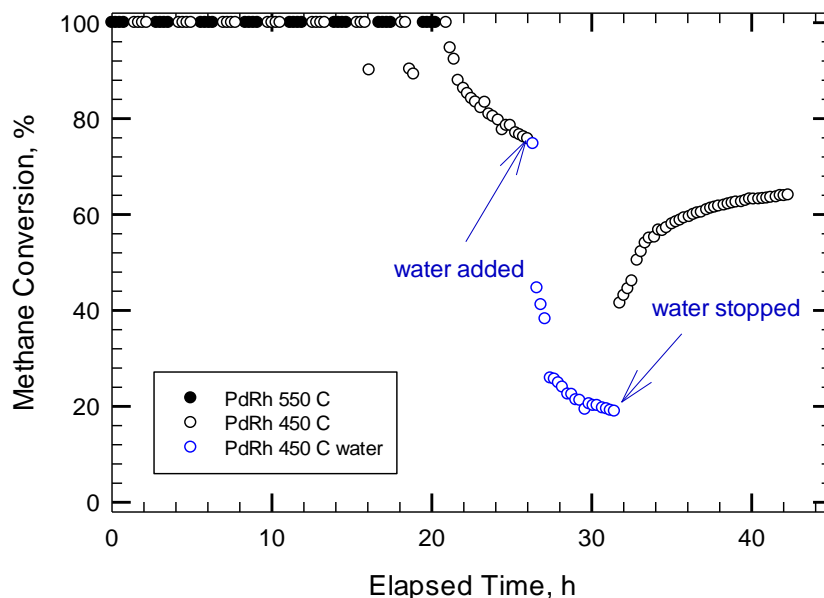


Figure 4.85. Variable temperature thermal ageing test of methane conversion of PdRh catalyst (MI-350) (CH<sub>4</sub> 4100±50 ppm, 5% vol. water, total flow rate 235 cc/min)

Figure 4.86 compares the experimental results of variable temperature thermal ageing test at 350°C and 450°C. The big difference in the catalytic activity can be explained by the effect of water as a function of temperature: at 450°C and above, water plays a less important role in the catalyst deactivation compared with lower temperatures. No phase transformation of Pd takes place at 450°C, and in consequence it is assumed that the difference in methane conversion for the two tests is just due to the difference in the way water is adsorbed on Pd surface at the two temperatures.

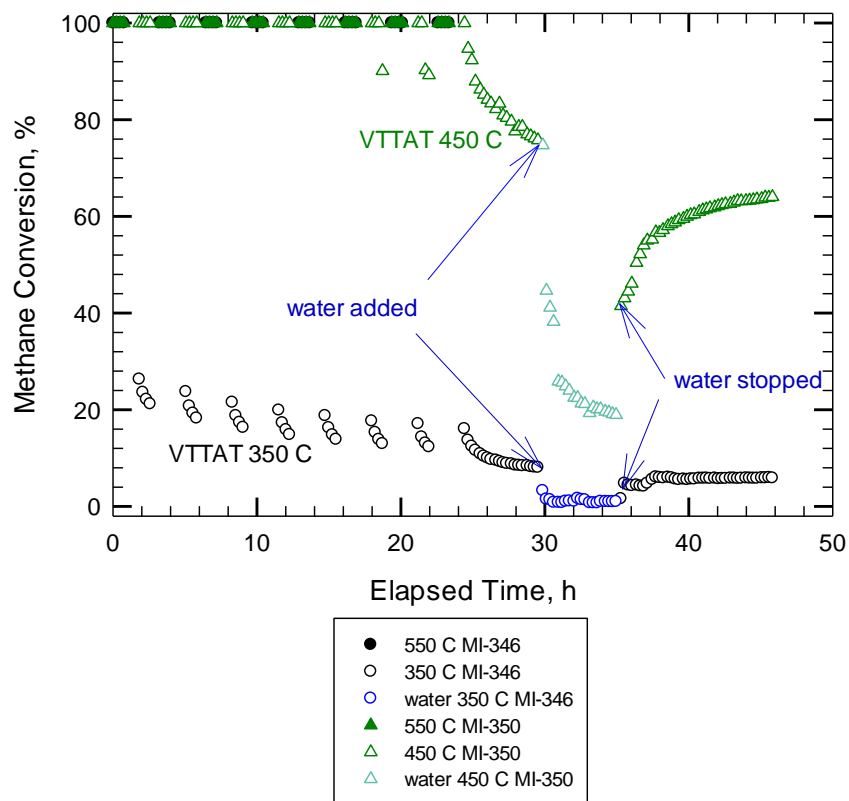


Figure 4.86. Comparison of VTTA 350 (MI-346) and VTTA 450 (MI-350) tests of methane conversion of PdRh catalyst (CH<sub>4</sub> 4100±50 ppm, 5% vol. water, total flow rate 235 cc/min)

#### 4.7.1.4. PtPdRh catalyst

A thermal ageing sequence was performed for PtPdRh catalyst: ignition-extinction (MI-323), variable temperature thermal ageing test (MI-327), ignition extinction after VTTAT (MI-328) and ignition-extinction in the presence of water (MI-329).

Figure 4.87 compares the ignition-extinction curves before (MI-323) and after (MI-328) thermal ageing test, as well as in the presence of water (MI-329). 100% conversion of methane was obtained at 500°C for the first ignition-extinction cycle. The presence of a negative hysteresis can be observed (i.e. ignition more active than extinction). T<sub>50</sub> of the light off curve was 370°C. As a result of VTTA test, the activity of the catalyst decreases (MI-328). 100% conversion of methane

was obtained at 550°C. T50 for the light off curve was 480°C. A small positive hysteresis can be observed. In presence of water, 71% conversion of methane was obtained at 550°C. T50 of the light off curve was 510°C. A small negative hysteresis can be observed. From the ignition-extinction results it can be concluded that PtPdRh catalyst show a low activity and stability in the conversion of methane.

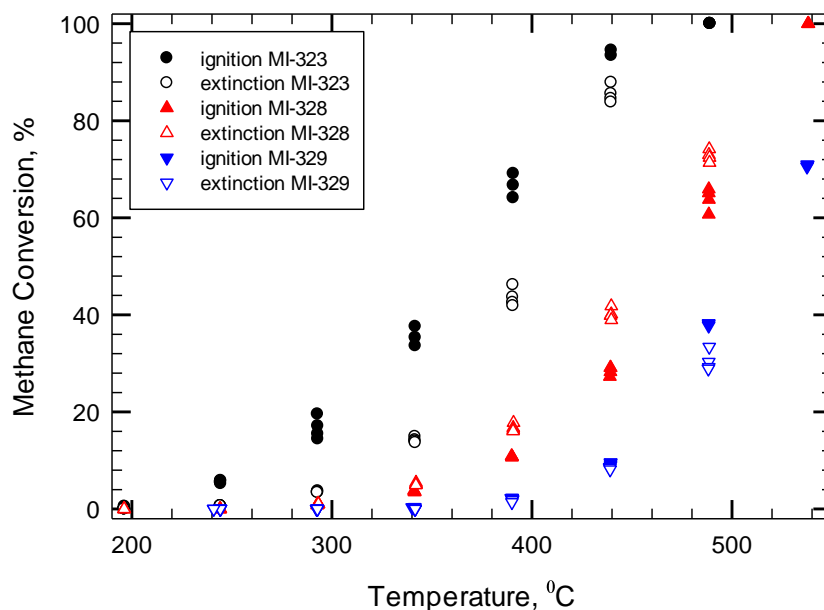


Figure 4.87. Ignition-extinction curves of methane conversion of PtPdRh catalyst: before (MI-323) and after (MI-328) thermal ageing, and in the presence of water (MI-329) (CH<sub>4</sub> 4100±50 ppm, 5% vol. water, total flow rate 235 cc/min)

The experimental results of variable temperature thermal ageing test are presented in figure 4.88. The initial activity for the first 450°C interval was around 70% conversion and it dropped to 61% conversion. The activity drops during each 450°C interval. Also, the activity at the beginning of each 450°C interval is higher than the activity at the end of the previous 450°C interval. However, the activity of the 450°C intervals is decreasing continuously. After 26 hours of thermal ageing, the conversion of methane was around 42% conversion. When water was

switched on the activity dropped to nearly 20% conversion and decreases continuously for the next 5 hours of water treatment, down to 10% conversion. When the water was switched off, the conversion jumped to 20% conversion and continued to increase up to 40% conversion, in 10 the next hours.

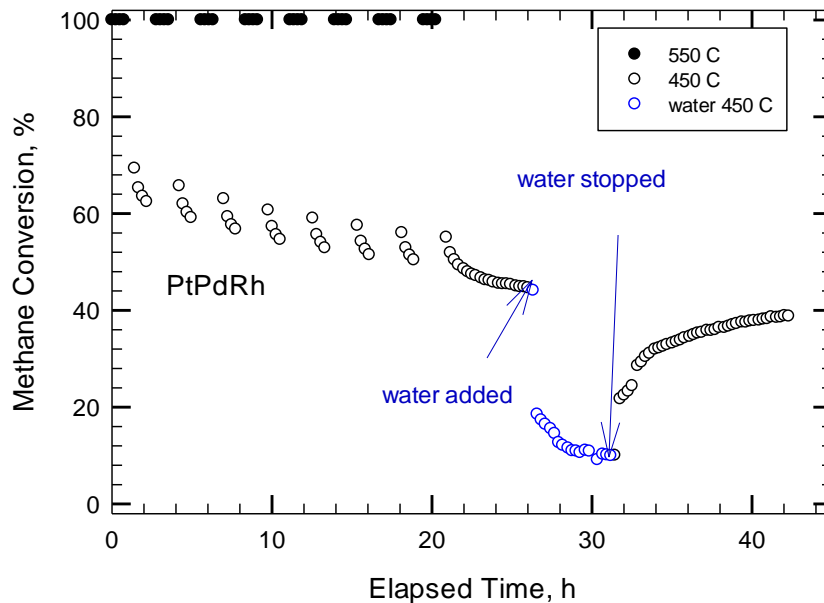


Figure 4.88. Variable temperature thermal ageing test of methane conversion of PtPdRh catalyst (MI-327) (CH<sub>4</sub> 4100±50 ppm, 5% vol. water, total flow rate 235 cc/min)

#### 4.4.1.6. Pt-Pd (1:5) catalyst

##### Variable temperature thermal ageing test at 350°C

Due to the high activity in methane conversion of Pt-Pd (1:5) catalyst, a thermal ageing test at 550°C with activity measured at 350°C was performed.

Figure 4.89 compares the ignition-extinction curves before thermal ageing (MI-286) and after thermal ageing (MI-290). 100% conversion of methane was obtained at 350°C for the first ignition-extinction cycle (MI-286). The presence of a small negative hysteresis can be observed (i.e. ignition more active than

extinction). T50 of the light off curve was 280°C. The strong effect of thermal ageing can be observed from the shift of the ignition-extinction curves toward higher temperatures (MI-290). For example, at 350°C, the conversion of methane was 100% before the VTTA test and just 10% after the thermal ageing process. 100% conversion of methane was obtained at 500°C and T50 of the light off curve was 415°C.

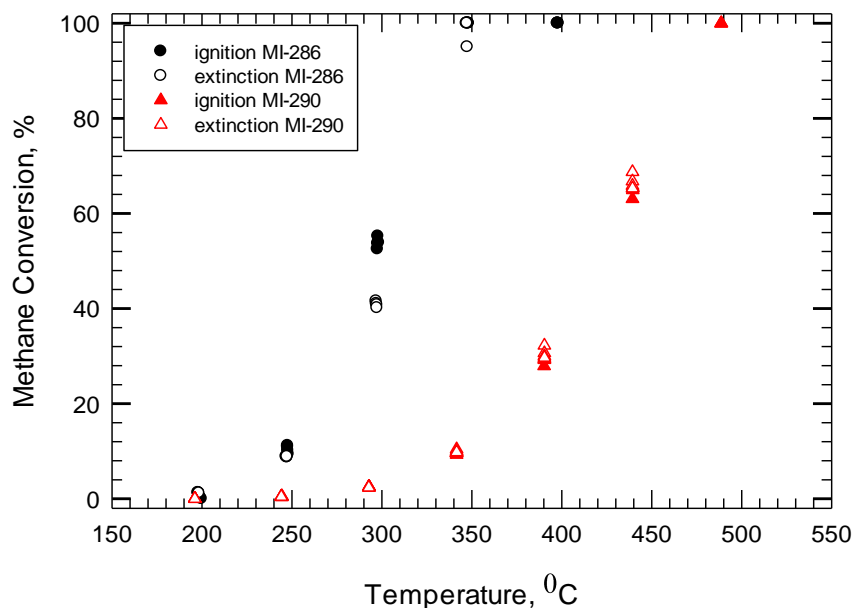


Figure 4.89. Ignition-extinction curves of methane conversion in presence of Pt-Pd (1:5) catalyst: before (MI-286) and after (MI-290) thermal ageing test (CH<sub>4</sub> 4100±50 ppm, total flow rate 235 cc/min)

The experimental results of variable temperature thermal ageing test are presented in figure 4.90. The initial activity of the first 350°C interval was around 80% conversion and it dropped to 77% conversion. The activity drops during each 350°C interval. Similar with Pd catalysts, the activity at the beginning of each 350°C interval is higher than the activity at the end of the previous 350°C interval. The activity of the 350°C intervals is decreasing continuously. After 30 hours of thermal ageing, the conversion of methane was around 68% conversion.

When water was switched on the activity dropped to 15% conversion. When the water was switched off, the activity jumped to 22% and 49% conversion in less than an hour, and continued to increase for another 9 hours, up to 62% conversion.

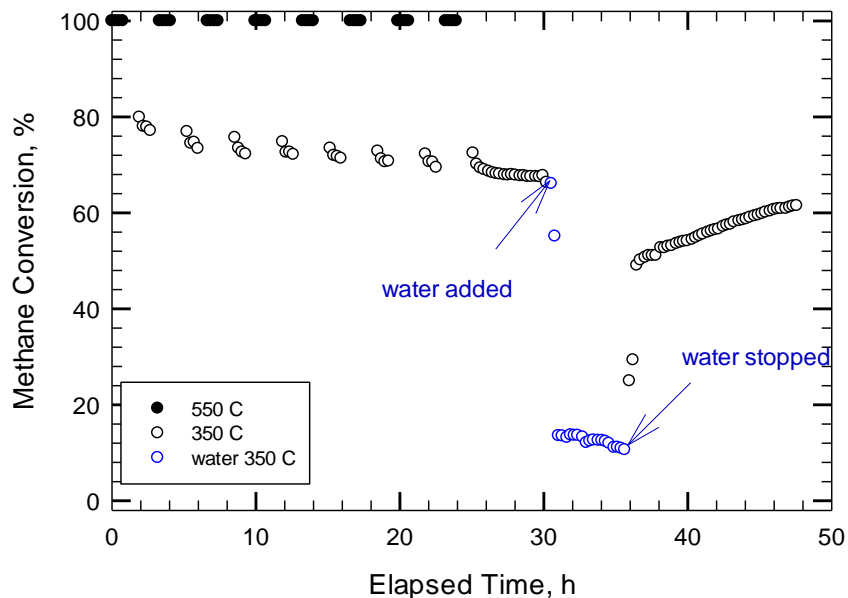


Figure 4.90. Variable temperature thermal ageing test of methane conversion of Pt-Pd (1:5) catalyst (MI-289) (CH<sub>4</sub> 4100±50 ppm, 5% vol. water, total flow rate 235 cc/min)

## Conclusions

### *Contribution of Rh to the activity of Pd 122 catalyst*

Figure 4.91 compares the initial activities of Pd 122 and Pd Rh catalysts. It can be observed that the activity of the catalysts is similar. 100% conversion was obtained at 450°C. T50 of the light off curve was 350°C. Both catalysts show a large negative hysteresis. The activity of Pt 122 and PdRh does not appear to be stable.

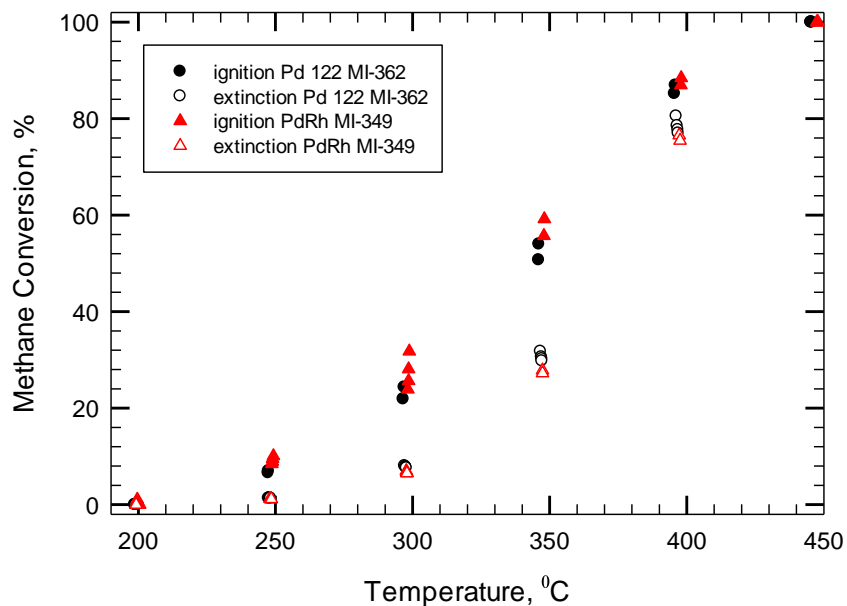


Figure 4.91. Ignition-extinction curves of methane conversion of Pd 122 (MI-362) and PdRh (MI-349) catalysts (CH<sub>4</sub> 4100±50 ppm, total flow rate 235 cc/min)

Figure 4.92 compares the experimental results of variable temperature thermal ageing test of Pd 122 and PdRh catalysts. It can be observed that PdRh catalyst starts to deactivate at the sixth 450°C interval compared with Pd 122 which starts to deactivate at the fourth 450°C interval. After 26 hours of thermal ageing, both catalysts show a drop down to 78% conversion of methane. However, when water is added to the catalysts, Pd 122 catalyst shows a better resistance to water deactivation. The activity of the catalysts decreases 22% conversion for Pd 122 compared with 19% conversion for PdRh catalyst. Interestingly, when water is switched off, the activity of both catalysts jumps to 40% conversion and continues to increase up to 62% in the next 10 hours.

Figure 4.93 compares the activities of Pd 122 and PdRh catalyst after the VTTA test. It can be observed that the Pd 122 and PdRh catalysts show similar activities, i.e. 100% conversion was obtained at 500°C. T<sub>50</sub> of the light off curve was 425°C.

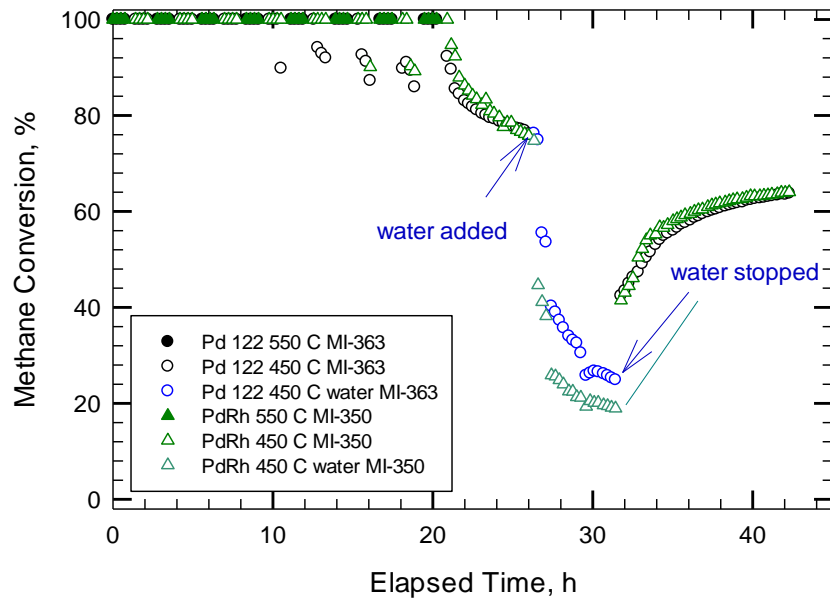


Figure 4.92. Variable temperature thermal ageing test of methane conversion of Pd 122 (MI-363) and PdRh (MI-350) catalysts (CH<sub>4</sub> 4100±50 ppm, 5% vol. water, total flow rate 235 cc/min)

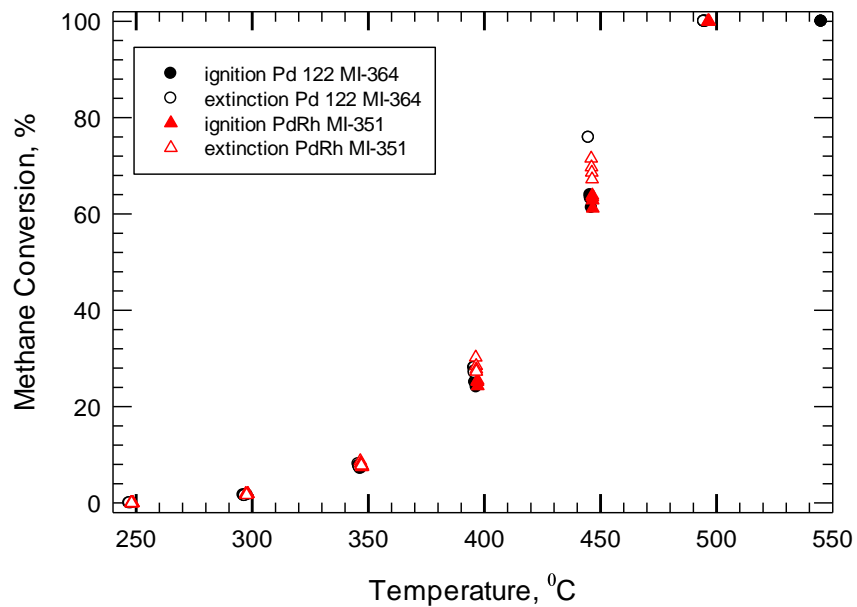


Figure 4.93. Ignition-extinction curves of methane conversion of Pd 122 (MI-364) and PdRh (MI-351) after VTTA test (CH<sub>4</sub> 4100±50 ppm, total flow rate 235 cc/min)

### Contribution of Pt to the activity of PdRh catalyst

Figure 4.94 compares the ignition-extinction curves of methane conversion over PdRh (MI-349) and PtPdRh (MI-323) catalysts. It can be observed that PdRh catalyst shows a slightly higher activity of methane conversion compared with PtPdRh catalyst.

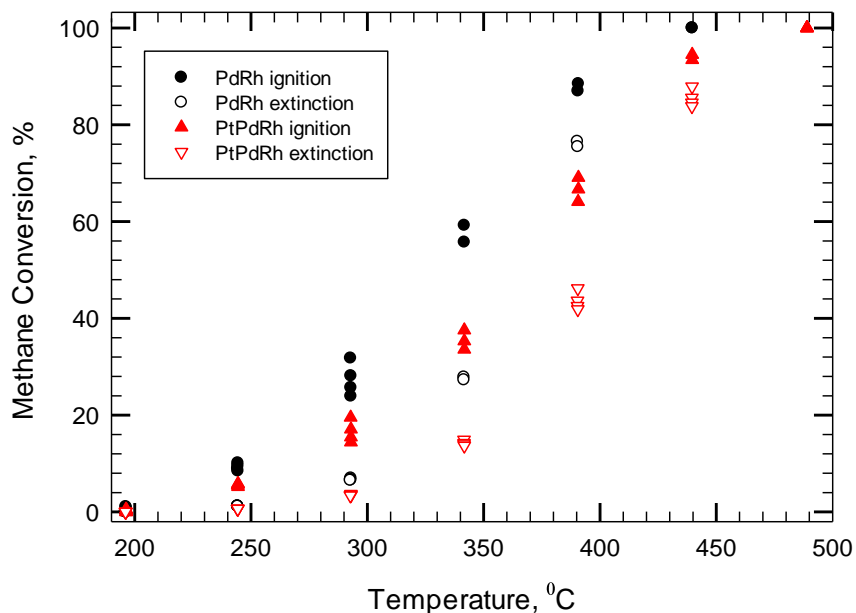


Figure 4.94. Ignition-extinction curves of methane conversion of PdRh (MI-349) and PtPdRh (MI-323) catalysts (CH<sub>4</sub> 4100±50 ppm, total flow rate 235 cc/min)

Figure 4.95 compares the experimental results for variable temperature thermal ageing test for PdRh and PtPdRh catalysts. Even if the lower temperature is the same for both catalysts, PtPdRh show a lower activity in methane conversion. The lower activity in PtPdRh can be assumed to be due to lower Pd loading. However, in presence of water, the drop in PtPdRh catalytic activity is smaller than for PdRh catalyst. This behaviour is assumed to be due to the presence of Pt, which brings resistance to water deactivation.

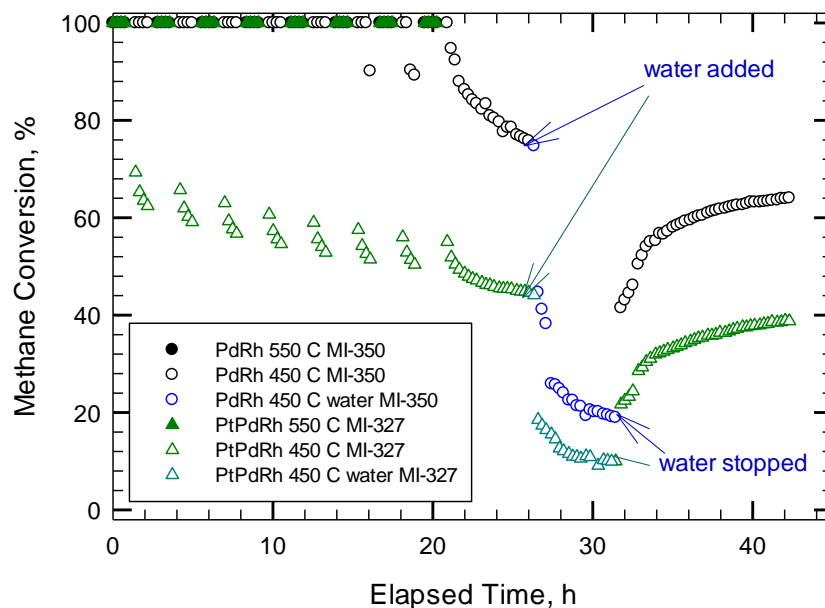


Figure 4.95. Variable temperature thermal ageing test for methane conversion over PdRh (MI-350) and PtPdRh catalysts (MI-327) ( $\text{CH}_4$   $4100 \pm 50$  ppm, 5% vol. water, total flow rate 235 cc/min)

Figure 4.96 compares the experimental results of methane conversion after variable temperature thermal ageing test for PdRh (MI-351) and PtPdRh (MI-328) catalysts. One can observe that PdRh catalyst shows a higher catalytic activity of methane conversion compared with PtPdRh catalyst. For example, if we look at the light off curve, at  $450^\circ\text{C}$  a conversion of methane of 63% was obtained for PdRh catalyst, compared with 30% conversion of methane for the PtPdRh catalyst.

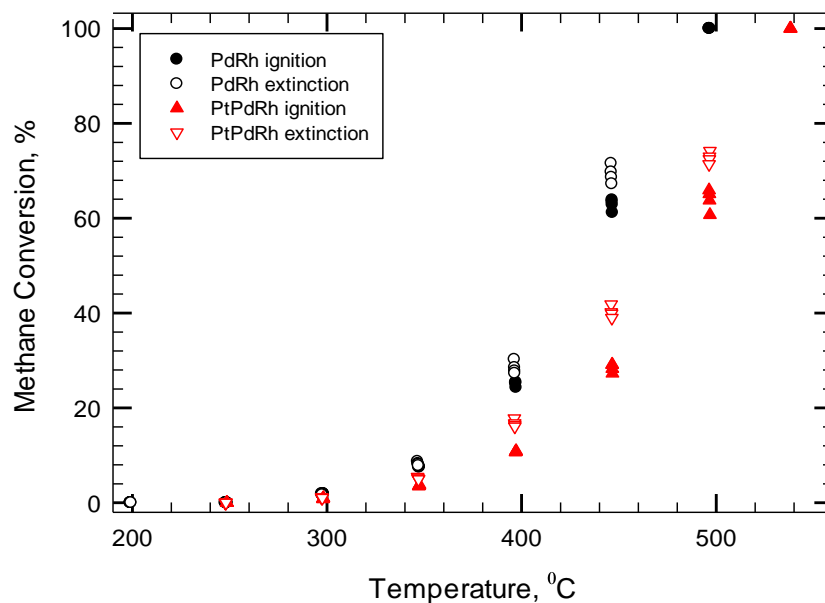


Figure 4.96. Ignition-extinction curves of methane conversion after VTTAT, of PdRh (MI-351) and PtPdRh (MI-328) catalysts (CH<sub>4</sub> 4100±50 ppm, total flow rate 235 cc/min)

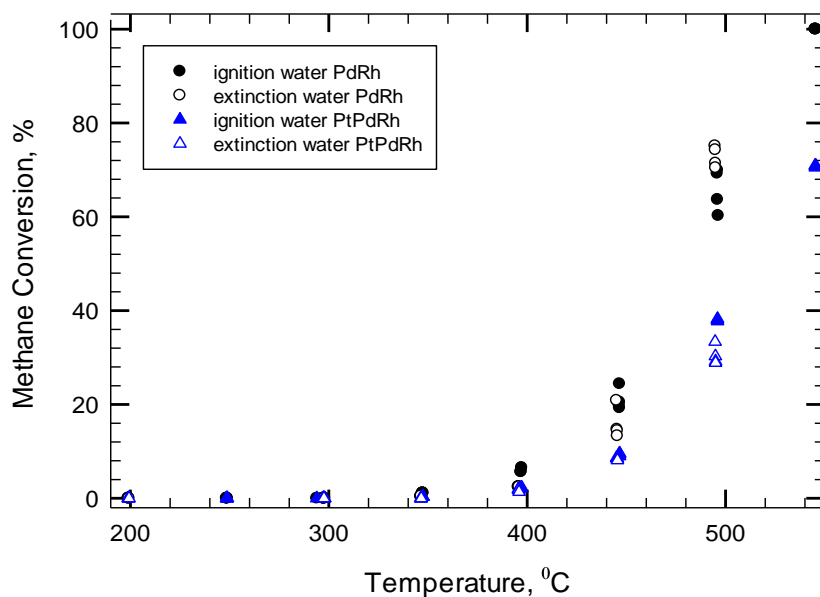


Figure 4.97. Ignition-extinction of methane conversion in presence of water of PdRh (MI-352) and PtPdRh (MI-329) catalysts (CH<sub>4</sub> 4100±50 ppm, 5% vol. water, total flow rate 235 cc/min)

Figure 4.97 compares the experimental results of methane conversion in presence of water for PdRh and PtPdRh catalysts. One can observe that PtPdRh catalyst shows a lower resistance to water inhibition compared with PdRh catalyst. For example for the light off curve, 64% conversion of methane is obtained for PdRh catalyst at 500°C, compared with just 40% conversion of methane for PtPdRh catalyst.

*Contribution of Pt to the activity of Pd catalyst*

Figure 4.98 compares the experimental results of Pd 150 (MI-374) and Pt-Pd (1:5) (MI-286) catalysts. It can be observed that Pt-Pd (1:5) catalyst show a higher activity in methane conversion. For example, the activity of Pt-Pd (1:5) at 300°C is 57% conversion and the activity of Pd 150 at 300°C is 46% conversion. This can be assumed to be due to the effect of Pt.

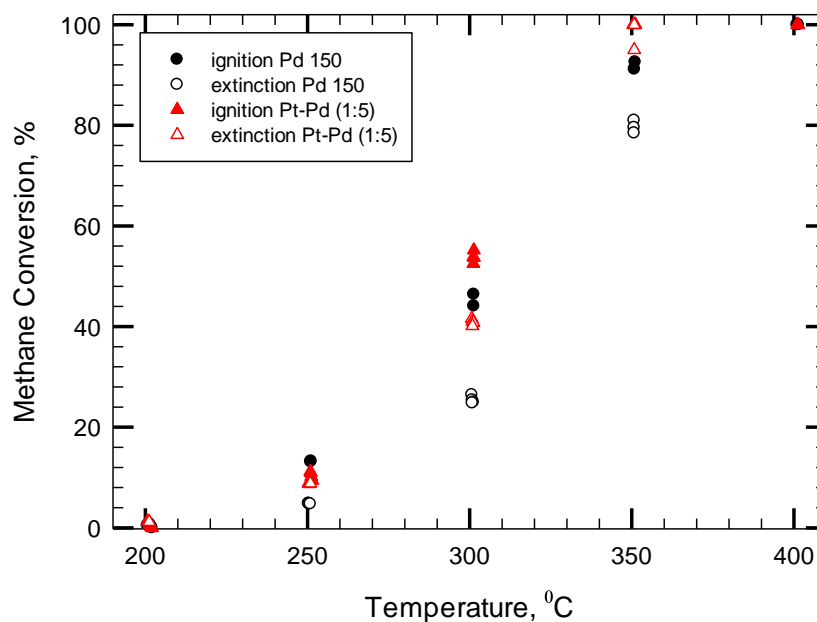


Figure 4.98. Ignition-extinction curves for methane conversion over Pd 150 (MI-374) and Pt-Pd (1:5) (MI-286) catalysts (CH<sub>4</sub> 4100±50 ppm, total flow rate 235 cc/min)

Figure 4.99 compares the experimental results of VTTA test of Pd 150 and Pt-Pd (1:5) catalysts. In absence of water added to the reactant stream, Pt-Pd (1:5) catalysts shows a higher stability during the thermal ageing test, compared with Pd 150 catalyst. The difference in catalytic activity is assumed to be due to the presence of Pt catalyst.

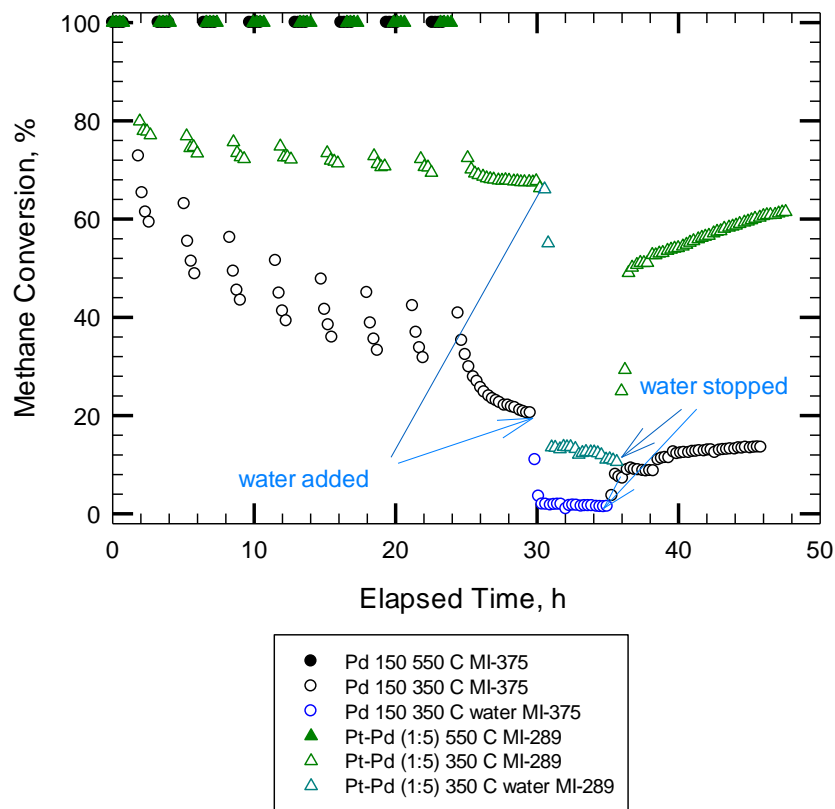


Figure 4.99. Variable temperature thermal ageing test for Pd 150 (MI-375) and Pt-Pd (1:5) (MI-289) catalysts (CH<sub>4</sub> 4100±50 ppm, total flow rate 235 cc/min)

Figure 4.100 compares the ignition-extinction results of methane conversion after VTTA test of Pd 150 (MI-376) and Pt-Pd (1:5) (MI-290) catalysts. After the thermal ageing test, Pd 150 shows a higher activity compared with Pt-Pd (1:5) catalyst.

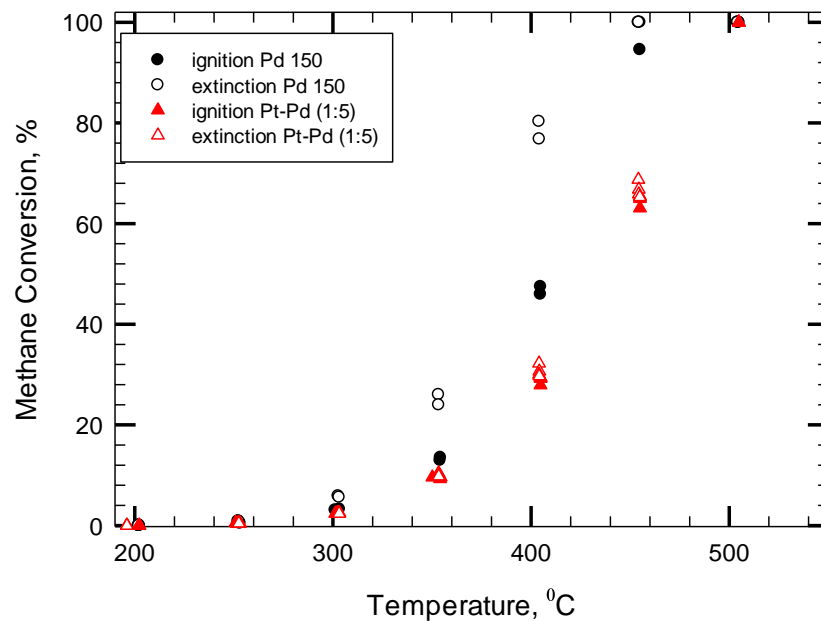


Figure 4-100. Ignition-extinction curves of methane conversion of Pd 150 (MI-376) and Pt-Pd (1:5) (MI-290) catalysts (CH<sub>4</sub> 4100±50 ppm, total flow rate 235 cc/min)

#### 4.7.2. Variable temperature hydrothermal ageing test (VTHTAT), hydrothermally aged at 550°C

In the beginning of the sequence, an ignition-extinction test was performed to assess the activity of the catalyst.

The variable temperature hydrothermal ageing test was designed to hydrothermally age the catalyst at 550°C and measure the activity in presence of water at a lower temperature, depending on the initial activity of the catalyst.

Another ignition-extinction test was performed to assess the changes in the catalytic activity. For some sequences, the activity of the catalyst was also assessed in presence of water.

#### 4.7.2.1. Pd 150 catalyst

##### *Variable temperature hydrothermal ageing at 450°C*

The changes in catalytic activity of the sample were assessed from the change in ignition-extinction curves before thermal ageing (MI-339), after thermal ageing (MI-342) and in the presence of water (MI-343) (figure 4.101). A small negative hysteresis can be observed for the first ignition-extinction cycle (MI-339). 100% conversion of methane was obtained at 400°C. T50 of the light off curve was 310°C. No hysteresis was observed for the ignition-extinction cycle after the thermal ageing. 100% conversion of methane was obtained at 400°C. T50 for the light off curve was 605°C. The decrease in catalytic activity observed after the hydrothermal ageing of the Pd 150 catalyst is assumed to be due to the sintering of metal particles. In the presence of water, a negative hysteresis can be observed. 100% conversion of methane was obtained at 550°C. T50 for the light off curve was 470°C.

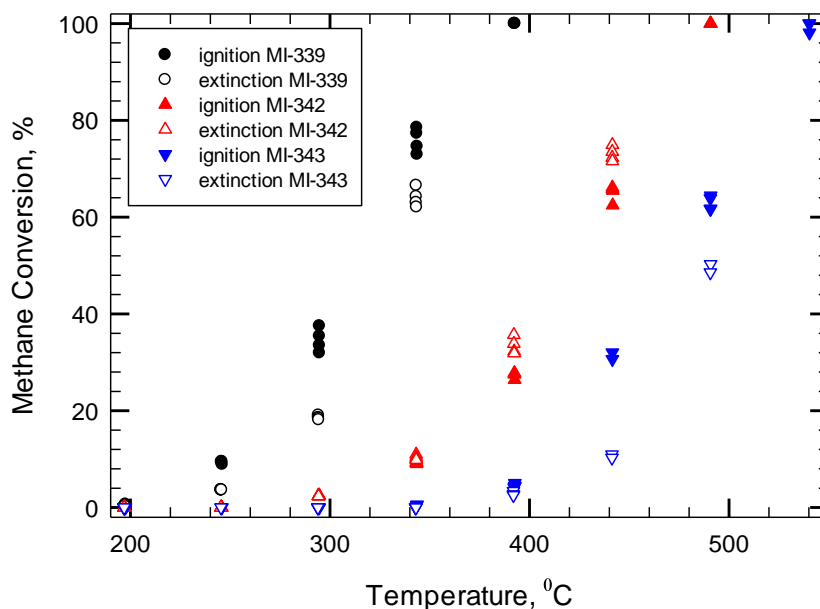


Figure 4.101. Ignition-extinction curves of methane conversion of Pd 150 catalyst: before (MI-339) and after (MI-342) thermal ageing, and in the presence of water (MI-343) (CH<sub>4</sub> 4100±50 ppm, 5% vol. water, total flow rate 235 cc/min)

From the VTHTA test results for Pd 150 catalyst it can be observed that the first activity point at 450°C interval was about 77% methane conversion and the activity dropped to 40% conversion (figure 4.102). The activity drops during each 450°C interval, as previously was seen for Pd 150 catalyst. However, the activity at the beginning of each 450°C interval is higher than the activity at the end of the previous 450°C interval. The activity of the 450°C intervals is decreasing continuously. After 33 hours of hydrothermal ageing, the conversion of methane was around 10% conversion. When water was switched off the activity jumped to 30% conversion and continued to increase up to 66% conversion in 10 hours. The decrease of catalytic activity of methane conversion in presence of water is assumed to be due to the strong inhibition effect of water on Pd catalyst.

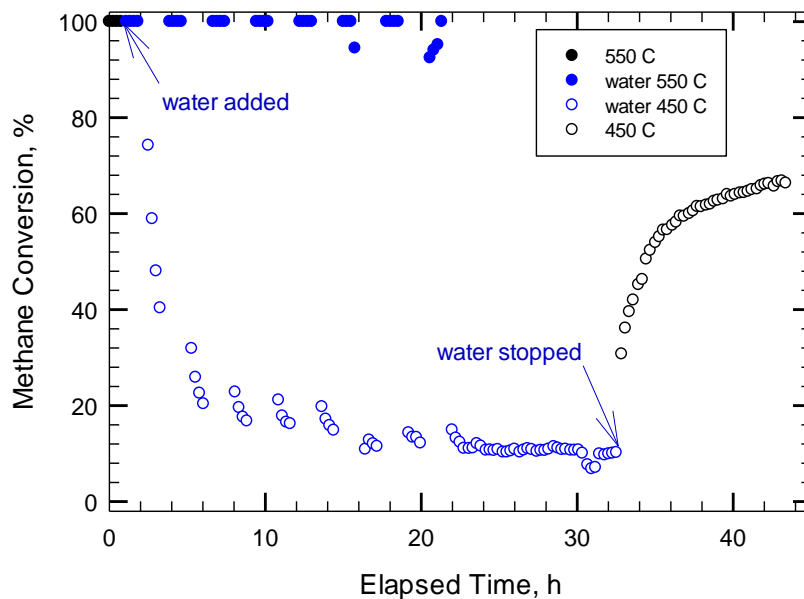


Figure 4.102. Variable temperature hydrothermal ageing test of methane conversion of Pd 150 catalyst (MI-341) (CH<sub>4</sub> 4100±50 ppm, 5% vol. water, total flow rate 235 cc/min)

#### 4.7.2.2. Pd 122 catalyst

Figure 4.103 compares the ignition-extinction curves of Pd 122 catalyst before (MI-357) and after (MI-359) the thermal treatment as well as in the presence of water. 100% conversion for the first ignition-extinction cycle was obtained at

450°C. T50 of the light off curve was 350°C. A small negative hysteresis can be observed. However, the activity does not appear to be stable for the light off curve. For the ignition-extinction cycle after VTHTA test it is interesting to observe that Pd 122 catalyst presents a small negative hysteresis loop. All previously tested Pd catalysts (i.e. Pd 150, Pt-Pd (1:5)) presented a positive hysteresis after the VTHTA test. However, 100% conversion of methane was obtained at 500°C. T50 of the light off curve was 415°C. The strong effect of water on the catalytic activity of Pd 122 can be observed from the drop in the conversion, i.e. at 500 C, 100% conversion of methane was obtained in absence of water, compared with 55% conversion of methane in presence of water. 100% conversion was obtained at 550°C. T50 of the light off curve was 485°C.

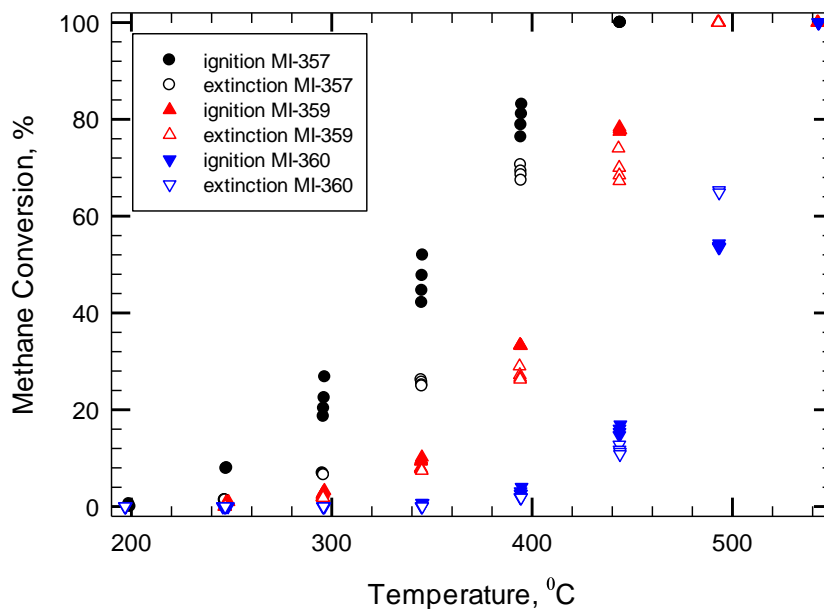


Figure 4.103. Ignition-extinction curves for methane conversion over Pd 122 catalyst: before (MI-357) and after (MI-359) VTHTAT, and in the presence of water (MI-360) (CH<sub>4</sub> 4100±50 ppm, 5% vol. water, total flow rate 235 cc/min)

Figure 4.104 presents the experimental results of variable temperature hydrothermal ageing test of Pd 122 catalyst. The strong effect of water on the catalytic activity can be observed from the decrease in activity. It can be observed that the first activity point at 450°C interval was about 69% methane conversion

and it dropped to 41% conversion. Similar like Pd 150 catalyst, the activity drops during each 450°C interval. The activity at the beginning of each 450°C interval is higher than the activity at the end of the previous 450°C interval. The activity of the 450°C intervals was decreasing continuously. After 33 hours of hydrothermal ageing, the conversion of methane was around 10% conversion. When water was switched off the activity jumped to 21% conversion and continued to increase up to 45% conversion in 10 hours.

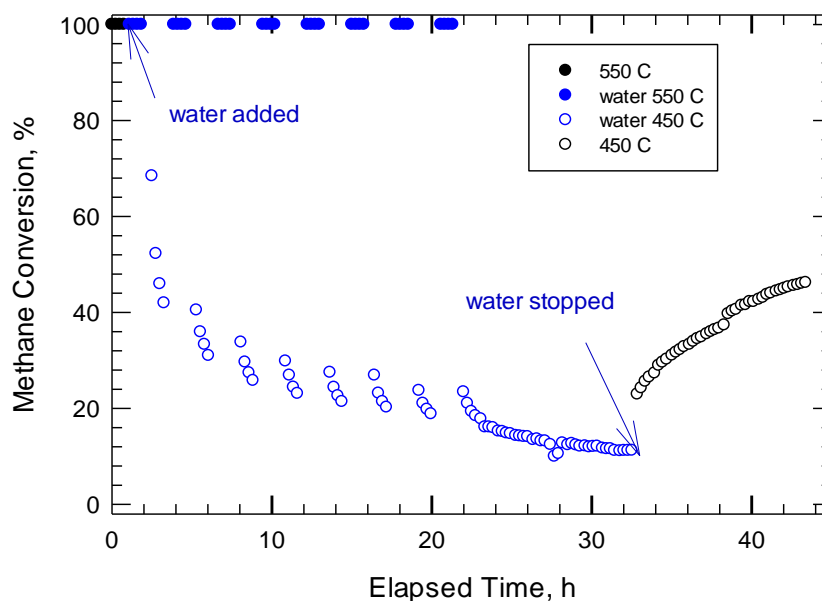


Figure 4.104. Variable temperature hydrothermal ageing test of methane conversion of Pd 122 catalyst (MI-358) (CH<sub>4</sub> 4100±50 ppm, total flow rate 235 cc/min)

#### 4.7.2.3. PdRh catalyst

A similar hydrothermal ageing sequence was performed for PdRh catalyst: ignition-extinction (MI-370), variable temperature hydrothermal ageing test (MI-371), ignition extinction after VTHTAT (MI-372) and ignition-extinction in the presence of water (MI-373).

Figure 4.105 compares the ignition-extinction curves of methane conversion before hydrothermal ageing (MI-370), after the hydrothermal ageing (MI-372) and in the presence of water (MI-373). The presence of a large negative hysteresis can be observed for the first ignition-extinction cycle. 100% conversion was obtained at 450°C. T50 for the light off curve was 350°C. However, the activity of the light off curve does not seem to be stable. After the VTHTA test, a positive hysteresis loop can be observed. 100% conversion was obtained at 550°C. T50 of the light off curve was 450°C. No hysteresis was observed for methane conversion cycle in presence of water. 84% conversion of methane was obtained at 550°C. T50 of the light off curve was 500°C.

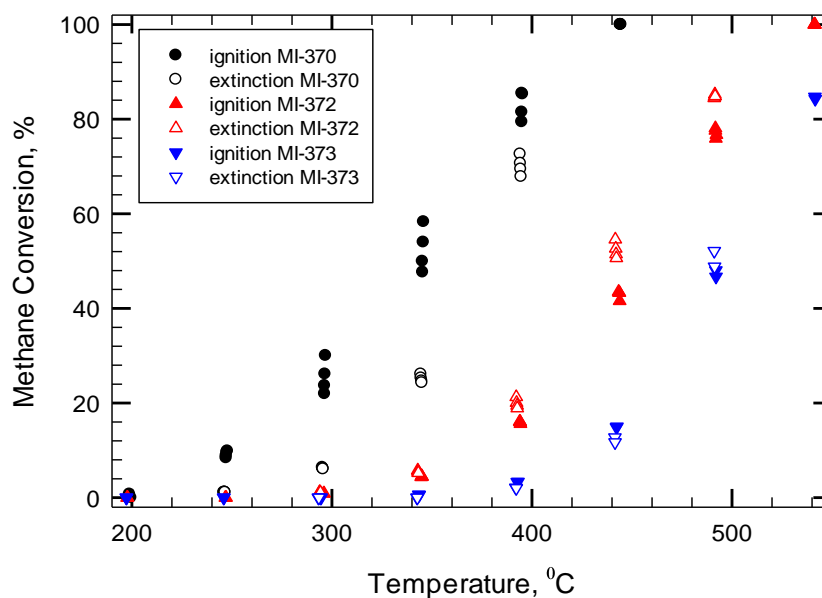


Figure 4.105. Ignition-extinction curve for methane conversion over PdRh catalyst: before (MI-370) and after (MI-372) thermal ageing and in the presence of water (MI-373) (CH<sub>4</sub> 4100±50 ppm, 5% vol. water, total flow rate 235 cc/min)



#### 4.7.2.4. PtPdRh catalyst

Figure 4.107 shows the changes in the catalytic activity as a result of hydrothermal ageing, as well as the water effect on the catalytic activity. The ignition-extinction cycle performed to assess the initial catalytic activity (MI-319) was compared with the ignition-extinction cycle after VTHTA test (MI-321) and with the ignition-extinction cycle performed in the presence of water (MI-322). A large negative hysteresis loop can be observed from the first ignition-extinction cycle. 100% conversion of methane was obtained at 500°C. T50 of the light off curve was 365°C. However, after the hydrothermal ageing, a small positive hysteresis can be observed, similar as for PdRh catalyst (MI-321). 100% conversion of methane was obtained at 550°C. T50 of the light off curve was 470°C. The decrease in activity is assumed to be due to the sintering process of the metal particles, i.e. at 450°C, the activity of the light off curve of PtPdRh catalyst decreases from 95% conversion (MI-319) to 33% conversion (MI-321). The effect of water on the catalytic activity can be observed from the third ignition-extinction cycle (MI-322). Around 75% conversion of methane was obtained at 550°C. T50 of the light off curve was 520°C. The inhibition effect of water can be observed from the decrease in the conversion of methane from 64% in absence of water (MI-321) to 30% conversion in presence of water (MI-322). These results highlight the poor resistance to water deactivation of PtPdRh catalyst.

Figure 4.108 presents the experimental results of variable hydrothermal ageing test for methane conversion of PtPdRh catalyst. It can be observed that the first activity point at 450°C interval was about 25% methane conversion and it dropped to 17% conversion. The activity drops during each 450°C interval, as previously was seen for PdRh catalyst. Similar, the activity at the beginning of each 450°C interval is higher than the activity at the end of the previous 450°C interval. It can also be observed that the activity of the 450°C intervals is decreasing continuously.

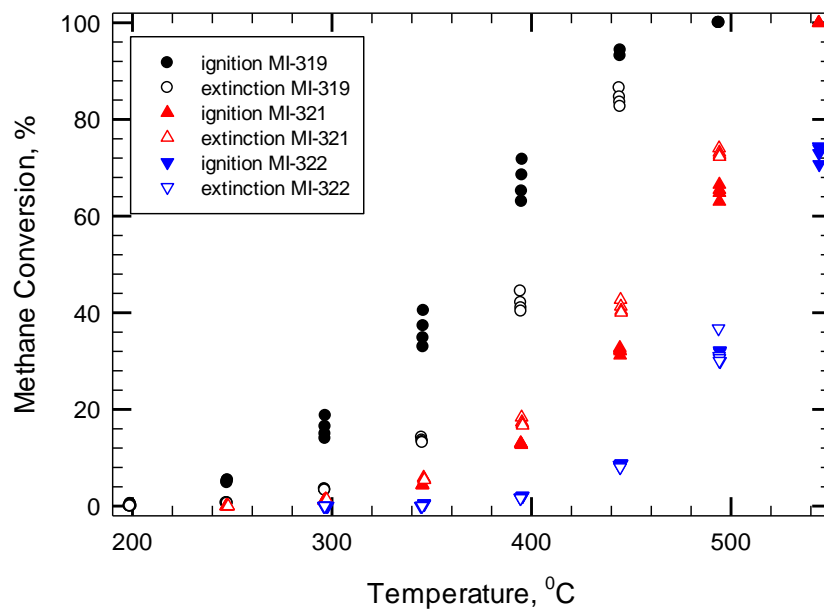


Figure 4.107. Ignition-extinction curve of methane conversion over PtPdRh catalyst (MI-319) (CH<sub>4</sub> 4100±50 ppm, 5% vol. water, total flow rate 235 cc/min)

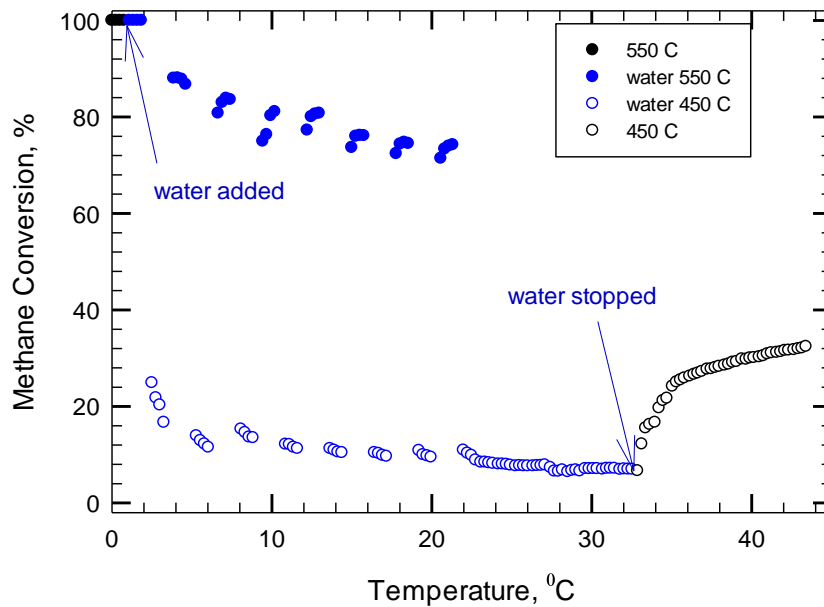


Figure 4.108. Variable temperature hydrothermal ageing test of methane conversion of PtPdRh catalyst (MI-320) (CH<sub>4</sub> 4100±50 ppm, 5% vol. water, total flow rate 235 cc/min)

A decline in catalytic activity of the 550°C thermal ageing interval can also be observed for PtPdRh catalyst. The decline starts with the second 550°C interval. The first activity for the second 550°C interval was about 88% conversion and it dropped to 86% conversion. The activity drops during each 550°C interval. However, one can observe that for the third and all the subsequent 550°C, there is a recovery in the activity of the 550°C intervals, i.e. the activity at the end of the 550°C interval is higher than the activity at the beginning of the interval. A similar trend was observed for the PtPd (4:1) catalyst. However, the activity at the end of the 550°C was 76% conversion.

It is interesting that for the 450°C intervals, the activity of each interval starts higher than the previous interval and then it drops, while for the 550°C intervals, the activity of each intervals starts with a lower activity and then it rises. It can be assumed that for higher temperatures, the behaviour observed for the PtPd (1:4) catalyst is pronounced and for lower temperatures the behaviour of Pd is pronounced. For higher temperatures (550°C), Pt catalyst is expected to become active in the conversion of methane. For lower temperatures (450°C), Pd catalyst is expected to be active in conversion of methane.

After 33 hours of hydrothermal ageing, the conversion of methane of the 450°C interval was around 8% conversion. When water was switched off the activity increased continuously up to 33% conversion after. It can be concluded that PtPdRh catalyst show a low catalytic activity as well as low stability in methane conversion.

#### 4.7.2.5. Pt-Pd (1:5) catalyst

The same sequence of experiments was performed for Pt-Pd (1:5) catalyst: ignition-extinction (MI-301), variable temperature hydrothermal ageing test (MI-302) and ignition-extinction after VTTAT (MI-304).

Figure 4.109 compares the ignition-extinction curves before (MI-301) and after (MI-304) hydrothermal ageing test. A small positive hysteresis can be observed from the first ignition-extinction cycle. 100% conversion of methane was obtained at 400°C. T50 of the light off curve was 310°C. No hysteresis was observed after the hydrothermal ageing test. 100% conversion of methane was obtained at 400°C. T50 of the light off curve was 340°C. The decrease in activity after hydrothermal ageing is assumed to be due to the sintering process of metal particles.

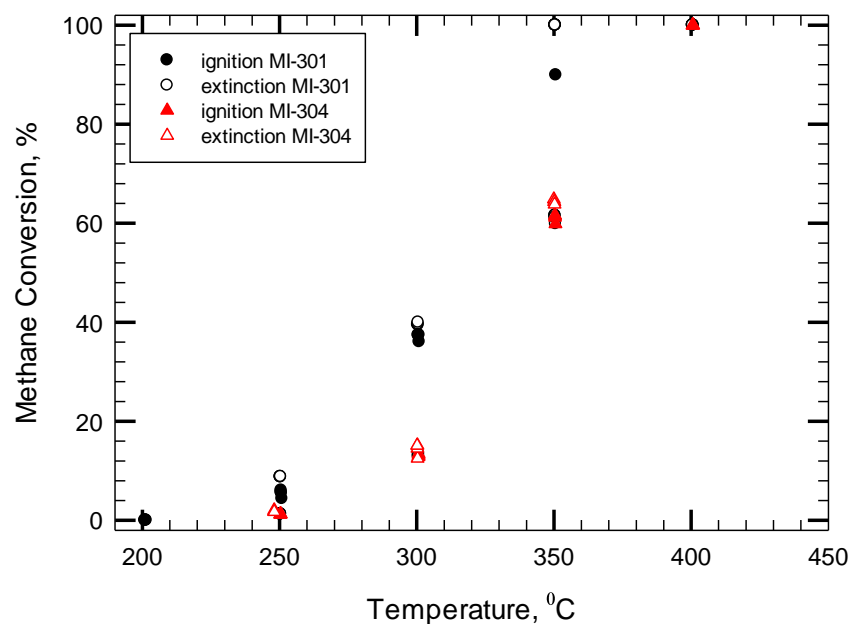


Figure 4.109. Ignition-extinction curves of methane conversion over Pt-Pd (1:5) catalyst: before (MI-301) and after (MI-304) hydrothermal ageing test (CH<sub>4</sub> 4100±50 ppm, total flow rate 235 cc/min)

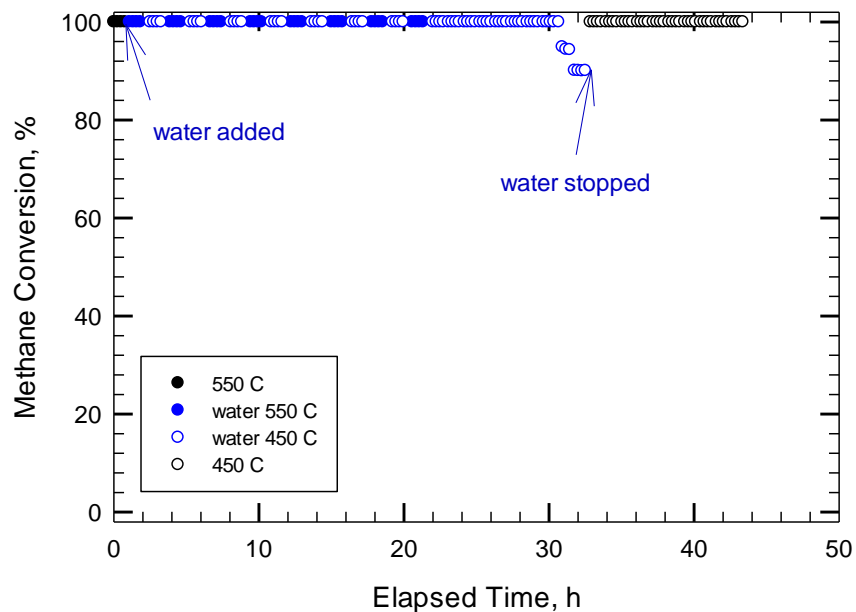


Figure 4.110. Variable temperature thermal ageing test of methane conversion over Pt-Pd (1:5) catalyst (MI-302) (CH<sub>4</sub> 4100±50 ppm, 5% vol. water, total flow rate 235 cc/min)

Figure 4.110 presents the experimental results of variable temperature hydrothermal ageing test for the Pt-Pd (1:5) catalyst. From the VTHTA test results it can be observed that the activity of the catalyst starts to decline after 32 hours of hydrothermal ageing. After 34 hours of hydrothermal ageing, the conversion of methane was around 90% conversion. When water was switched off the activity jumped to 100% conversion. It can be concluded that Pt-Pd (1:5) catalyst show a high activity and stability of methane conversion.

## Conclusions

### *The influence of precious metal loading on the catalytic activity*

Figure 4.111 compares the catalytic activity of Pd 122 (MI-357) with the catalytic activity of Pd 150 catalyst (MI-339). Both catalysts show a negative hysteresis. However, Pd 150 shows a higher activity in methane conversion compared with

Pd 122 catalyst. For example at 350°C, the conversion of methane over Pd 150 is 78% compared with just 50% conversion over Pd 122 catalyst. This is assumed to be due to higher metal loading of Pd 150 compared with Pd 122 catalyst.

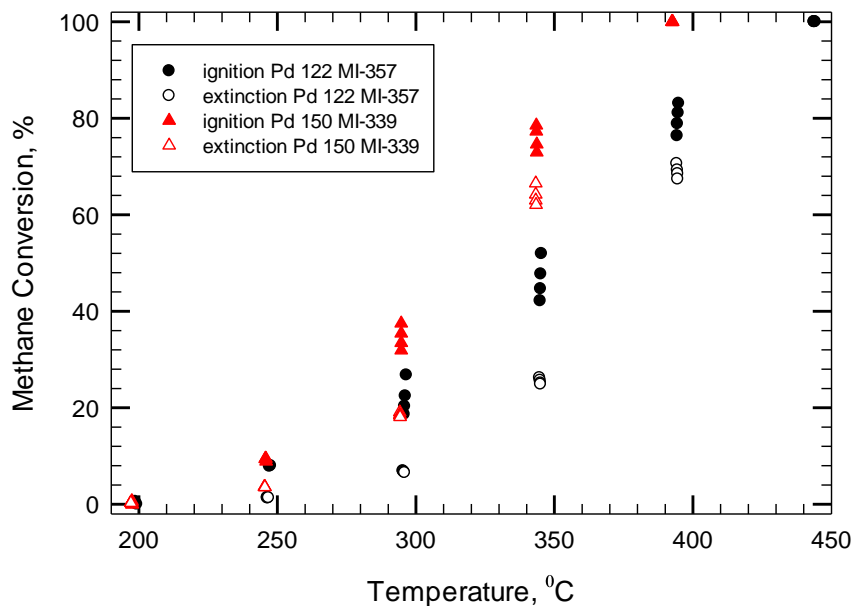


Figure 4.111. Ignition-extinction curves for methane conversion over Pd 122 (MI-357) and Pd 150 (MI-339) catalysts (CH<sub>4</sub> 4100±50 ppm, total flow rate 235 cc/min)

Figure 4.112 compares the experimental results of VTHTA test of methane conversion over Pd 122 (MI-358) and Pd 150 (MI-341) catalyst. It is interesting to observe that in presence of water added to the reactant stream, the activity of Pd 122 catalyst of the 450°C intervals is slightly higher compared with the activity of Pd 150 of the 450°C intervals. However, after 33 hours on the stream, the activities of Pd 122 and Pd 150 catalysts are very close. After the water was switched off, Pd 150 showed a higher recovery in the activity compared with Pd 122 catalyst.

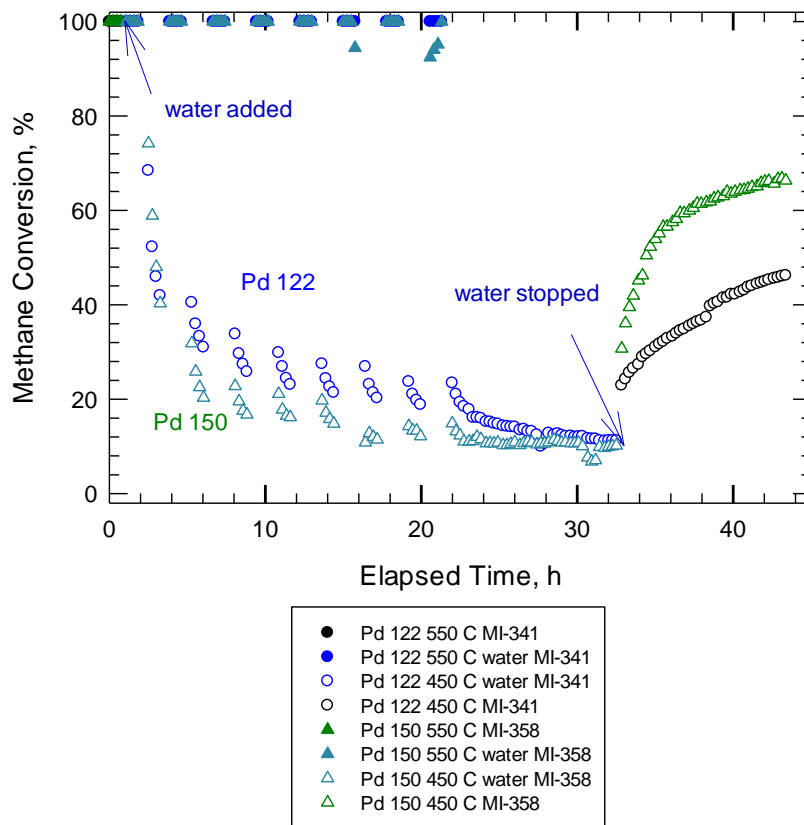


Figure 4.112. Variable temperature hydrothermal ageing test for methane conversion over Pd 122 (MI-341) and Pd 150 (MI-358) catalysts (CH<sub>4</sub> 4100±50 ppm, 5% vol. water, total flow rate 235 cc/min)

Figure 4.113 compares the ignition-extinction curves after the variable temperature hydrothermal ageing test of the Pd 122 (MI-359) and Pd 150 (MI-342) catalysts. It is interesting to observe that the hysteresis loops overlap, except they are inverted, i.e. Pd 122 shows a negative hysteresis while Pd 150 shows a positive hysteresis.

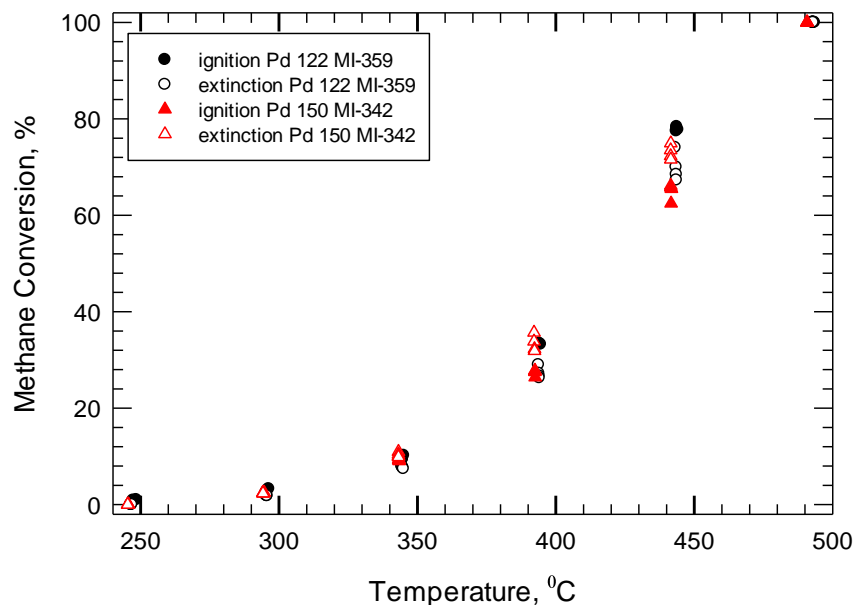


Figure 4.113. Ignition-extinction curves for methane conversion over Pd 122 (MI-359) and Pd 150 (MI-342) catalysts, after VTHTA test (CH<sub>4</sub> 4100±50 ppm, total flow rate 235 cc/min)

#### *The influence of Rh on Pd catalyst activity and stability*

Figure 4.114 compares the catalytic activities of Pd 122 (MI-357) and PdRh (MI-370) catalysts. For the light off curve, PdRh shows a slightly higher activity. However, the extinction curves show very close results for Pd 122 and PdRh catalysts. 100% conversion of methane was obtained at 450°C for both catalysts. The activity of both catalysts appears to don't be stable.

Figure 4.115 compares the experimental results for VTHTA test of methane conversion over Pd 122 and PdRh catalyst. It can be observed that the results of hydrothermal ageing are very close for both catalysts, in the presence of water as well as in the absence of water.

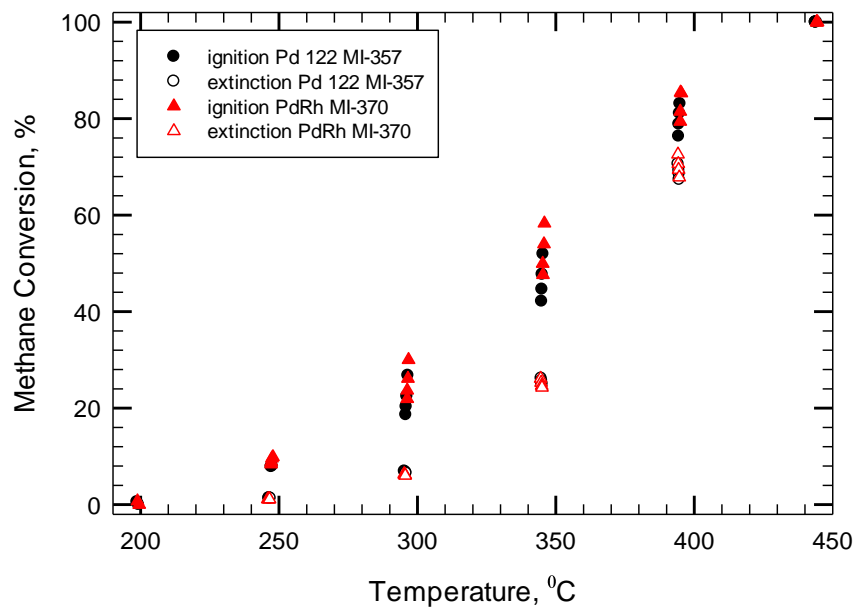


Figure 4.114. Ignition-extinction curves for methane conversion for Pd 122 (MI-357) and PdRh (MI-370) catalysts (CH<sub>4</sub> 4100±50 ppm, total flow rate 235 cc/min)

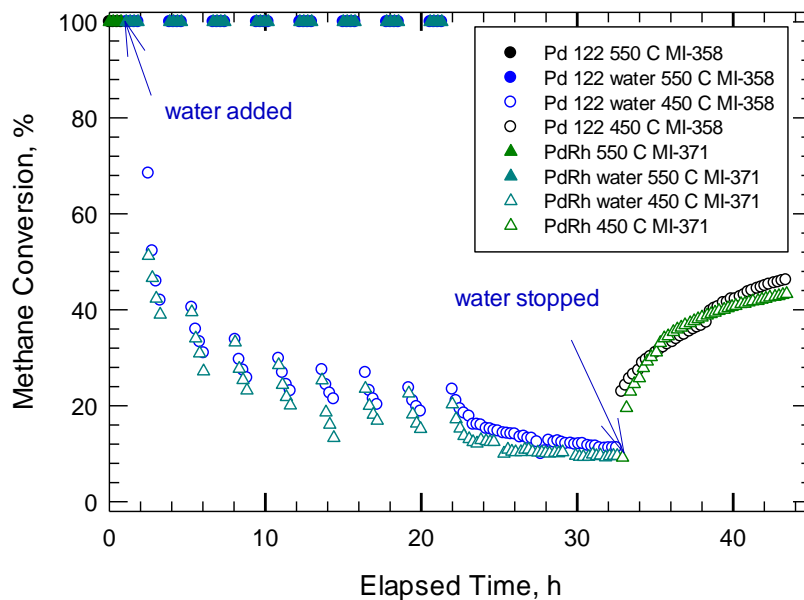


Figure 4.115. Variable temperature hydrothermal ageing test for methane conversion over Pd 122 (MI-358) and PdRh (MI-371) catalysts (CH<sub>4</sub> 4100±50 ppm, 5% vol. water, total flow rate 235 cc/min)

Figure 4.116 compares the ignition-extinction curves of methane conversion of Pd 122 (MI-359) and PdRh (MI-372) catalysts, after hydrothermal ageing test. It can be observed that Pd 122 catalyst shows a higher catalytic activity in conversion of methane. For example, 72% conversion of methane is obtained for Pd 122 at 450°C compare with 42% conversion of methane for PdRh catalyst.

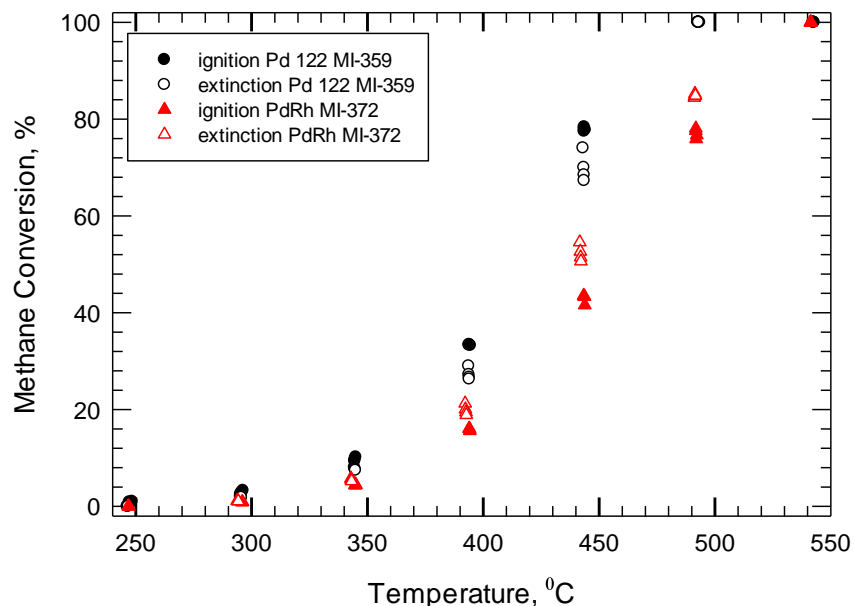


Figure 4.116. Ignition-extinction curves of methane conversion after hydrothermal ageing, for Pd 122 (MI-359) and PdRh (MI-372) catalysts (CH<sub>4</sub> 4100±50 ppm, total flow rate 235 cc/min)

Figure 4.117 compares the ignition-extinction curves of methane conversion in presence of water, of PdRh (MI-373) and Pd 122 (MI-360) catalysts. It can be observed that in presence of water, Pd 122 catalyst shows a higher activity of methane conversion.

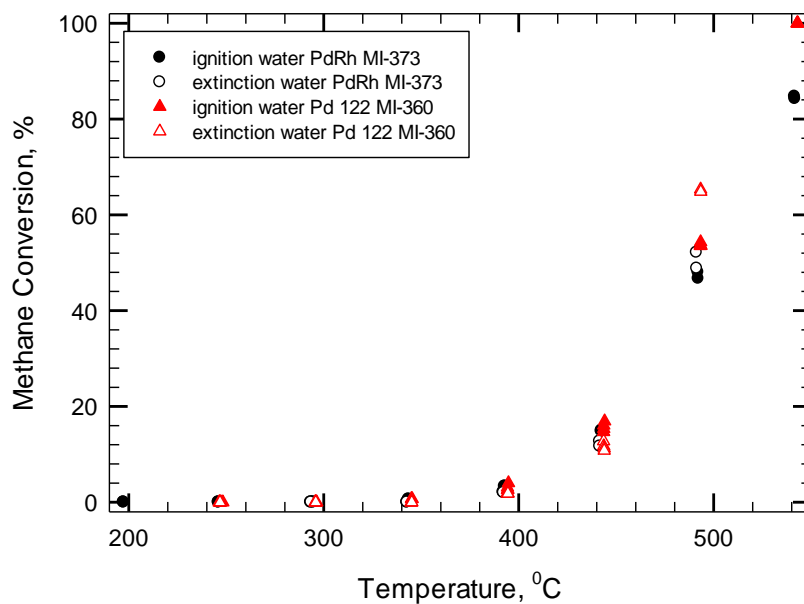


Figure 4.117. Ignition-extinction curves of methane conversion in presence of water, of PdRh (MI-373) and Pd 122 (MI-360) catalyst (CH<sub>4</sub> 4100±50 ppm, 5% vol. water, total flow rate 235 cc/min)

*The influence of Pt on the activity and stability of PdRh catalyst*

Figure 4.118 compares the experimental results of the catalytic activity of PdRh (MI-359) and PtPdRh (MI-319) catalysts. It can be observed that PdRh catalyst shows a higher activity of methane conversion compare with PtPdRh catalyst. This is assumed to be due to the lower loading of precious metal of PtPdRh catalyst compared with PdRh catalyst, as well as due to the Pt catalyst which replaces some of the Pd catalyst. 100% conversion of methane was obtained at 450°C for PdRh catalyst, and at 500 C for PtPdRh catalyst. However, the activity does not appear to be stable.

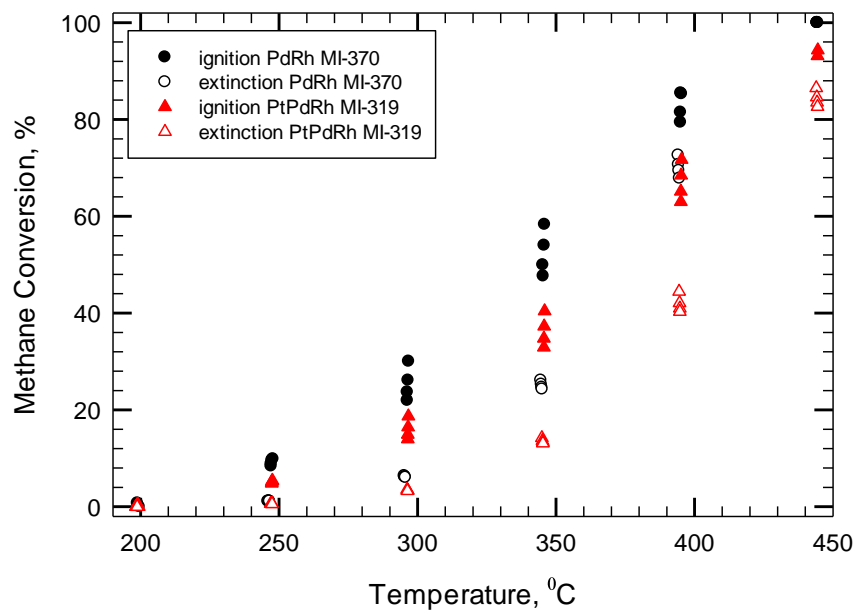


Figure 4.118. Ignition-extinction curves of methane conversion of PdRh (MI-370) and PtPdRh (MI-319) catalysts (CH<sub>4</sub> 4100±50 ppm, total flow rate 235 cc/min)

Figure 4.119 compares the experimental results of VTHTA test of methane conversion of PdRh (MI-371) and PtPdRh (MI-320) catalysts. The activity of the 450°C interval is higher for PdRh catalyst compared with PtPdRh catalyst. The activity of the 550°C interval is 100% conversion of methane for the PdRh catalyst while for PtPdRh catalyst is continuously decreasing and reaches 78% conversion of methane after 20 hours of water exposure. It is interesting to observe that after 33 hours, the conversion of methane in the presence of water was close to 10% conversion for both catalysts (10% conversion of methane for PdRh catalysts and 7% conversion of methane for PtPdRh catalyst). After the water was switched off, PdRh catalyst shows a higher recovery in activity compared with PtPdRh catalyst.

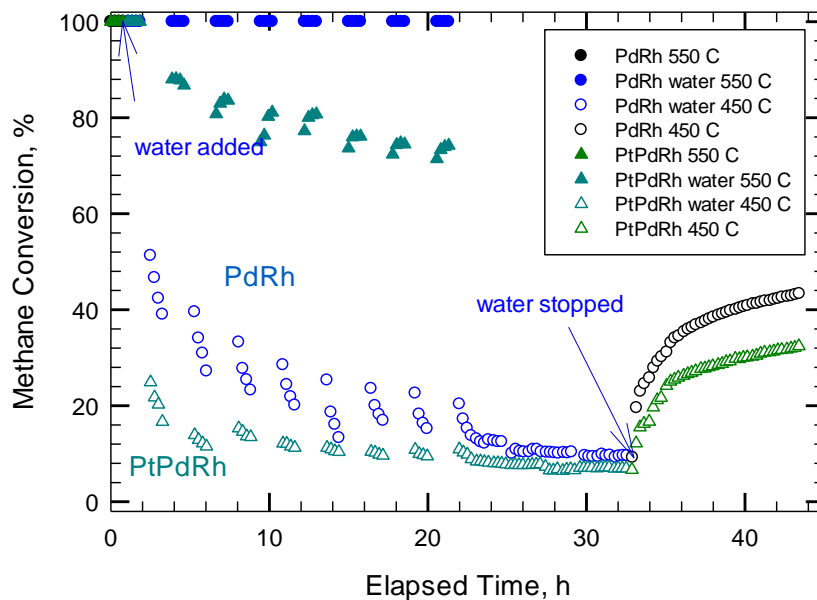


Figure 4.119. Variable temperature hydrothermal ageing test of methane conversion of PdRh (MI-371) and PtPdRh (MI-320) catalysts (CH<sub>4</sub> 4100±50 ppm, 5% vol. water, total flow rate 235 cc/min)

Figure 4.120 compares the ignition-extinction curves of PdRh (MI-372) and PtPdRh (MI-321) catalysts after the VTHTA test. One can observe that the PdRh catalyst shows a higher conversion of methane compared with PtPdRh catalyst after thermal ageing.

Figure 4.121 compares the experimental results of methane conversion in presence of water of PdRh and PtPdRh catalysts. PdRh catalyst shows a higher activity in methane conversion in presence of water. At 550°C, 84% conversion of methane in presence of water was obtained for PdRh catalyst, while 75% conversion of methane was obtained for PtPdRh catalyst.

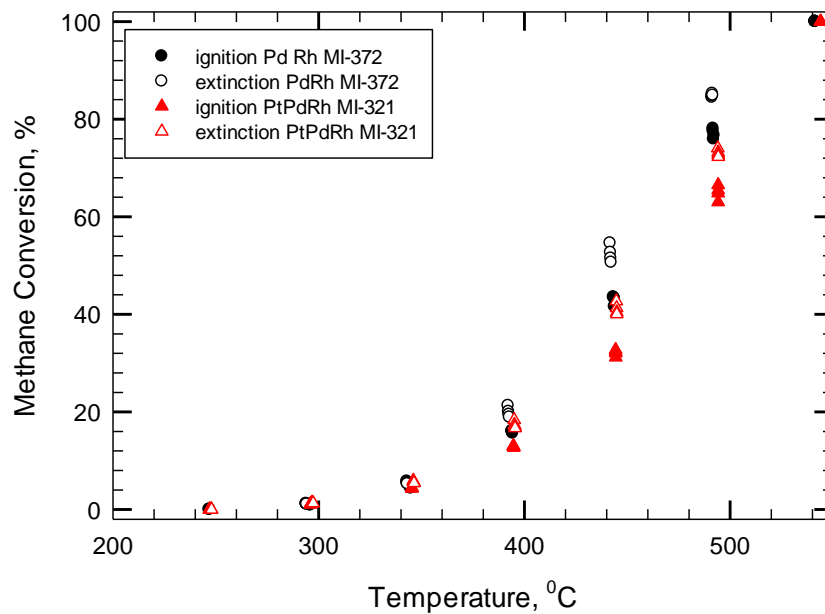


Figure 4.120. Ignition-extinction curves of methane conversion over PtPdRh (MI-321) and PdRh (MI-372) catalysts, after VTHTA test (CH<sub>4</sub> 4100±50 ppm, total flow rate 235 cc/min)

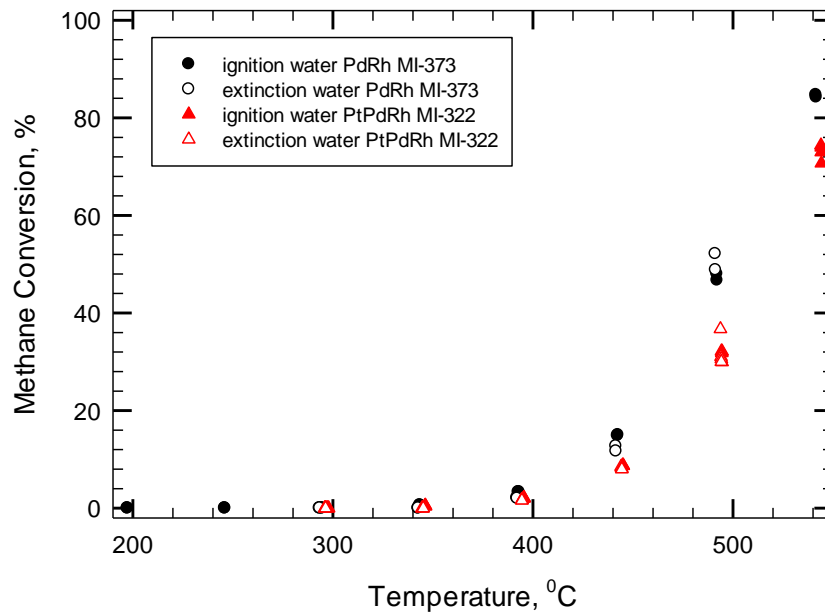


Figure 4.121. Ignition-extinction curves of methane conversion in the presence of water for PtPdRh (MI-322) and PdRh (MI-373) catalysts (CH<sub>4</sub> 4100±50 ppm, 5% vol. water, total flow rate 235 cc/min)

*The influence of Pt on Pd catalyst*

Figure 4-122 compares the ignition-extinction results of Pd 150 (MI-339) and Pt-Pd (1:5) (MI-301) catalysts. The bimetallic PtPd catalysts shows a higher conversion of methane compared with Pd only catalyst. This is assumed to be due to the behaviour of bimetallic Pt-Pd (1:5) catalyst (Pt promoting Pd catalyst).

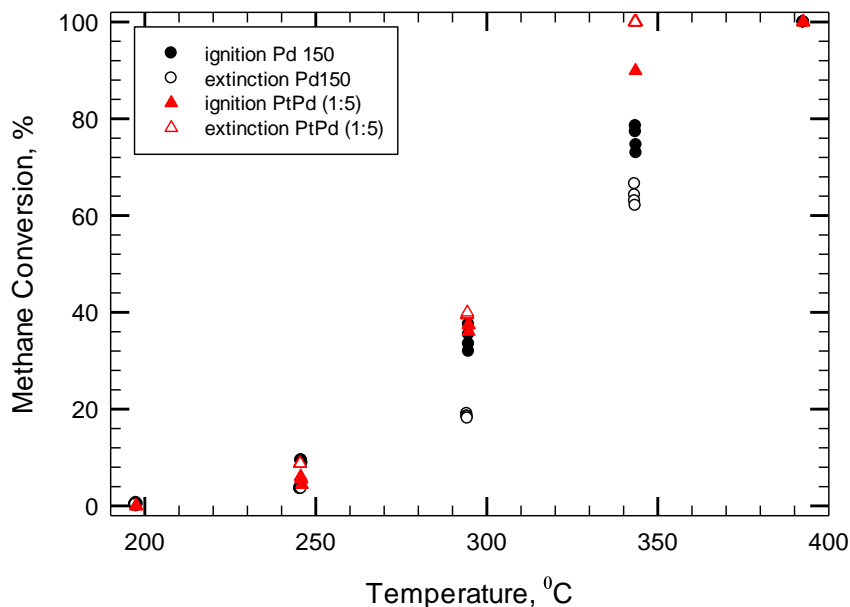


Figure 4.122. Ignition-extinction curves of methane conversion for Pt-Pd (1:5) (MI-301) and Pd 150 (MI-339) catalysts (CH<sub>4</sub> 4100±50 ppm, total flow rate 235 cc/min)

Figure 4.123 compares the experimental results of the VTТА test of methane conversion of 150 (MI-341) and Pd Pt-Pd (1:5) (MI-303) catalysts. One can observe that Pt-Pd (1:5) catalyst shows a higher resistance to water deactivation compared with Pd 150 catalyst. It is assumed that the high resistance to water deactivation of PtPd (1:5) catalyst is due to the presence of Pt as well as the interaction between Pt and Pd catalysts in the bimetallic Pt-Pd (1:5) catalyst.

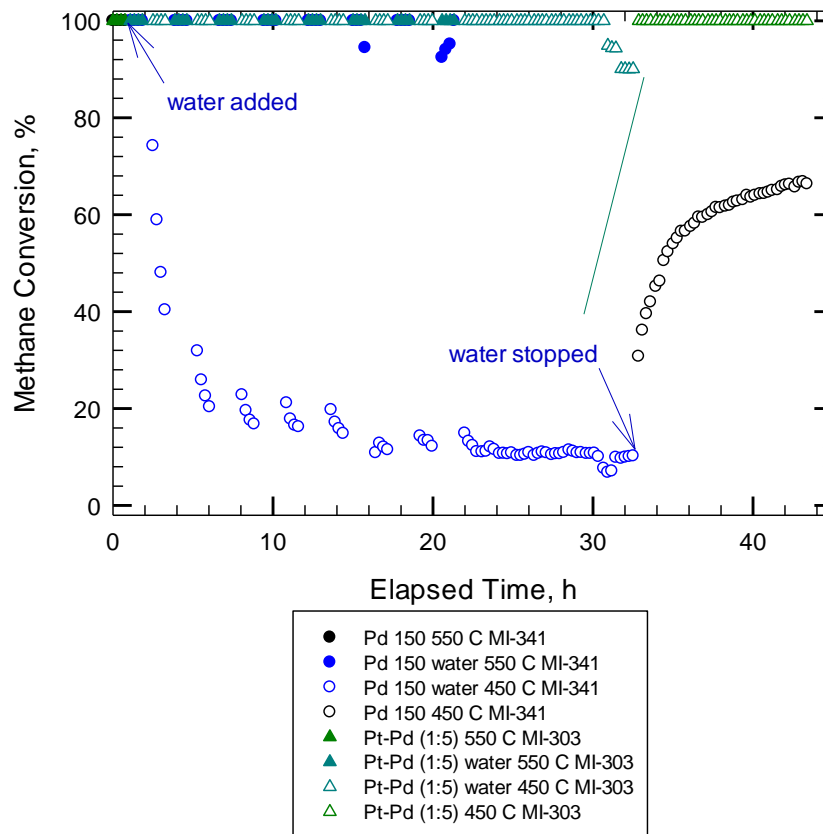


Figure 4.123. Variable temperature thermal ageing test of methane conversion for Pt-Pd (1:5) (MI-303) and Pd 150 (MI-341) catalysts (CH<sub>4</sub> 4100±50 ppm, 5% vol. water, total flow rate 235 cc/min)

Figure 4.124 compares the ignition-extinction curves of methane conversion after VTTA test, of Pd 150 (MI-342) and Pt-Pd (1:5) (MI-304) catalysts. It can be observed that Pt-Pd (1:5) catalyst shows a higher resistance to water deactivation compared with Pd 150 catalyst. This is assumed to be mainly due to the benefits the Pt metal brings to the bimetallic Pt-Pd (1:5) catalyst, i.e. resistance to water and sulphur deactivation.

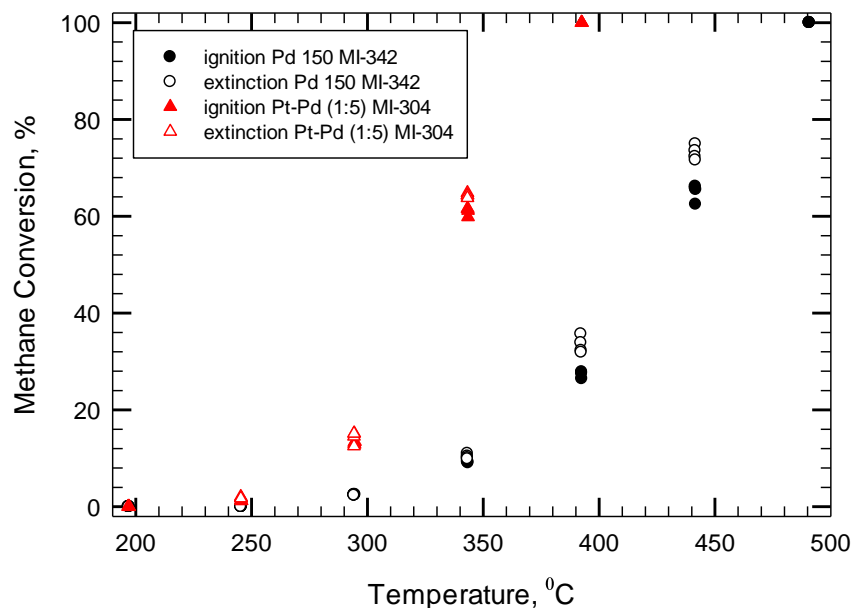


Figure 4.124. Ignition-extinction curves of methane deactivation after VTTA test, of Pd 150 (MI-342) and Pt-Pd (1:5) (MI-304) catalysts (CH<sub>4</sub> 4100±50 ppm, total flow rate 235 cc/min)

#### 4.8. De-greening temperature effect on the catalytic activity

It had been reported in the literature (Chapter 2) that the de-greened temperature in the presence of an oxidizing atmosphere, has an influence on the sintering of noble metals particles of supported catalysts, i.e. for temperatures between 400°C and 600°C, a re-dispersion of the catalyst articles was observed, while for temperatures above 600°C and below 400°C a sintering process of the catalyst particles was observed.

The experimental results of activity and stability of two different catalysts de-greened at 650°C and 550°C are compared (i.e. Pd 150 only, Pt-Pd (1:5)).

#### 4.8.1. Pd 150 catalyst

VTTA test sequence at 350°C

Figure 4.125 presents the ignition-extinction curves of Pd 150 de-greened at 650°C (MI-258) and 550°C (MI-374). The sample de-greened at 550°C shows a higher activity compared with the sample de-greened at 650°C, i.e. at 350°C the conversion of methane is 93% for the catalyst de-greened at 550°C compared with just 80% for the catalyst de-greened at 650°C. Wanke S. observed that a re-dispersion of the catalyst takes place when it is exposed to an oxygen atmosphere at a temperature between 500°C and 600°C (Wanke, S.E. et al., 1975). Outside of this range, a sintering of the metal particles was observed. Therefore, it is assumed that a re-dispersion of the metal particles took place for the samples de-greened at 550°C.

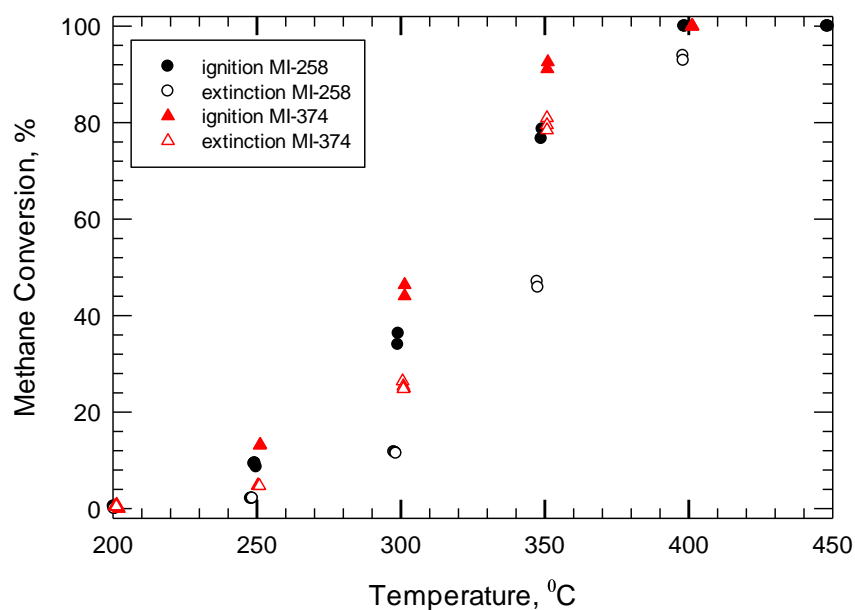


Figure 4.125. Ignition-extinction curves of methane conversion over Pd 150 catalyst de-greened at 650°C (MI-258) and 550°C (MI-374) (CH<sub>4</sub> 4100±50 ppm, total flow rate 235 cc/min)

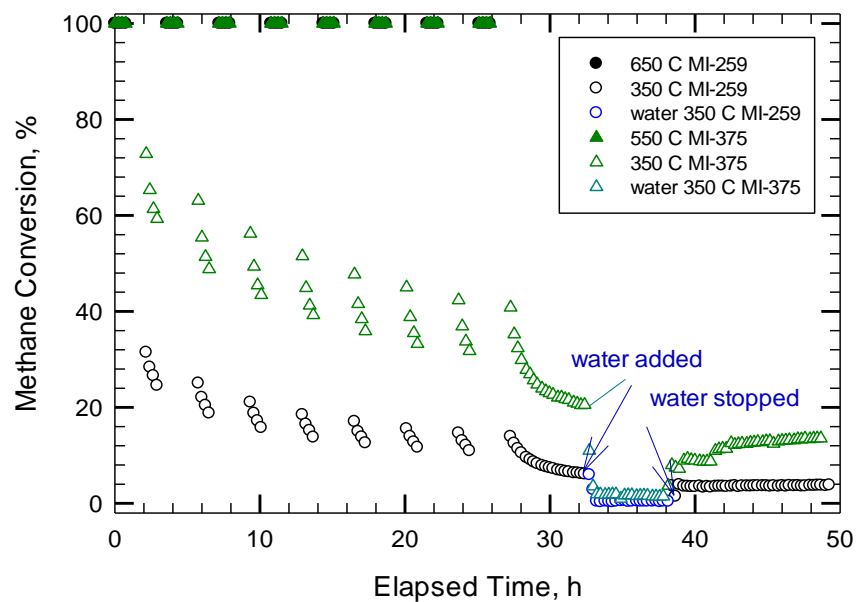


Figure 4.126. Variable temperature thermal ageing test of methane conversion over Pd 150 catalyst, de-greened at 650°C (MI-259) and 550°C (MI-375) (CH<sub>4</sub> 4100±50 ppm, 5% vol. water, total flow rate 235 cc/min)

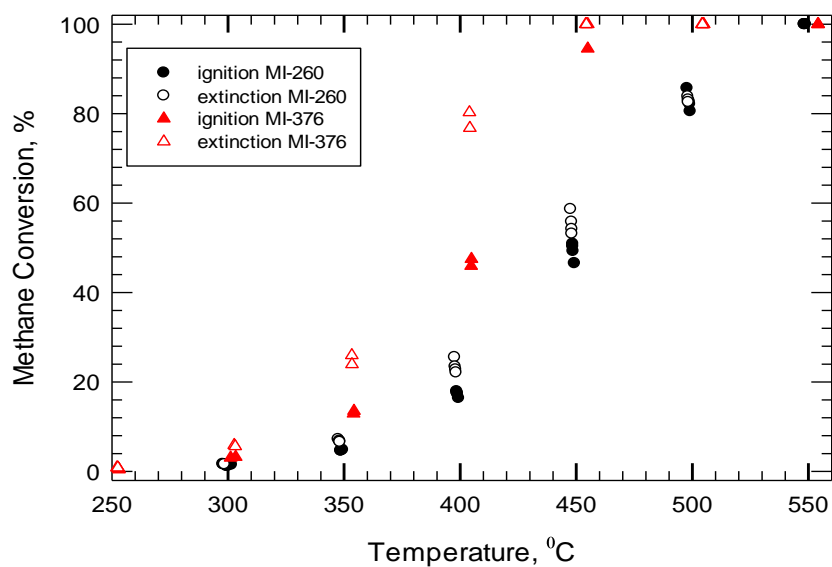


Figure 4.127. Ignition-extinction curves of methane conversion for Pd 150 catalyst de-greened at 650°C (MI-260) and 550 °C (MI-376) (CH<sub>4</sub> 4100±50 ppm, total flow rate 235 cc/min).

Figure 4.126 compares the experimental results of variable temperature thermal ageing test of methane conversion over Pd 150 catalyst, for the samples de-greened and 650°C and 550°C. It is interesting to observe that in the absence of water, the sample de-greened at 550°C (MI-374) shows a higher activity compared with the sample de-greened at 650°C (MI-258). However, when water was added to the reactant stream, the activities of the two samples were very close.

Figure 4.127 presents the ignition-extinction results of methane conversion after the VTHTA test. It can be observed that the sample de-greened at 550°C (MI-376) shows a higher activity compared with the sample de-greened at 650°C (MI-260).

#### VTHTA test at 450°C

Figure 4.128 compares the initial ignition-extinction curves of methane conversion of Pd 150 de-greened at 650°C (MI-278) and 550°C (MI-339).

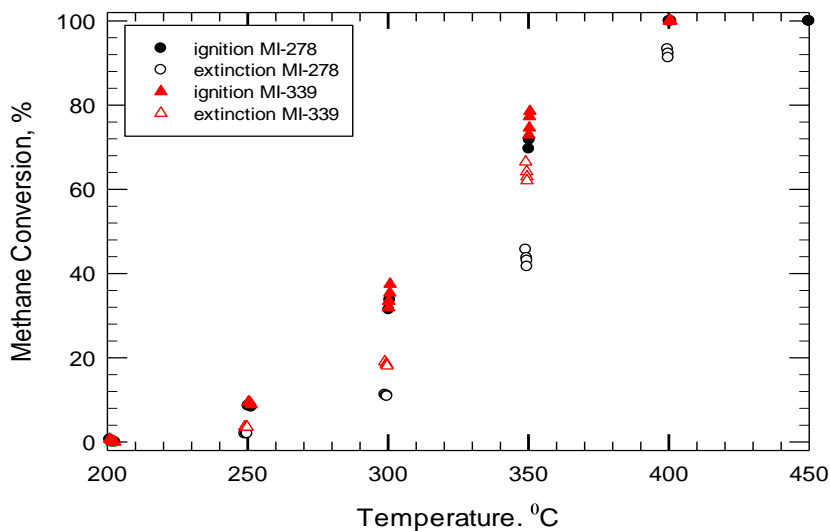


Figure 4.128. Ignition-extinction curve of methane conversion after VTHTA test, of Pd 150 catalyst de-greened at 650°C (MI-278) and 550°C (MI-339) (CH<sub>4</sub> 4100±50 ppm, total flow rate 235 cc/min)

One can observe that the Pd 150 sample de-greened at 550°C shows a slightly higher activity compared with the sample de-greened at 650°C. This is in accordance with what we observed for the VTTA test at 350°C.

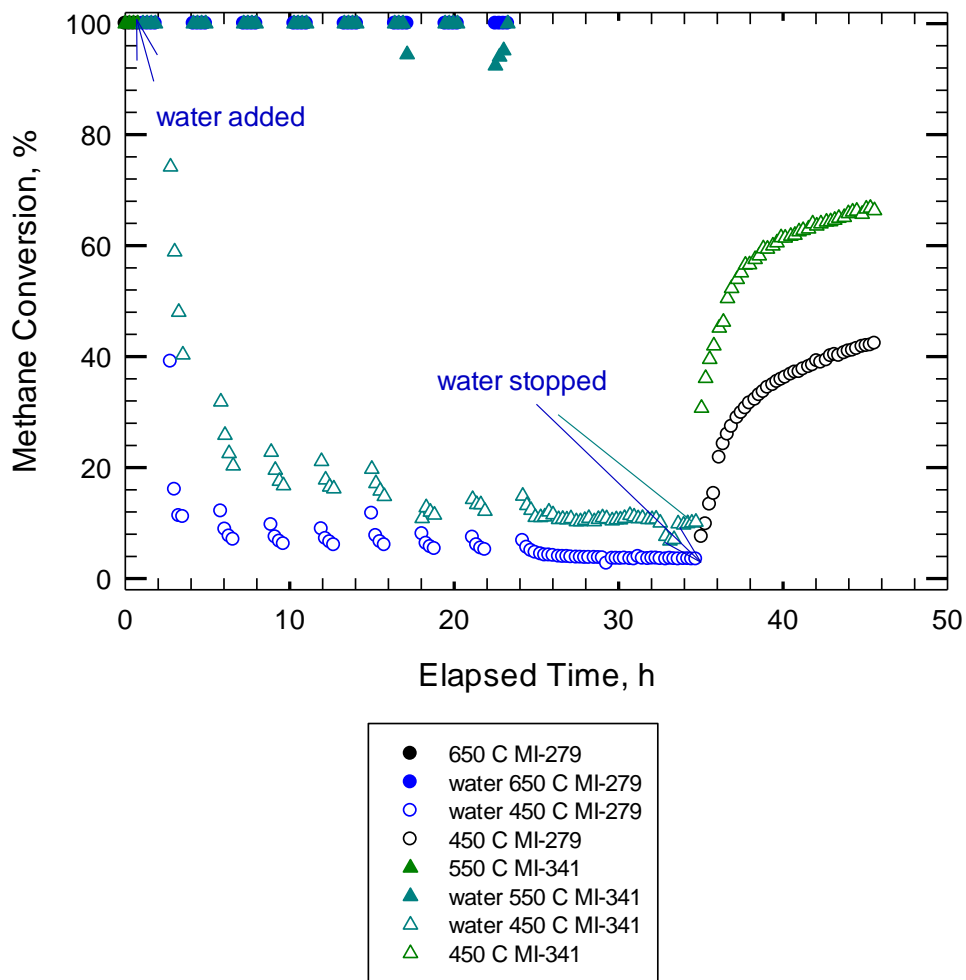


Figure 4.129. Variable temperature thermal ageing test of methane conversion over Pd 150 catalyst de-greened at 650°C (MI-279) and 550°C (MI-341) (CH<sub>4</sub> 4100±50 ppm, 5% vol. water, total flow rate 235 cc/min)

Figure 4.129 compares the experimental results of variable temperature hydrothermal ageing test Pd 150 catalys de-greened at 650°C (MI-279) and 550°C (MI-241). A slightly higher activity of the 450°C interval can be observed for the sample de-greened at 550°C, i.e. for the first 450°C interval, the activity of the first point is 75 % conversion and it's drops to 40 % conversion, while for the

sample de-greened at 650°C, the activity of the first point is 40% conversion and it's drops to 10 % conversion. After the water is switched off, the sample de-greened at 550°C shows a higher recovery of the activity. This is assumed to be a result of the de-greening temperature, as the sample de-greened at 550°C should offer a higher active surface compared with sample de-greened at 650°C.

Figure 4.130 compares the experimental results of ignition-extinction curves after VTHTA test of Pd 150 catalyst de-greened at 650°C (MI-280) and 550°C (MI-342).

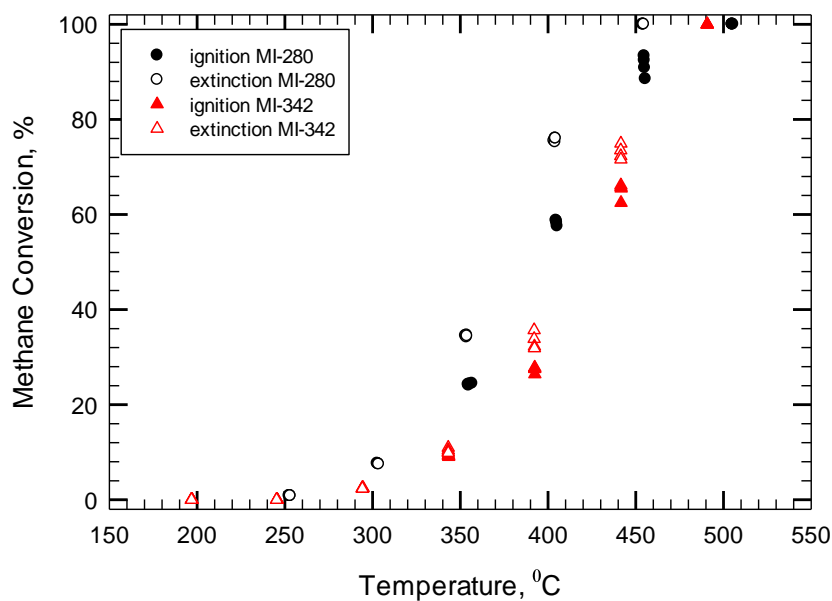


Figure 4.130. Ignition-extinction curves of methane conversion after VTHTA test for Pd 150 catalyst de-greened at 650°C (MI-280) and 550°C (MI-342) (CH<sub>4</sub> 4100±50 ppm, total flow rate 235 cc/min)

#### 4.8.2. Pt-Pd (1:5) catalyst

VTTA test at 350°C

Figure 4.131 presents the ignition-extinction curves for Pt-Pd (1:5) de-greened at 650°C (MI-232) and 550°C (MI-286). The catalyst de-greened at 550°C shows a slightly higher activity compared with the catalyst de-greened at 650°C. For example, at 250°C, the conversion of methane was 55% for the catalyst de-greened at 550°C compared with 45% for the catalyst de-greened at 650°C. Therefore, it is assumed that a re-dispersion of the metal particles took place for the samples de-greened at 550°C.

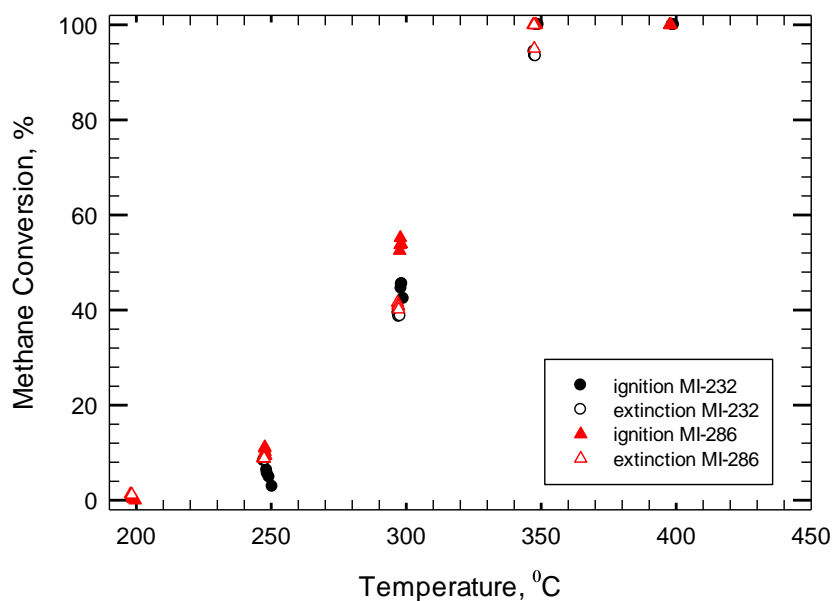


Figure 4.131. Ignition-extinction curves of methane conversion over Pt-Pd (1:5) catalyst de-greened at 650°C (MI-232) and 550°C (MI-286) (CH<sub>4</sub> 4100±50 ppm, total flow rate 235 cc/min)

Figure 4.132 compares the experimental results of variable temperature thermal ageing test of methane conversion of Pt-Pd (1:5) catalyst, for the two de-greening temperatures (650°C and 550°C). It is interesting to observe that in the absence of

water, the sample de-greened at 650°C (MI-233) shows a slightly higher activity compared with the sample de-greened at 550°C (MI-289). This is assumed to be due to the higher dispersion of the sample de-greened at 550°C, as more water will be formed during the reaction, which will block the active sites of the catalyst. However, after 33 hours on the stream, the activities of both samples are very close. When water is added to the reactant stream, the drop in activity is similar for both catalysts. After the water is switched off, the recovery in activity is slightly higher for the sample de-greened at 650°C (61% conversion of methane) compared with the sample de-greened at 550°C (58% conversion of methane).

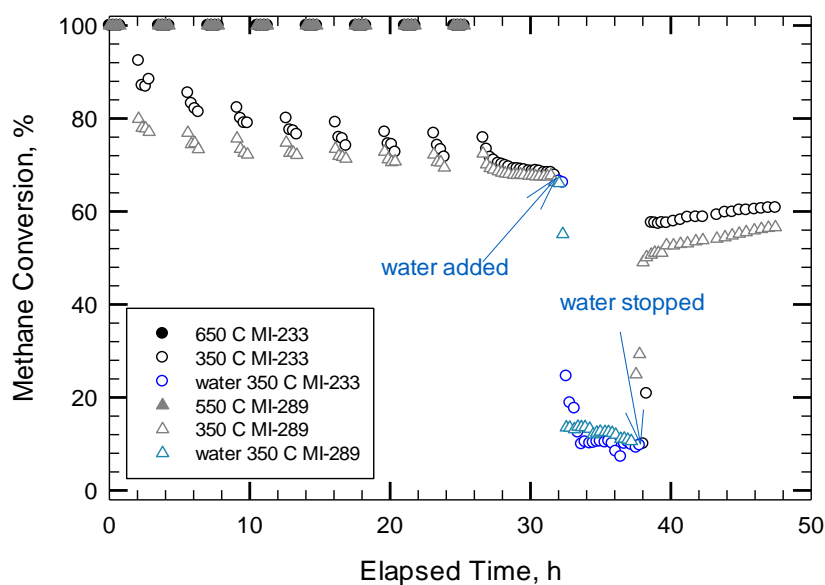


Figure 4.132. Variable temperature thermal ageing test of methane conversion of Pt-Pd (1:5) catalyst de-greened at 650°C (MI-233) and 550°C (MI-289) (CH<sub>4</sub> 4100±50 ppm, 5% vol. water, total flow rate 235 cc/min)

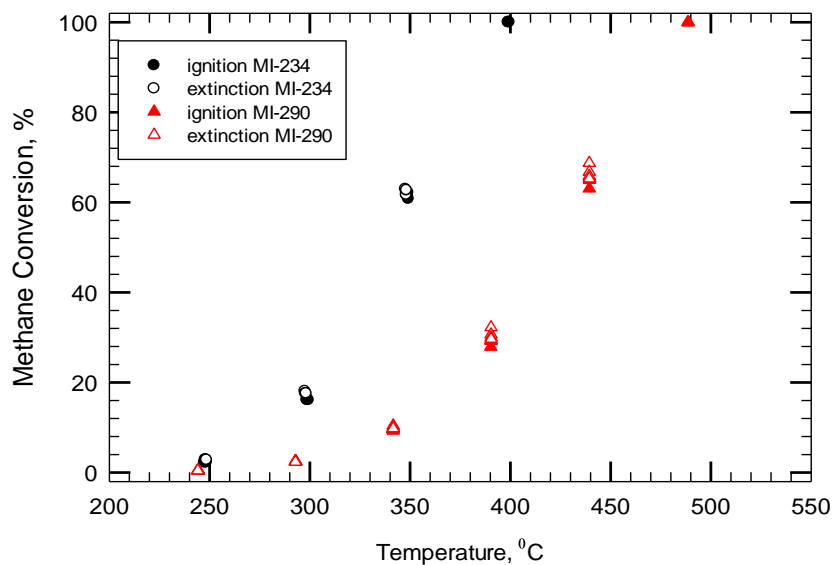


Figure 4.133. Ignition-extinction curves of methane conversion of Pt-Pd (1:5) catalyst de-greened at 650°C (MI-234) and 550°C (MI-290), after VTТА test (CH<sub>4</sub> 4100±50 ppm, total flow rate 235 cc/min)

Figure 4.133 compares the ignition-extinction curves of methane conversion, after variable temperature thermal ageing test, of Pt-Pd (1:5) catalyst de-greened at 650°C (MI-234) and 550°C (MI-290). One can observe that the activity of the Pt-Pd (1:5) sample de-greened at 650°C is higher than the activity of the sample de-greened at 550°C. This can be assumed to be due to the effect of water on the sintering process of metal particles.

#### *VTHTA 350°C*

Figure 4.134 presents the ignition-extinction curves of methane conversion over Pt-Pd (1:5) catalyst de-greened at 650°C (MI-228) and 550°C (MI-295). The activity of both samples show similar activities, which is consistent with the previous observation (figure 4.131).

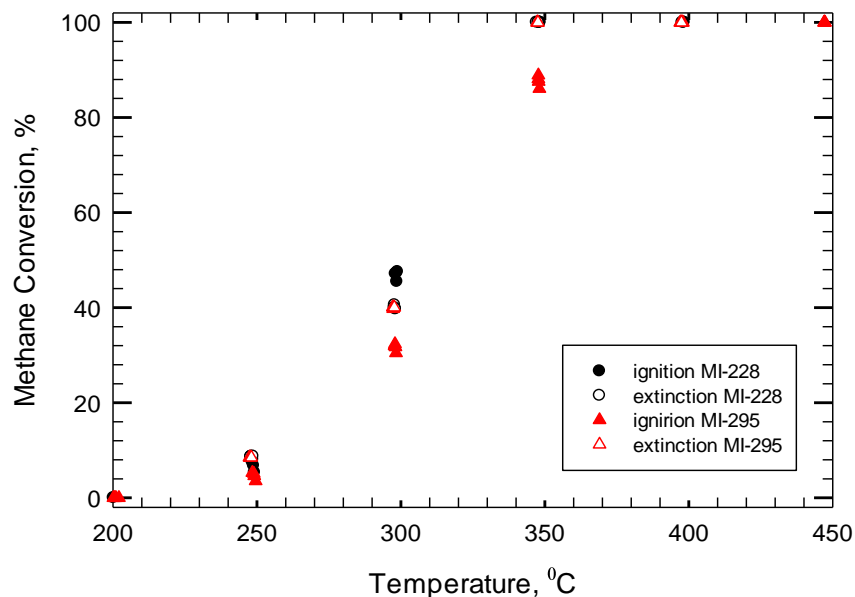


Figure 4.134. Ignition-extinction curves of methane conversion over Pt-Pd (1:5) catalyst de-greened at 650°C (MI-228) and 550°C (MI-295) (CH<sub>4</sub> 4100±50 ppm, total flow rate 235 cc/min)

Figure 4.135 compares the experimental results of variable temperature hydrothermal ageing test of the Pt-Pd (1:5) catalysts de-greened at 650°C (MI-229) and 550°C (MI-296). One can see that the 350°C temperature intervals show very close activity values. However, after the water was switched off, the sample de-greened at 550°C (MI-296) showed a higher recovery in activity compared with the sample de-greened at 650°C (MI-229).

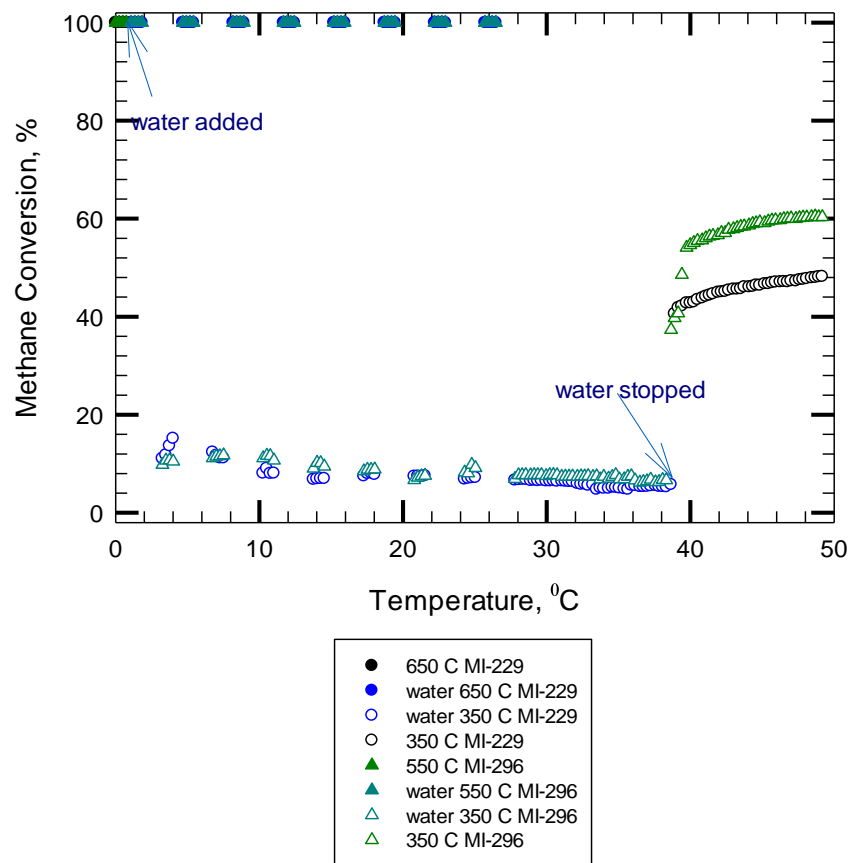


Figure 4.135. Variable temperature thermal ageing test of methane conversion over Pt-Pd (1:5) catalyst, de-greened at 650°C (MI-229) and 550°C (MI-296) (CH<sub>4</sub> 4100±50 ppm, 5% vol. water, total flow rate 235 cc/min)

Figure 4.136 compares the results of ignition-extinction curves of methane conversion after VTHTA test. It is interesting to observe that the Pt-Pd (1:5) sample de-greened at 650°C (MI-230) shows a higher activity compared with the sample de-greened at 550°C (MI-297), similar as for VTTA test at 350°C.

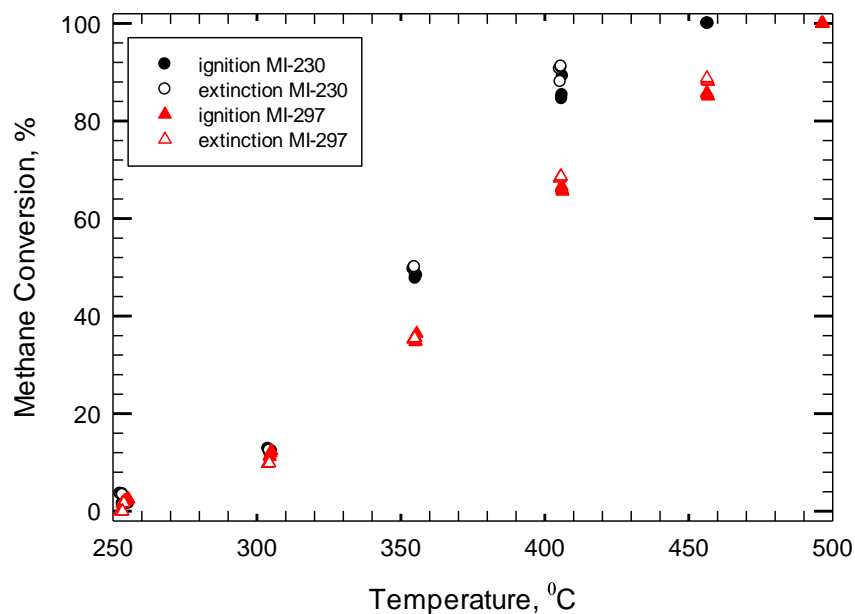


Figure 4.136. Ignition-extinction curve of methane conversion after VTHTA test, over Pt-Pd (1:5) catalyst de-greened at 650°C (MI-230) and 550°C (MI-297) (CH<sub>4</sub> 4100±50 ppm, total flow rate 235 cc/min)

#### *VTHTA at 450°C*

Figure 4.137 compares the ignition-extinction curves of methane conversion of Pt-Pd (1:5) catalyst de-greened at 650°C (MI-244) and 550°C (MI-301). It can be observed that both samples show similar catalytic activities of methane conversion.

Figure 4.138 compares the experimental results of variable temperature hydro thermal ageing test of methane conversion of the Pt-Pd (1:5) samples de-greened at 650°C and 550°C. It is interesting to observe that for the 450°C intervals, the sample de-greened at 550°C (MI-303) shows a decrease of methane conversion after 33 hours, while the sample de-greened at 650°C (MI-245) shows a decrease in methane conversion after just 7 hours.

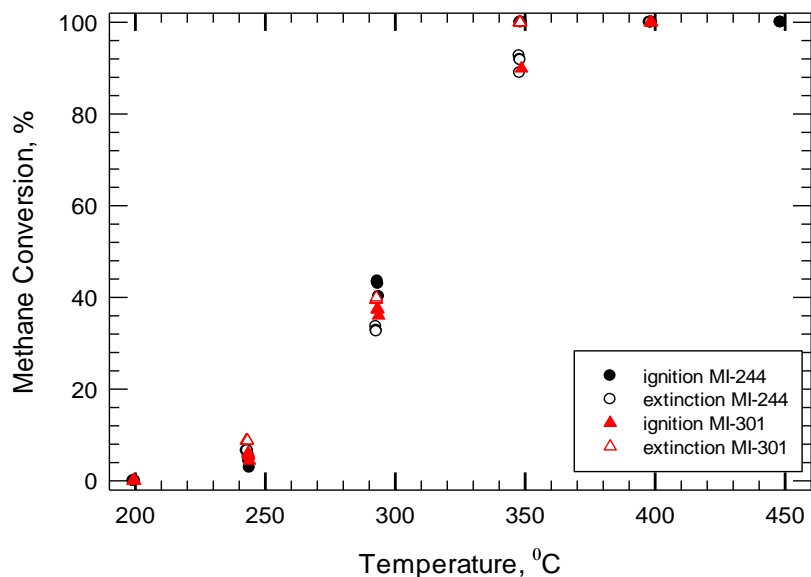


Figure 4.137. Ignition-extinction curves of methane conversion over Pt-Pd (1:5) catalyst de-greened at 650°C (MI-244) and 550°C (MI-301) (CH<sub>4</sub> 4100±50 ppm, total flow rate 235 cc/min)

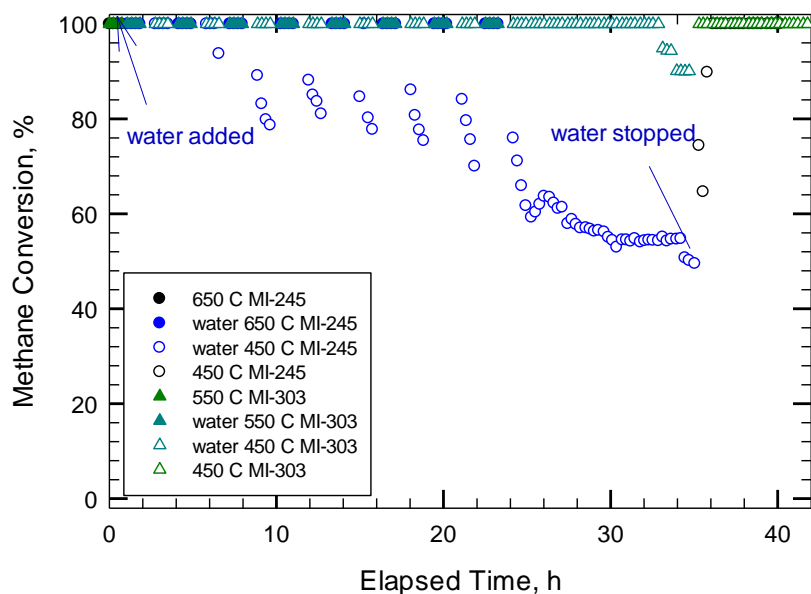


Figure 4.138. Variable temperature hydrothermal ageing test of methane conversion over Pt-Pd (1:5) catalyst de-greened at 650°C (MI-245) and 550°C (MI-303) (CH<sub>4</sub> 4100±50 ppm, 5% vol. water, total flow rate 235 cc/min)

This effect is assumed to be due to the higher dispersion of the sample de-greened at 550°C. In consequence, the sample de-greened at 550°C will have higher active surface area available for the reaction, compared with the sample de-greened at 650°C.

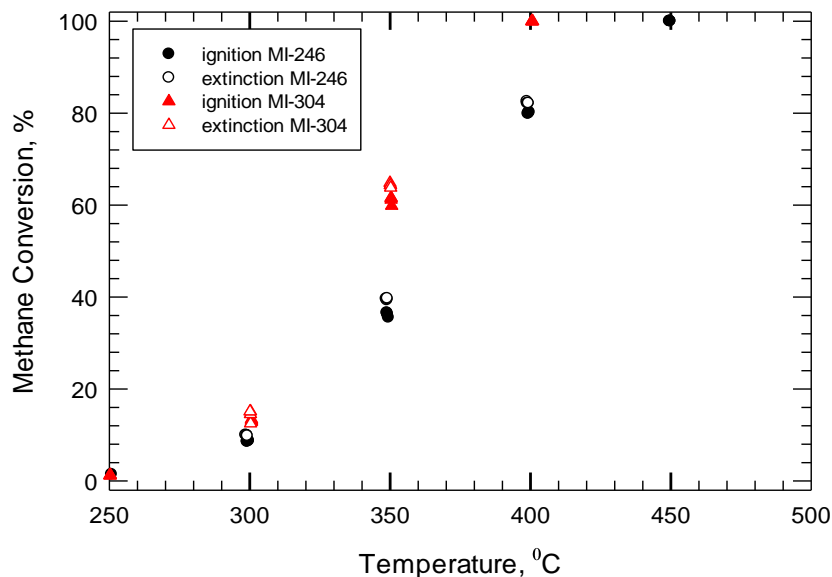


Figure 4.139. Ignition-extinction curves of methane conversion after VTHTA test for Pt-Pd (1:5) catalyst de-greened at 650°C (MI-246) and 550°C (MI-304)

Figure 4.139 compares the ignition-extinction curves of methane conversion after VTHTA test. It can be observed that the Pt-Pd (1:5) sample de-greened at 550°C (MI-304) shows a higher activity in methane conversion compared with the sample de-greened at 650°C (MI-246).

To better investigate the influence of de-green temperature on the activity of the Pt-Pd (1:5) catalyst, the sample used in the MI-301 VTHTA test sequence (550°C de-greened) was hydrothermally aged at 650°C-450°C without any pre-treatment. The results are presented in figure 4.140.

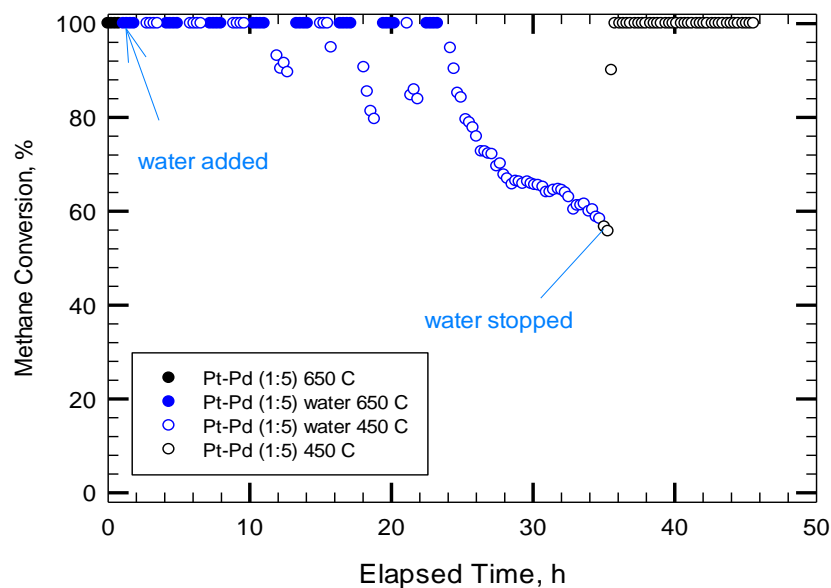


Figure 4.140. Variable temperature hydrothermal ageing test of methane conversion over Pt-Pd (1:5) catalyst (MI-310) (CH<sub>4</sub> 4100±50 ppm, 5% vol. water, total flow rate 235 cc/min)

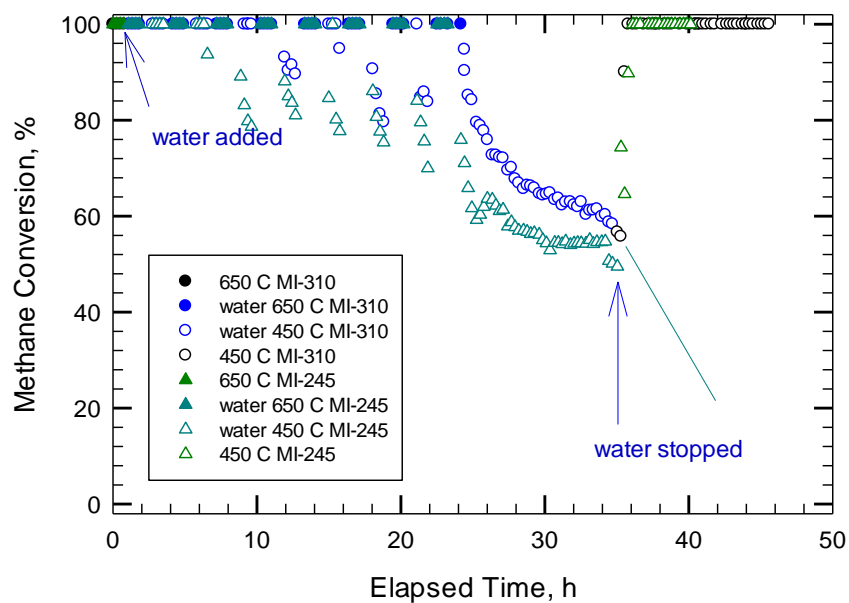


Figure 4.141. Variable temperature hydrothermal ageing test of methane conversion over Pt-Pd (1:5) catalyst de-greened at 550°C (MI-310) and 650°C (MI-245) (CH<sub>4</sub> 4100±50 ppm, 5% vol. water, total flow rate 235 cc/min)

One can see that the VTHTA test at 650°C-450°C (figure 4.140) shows similarities with the Pt-Pd (1:5) samples de-greened at 650°C and hydrothermally aged at 650°C-450°C. Figure 4.141 compares the hydrothermal ageing 650°C-450°C results of MI-310 test (de-greened at 550°C) with a previous test MI-245 (de-greened at 650°C). It can be seen that for the Pt-Pd (1:5) de-greened at 650°C, the activities of the 450°C intervals are slightly smaller compared with Pt-Pd (1:5) de-greened at 550°C. This is assumed to be due to the effect of the de-greening temperature on the particle size of the catalyst.

The same sample de-greened at 550°C was treated 16 hours at 600°C, in presence of air. After that a VTHTA test sequence was performed, i.e. ignition-extinction, VTHTA test, ignition-extinction. The experimental results of the VTHTA test are presented in figure 4.142. Figure 4.143 compares the VTHTA test results (650°C-450°C) of Pt-Pd (1:5) catalyst de-greened at 550°C (MI-310) and 600°C (MI-312). The sample de-greened at 600°C shows a slightly lower activity of the 450°C interval compared with the sample de-greened at 550°C. The higher activity of the sample de-greened at 550°C is assumed to be due to the re-dispersion of the catalyst particles, as Wanke S. showed in his study (Wanke, S.E. et al, 1975).

Figure 4.144 compares the experimental results of methane conversion of Pt-Pd (1:5) catalyst de-greened at 650°C (MI-245) and 600°C (MI-312). One can observe the close results of the activities of the 450°C intervals for the MI-245 and MI-312 experiments.

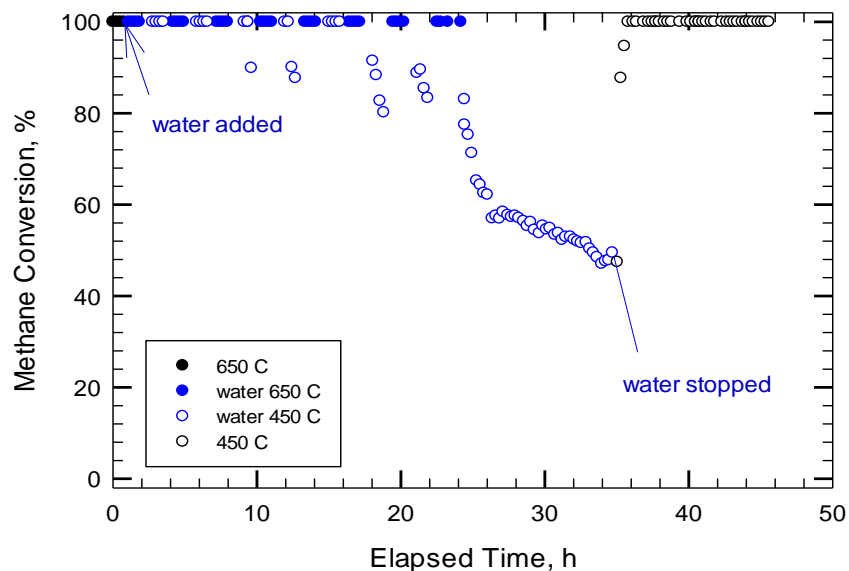


Figure 4.142. Variable temperature hydrothermal ageing test of methane conversion over Pt-Pd (1:5) de-greened at 600°C (MI-312) (CH<sub>4</sub> 4100±50 ppm, 5% vol. water, total flow rate 235 cc/min)

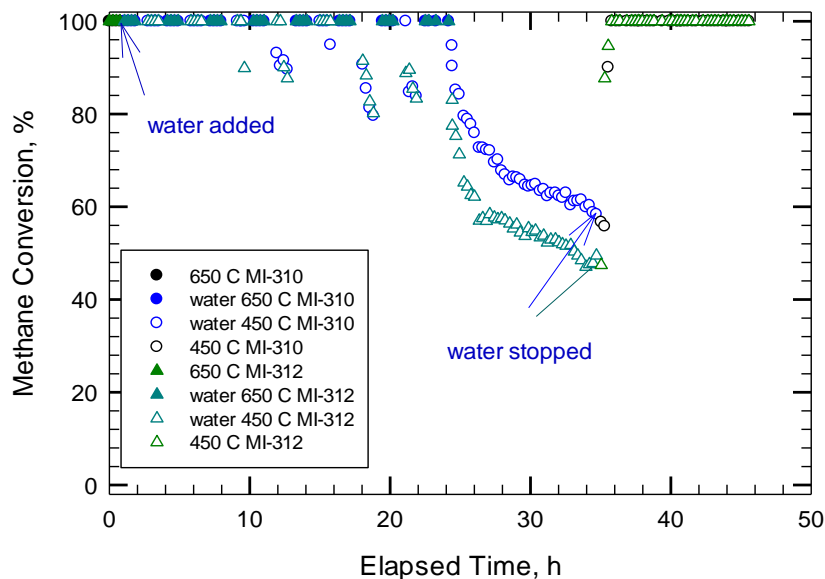


Figure 4.143. Variable temperature hydrothermal ageing test of methane conversion over Pt-Pd (1:5) catalyst de-greened at 550°C (MI-310) and 600°C (MI-312) (CH<sub>4</sub> 4100±50 pm, total flow rate 235 cc/min)

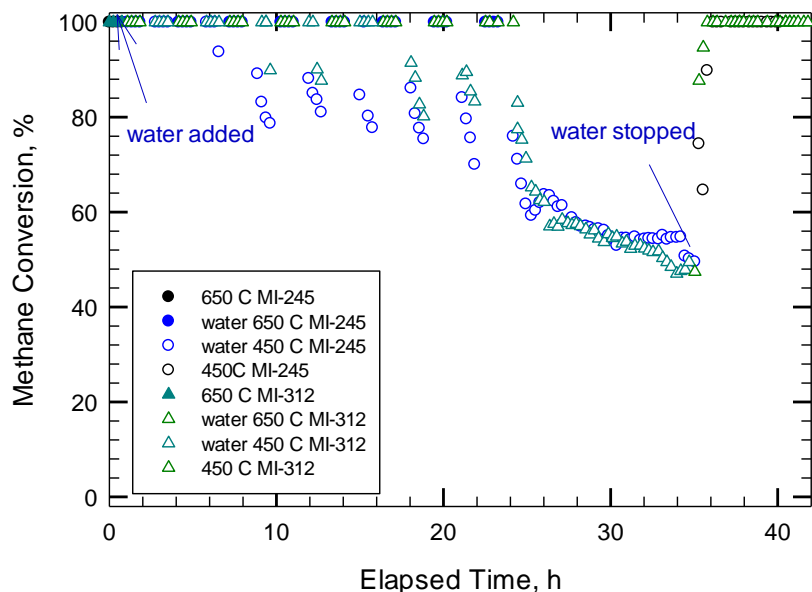


Figure 4.144. Variable temperature thermal ageing test of methane conversion of Pt-Pd (1:5) catalyst de-greened at 650°C (MI-245) and 600°C (MI-312) (CH<sub>4</sub> 4100±50 ppm, 5% vol. water, total flow rate 235 cc/min)

A new Pt-Pd (1:5) sample was de-greened at 550°C and a VTHTA 550°C-450°C was performed. The results are presented in figure 4.145. It can be observed that the results are similar with the results of MI-302 experiment. A decrease in the catalytic activity for the 450°C interval starts after 29 hours exposure to hydrothermal ageing. Figure 4.146 compares the experimental results of two VTHTA tests 550°C-450°C of Pt-Pd (1:5) catalyst de-greened at 550°C.

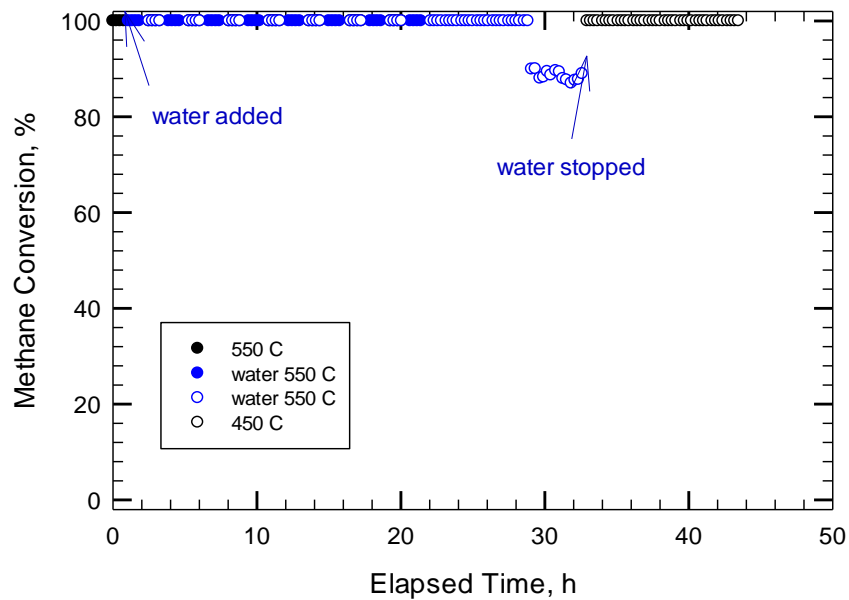


Figure 4.145. Variable temperature hydrothermal ageing of Pt-Pd (1:5) catalyst, de-greened at 550°C (MI-331) (CH<sub>4</sub> 4100±50 ppm, 5% vol. water, total flow rate 235 cc/min)

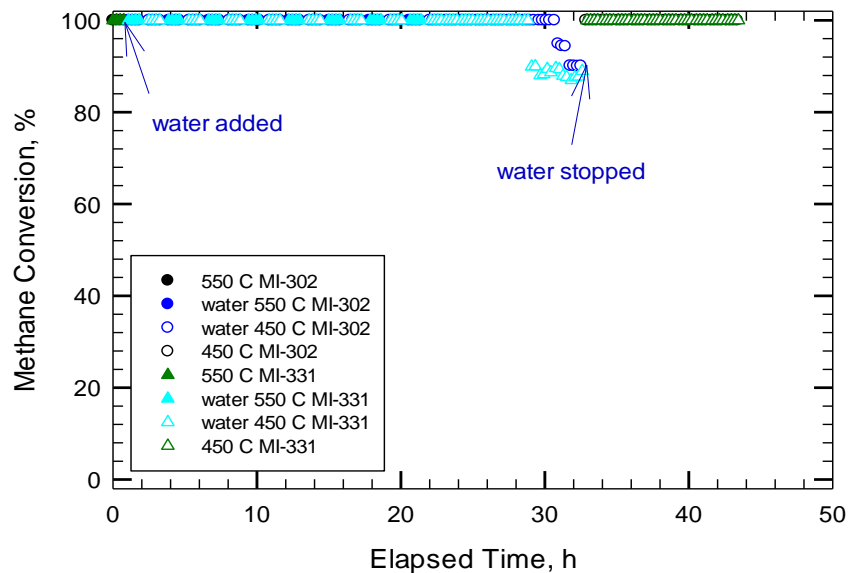


Figure 4.146. Variable temperature hydrothermal ageing of methane conversion of Pt-Pd (1:5) catalyst de-greened at 550°C (MI-302 vs MI-331) (CH<sub>4</sub> 4100±50 ppm, 5% vol. water, total flow rate 235 cc/min)

A new Pt-Pd (1:5) sample was de-greened at 600°C and a VTHTA test 650°C-450°C was performed. The results are presented in figure 4.147. Figure 4.148 compares the experimental results of VTHTA tests 650°C-450°C MI-312 and MI-336 (both tested samples de-greened at 600°C and hydrothermally aged 650°C-450°C). It can be observed that the activities and deactivation of the samples are very similar. This highlights the good reproducibility of the tests as well as the influence of de-green temperature on the activity of Pt-Pd (1:5) catalyst.

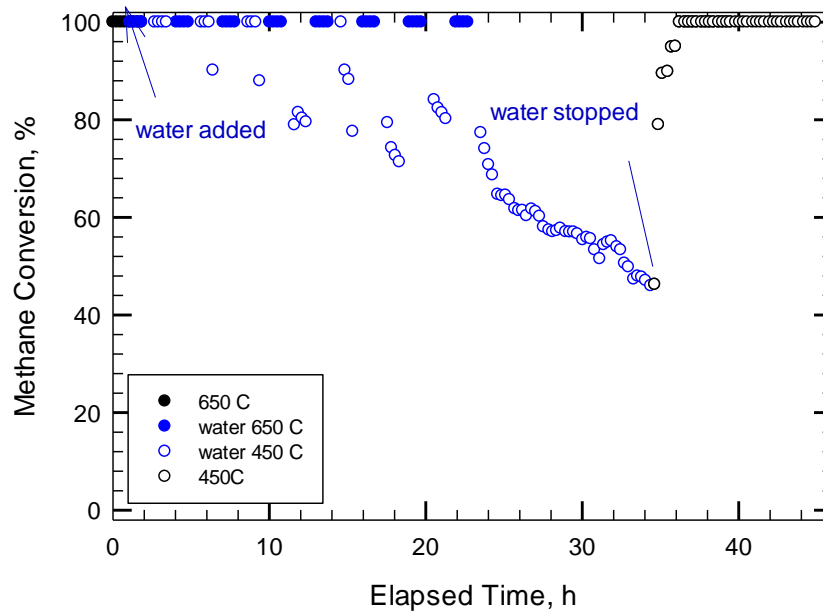


Figure 4.147. Variable temperature hydrothermal ageing of methane conversion of Pt-Pd (1:5) catalyst de-greened at 600°C (MI-336) (CH<sub>4</sub> 4100±50 ppm, 5% vol. water, total flow rate 235 cc/min)

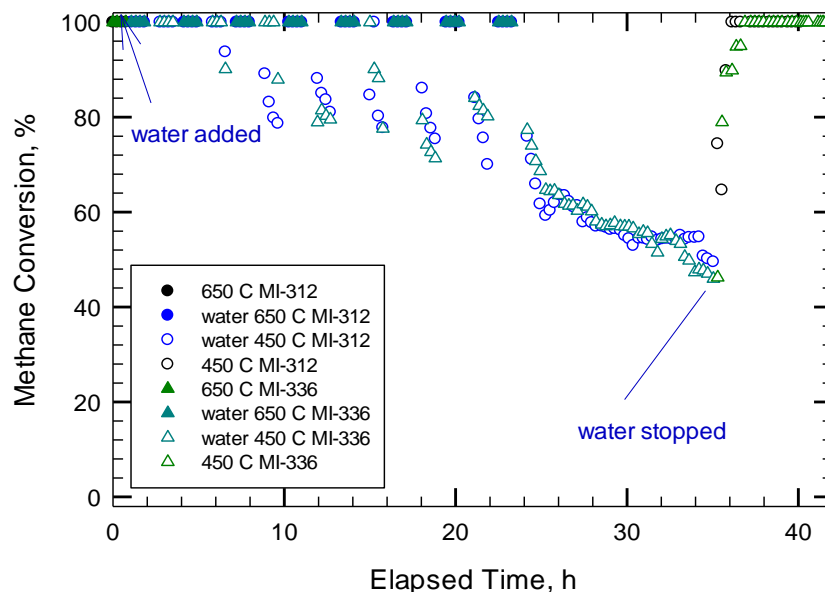


Figure 4.148. Variable temperature hydrothermal ageing test of methane conversion of Pt-Pd (1:5) catalyst de-greened at 600°C (MI-312 vs MI-336) (CH<sub>4</sub> 4100±50 ppm, 5% vol. water, total flow rate 235 cc/min)

## Conclusions:

### *Pd 150 catalyst*

The de-green temperature of the Pd 150 catalyst has an influence on the stability of the catalyst, i.e. results for 550°C shows slightly higher activity and stability of the catalyst

The de-green temperature of the Pd 150 catalyst has an influence on the stability of the catalyst, i.e. results for 550°C shows slightly higher activity and stability of the catalyst

#### *Pt-Pd (1:5) catalyst*

For thermal ageing test the Pt-Pd (1:5) catalyst de-greened at 650°C showed a higher resistance to water deactivation compared with the sample de-greened at 550 °C.

However, for hydrothermal ageing, higher activity and higher resistance to water deactivation was observed for de-greening temperature of 550°C.

### **4.9. Hydrogen effect on the activity of the catalyst**

The effect of hydrogen pre-treatment on the catalytic activity was investigated. The presence of a hysteresis loop after reduction of the catalysts was observed for Pd and predominantly Pd catalyst, hysteresis which changes or disappears after thermal and hydrothermal ageing of the samples.

#### *4.9.1. Pd 80 catalyst (CH<sub>4</sub> 4700±50 ppm)*

Figure 4.149 compares the experimental results of ignition-extinction curves of the initial activity of the catalyst (MI-089) and the activity after some ageing of the catalyst, in absence of water (MI-098). It can be observed that the ignition-extinction curves shifted toward higher temperatures due to a decrease in the catalytic activity. The decrease in the catalytic activity is assumed to be due to sintering of the particles. It also can be observed that the hysteresis loop of the ignition-extinction curves disappears after the thermal ageing experiments.

Figure 4.150 compares a similar situation as described above: ignition-extinction before thermal ageing (MI-106) and ignition-extinction after the thermal ageing (MI-111). A decrease in the size of the hysteresis loop can be observed, as well as a shift towards higher temperatures of the ignition-extinction curves after the thermal ageing.

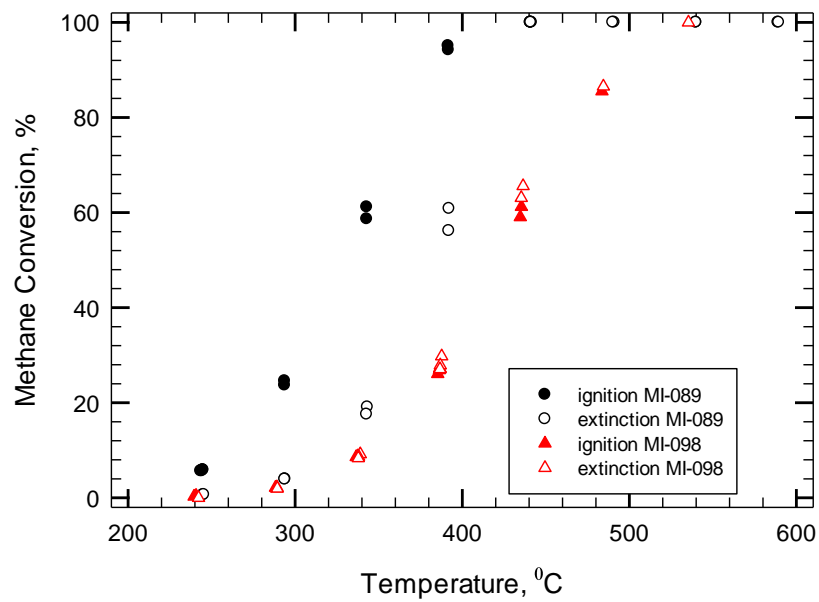


Figure 4.149. Ignition-extinction curves of methane conversion of Pd 80 catalyst before (MI-089) and after (MI-098) thermal ageing (CH<sub>4</sub> 4700±50 ppm, total flow rate 235 cc/min)

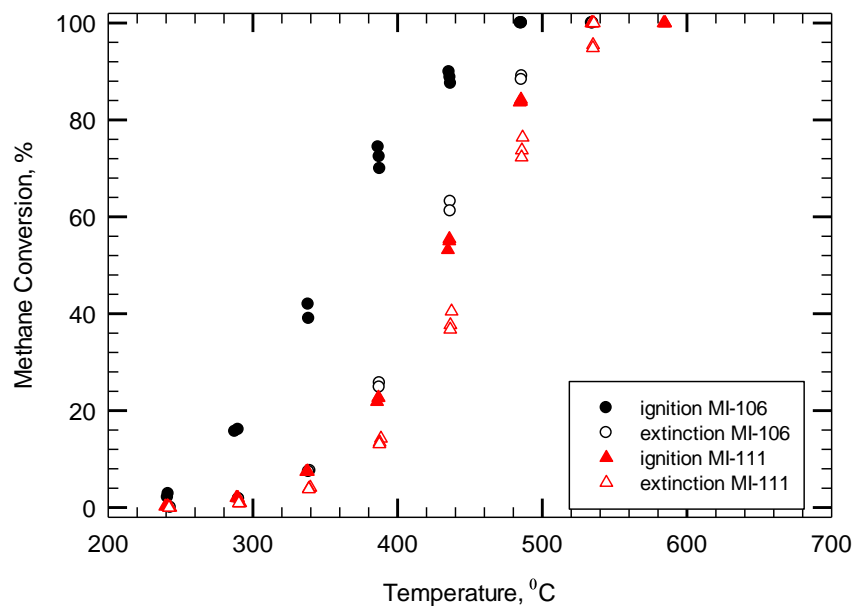


Figure 4.150. Ignition-extinction curves of methane conversion of Pd 80 catalyst before (MI-106) and (MI-111) after thermal ageing (CH<sub>4</sub> 4700±50 ppm, total flow rate 235 cc/min)

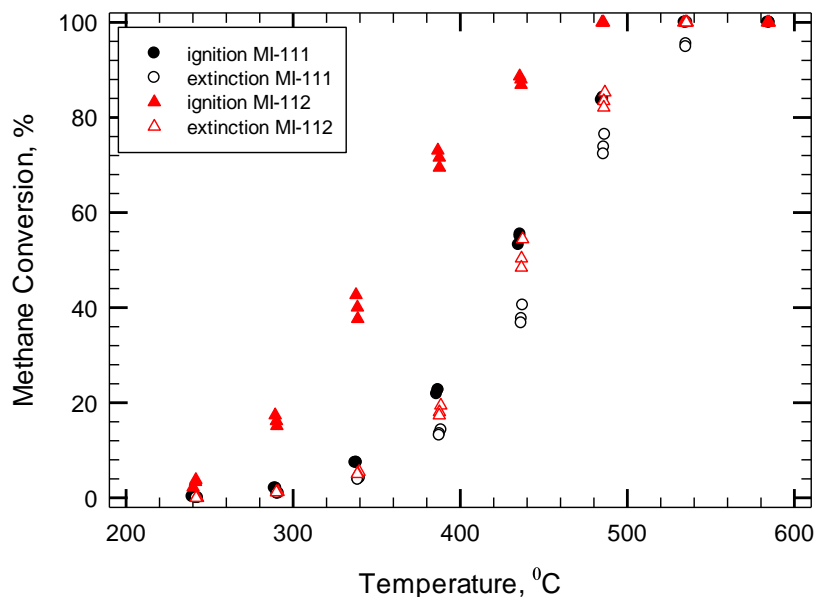


Figure 4.151. Ignition-extinction curves of methane conversion of Pd 80 catalyst after the thermal ageing experiments (MI-111) and after the sample was reduced (MI-112) (CH<sub>4</sub> 4700±50 ppm, total flow rate 235 cc/min)

Figure 4.151 compares the ignition-extinction results after thermal ageing (MI-111) and the ignition-extinction results after reduction of the same sample (MI-112). It can be observed that the ignition-curve shifted toward lower temperatures. This is assumed to be due to the hydrogen activation of the sample.

Figure 4.152 compares the ignition-extinction curves of methane conversion over Pd 80 catalyst. The experiment MI-106 was performed with a fresh de-greened and reduced sample, while experiment MI-112 was performed with a thermally aged and reduced sample. It can be observed that both experiments show similar activities. It was therefore concluded that the reduction of the catalyst brings back the initial activity.

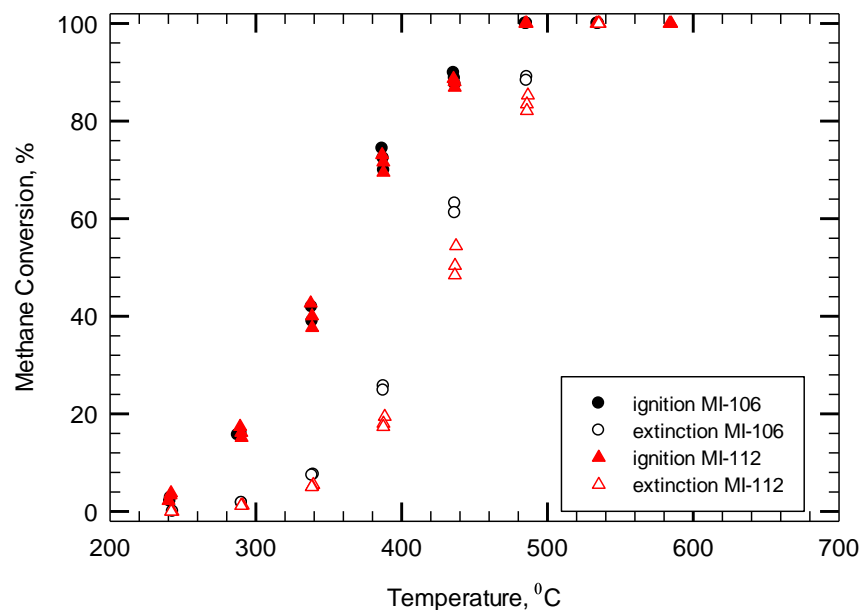


Figure 4.152. Ignition-extinction curves of methane conversion over Pd 80 catalyst: MI-106 fresh and reduced sample, MI-112 thermally aged and reduced sample (CH<sub>4</sub> 4700±50 ppm, total flow rate 235 cc/min)

#### 4.9.2. Pd 150 catalyst (CH<sub>4</sub> 4100±50 ppm)

The presence of a hysteresis loop was also observed for Pd 150 catalyst. To assess the changes in the catalytic activity, 2 ignition-extinction cycles were performed one after another (MI-339 and MI-340). Figure 4.153 compares the experimental results of the two ignition-extinction curves. It can be observed that the activity of the second ignition-extinction cycle shifted towards higher temperatures compared with activity of the first ignition-extinction curve, i.e. 78% conversion for the first light off curve at 350°C compared with 58% conversion for the second light off curve. However, 100% conversion of methane is obtained at 400°C for both samples.

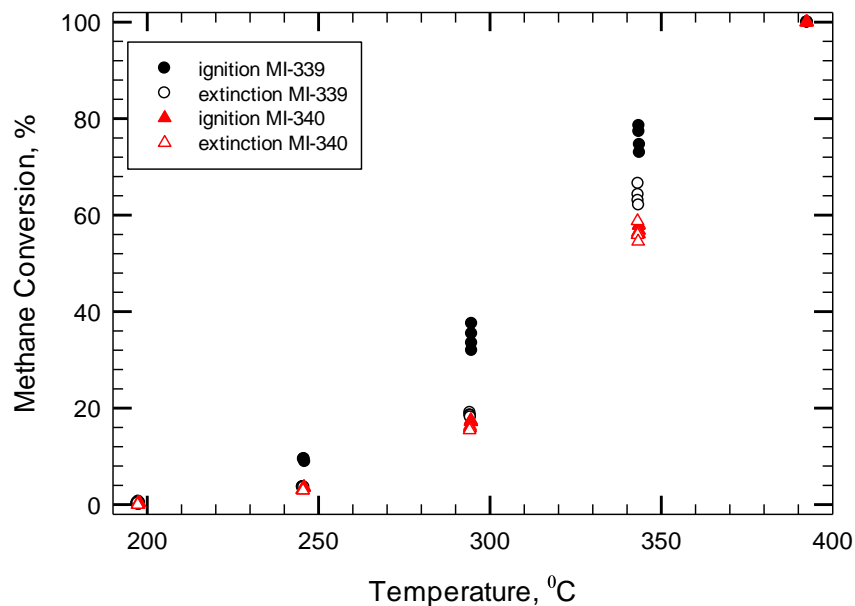


Figure 4.153. Ignition-extinction curves of methane conversion of Pd 150 catalyst: MI-339 fresh and reduced sample; MI-340 thermally aged and non-reduced sample (CH<sub>4</sub> 4100±50 ppm, total flow rate 235 cc/min)

#### 4.9.3. Pd Rh catalyst (CH<sub>4</sub> 4100±50 ppm)

The presence of a hysteresis loop observed for PdRh catalyst was investigated. Two ignition-extinction cycles were performed one after another (MI-315 and MI-316). Figure 4.154 compares the experimental results of the two ignition-extinction curves. As in the case of Pd 150 catalyst, the activity of the second ignition-extinction cycle was lower compared with the activity of the first ignition-extinction cycle. The hysteresis loop that was observed in the first ignition-extinction cycle is not observed in the second ignition-extinction cycle. However, 100% conversion of methane was obtained for both samples at 450°C.

Similar results were obtained for experiments MI-344 and MI-345: ignition-extinction performed for the fresh and reduced sample (MI-344) followed by another ignition-extinction curve for the thermally aged sample (MI-345) (figure 4.155).

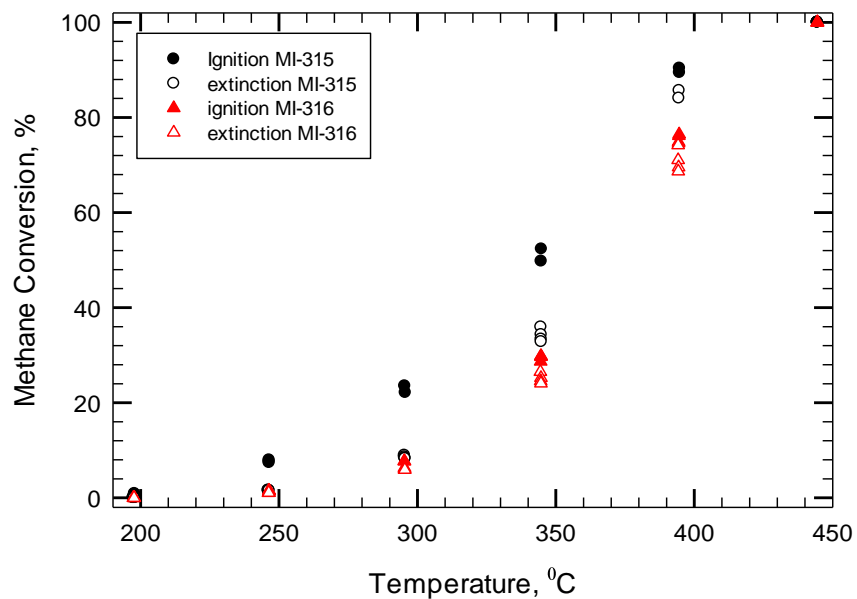


Figure 4.154. Ignition-extinction curves of methane conversion of PdRh catalyst: MI-315 fresh and reduced sample; MI-316 thermally aged sample (CH<sub>4</sub> 4100±50 ppm, total flow rate 235 cc/min)

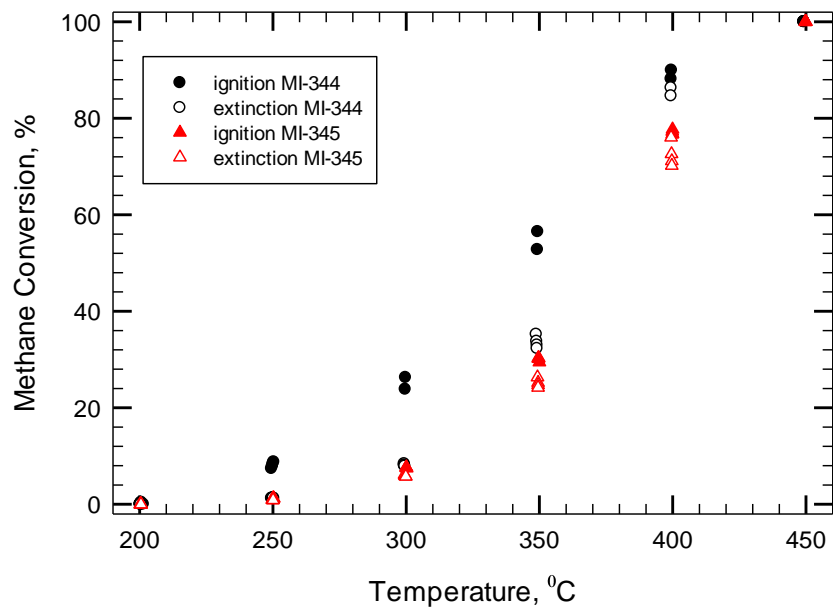


Figure 4.155. Ignition-extinction curves of methane conversion of PdRh catalyst: MI-344 fresh and reduced sample; MI-345 thermally aged sample (CH<sub>4</sub> 4100±50 ppm, total flow rate 235 cc/min)

#### 4.9.4. PtPdRh catalyst ( $CH_4$ $4100 \pm 50$ ppm)

Four ignition-extinction cycles of methane conversion, one after another, were performed for PtPdRh catalyst: MI-323 for the fresh and reduced sample, MI-324 for the thermally aged sample, MI-325 for the thermally aged sample and MI-326 for the thermally aged sample. Figure 4.156 compares the experimental results of the first two ignition-extinction cycles: MI-323 and MI-324. 100% conversion of methane was obtained at 500°C for both experiments. However, the catalytic activity of the second ignition-extinction cycle was lower compared with the initial ignition-extinction cycle. Figure 4.157 compares the ignition-extinction results of the thermally aged samples MI-325 and MI-326. A slight decrease in catalytic activity can be observed for the MI-326 experiment. However, 100% conversion of methane at 500°C was obtained for both experiments.

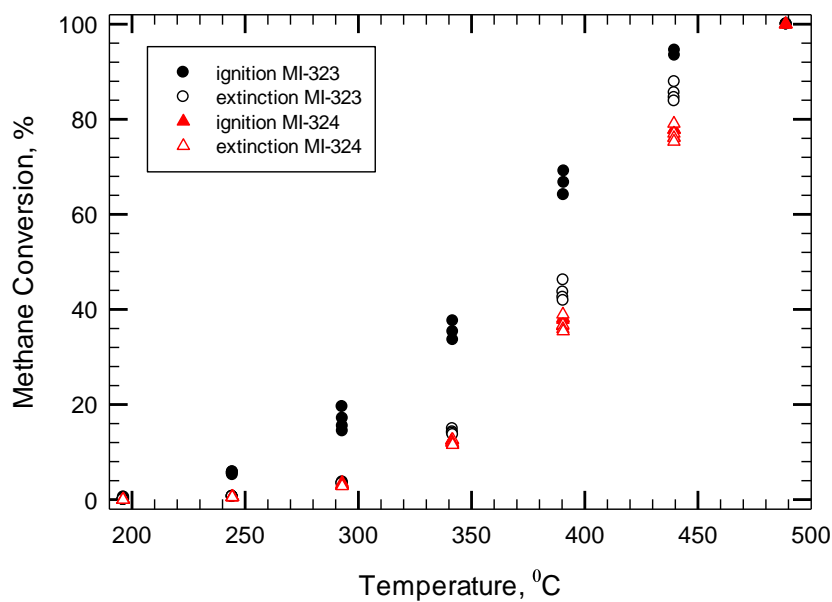


Figure 4.156. Ignition-extinction curves of methane conversion of PtPdRh catalyst: MI-323 fresh and reduced sample; MI-324 thermally aged sample ( $CH_4$   $4100 \pm 50$  ppm, total flow rate 235 cc/min)

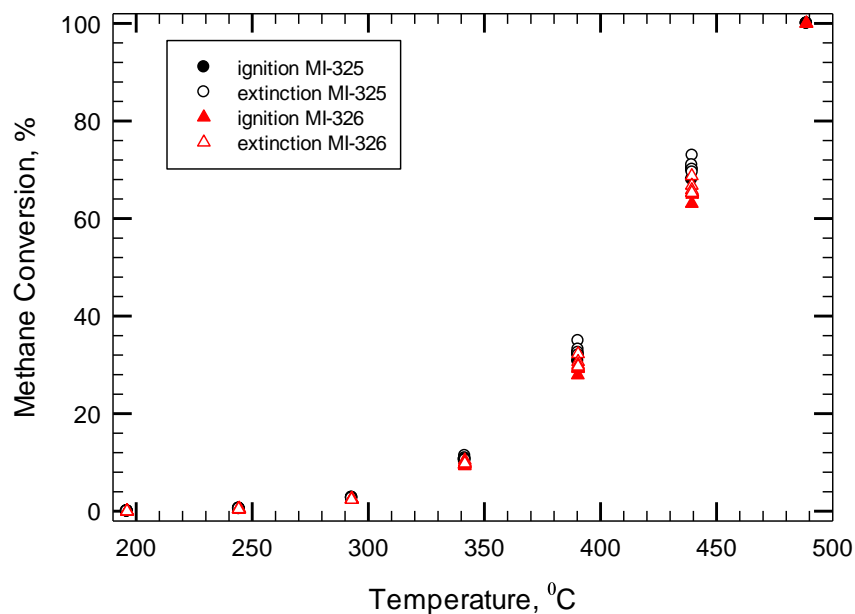


Figure 4.157. Ignition-extinction curves of methane conversion over PtPdRh catalyst: MI-325 the third ignition-extinction cycle; MI-326 the fourth ignition-extinction cycle ( $\text{CH}_4$   $4100 \pm 50$  ppm, total flow rate 235 cc/min)

#### 4.9.5. Pd 122 catalyst ( $\text{CH}_4$ $4100 \pm 50$ ppm)

The presence of a similar hysteresis loop was also observed for Pd 122 catalyst. A sequence of tests was performed to investigate the nature of hysteresis loop: a fresh sample was de-greened and reduced; then an ignition-extinction cycle was performed (MI-379); the change in hysteresis loop was assessed by performing another ignition-extinction cycle (MI-380); then the same sample was reduced again and one ignition-extinction cycle was performed to assess the activity of the catalyst (MI-381), followed by another ignition-extinction cycle to assess the changes in catalytic activity (MI-382); an ignition-extinction cycle was performed on a fresh de-greened sample, with no reduction of the sample (MI-383); another ignition-extinction cycle was performed to assess the changes in the catalytic activity (MI-384).

Figure 4.158 compares the ignition-extinction results of methane conversion over reduced (MI-379) and thermally aged (MI-380) Pd 122 catalyst. No hysteresis loop was observed for the thermally aged Pd 122 catalyst.

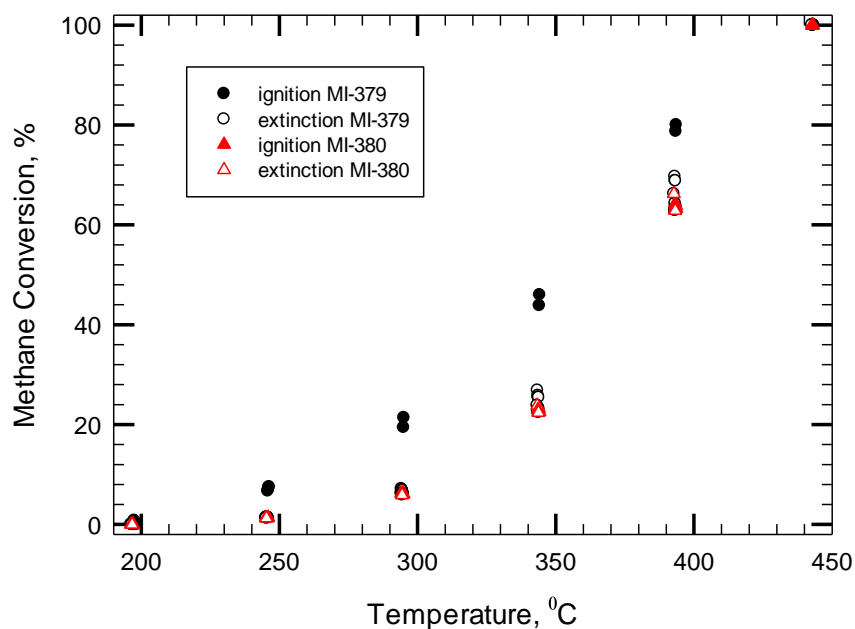


Figure 4.158. Ignition-extinction curves of methane conversion of Pd 122 catalyst: MI-379 fresh and reduced sample; MI-380 thermally aged sample (CH<sub>4</sub> 4100±50 ppm, total flow rate 235 cc/min)

Figure 4.159 compares the ignition-extinction curves of the reduced Pd 122 catalyst samples (MI-379 and MI-381). It can be observed that after hydrogen exposure, the activity of the catalyst returns to the initial values.

Figure 4.160 compares the ignition-extinction results of thermally aged Pd 122 sample (MI-380) and a reduced Pd 122 sample. It can be observed that the extinction curve of the reduced sample (MI-381) shows the same activity as the thermally aged sample (MI-380). However the ignition curve of the reduced samples shows higher activity than the thermally aged sample.

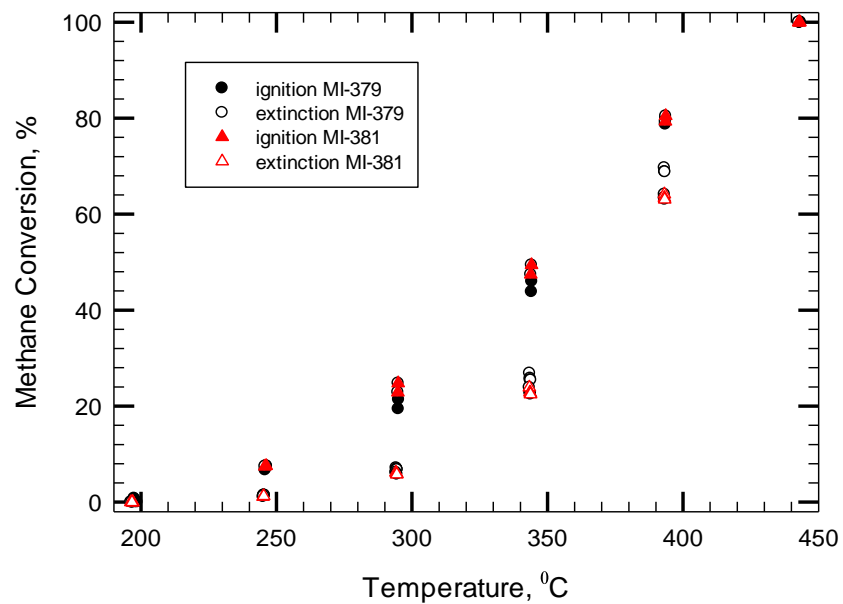


Figure 4.159. Ignition-extinction curves of methane conversion of Pd 122 reduced sample: MI-379 vs MI-381 (CH<sub>4</sub> 4100±50 ppm, total flow rate 235 cc/min)

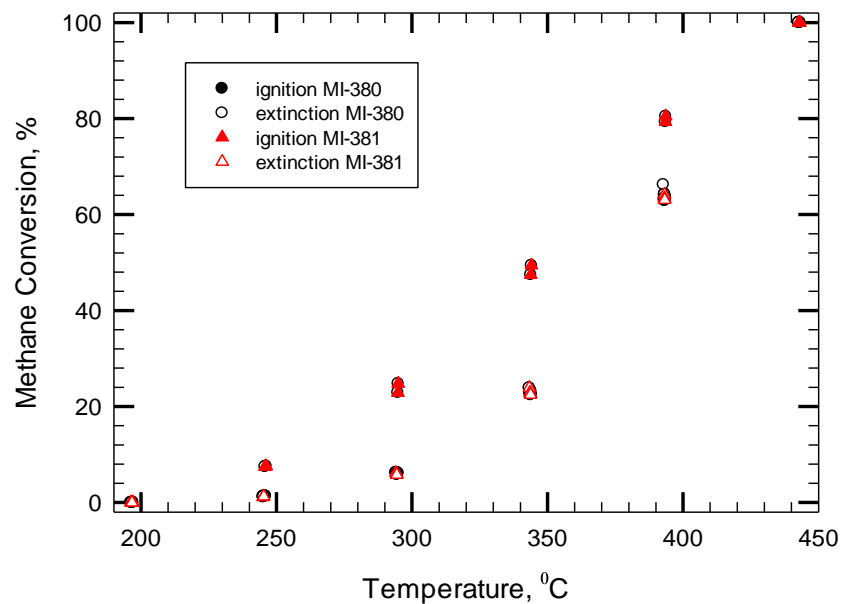


Figure 4.160. Ignition-extinction curves of methane conversion of Pd 122 catalyst: MI-380 thermally aged sample; MI-381 reduced sample (CH<sub>4</sub> 4100±50 ppm, total flow rate 235 cc/min)

Figure 4.161 compares the ignition-extinction curves of reduced sample (MI-381) and thermally aged sample (MI-382). It can be observed that 100% conversion of methane is obtained at higher temperature than for the reduced sample. A hysteresis loop can be observed for the reduced sample and no hysteresis loop for the thermally aged sample.

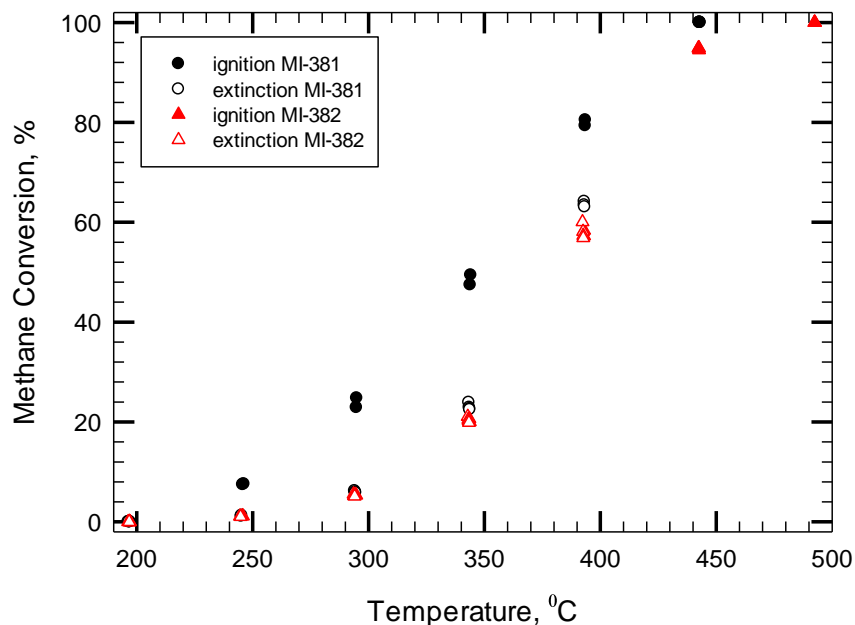


Figure 4.161. Ignition-extinction curves of methane conversion of Pd 122 catalyst: MI-381 reduced sample; MI-382 thermally aged sample (CH<sub>4</sub> 4100±50 pm, total flow rate 235 cc/min)

Figure 4.162 presents the experimental results of just de-greened sample (no reduction) (MI-383). It can be observed that there is no hysteresis loop. However, 100% conversion of methane was obtained at 450°C, similar as for the reduced samples (i.e. MI-381).

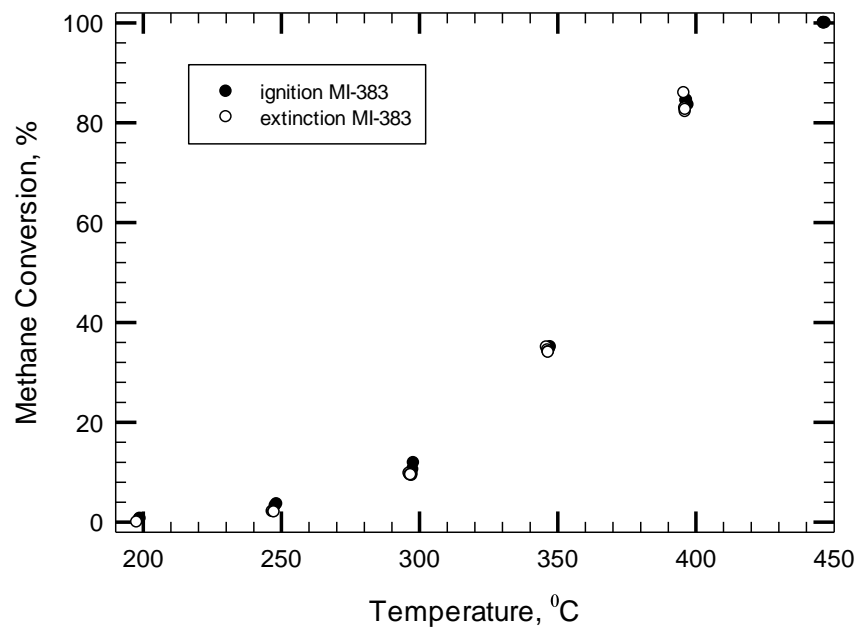


Figure 4.162. Ignition-extinction curves of methane conversion of Pd 122 catalyst: MI-383 de-greened sample, non-reduced (CH<sub>4</sub> 4100±50 ppm, total flow rate 235 cc/min)

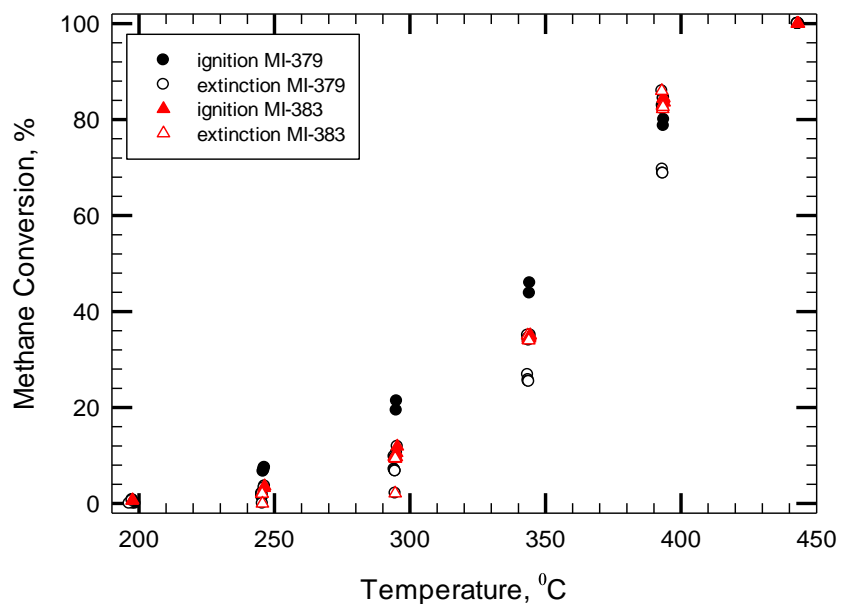


Figure 4.163. Ignition-extinction curves of methane conversion over Pd 122 catalyst: MI-379 de-greened and reduced sample; MI-383 just de-greened sample (CH<sub>4</sub> 4100±50 ppm, total flow rate 235 cc/min)

Figure 4.163 compares the ignition-extinction curves of just de-greened sample (MI-383) with de-greened and reduced sample (MI-379). It is interesting to observe that for temperatures up to 300°C, the ignition activity of the just de-greened sample (MI-383) is similar with the extinction activity of the de-greened and reduced sample (MI-379). However, for 450°C and above, the activity of just de-greened sample is similar with the ignition activity of the de-greened and reduced sample.

Another ignition-extinction cycle was performed for the previously just de-greened sample to assess the changes in catalytic activity as a function of thermal ageing (MI-384). Figure 4.164 compares the experimental results of MI-383 and MI-384 tests. No hysteresis loop was observed for the MI-384 experiment. There was no significant changes in the catalytic activity of the sample, i.e. for 400°C, 84% conversion was obtained for MI-383 test and 80% conversion was obtained for MI-384 test.

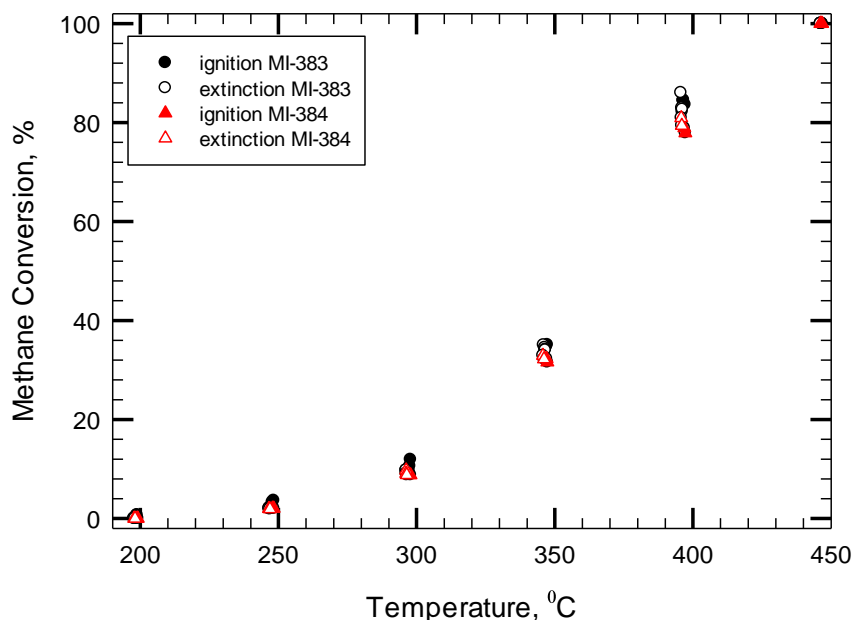


Figure 4.164. Ignition-extinction curves of methane conversion of Pd 122 catalyst: MI-383 just de-greened sample; MI-384 used sample (CH<sub>4</sub> 4100±50 pm, total flow rate 235 cc/min)

## Conclusions:

For Pd and predominantly Pd samples, the reduction process brings an increase in the initial catalytic activity. However, the effect of reduction disappears after a short thermal ageing treatment. The activity of just de-greened samples seems to don't be affected by short thermal ageing treatments.

### 4.10. The influence of catalyst loading on the activity and stability of the catalyst

Figure 4.165 compares the ignition-extinction curves of Pd 122 and Pd 150 catalyst. Both catalysts show a negative hysteresis. It can also be observed that Pd 150 shows a higher activity of methane conversion compared with Pd 122 catalyst. For example 92% conversion of methane was obtained at 350°C for Pd 150 catalyst, compare with 53% conversion for Pd 122 catalyst.

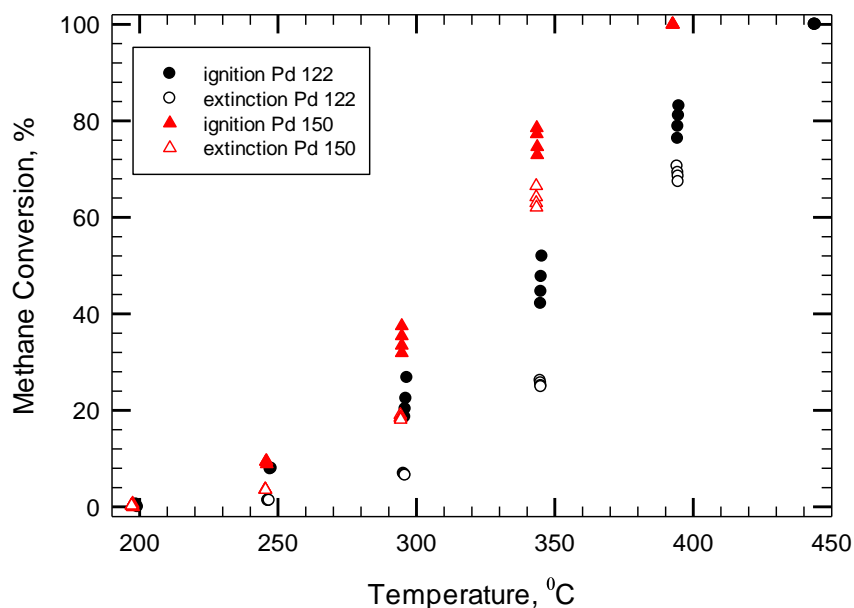


Figure 4.165. Ignition-extinction curves of methane conversion over Pd 122 (MI-357) and Pd 150 (MI-339) catalysts (CH<sub>4</sub> 4100±50 ppm, total flow rate 235 cc/min)

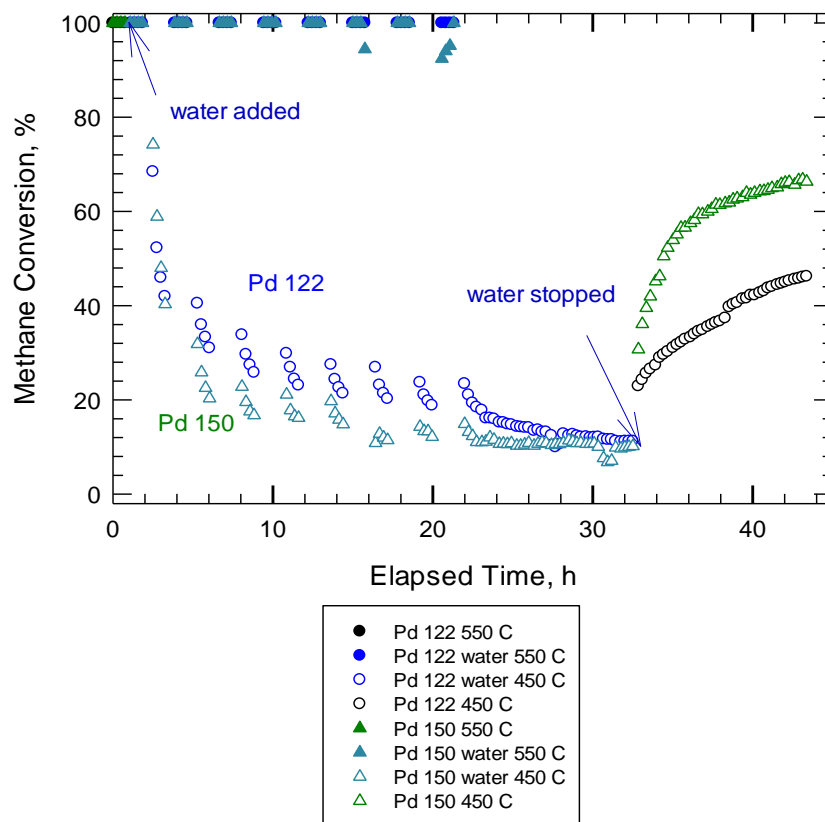


Figure 4.166. Variable temperature hydrothermal ageing test of methane conversion over Pd 122 (MI-358) and Pd 150 (MI-341) ( $\text{CH}_4$  4100 $\pm$ 50 ppm, 5% vol. water, total flow rate 235 cc/min)

Figure 4.166 compares the experimental results of variable temperature hydrothermal ageing of Pd 122 and Pd 150 catalysts. It has been previously shown that the loading of the catalyst has an influence on the activity and stability of the catalyst (Flynn et al., 1975, Fiedorow et al., 1976) The experimental results presented in figure 4.166 are in good agreement with the observation of Flynn, P.C. and Fiedorow, R. M. regarding the influence of catalyst particles loading on the deactivation of the catalysts. It was shown that a higher loading of a catalyst brings a higher activity of the catalyst. However, the sintering of particles is also a function of the loading. Wanke S. concluded that the sintering process is a function of the distance between catalysts particles, i.e. the higher the loading of supported catalyst the higher the sintering process of the catalyst particles (Wanke et al., 1975). For the 450°C temperature intervals it can be observed that Pd 150

shows a lower activity of methane conversion compared with Pd 122 catalyst. This can be assumed to be due to the more pronounced effect of the metal particles sintering of Pd 150 catalyst, compared with Pd 122 catalyst. However, after 33 hours in presence of water, the activities of the catalysts are similar. After the water was switched off the recovery in activity of Pd 150 catalyst is higher compared with Pd 122 catalyst.

Figure 4.167 compares the ignition-extinction curves of methane conversion over Pd 122 (MI-359) and Pd 150 (MI-342) catalysts. Both samples present similar activity in conversion of methane after VTHTA test.

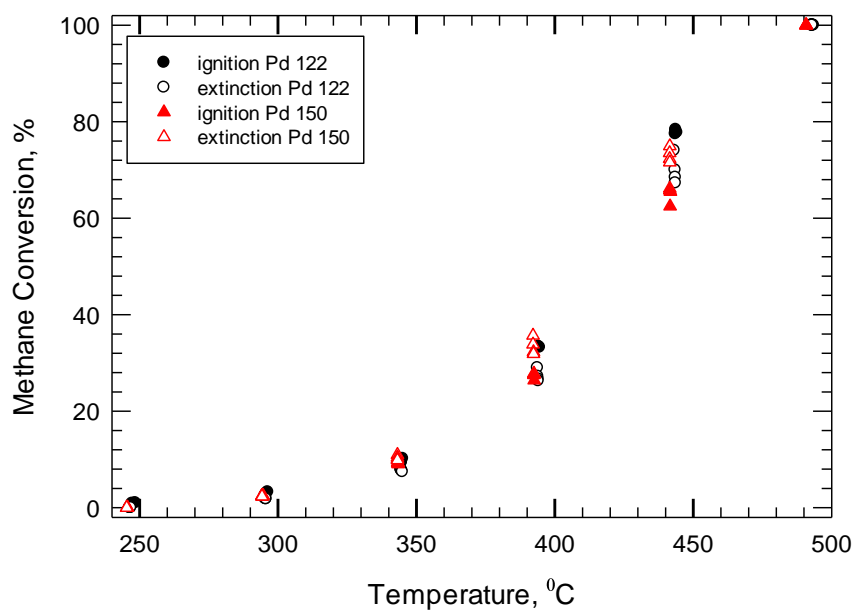


Figure 4.167. Ignition-extinction curves of methane conversion over Pd 122 (MI-359) and Pd 150 (MI-342) catalysts, after VTHTA test (CH<sub>4</sub> 4100±50 ppm, total flow rate 235 cc/min)

## Conclusions

It was observed that an increase in the catalyst loading brings an increase in the catalytic activity.

It was also observed that an increase in loading brings a decrease in conversion of methane in presence of water.

## 5.1 Summary of experimental results

### 5.1.1 General behaviour of the catalysts

Pt only and Pd 80 only catalyst showed a negative hysteresis (ignition more active than extinction curves), while bimetallic Pt-Pd (4:1) catalyst showed a positive hysteresis (extinction curve more active than ignition curve). Pd 80 only showed the highest activity in methane conversion, Pt catalyst showed the lowest conversion and both bimetallic Pt-Pd catalysts showed intermediate conversion.

The three way catalysts (Pd 122, PdRh and PtPdRh) showed negative hysteresis. The highest activity in methane conversion was observed for Pd 122 and PdRh catalysts.

### 5.1.2. Diesel oxidation catalysts: Pd 80, Pd 150, Pt, Pt-Pd (4:1), Pt-Pd (1:5) catalysts

-The dependence of catalytic activity on the temperature and atmosphere present in the reactor during the heating up process of reactor was clearly observed just for Pt-Pd (4:1) catalyst and not for Pd 80 only and Pt only catalysts. From CO chemisorption results it was concluded that the change in particle size as a result of thermal treatment in presence of oxygen or inert gas is insignificant for Pt, Pd 80 and Pt-Pd (4:1) catalysts. In consequence, sintering process of metal particles is not the culprit of the change in catalytic activity. From the TPR result was concluded that Pt-Pd (4:1) catalyst is an alloy rather than mixture of Pt and Pd catalysts. It was assumed that the specific behaviour of Pt-Pd (4:1) catalyst is due to the structure of the catalyst.

- Different patterns were observed, as a function of time for thermal ageing at constant temperature test of Pt, Pd 80 and Pt-Pd (4:1) catalysts: a slight decrease of methane conversion for Pt catalyst, a strong decrease in activity for Pd 80 catalyst while a slight increase in activity was observed for Pt-Pd (4:1) catalyst. It

was therefore concluded that the addition of Pd to Pt catalyst brings an increase in the performance of the catalyst for methane combustion.

-The experimental results of variable temperatures thermal ageing test of Pd150, Pt, Pt-Pd (4:1) and Pt-Pd (1:5) catalysts showed that Pd 150 and Pd predominantly catalysts show the highest activity in methane conversion. It was also observed that all catalysts show a negative hysteresis except the Pt and predominantly Pt bimetallic catalyst (Pt-Pd (4:1)). A better resistance to thermal ageing deactivation was observed for Pd formulated catalysts, Pt-Pd (1:5) and Pt-Pd (4:1), compared with Pd 150 catalyst. The addition of small amounts of Pt to Pd catalysts (i.e. Pt-Pd (1:5) catalysts) resulted in overall better activity and stability in conversion of methane. The increase in Pt content contributed to the stability and activity of Pd catalyst.

-For hydrothermal ageing at constant temperature, bimetallic Pt-Pd (4:1) showed higher activity of methane conversion and good resistance to water deactivation compared with Pt catalyst.

- For the variable temperature hydrothermal ageing test (VTHTAT) the conversion of methane for Pt, Pd 150, Pt-Pd (4:1), Pt-Pd (1:5) showed that Pd and predominantly Pd catalyst (Pt-Pd (1:5)) are the most active. A decrease in activity as a result of hydrothermal treatment was observed for all four catalysts.

### *5.1.3. Three way catalytic converters: Pd 150, Pd 122, Pt-Pd (1:5), Pd Rh, PtPdRh*

-For variable temperature thermal ageing test (VTTAT), Pd 122 and PdRh catalysts showed similar behaviours and catalytic activities. This was assumed to be due to a very similar precious metal loading (0.816 % Pd for Pd 122 catalyst and 0.8 % Pd for PdRh catalyst). In the presence of water the activity of both catalysts decreased in the same fashion. The higher activity, stability and resistance to water deactivation observed for PdRh catalyst compared with PtPdRh catalyst was also assumed to be due to the precious metal loading (0.80 %

Pd, 0.02% Rh for PdRh catalyst and 0.13% Pt, 0.49 % Pd, 0.02% Rh for PtPdRh catalyst). For the Pd 150 (1% Pd) and Pt-Pd (1:5) (0.16 % Pt, 0.835 % Pd) catalysts de-greened at 550°C, the structure of Pt-Pd (1:5) particles was assumed to be responsible for higher activity and resistance to water deactivation.

-For the variable temperature hydrothermal ageing test (VTHTAT) catalyst, similar activity and stability of methane conversion were observed for Pd 122 and PdRh. When compared with PtPdRh catalyst, the PdRh catalyst showed higher activity and resistance to water deactivation which was assumed to be due to the loading of precious metal.

The higher activity and resistance to water deactivation of Pt-Pd (1:5) catalyst compared with Pd 150 catalyst was assumed to be due to the structure of Pt-Pd (1:5) particles.

-The influence of metal loading for Pd 122 and Pd 150 catalysts showed that Pd 150 catalyst had a higher activity. However, in presence of water Pd 122 showed a higher stability. This behaviour was assumed to be a consequence of the sintering effect as a function of metal loading, i.e. the sintering effect of metal particles increases with the increase of metal loading.

-The experimental results of catalytic activity of Pd 150 and Pt-Pd (1:5) catalysts as a function of de-greening temperature showed that for Pd 150 catalyst the de-greening at 550 °C compared with 650 °C brings an increase in activity and stability of the catalyst for both thermal and hydrothermal ageing tests. For Pt-Pd (1:5) catalyst for thermal ageing test, the sample de-greened at 650°C showed a higher resistance to water deactivation compared with the sample de-greened at 550 °C. For hydrothermal ageing, however, higher activity and higher resistance to water deactivation was observed for the sample de-greened at 550°C.

-The experimental results showed that reduction pre-treatment of the samples have a positive effect on Pd only catalysts (80, 122 and 150 g/ft<sup>3</sup>) as well as Pd formulated catalysts (Pt-Pd (4:1), Pt-Pd (1:5), PdRh, PtPdRh).

-The concentration of methane on the catalytic activity was observed for Pt-Pd (4:1) catalyst, i.e. the ignition-extinction curve shifted toward higher temperatures for 4700 ppm compared with 4100 ppm.

-The negative effect of water on the catalytic activity was observed for all catalysts. The effect was stronger on the Pd only (80, 122 and 150 g/ft<sup>3</sup>) and Pd formulated catalysts (Pt-Pd (4:1), Pt-Pd (1:5), PdRh, PtPdRh). However, all catalysts showed no hysteresis in presence of water, except Pt-Pd (4:1) catalyst, which showed a large negative hysteresis.

## **5.2. Further work**

### *5.2.1. Gas constituents*

The study of the catalytic activity should be conducted for more complex compositions and different concentrations of reactants. The composition of the reactants used in this project was much simpler than real vehicle exhaust from internal combustion engines. Carbon Monoxide, nitrogen oxides are also presents beside the methane, CO<sub>2</sub> and water. It is expected that the behavior of the catalysts will be affected by complex exhaust gases, considering that some of the components may improve or inhibit the reaction. It is expected that higher amounts of water will be produced in the real exhaust gas then the ones used in the project.

### *5.2.2. Characterisation of the catalysts*

The activity of the catalyst depends on the state of the precious metal articles. X-Ray photoelectron spectroscopy (XPS) will be a useful tool in determining the oxidation state of the active metal after exposure of the samples to various conditions of reaction. The study of morphological changes of the support and catalyst will be important as it can provide information about the changes that take place during the reaction. Scanning electron microscopy (SEM) might be an appropriate method of determining the morphology changes. Detailed

investigation of the catalysts can provide useful information about the processes that takes place during the reaction.

### *5.2.3. Study and development of different catalyst formulations*

The interesting behaviour of bimetallic Pt-Pd (4:1) and Pt-Pd (1:5) catalyst studied in this project suggests that the effect of Pt ratio on the activity and the stability of Pd catalyst should be studied further investigated. The effect of different earth metal on the catalyst performance should be investigated. Haruta showed that highly dispersed gold on reducible semiconductors shows high conversion of CO, otherwise considered less active than platinum group metals (Haruta et al. 1994).

## References

Akhtar, M., Tompkins, F. C., (1971, a), The hydrogen/oxygen titration on platinum film. Determination of the catalytically active area, *Trans. Faraday. Soc.*, 67, p. 2454

Akhtar, M., Tompkins, F. C., (1971, b), Effect of presorption on platinum films on the catalytic oxidation of hydrogen; and area determination by carbon monoxide/oxygen titration, *Trans. Faraday. Soc.*, 67, p. 2461

Anderson, R.B., Stein, K. C. Feenan, J.J. and Hofer, L. J. E., (1961), Catalytic oxidation of methane, *Industrial and Engineering Chemistry Research*, 53, p. 809

Ayoub, M., Irfan, M. F., Yoo, K.-S., (2011), Surfactants as additives for NO<sub>x</sub> reduction during SNCR process with urea solution as reducing agent, *Energy Conversion and Management*, vol 52 (10), p. 3083, Retrieved August 23, 2013 from <http://www.sciencedirect.com/science/article/pii/S0196890411001403>

Bagley, R. D., (1974), US Patent 3,790,654, Washington, DC (Ed.), US

Baird, T., Paal, Z., Thomson, S. J., (1973, a), Sintering studies on platinum black catalysts. Part 1. Effect of pre-treatment and reaction on particle size, *J. Chem. Soc., Faraday Trans. 1*, 69, p. 50

Baird, T., Paal, Z., Thomson, S. J., (1973, b), Sintering studies on platinum black catalysts. Part 2. Effect of temperature of treatment and method of preparation on the sintering process, *J. Chem. Soc., Faraday Trans. 1*, 69, p. 1237



Choudhary, V., Rane, V., (1992), Pulse micro reactor studies on conversion of methane, ethane, and ethylene over rare earth oxides in the absence of free oxygen, *J. of Catal.*, 135 (1), p. 310

Choudhary, V. R., Rane, V. H., Chaudhari, S. T., (1997), Surface properties of rare earth promote MgO catalysts and their activity/selectivity in oxidative coupling of methane, *Appl. Catal. A: General*, 158 (1-2), p. 121

Church, M. L., Cooper, B. J. Willson, P. J., (2006), Catalyst formulation 1960 to present, S.A.E. Technical Paper Series, Paper 890815, *Advanced three-way catalysts*, Warrendale, Pa.: Society of Automotive Engineers, p. 217

Corning Environmental Technologies, (n.d.), Diesel Particulate Filter, *Corning Incorporated: Home: Products & Services: Diesel Particulate Filters*, Retrieved August 23, 2013, from

[http://www.corning.com/environmentaltechnologies/products\\_services/particulate\\_filters.aspx](http://www.corning.com/environmentaltechnologies/products_services/particulate_filters.aspx)

Culley, S. A., McDonnell, T. F., Ball, D. J., Kirby, C. W., Hawes, S. W., (2006), The impact of passenger car motor oil phosphorus levels on automotive emissions control systems, SAE Technical Paper 961898, *Advanced three-way catalysts*. Warrendale, Pa.: Society of Automotive Engineers, p. 555

Dadyburjor, D. B., (1979), Splitting of supported metal catalysts, *Journal of Catalysis*, 57, p. 504

Davis Recycling Inc., (2007), Catalytic Converters: Types of Converters: Pellet, *Davis Recycling Inc.*, Retrieved August 23, 2013, from <http://davisconverters.com/Pellet-Converter.shtml>

Diesel Technology Forum, (2007), About Clean Diesel: What is SCR?. *Diesel Technology Forum: Home Page*, Retrieved August 23, 2013, from <http://www.dieselforum.org/index.cfm?objectid=99731DF0-B3D1-11E0-861B000C296BA163>

Eckhoff, S., Mueller, W., Lindner, D., Leyrer, J., Kreuzer, T., Vent, G., Schoen, C., Schmidt, J., Franz, J., (2006), Catalyst design for high performance engines capable to fulfill future legislation, SAE Technical Paper 2004-01-1276, *Advanced three-way catalysts*, Warrendale, Pa.: Society of Automotive Engineers, p. 17

Fiedorow, R. M. J., Wanke, S. E., (1976). The sintering of supported metal catalysts. I. Redispersion of supported Platinum in oxygen, *J. Catal.*, 43, p. 34

Flynn, P. C., Wanke, S. E., (1974). A model of supported metal catalysts sintering. I. Development of model, *J. Catal.*, 34, p. 390

Flynn, P. C., Wanke, S. E., (1975), Experimental studies of sintering of supported platinum catalysts, *J. Catal.*, 37, p. 432

Gavin Schmidt, (2004), Methane: A Scientific Journey from Obscurity to Climate Super-Stardom, NASA GISS: Research Features, Retrieved June 18, 2013, from [http://www.giss.nasa.gov/research/features/200409\\_methane/](http://www.giss.nasa.gov/research/features/200409_methane/).

Gelin, P., Urfels, L., Primet, M., Tena, E., (2003), Complete oxidation of methane at low temperature over Pt and Pd catalysts for the abatement of lean-burn natural gas fuelled vehicles emissions: Influence of water and sulphur containing compounds, *Catal. Today*, 83 (1-4), p. 45

Goldsmith, J., Rogers, L. (1959). Health hazards of automobile exhaust, *Public Health Reports*, 74 (6), p. 551, Retrieved November 19, 2013, from <http://www.ncbi.nlm.nih.gov/pmc/articles/PMC1929251/pdf/pubhealthreporig00126-0083.pdf>

Government of Canada, (2012), [Cars, Trucks, Vans and Sport Utility Vehicles \(SUVs\)](#), *Government of Canada, Environment Canada*, Retrieved November 17, 2013, from <http://www.ec.gc.ca/air/default.asp?lang=En&n=EC8E75D0-1>

Gruber, H. L., (1962 a), Chemisorption studies on supported platinum, *J. Phys. Chem.*, 66, (1), p. 48, Retrieved November 17, 2013, from <http://pubs.acs.org/doi/abs/10.1021/j100807a010>

Gruber, H. L., (1962 b), An adsorption flow method for specific metal surface area determination, *Analytical Chemistry*, 34, (13), p. 1828, Retrieved November 17, 2013, from <http://pubs.acs.org/doi/abs/10.1021/ac60193a045>

Haagen-Smit, Arie J. (1954), The Control of Air Pollution in Los Angeles, *Engineering and Science*, 18 (3), p. 11. Retrieved November 16, 2013 from <http://resolver.caltech.edu/CaltechES:18.3.haagen>

Haagen-Smit, Arie J., (1952), Smog Research Pays Off, *Engineering and Science*, 15 (8), p. 11. Retrieved November 16, 2013 from <http://resolver.caltech.edu/CaltechES:15.8.Haagen>

Haagen-Smit, Arie J., (1958), *Progress in Smog Control*. *Engineering and Science*, 21 (9), p. 5. Retrieved November 16, 2013 from <http://resolver.caltech.edu/CaltechES:21.9.haagensmit>

Haagen-Smit, Arie J., (1961), The Air We Breathe, *Engineering and Science*, 24 (7), p. 6. Retrieved November 16, 2013 from <http://resolver.caltech.edu/CaltechES:24.7.books>

Haagen-Smit, Arie J. (1962) Smog Control, *Engineering and Science*, 26 (2), p. 9. Retrieved November 16, 2013 from <http://resolver.caltech.edu/CaltechES:26.2.smog>

Haagen-Smit, Arie J., (1973), The Sins of Waste, *Engineering and Science*, 36 (4). p. 16. Retrieved November 16, 2013 from <http://resolver.caltech.edu/CaltechES:36.4.sins>

Hansen, K., (2008), Water Vapor Confirmed as Major Player in Climate Change, *NASA GSFC: News & Features: New Topics: Earth*, Retrieved November 19, 2013, from [http://www.nasa.gov/topics/earth/features/vapor\\_warming.html](http://www.nasa.gov/topics/earth/features/vapor_warming.html)

Haruta, M., Ueda, A., Bamwenda, G. R., Taniguchi, R., Azuma, M., (1994), Low temperature catalytic combustion over supported gold. In Proc. International workshop on catalytic combustion, Arai, H. (Ed), *Catalysis Society of Japan*, Tokyo, Japan, p. 2

Hayes, R.E., Kolaczkowski, S.T., (1997), Introduction to Catalytic Combustion. 1st Edn., *Gordon and Breach*, Australia

Henderson, Y. (1922). Automobile Exhaust Gas As A Health Hazard. *The Boston Medical and Surgical Journal*, 187(5), 180

Hicks, R. F. Qi, H. Young, M. L., Lee, R. G. (1990). Structure sensitivity of methane oxidation over platinum and palladium, *J. catal*, 122 (2), p. 280

Houdry, J. H., Hayes, C. T., (1958), Platinum oxidation catalysts in the control of air pollution, *Platinum Metals Rev.*, 2, (4), p. 110

Houdry, E. J., (1956), US Patent 2,742,437, Washington, DC: US

Hunt, L. B., (1979), Sir Humphry Davy on Platinum, *Platinum Metals Rev.*, 23, (1), p. 29

Hurtado, P., Ordonez, S. Sastre H., Diez, F., (2004), Combustion of methane over palladium catalyst in the presence of inorganic compounds: inhibition and deactivation phenomena, *Appl. Cat. B: Environmental*, 47 (2), p. 85

Jones, A., McNicol, B. D., (1986), Temperature-programmed reduction for solid materials characterization, *New York: M. Dekker, USA*

Kanazawa, T., Sakurai, K., (2006), Development of the automotive exhaust hydrocarbon adsorbent, SAE Technical Paper 2001-01-0660, *Advanced three-way catalysts*. Warrendale, Pa.: Society of Automotive Engineers, p. 61

Knight D., (1992), Humphry Davy, *Science and Power*, Cambridge University Press (Ed.), UK

Lassi, U., Polvinen, R., Suhonen, S., Kallinen, K., Savimaki, A., Harkonen, M., Valden, M., Keiski, R. L., (2004), Effect of ageing atmosphere on the deactivation of Pd/Rh automotive exhaust gas catalyst: catalytic activity and XPS studies, *Applied Catalysis A: General*, 263 (2), p. 241

LA Weekly, (2005), [History of Smog, LA Weekly: News: Clear and present danger](http://www.laweekly.com/2005-09-22/news/history-of-smog/), Retrieved November 17, 2013, from <http://www.laweekly.com/2005-09-22/news/history-of-smog/>

Lee, J. H., Trimm, D. L., (1995), Catalytic combustion of methane, *Fuel Processing Technology*, 42 (2-3), p. 339

Lee, Sunggyu, (1997), Methane and its derivative, *Marcel Dekker, Inc.* (Ed), New York

Lietz, G., Lieske, H., Spindler, H., Hanke, W., Volter, J., (1983), Reactions of platinum in oxygen- and hydrogen- treated Pt gamma Al<sub>2</sub>O<sub>3</sub> catalysts, *Journal of catalysis*, 81, p. 17

Liu, J.P., Curry, J.A., Wang, H., Song, M., Horton, R.M., (2012), Impact of declining Arctic sea ice on winter snowfall. *Proc. Natl. Acad. Sci.*, 109, p. 4074

Lui, Y.-K., Dettling, J. C., (2006), Evolution of Pd-Rh TWC Catalyst Technology, SAE Technical Paper 930249, *Advanced three-way catalysts*, Warrendale, Pa.: Society of Automotive Engineers, p. 187

Maeland, A., Flanagan, T.B., (1966), The hydrogen-palladium system, *Platinum Metal Rev*, 10 (1), p. 20

Manna, A. M, (2006), Microstructured and thermally integrated catalytic reactor for hydrogen production, (PhD Thesis), *Universita Degli Studi Di Salerno*, Retrieved Nov 26, 2013, from

[https://www.google.ca/url?sa=t&rct=j&q=&esrc=s&source=web&cd=20&cad=rja&ved=0CGQQFjAJOAo&url=http%3A%2F%2Fwww.unisa.it%2Fsecure%2Fget%2Ffile%2F40.tesi\\_antionietta\\_manna.pdf%2Fid%2F1270&ei=x3qUUtjVGsbqoATLkIG4Bg&usg=AFQjCNGsmby8T\\_HfeCqc5O401ZMPeqRwPQ&bvm=bv.57155469,d.cGU](https://www.google.ca/url?sa=t&rct=j&q=&esrc=s&source=web&cd=20&cad=rja&ved=0CGQQFjAJOAo&url=http%3A%2F%2Fwww.unisa.it%2Fsecure%2Fget%2Ffile%2F40.tesi_antionietta_manna.pdf%2Fid%2F1270&ei=x3qUUtjVGsbqoATLkIG4Bg&usg=AFQjCNGsmby8T_HfeCqc5O401ZMPeqRwPQ&bvm=bv.57155469,d.cGU)

Manninger, I., (1984), The kinetics of Pt-black catalyst sintering in different atmospheres, *Journal of catalysis*, 89, p. 164

Meeyoo, V., Trimm, D. L., Cant, N. W. (1998), The effect of sulphur containing pollutants on the oxidation activity of precious metals used in vehicle exhaust catalysts, *Appl. Cat. B: Environmental*, 16: L-101-104

Mooney, J. J., (n.d.), An AIChE mini-history of John Mooney, *New Jersey Institute of Technology: Chemical Biological and Pharmaceutical Engineering*, Retrieved Aug 22, 2013 from <http://chemicaleng.njit.edu/news/JMooney.php>

National Research Council, (2011) America's Climate Choices, *Washington, DC: The National Academies Press*, Retrieved November 16, 2013, from [http://www.nap.edu/openbook.php?record\\_id=12781&page=15](http://www.nap.edu/openbook.php?record_id=12781&page=15)

Niemantsverdriet, J. W. (2007). Spectroscopy in Catalysis: An Introduction, Third Edition, *WileyVCH Verlag GmgH & Co. KGaA*, Weinheim, Germany, p.13

Nunan, J. G., Williamson, W. B., Robota, H. J., Henk, M. G., (1995) Impact of Pt-Rh and Pd-Rh Interactions on Performance Features for Bimetallic Catalysts, *SAE Paper 950258*, p. 1422

Patel, B. S., Patel, K. D., (2012), A review paper on catalytic converter for automobile exhaust emission, *International Journal of applied Engineering Research*, vol 7, no. 11, p. 1398

Persson, K., Ersson, A., Jansson, K. Iverlund, N, Jaras, S. (2005), Influence of co-metals on bimetallic palladium catalysts for methane combustion, *Journal of catalysis*, 231 (1), p. 139

Priestley, J., (1774), Experiments and Observations on Different Kinds of Air, *London W. Bowyer and J. Nichols*, Retrieved June 18, 2013 from <http://archive.org/stream/experimentsobser01prie#page/322/mode/2up/search/Franklin>

Punke, A., Dahle, U., Tauster, S. J., Rabinowitz, H. N., Yamada, T., (2006), Trimetallic three-way catalysts, SAE Technical Paper 950255, *Advanced three-way catalysts*, Warrendale, Pa.: Society of Automotive Engineers, p. 157

Renault.com-Car Manufacturer Renault's official international website-Renault, (2013), NOx Trap, *Home: Innovation: Powertrain Range*, Retrieved August 22, 2013, from <http://www.renault.com/en/innovation/gamme-mecanique/pages/nox-trap.aspx>

Ruckenstein, E., Dadyburjor, D., (1977), Mechanism of ageing of supported metal catalyst, *Journal of Catalysis*, 48, p. 73

Schleyer, C. H., Gorse, R. A., Freel, J., Gunst, R. F., Barnes, G. J., Natarajan, M., Eckstrom, J., Eng, K. D., Schleneker, A. M., (2006), Effect of fuel sulfur on emissions in California low emission vehicles, SAE Technical Paper 982726, *Advanced three-way catalysts*, Warrendale, Pa.: Society of Automotive Engineers, p. 513

Schmidt, J., Busch, M., Waltner, A., Enderle, C., Heil, B., Lindler, D., Mueller, W., Musmann, L., Lox, E. S., Kreuzer, T., (2006), Utilization of advanced Pt-Rh three-way catalyst technologies for advanced gasoline applications with different cold start strategies, SAE Technical Paper 2001-01-0927, *Advanced three-way catalysts*, Warrendale, Pa.: Society of Automotive Engineers, p. 51

Solomon, S., D. Qin, M. Manning, Z. Chen, M. Marquis, K.B. Averyt, M. Tignor and H.L. Miller et al., (2007). IPCC, 2007: Summary for Policymakers. In: Climate Change 2007: The Physical Science Basis. Contribution of Working Group I to the Fourth Assessment Report of the Intergovernmental Panel on Climate Change, *Cambridge University Press*, Cambridge, United Kingdom and New York, NY, USA. Retrieved November 16, 2013, from [http://www.ipcc.ch/publications\\_and\\_data/ar4/wg1/en/spmsspmpm-projections-of.html](http://www.ipcc.ch/publications_and_data/ar4/wg1/en/spmsspmpm-projections-of.html)

Sperling, D., Gordon, D., (2009), Two billion cars: driving toward sustainability, *Oxford University Press*, New York. p. 93

Tanaka, H., Uenishi, M., Tan, Isao, Kimura, M., Mizuki, J., Nishihata, Y., (2006), An intelligent catalyst, SAE Technical Paper 2001-01-1301, *Advanced three-way catalysts*, Warrendale, Pa.: Society of Automotive Engineers, p. 43

ThinkQuest team, (2000), Start your engines!.*ThinkQuest*. Retrieved November 17, 2013, from

<http://library.thinkquest.org/C006011/english/sites/gasmotoren.php3?v=2>

UK Weather Forecast, (n.d.), The Great Smog of 1952, *Met Office Education: Education: For Teens: Case Studies*, Retrieved November 16, 2013, from

<http://www.metoffice.gov.uk/education/teens/case-studies/great-smog>

US Department of Energy, (2004), Greenhouse Gases, Climate Change, and Energy. *US Energy Information Administration*. Retrieved November 17, 2013, from

<http://www.eia.gov/oiaf/1605/ggcebro/chapter1.html>

US Environmental Protection Agency, (1994), Milestones in Auto Emissions Control. *Office of Mobile Sources*. Retrieved June 17, 2013, from

<http://www.epa.gov/oms/consumer/12-miles.pdf>.

US Environmental Protection Agency. (1973). EPA Requires Phase-Out of Lead in All Grades of Gasoline. *EPA Home: About EPA*. Retrieved June 17, 2013, from

<http://www.epa.gov/history/topics/lead/03.html>

US Department of Energy, (2013), DOE - Fossil Energy: A Brief History of Natural Gas, *Fossil Energy Office of Communication* Retrieved November 17, 2013, from

<http://fossil.energy.gov/education/energyle>

US Environmental Protection Agency, (n.d.), Fuel Oil Combustion, *External Combustion Sources*, Retrieved November 18, 2013, from

<http://www.epa.gov/ttnchie1/ap42/ch01/final/c01s03.pdf>

US Environmental Protection Agency, (2013), Carbon Dioxide Emissions, *US Environmental Protection Agency*, Retrieved November 18, 2013, from <http://www.epa.gov/climatechange/ghgemissions/gases/co2.html>

US Patent and Trademark Office, (2012), 2002 Laureats, *The USPTO: Home Page: About us: National Medal of Technology and Innovation: Recipients*, Retrieved on Aug 22, 2013 from <http://www.uspto.gov/about/nmti/recipients/2002.jsp>

van Helder, R., Verbeek, R., Willems, F. Van der Welle, R., (2004), Optimization of urea SCR de NOx systems for HD diesel engines, SAE Technical paper 2004-01-0154, Retrieved August 23, 2013 from <http://www.mate.tue.nl/mate/pdfs/7933.pdf>

van Giezen, J. C., (1997), *The Catalytic Combustion of Methane* (PhD Thesis), *University of Utrecht*, Utrecht, Netherlands. Print.

Votsmeier, M., Bog., T., Lindner, D., Gieshoff, J., Lox, E. S., Kreuzer, T., (2006), A systematic approach towards low precious metal three-way catalysts application, *Advanced three-way catalysts*, Warrendale, Pa.: Society of Automotive Engineers, p. 25

Wan Abu Bakar, W. A., & Buang, N. A. (2010, June 1). The Catalytic Combustion For Natural Gas. - *Universiti Teknologi Malaysia Institutional Repository*. Retrieved November 26, 2013, from <http://eprints.utm.my/2685/>

Wanke, S. E., Flynn, P. C., (1975), The sintering of supported metal catalysts, *Catalysis Reviews: Science and Engineering*, 12 (1), p.93

Washington Gas Light Co., (2013). Washington Gas - Natural Gas Vehicles. *Washington Gas Light Co.*. Retrieved November 17, 2013, from <http://www.washgas.com/pages/NaturalGasVehicles>

Windmann, J., Braun, J., Zacke, P. Tischer, S., Deutchmann, O., Warnatz, J. (2002), Impact of the inlet flow distribution on the light-off behavior of a 3-way catalytic converter, SAE 2003-01-0937, Retrieved November 26, 2013 from [http://www.itcp.kit.edu/deutschmann/img/content/40\\_OD\\_03\\_SAE\\_Windmannetal.pdf](http://www.itcp.kit.edu/deutschmann/img/content/40_OD_03_SAE_Windmannetal.pdf)

Yamamoto, S., Matsushita, K., Etoh, S., Takaya, M., (2006), In-line hydrocarbon (HC) adsorber system for reducing cold-start emissions, SAE Technical Paper 2000-01-0892, *Advanced three-way catalysts*, Warrendale, Pa.: Society of Automotive Engineers, p. 67

Zhang, J. (n.d.). Catalytic Converter – Part I of Automotive After-treatment System, *Bowmannz.com*, Retrieved August 22, 2013, from [http://www.bowmannz.com/yahoo\\_site\\_admin/assets/docs/CatalyticConverter.92123507.pdf](http://www.bowmannz.com/yahoo_site_admin/assets/docs/CatalyticConverter.92123507.pdf)

Zhu G., Han H., Zemlyanov D. Y., Ribeiro F. H., (2005), Temperature dependence of the kinetics for the complete oxidation of methane on palladium and palladium oxide, *J. Phys. Chem. B*, 109 (9), p. 2331

Appendix A. Summary of experiments

Exp.	Catalyst	Cycle
De-greened at 650 °C		
MI-001	Pt-Pd 95, 200-400 $\mu\text{m}$ , 4700	Ignition
MI-002	Pt-Pd 95, 200-400 $\mu\text{m}$ , 4700	Extinction
MI-003	Pt-Pd 95, 200-400 $\mu\text{m}$ , 4700	Extinction
MI-004	Pt-Pd 95, 200-400 $\mu\text{m}$ , 4700	Ignition
MI-005	Pt-Pd 95, 200-400 $\mu\text{m}$ , 4700	Extinction
MI-006	Pt-Pd 95, 200-400 $\mu\text{m}$ , 4700	Extinction
MI-007	Pt-Pd 95, 200-400 $\mu\text{m}$ , 4700	Ignition-extinction
MI-008	Pt-Pd 95, 200-400 $\mu\text{m}$ , 4700	Ignition
MI-009	Pt-Pd 95, 200-400 $\mu\text{m}$ , 4700	Extinction
MI-010	Pt-Pd 95, 200-400 $\mu\text{m}$ , 4700	Extinction
MI-011	Pt-Pd 95, 200-400 $\mu\text{m}$ , 4700	Ignition
MI-012	Pt-Pd 95, <200 $\mu\text{m}$ , 4700	Ignition-extinction
MI-013	Pt-Pd 95, <200 $\mu\text{m}$ , 4700	Ignition-extinction
MI-014	Pt-Pd 95, 200-400 $\mu\text{m}$ , 4700	Ignition-extinction
MI-015	Pt-Pd 95, 200-400 $\mu\text{m}$ , 4700	Ignition
MI-016	Pt-Pd 95, 200-400 $\mu\text{m}$ , 4700	Extinction
MI-017	Pt-Pd 95, 200-400 $\mu\text{m}$ , 4700	Extinction
MI-018	Pt-Pd 95, 200-400 $\mu\text{m}$ , 4700	Extinction
MI-019	Pt-Pd 95, 200-400 $\mu\text{m}$ , 4700	Extinction
MI-020	Pt-Pd 95, 200-400 $\mu\text{m}$ , 4700	Ignition-extinction
MI-021	Pt-Pd 95, 200-400 $\mu\text{m}$ , 4700	Ignition-extinction
MI-022	Pt-Pd 95, 200-400 $\mu\text{m}$ , 4700	Ignition
MI-023	Pt-Pd 95, 200-400 $\mu\text{m}$ , 4700	Extinction
MI-024	Pt-Pd 95, 200-400 $\mu\text{m}$ , 4700	Extinction
MI-025	Pt-Pd 95, 200-400 $\mu\text{m}$ , 4700	Extinction
MI-026	Pt-Pd 95, 200-400 $\mu\text{m}$ , 4700	Extinction
MI-027	Pt-Pd 95, 200-400 $\mu\text{m}$ , 4700	Extinction
MI-028	Pt-Pd 95, 200-400 $\mu\text{m}$ , 4700	Ignition-extinction
MI-029	Pt-Pd 95, 200-400 $\mu\text{m}$ , 4700	Extinction
MI-030	Pt-Pd 95, 200-400 $\mu\text{m}$ , 4700	Extinction
MI-031	Pt-Pd 95, 200-400 $\mu\text{m}$ , 4700	Extinction
MI-032	Pt-Pd 95, 200-400 $\mu\text{m}$ , 4700	Extinction
MI-033	Pt-Pd 95, 200-400 $\mu\text{m}$ , 4700	Extinction
MI-034	Pt-Pd 95, 200-400 $\mu\text{m}$ , 4700	Extinction
MI-035	Pt-Pd 95, 200-400 $\mu\text{m}$ , 4700	Ignition-extinction
MI-036	Pt-Pd 95, 200-400 $\mu\text{m}$ , 4700	Ignition-extinction
MI-037	Pt-Pd 95, 200-400 $\mu\text{m}$ , 4700	Ignition
MI-038	Pt-Pd 95, 200-400 $\mu\text{m}$ , 4700	Ignition-extinction

MI-039	Pt-Pd 95, 200-400 $\mu\text{m}$ , 4700	Extinction
MI-040	Pt-Pd 95, 200-400 $\mu\text{m}$ , 4700	Extinction
MI-041	Pt-Pd 95, 200-400 $\mu\text{m}$ , 4700	Extinction
MI-042	Pt-Pd 95, 200-400 $\mu\text{m}$ , 4700	Extinction
MI-043	Pt-Pd 95, 200-400 $\mu\text{m}$ , 4700	Extinction
MI-044	Pt-Pd 95, 200-400 $\mu\text{m}$ , 4700	Extinction
MI-045	Pt-Pd 95, 200-400 $\mu\text{m}$ , 4700	Extinction
MI-046	Pt-Pd 95, 200-400 $\mu\text{m}$ , 4700	Extinction
MI-047	Pt-Pd 95, 200-400 $\mu\text{m}$ , 4700	Extinction
MI-048	Pt-Pd 95, 200-400 $\mu\text{m}$ , 4700	Extinction
MI-049	Pt-Pd 95, 200-400 $\mu\text{m}$ , 4700	Extinction
MI-050	Pt-Pd 95, 200-400 $\mu\text{m}$ , 4700	Extinction
MI-051	Pt-Pd 95, 200-400 $\mu\text{m}$ , 4700	Extinction
MI-052	Pt-Pd 95, 200-400 $\mu\text{m}$ , 4700	Extinction
MI-053	Pt-Pd 95, 200-400 $\mu\text{m}$ , 4700	Extinction
MI-054	Pt-Pd 95, 200-400 $\mu\text{m}$ , 4700	Extinction
MI-055	Pt-Pd 95, 200-400 $\mu\text{m}$ , 4700	Extinction
MI-056 reduced	Pt 95, 200-400 $\mu\text{m}$ , 4700	Extinction
MI-057	Pt 95, 200-400 $\mu\text{m}$ , 4700	Extinction
MI-058	Pt 95, 200-400 $\mu\text{m}$ , 4700	Ignition-extinction
MI-059	Pt 95, 200-400 $\mu\text{m}$ , 4700	Extinction
MI-060	Pt 95, 200-400 $\mu\text{m}$ , 4700	Extinction
MI-061	Pt 95, 200-400 $\mu\text{m}$ , 4700	Extinction
MI-062	Pt-Pd 95, 200-400 $\mu\text{m}$ , 4700	Ignition
MI-063	Pt-Pd 95, 200-400 $\mu\text{m}$ , 4700	Extinction
MI-064	Pt-Pd 95, 200-400 $\mu\text{m}$ , 4700	Extinction
MI-065	Pt-Pd 95, 200-400 $\mu\text{m}$ , 4700	Extinction
MI-066	Pd 80, 200-400 $\mu\text{m}$ , 4700	Ignition-extinction
MI-067	Pd 80, 200-400 $\mu\text{m}$ , 4700	Extinction
MI-068	Pd 80, 200-400 $\mu\text{m}$ , 4700	Extinction
MI-069	Pd 80, 200-400 $\mu\text{m}$ , 4700	Steady-state 200 C
MI-070	Pd 80, 200-400 $\mu\text{m}$ , 4700	Steady-state 400 C
MI-071	Pd 80, 200-400 $\mu\text{m}$ , 4700	Steady-state 350 C
MI-072	Pd 80, 200-400 $\mu\text{m}$ , 4700	Steady-state 325 C
MI-073	Pt 95, 200-400 $\mu\text{m}$ , 4700	Steady-state 500 C
MI-074	Pt 95, 200-400 $\mu\text{m}$ , 4700	Steady-state 400 C
MI-075	Pt 95, 200-400 $\mu\text{m}$ , 4700	Steady-state 300 C
MI-076 reduced	Pd 80, 200-400 $\mu\text{m}$ , 4700	400 C-450 C-400 C
MI-077	Pd 80, 200-400 $\mu\text{m}$ , 4700	Ignition-extinction
MI-078	Pd 80, 200-400 $\mu\text{m}$ , 4700	Ignition-extinction
MI-079	Pd 80, 200-400 $\mu\text{m}$ , 4700	Steady-state pulse 400 C

MI-080 Reduced- no air exposure	Pd 80, 200-400 $\mu\text{m}$ , 4700	Ignition-extinction
MI-081 Reduced	Pd 80, 200-400 $\mu\text{m}$ , 4700	Ignition-extinction
MI-082 1degree/min	Pd 80, 200-400 $\mu\text{m}$ , 4700	Ignition-extinction ramping
MI-083 120/min	Pd 80, 200-400 $\mu\text{m}$ , 4700	Ignition-extinction
MI-084 120/min	Pd 80, 200-400 $\mu\text{m}$ , 4700	Ignition-extinction ramping
MI-085 60/min	Pd 80, 200-400 $\mu\text{m}$ , 4700	Ignition-extinction ramping
MI-086	Pd 80, 200-400 $\mu\text{m}$ , 4700	Ignition-extinction
MI-087 reduced tc	Pd 80, 200-400 $\mu\text{m}$ , 4700	Ignition-extinction
MI-088 reduced	Pd 80, 200-400 $\mu\text{m}$ , 4700	Ignition-extinction
MI-089 Aged 600 C/10h, reduced	Pd 80, 200-400 $\mu\text{m}$ , 4700	Ignition-extinction
MI-090	Pd 80, 200-400 $\mu\text{m}$ , 4700	Extinction
MI-091	Pd 80, 200-400 $\mu\text{m}$ , 4700	Extinction
MI-092	Pd 80, 200-400 $\mu\text{m}$ , 4700	Extinction
MI-093	Pd 80, 200-400 $\mu\text{m}$ , 4700	Steady-state 450 C
MI-094	Pd 80, 200-400 $\mu\text{m}$ , 4700	Steady-state 350 C
MI-095	Pd 80, 200-400 $\mu\text{m}$ , 4700	Steady-state 400 C
MI-096	Pd 80, 200-400 $\mu\text{m}$ , 4700	Steady-state 300 C
MI-097	Pd 80, 200-400 $\mu\text{m}$ , 4700	Steady-state 500 C
MI-098	Pd 80, 200-400 $\mu\text{m}$ , 4700	Ignition-extinction
MI-099 Aged 650 C/24 h Not reduced	Pd 80, 200-400 $\mu\text{m}$ , 4700	Ignition-extinction
MI-100	Pd 80, 200-400 $\mu\text{m}$ , 4700	Steady-state 500 C
MI-101	Pd 80, 200-400 $\mu\text{m}$ , 4700	Steady-state 350 C
MI-102	Pd 80, 200-400 $\mu\text{m}$ , 4700	Steady-state 450 C
MI-103	Pd 80, 200-400 $\mu\text{m}$ , 4700	Steady-state 300 C
MI-104	Pd 80, 200-400 $\mu\text{m}$ , 4700	Steady-state 400 C
MI-105	Pd 80, 200-400 $\mu\text{m}$ , 4700	400 C-450 C-400 C-450C
MI-106 reduced	Pd 80, 200-400 $\mu\text{m}$ , 4700	Ignition-extinction
MI-107	Pd 80, 200-400 $\mu\text{m}$ , 4700	Steady-state 500 C
MI-108	Pd 80, 200-400 $\mu\text{m}$ , 4700	Steady-state 350 C
MI-109	Pd 80, 200-400 $\mu\text{m}$ , 4700	Steady-state 450 C
MI-110	Pd 80, 200-400 $\mu\text{m}$ , 4700	Steady-state 400 C
MI-111	Pd 80, 200-400 $\mu\text{m}$ , 4700	Ignition-extinction

MI-112 reduced	Pd 80, 200-400 $\mu\text{m}$ , 4700	Ignition-extinction
MI-113	Pd 80, 200-400 $\mu\text{m}$ , 4700	Steady-state 400 C
MI-114	Pd 80, 200-400 $\mu\text{m}$ , 4700	Steady-state 400 C
MI-115	Pd 80, 200-400 $\mu\text{m}$ , 4700	Steady-state 400 C
MI-116	Pd 80, 200-400 $\mu\text{m}$ , 4700	Steady-state 400 C
MI-117	Pd 80, 200-400 $\mu\text{m}$ , 4700	Ignition-extinction
MI-118 +repeat	Pd 80, 200-400 $\mu\text{m}$ , 4700	Ignition-extinction
MI-119	Pd 80, 200-400 $\mu\text{m}$ , 4700	Steady-state 400 C
MI-120	Pd 80, 200-400 $\mu\text{m}$ , 4700	Steady-state 400 C
MI-121	Pd 80, 200-400 $\mu\text{m}$ , 4700	Steady-state 400 C
MI-122	Pd 80, 200-400 $\mu\text{m}$ , 4700	Ignition-extinction
MI-123 Same sample red.	Pd 80, 200-400 $\mu\text{m}$ 4700	Ignition-extinction
MI-124	Pd 80, 200-400 $\mu\text{m}$ 4700	Steady-state 400 C
MI-125	Pd 80, 200-400 $\mu\text{m}$ 4700	Steady-state 400 C
MI-126	Pd 80, 200-400 $\mu\text{m}$ 4700	Steady-state 400 C
MI-127	Pd 80, 200-400 $\mu\text{m}$ 4700	Steady-state 400 C
MI-128 repeat	Pd 80, 200-400 $\mu\text{m}$ 4700	Steady-state 400 C
MI-129	Pd 80, 200-400 $\mu\text{m}$ 4700	Steady-state 400 C
MI-130	Pd 80, 200-400 $\mu\text{m}$ 4700	Steady-state 400 C
MI-131	Pd 80, 200-400 $\mu\text{m}$ 4700	Steady-state 400 C
MI-132	Pd 80, 200-400 $\mu\text{m}$ 4700	Ignition-extinction
MI-133	Pt-Pd 95, 200-400 $\mu\text{m}$ , 4100	Ignition
MI-134	Pt-Pd 95, 200-400 $\mu\text{m}$ , 4100	Ignition-extinction
MI-135	Pt-Pd 95, 200-400 $\mu\text{m}$ , 4100	Ignition-extinction
MI-136	Pt-Pd 95, 200-400 $\mu\text{m}$ , 2100	Ignition-extinction
MI-137	Pt-Pd 95, 200-400 $\mu\text{m}$ , 4100	Ignition-extinction
MI-138	Pt-Pd 95, 200-400 $\mu\text{m}$ , 4100	Ignition-extinction
MI-139	Pt-Pd 95, 200-400 $\mu\text{m}$ , 4100	Ignition-extinction
MI-140	Pt-Pd 95, 200-400 $\mu\text{m}$ , 4100	Ignition-extinction
MI-141	Pt-Pd 95, 200-400 $\mu\text{m}$ , 4100	Ignition-extinction
MI-142	Pt-Pd 95, 200-400 $\mu\text{m}$ , 4100	Ignition-extinction
MI-143 Same catalyst	Pt-Pd 95, 200-400 $\mu\text{m}$ , 4100	Ignition-extinction
MI-144	Pt-Pd 95, 200-400 $\mu\text{m}$ , 4100	VTTAT 440-650 C
MI-145	Pt-Pd 95, 200-400 $\mu\text{m}$ , 4100	Steady-state 400 C
MI-146	Pt-Pd 95, 200-400 $\mu\text{m}$ , 4100	Ignition-extinction
MI-147	Pt-Pd 95, 200-400 $\mu\text{m}$ , 4100	Steady-state 400 C
MI-148	Pt-Pd 95, 200-400 $\mu\text{m}$ , 4700	Ignition-extinction
MI-149	Pt-Pd 95, 200-400 $\mu\text{m}$ , 4100	Steady-state 400 C

MI-150	Pt-Pd 95, 200-400 $\mu\text{m}$ , 4100	Steady-state 400 C
MI-151	Pt-Pd 95, 200-400 $\mu\text{m}$ , 4100	Ignition-extinction
MI-152	Pt 95, 200-400 $\mu\text{m}$ , 4100	Ignition-extinction
MI-153	Pt 95, 200-400 $\mu\text{m}$ , 4100	Ignition-extinction
MI-154	Pt 95, 200-400 $\mu\text{m}$ , 4100	Ignition-extinction
MI-155	Pt 95, 200-400 $\mu\text{m}$ , 4100	Ignition-extinction
MI-156	Pt 95, 200-400 $\mu\text{m}$ , 4100	VTTAT 650-550-650 C
MI-157	Pt 95, 200-400 $\mu\text{m}$ , 4100	Steady-state 400 C
MI-158	Pt 95, 200-400 $\mu\text{m}$ , 4100	Ignition-extinction
MI-159	Pt 95, 200-400 $\mu\text{m}$ , 4100	Ignition-extinction
MI-160	Pt 95, 200-400 $\mu\text{m}$ , 4100	Ignition-extinction
MI-161	Pt 95, 200-400 $\mu\text{m}$ , 4100	Ignition-extinction
MI-162	Pt 95, 200-400 $\mu\text{m}$ , 4100	CTHTAT 450 C
MI-163	Pt 95, 200-400 $\mu\text{m}$ , 4100	Ignition-extinction
MI-164	Pt 95, 200-400 $\mu\text{m}$ , 4100	CTHTAT 650 C
MI-165	Pt 95, 200-400 $\mu\text{m}$ , 4100	CTHTAT 600 C
MI-166	Pt 95, 200-400 $\mu\text{m}$ , 4100	VTHTAT 650-600 C
MI-167	Pt 95, 200-400 $\mu\text{m}$ , 4100	Ignition-extinction
MI-168	Pt 95, 200-400 $\mu\text{m}$ , 4100	Ignition-extinction water
MI-169	Pt-Pd 95, 200-400 $\mu\text{m}$ , 4100	Ignition-extinction
MI-170	Pt-Pd 95, 200-400 $\mu\text{m}$ , 4100	Ignition-extinction
MI-171	Pt-Pd 95, 200-400 $\mu\text{m}$ , 4100	Ignition-extinction
MI-172	Pt-Pd 95, 200-400 $\mu\text{m}$ , 4100	Ignition-extinction
MI-173	Pt-Pd 95, 200-400 $\mu\text{m}$ , 4100	Ignition-extinction
MI-174	Pt-Pd 95, 200-400 $\mu\text{m}$ , 4100	CTHTAT 550C
MI-175	Pt-Pd 95, 200-400 $\mu\text{m}$ , 4100	CTHTAT 550C
MI-176	Pt-Pd 95, 200-400 $\mu\text{m}$ , 4100	CTHTAT 500C
MI-177	Pt-Pd 95, 200-400 $\mu\text{m}$ , 4100	Ignition-extinction
MI-178	Pt-Pd 95, 200-400 $\mu\text{m}$ , 4100	Ignition-extinction water
MI-179	Pt-Pd 95, 200-400 $\mu\text{m}$ , 4100	Ignition-extinction
MI-180	Pt 95, 200-400 $\mu\text{m}$ , 4100	Ignition-extinction
MI-181	Pt 95, 200-400 $\mu\text{m}$ , 4100	CTHTAT 650 C
MI-182	Pt 95, 200-400 $\mu\text{m}$ , 4100	CTHTAT 600 C
MI-183	Pt 95, 200-400 $\mu\text{m}$ , 4100	CTHTAT 600 C
MI-184	Pt 95, 200-400 $\mu\text{m}$ , 4100	Ignition-extinction
MI-185	Pt 95, 200-400 $\mu\text{m}$ , 4100	Ignition-extinction
MI-186	Pt 95, 200-400 $\mu\text{m}$ , 4100	Ignition-extinction
MI-187	Pt 95, 200-400 $\mu\text{m}$ , 4100	Ignition-extinction
MI-188	Pt 95, 200-400 $\mu\text{m}$ , 4100	CTHTAT 600C
MI-189	Pt 95, 200-400 $\mu\text{m}$ , 4100	Ignition-extinction
MI-190	Pt 95, 200-400 $\mu\text{m}$ , 4100	Ignition-extinction water
MI-191	Pt 95, 200-400 $\mu\text{m}$ , 4100	Ignition-extinction

MI-192	Pt 95, 200-400 $\mu\text{m}$ , 4100	Ignition-extinction
MI-193	Pt 95, 200-400 $\mu\text{m}$ , 4100	Ignition-extinction
MI-194	Pt 95, 200-400 $\mu\text{m}$ , 4100	Ignition-extinction
MI-195	Pt 95, 200-400 $\mu\text{m}$ , 4100	CTHTAT 550 C
MI-196	Pt 95, 200-400 $\mu\text{m}$ , 4100	Ignition-extinction
MI-197	Pt 95, 200-400 $\mu\text{m}$ , 4100	Ignition-extinction
MI-198	Pt 95, 200-400 $\mu\text{m}$ , 4100	VTTAT 650-550 C water
MI-199	Pt 95, 200-400 $\mu\text{m}$ , 4100	Ignition-extinction
MI-200	Pt 95, 200-400 $\mu\text{m}$ , 4100	VTTAT water
MI-201	Pt 95, 200-400 $\mu\text{m}$ , 4100	Ignition-extinction
MI-202	Pt 95, 200-400 $\mu\text{m}$ , 4100	Ignition-extinction water
MI-203	Pt 95, 200-400 $\mu\text{m}$ , 4100	Ignition-extinction
MI-204	Pt 95, 200-400 $\mu\text{m}$ , 4100	Ignition-extinction
MI-205	Pt 95, 200-400 $\mu\text{m}$ , 4100	Ignition-extinction
MI-206	Pt 95, 200-400 $\mu\text{m}$ , 4100	VHTAT 650-550
MI-207	Pt 95, 200-400 $\mu\text{m}$ , 4100	Ignition-extinction
MI-208	Pt 95, 200-400 $\mu\text{m}$ , 4100	Ignition-extinction
MI-209	Pt 95, 200-400 $\mu\text{m}$ , 4100	Ignition-extinction
MI-210	Pt 95, 200-400 $\mu\text{m}$ , 4100	Ignition-extinction
MI-211	Pt-Pd 95, 200-400 $\mu\text{m}$ , 4100	Ignition-extinction
MI-212	Pt-Pd 95, 200-400 $\mu\text{m}$ , 4100	VTTAT 650-450 water
MI-213	Pt-Pd 95, 200-400 $\mu\text{m}$ , 4100	Ignition-extinction
MI-214	Pt-Pd 95, 200-400 $\mu\text{m}$ , 4100	Ignition-extinction water
MI-215	Pt-Pd 95, 200-400 $\mu\text{m}$ , 4100	Ignition-extinction
MI-216	Pt-Pd 95, 200-400 $\mu\text{m}$ , 4100	Ignition-extinction
MI-217	Pt-Pd 95, 200-400 $\mu\text{m}$ , 4100	Ignition-extinction
MI-218	Pt-Pd 95, 200-400 $\mu\text{m}$ , 4100	VHTAT 650-450 C
MI-219	Pt-Pd 95, 200-400 $\mu\text{m}$ , 4100	Ignition-extinction
MI-220	Pt-Pd 95, 200-400 $\mu\text{m}$ , 4100	Ignition-extinction water
MI-221	Pt-Pd 150, 200-400 $\mu\text{m}$ , 4100	Ignition-extinction
MI-222	Pt-Pd 150, 200-400 $\mu\text{m}$ , 4100	VTTAT 650-300 C
MI-223	Pt-Pd 150, 200-400 $\mu\text{m}$ , 4100	Ignition-extinction
MI-224	Pt-Pd 150, 200-400 $\mu\text{m}$ , 4100	Ignition-extinction water
MI-225	Alumina, 200-400 $\mu\text{m}$ , 4100	Ignition-extinction
MI-226	Alumina, 200-400 $\mu\text{m}$ , 4100	Ignition-extinction
MI-227	Alumina, 200-400 $\mu\text{m}$ , 4100	Ignition-extinction
MI-228	Pt-Pd 150, 200-400 $\mu\text{m}$ , 4100	Ignition-extinction
MI-229	Pt-Pd 150, 200-400 $\mu\text{m}$ , 4100	VHTAT 650-350 C
MI-230	Pt-Pd 150, 200-400 $\mu\text{m}$ , 4100	Ignition-extinction
MI-231	Pt-Pd 150, 200-400 $\mu\text{m}$ , 4100	Ignition-extinction water
MI-232	Pt-Pd 150, 200-400 $\mu\text{m}$ , 4100	Ignition-extinction
MI-233	Pt-Pd 150, 200-400 $\mu\text{m}$ , 4100	VTTAT 650-350 C water

MI-234	Pt-Pd 150, 200-400 $\mu\text{m}$ , 4100	Ignition-extinction
MI-235	Pt-Pd 150, 200-400 $\mu\text{m}$ , 4100	Ignition-extinction
MI-236	Pt-Pd 150, 200-400 $\mu\text{m}$ , 4100	VTHAT 650-450 C
MI-237	Pt-Pd 95, 200-400 $\mu\text{m}$ , 4100	Ignition-extinction
MI-238	Pt-Pd 95, 200-400 $\mu\text{m}$ , 4100	Ignition-extinction
MI-239	Pt-Pd 95, 200-400 $\mu\text{m}$ , 4100	Ignition-extinction
MI-240	Pt-Pd 95, 200-400 $\mu\text{m}$ , 4100	VTHAT 650-450 C
MI-241	Pt-Pd 95, 200-400 $\mu\text{m}$ , 4100	Ignition-extinction
MI-242	Pt-Pd 95, 200-400 $\mu\text{m}$ , 4100	Ignition-extinction water
MI-243	Pt-Pd 150, 200-400 $\mu\text{m}$ , 4100	Ignition-extinction
MI-244	Pt-Pd 150, 200-400 $\mu\text{m}$ , 4100	Ignition-extinction
MI-245	Pt-Pd 150, 200-400 $\mu\text{m}$ , 4100	VTHAT 650-450 C
MI-246	Pt-Pd 150, 200-400 $\mu\text{m}$ , 4100	Ignition-extinction
MI-247	Pt-Pd 150, 200-400 $\mu\text{m}$ , 4100	Ignition-extinction
MI-248	Pd 150, 200-400 $\mu\text{m}$ , 4100	Ignition-extinction
MI-249	Pd 150, 200-400 $\mu\text{m}$ , 4100	VTHAT 650-450 C
MI-250	Pd 150, 200-400 $\mu\text{m}$ , 4100	Ignition-extinction
MI-251	Pd 150, 200-400 $\mu\text{m}$ , 4100	VTHAT 650-450 C
MI-252	Pd 150, 200-400 $\mu\text{m}$ , 4100	Ignition-extinction
MI-253	Pd 150, 200-400 $\mu\text{m}$ , 4100	Ignition-extinction water
MI-254	Pd 150, 200-400 $\mu\text{m}$ , 4100	Ignition-extinction
MI-255	Pd 150, 200-400 $\mu\text{m}$ , 4100	VTHAT 650-350 C
MI-256	Pd 150, 200-400 $\mu\text{m}$ , 4100	Ignition-extinction
MI-257	Pd 150, 200-400 $\mu\text{m}$ , 4100	Ignition-extinction
MI-258	Pd 150, 200-400 $\mu\text{m}$ , 4100	Ignition-extinction
MI-259	Pd 150, 200-400 $\mu\text{m}$ , 4100	VTHAT 650-350 C water
MI-260	Pd 150, 200-400 $\mu\text{m}$ , 4100	Ignition-extinction
MI-261	Pd 150, 200-400 $\mu\text{m}$ , 4100	Ignition-extinction
MI-262	Pd 150, 200-400 $\mu\text{m}$ , 4100	VTHAT 650-350 C
MI-263	Pd 150, 200-400 $\mu\text{m}$ , 4100	Ignition-extinction
MI-264	Pd 150, 200-400 $\mu\text{m}$ , 4100	Ignition-extinction
MI-265	Pd 150, 200-400 $\mu\text{m}$ , 4100	VTHAT 650-450 C
MI-266	Pd 150, 200-400 $\mu\text{m}$ , 4100	Ignition-extinction
MI-267	Pd 150, 200-400 $\mu\text{m}$ , 4100	Ignition-extinction
MI-268	Pd 150, 200-400 $\mu\text{m}$ , 4100	Ignition-extinction
MI-269	Pd 150, 200-400 $\mu\text{m}$ , 4100	VTHAT 650-450 C
MI-270	Pd 150, 200-400 $\mu\text{m}$ , 4100	Ignition-extinction
MI-271	Pt 95, 200-400 $\mu\text{m}$ , 4100	Ignition-extinction
MI-272	Pt 95, 200-400 $\mu\text{m}$ , 4100	Ignition-extinction
MI-273	Pt 95, 200-400 $\mu\text{m}$ , 4100	VTHAT 650-550 C
MI-274	Pt 95, 200-400 $\mu\text{m}$ , 4100	Ignition-extinction
MI-275	Pt 95, 200-400 $\mu\text{m}$ , 4100	VTHAT 650-550 C

MI-276	Pt 95, 200-400 $\mu\text{m}$ , 4100	Ignition-extinction
MI-277	Pt 95, 200-400 $\mu\text{m}$ , 4100	Ignition-extinction water
MI-278	Pd 150, 200-400 $\mu\text{m}$ , 4100	Ignition-extinction
MI-279	Pd 150, 200-400 $\mu\text{m}$ , 4100	VHTAT 650-450 C
MI-280	Pd 150, 200-400 $\mu\text{m}$ , 4100	Ignition-extinction
MI-281	Pd 150, 200-400 $\mu\text{m}$ , 4100	Ignition-extinction
MI-282	Pt-Pd 150, 200-400 $\mu\text{m}$ , 4100	Ignition-extinction
MI-283	Pt-Pd 150, 200-400 $\mu\text{m}$ , 4100	VHTAT 650-450 C
MI-284	Pt-Pd 150, 200-400 $\mu\text{m}$ , 4100	Ignition-extinction
MI-285	Pt-Pd 150, 200-400 $\mu\text{m}$ , 4100	Ignition-extinction water
De-greened at 550 °C		
MI-286	Pt-Pd 150, 200-400 $\mu\text{m}$ , 4100	Ignition-extinction 1
MI-287	Pt-Pd 150, 200-400 $\mu\text{m}$ , 4100	Ignition-extinction 2
MI-288	Pt-Pd 150, 200-400 $\mu\text{m}$ , 4100	Ignition-extinction 3
MI-289	Pt-Pd 150, 200-400 $\mu\text{m}$ , 4100	VHTAT 550-350 water
MI-290	Pt-Pd 150, 200-400 $\mu\text{m}$ , 4100	Ignition-extinction
MI-291	Pt-Pd 150, 200-400 $\mu\text{m}$ , 4100	Ignition-extinction 2
MI-292	Pt-Pd 150, 200-400 $\mu\text{m}$ , 4100	Ignition-extinction water
MI-293	Pt-Pd 150, 200-400 $\mu\text{m}$ , 4100	Ignition-extinction
MI-294	Pt-Pd 150, 200-400 $\mu\text{m}$ , 4100	Ignition-extinction
MI-295	Pt-Pd 150, 200-400 $\mu\text{m}$ , 4100	Ignition-extinction
MI-296	Pt-Pd 150, 200-400 $\mu\text{m}$ , 4100	VHTAT 550-350 C
MI-297	Pt-Pd 150, 200-400 $\mu\text{m}$ , 4100	Ignition-extinction 1
MI-298	Pt-Pd 150, 200-400 $\mu\text{m}$ , 4100	Ignition-extinction 2
MI-299	Pt-Pd 150, 200-400 $\mu\text{m}$ , 4100	Ignition-extinction 3
MI-300	Pt-Pd 150, 200-400 $\mu\text{m}$ , 4100	Ignition-extinction water
MI-301	Pt-Pd 150, 200-400 $\mu\text{m}$ , 4100	Ignition-extinction
MI-302	Pt-Pd 150, 200-400 $\mu\text{m}$ , 4100	VHTAT 550-450 C
MI-303	Pt-Pd 150, 200-400 $\mu\text{m}$ , 4100	Ignition-extinction 1
MI-304	Pt-Pd 150, 200-400 $\mu\text{m}$ , 4100	Ignition-extinction 2
MI-305	Pt-Pd 150, 200-400 $\mu\text{m}$ , 4100	Ignition-extinction water
MI-306	Pt-Pd 150, 200-400 $\mu\text{m}$ , 4100	Ignition-extinction water
MI-307	Cordierite, 200-400 $\mu\text{m}$ , 4100	Ignition-extinction
MI-308	Cordierite, 200-400 $\mu\text{m}$ , 4100	VHTAT 550-500 C water
MI-309	Cordierite, 200-400 $\mu\text{m}$ , 4100	Ignition-extinction
MI-310 (used cat MI-302)	Pt-Pd 150, 200-400 $\mu\text{m}$ , 4100	VHTAT 650-450 C
MI-311 (600)	Pt-Pd 150, 200-400 $\mu\text{m}$ , 4100	Ignition-extinction
MI-312	Pt-Pd 150, 200-400 $\mu\text{m}$ , 4100	VHTAT 650-450 C
MI-313	Pt-Pd 150, 200-400 $\mu\text{m}$ , 4100	Ignition-extinction
MI-314	Reactor, 4100	Ignition-extinction 1

MI-315	PdRh, 200-400 $\mu\text{m}$ , 4100	Ignition-extinction 1
MI-316	PdRh, 200-400 $\mu\text{m}$ , 4100	Ignition-extinction 2
MI-317	PdRh, 200-400 $\mu\text{m}$ , 4100	VTHAT 550-400 C
MI-318	PdRh, 200-400 $\mu\text{m}$ , 4100	Ignition-extinction
MI-319 (550)	PtPdRh, 200-400 $\mu\text{m}$ , 4100	Ignition-extinction
MI-320	PtPdRh, 200-400 $\mu\text{m}$ , 4100	VHTA 550-450 C
MI-321	PtPdRh, 200-400 $\mu\text{m}$ , 4100	Ignition-extinction
MI-322	PtPdRh, 200-400 $\mu\text{m}$ , 4100	Ignition-extinction water
MI-323 (550)	PtPdRh, 200-400 $\mu\text{m}$ , 4100	Ignition-extinction 1
MI-324	PtPdRh, 200-400 $\mu\text{m}$ , 4100	Ignition-extinction 2
MI-325	PtPdRh, 200-400 $\mu\text{m}$ , 4100	Ignition-extinction 3
MI-326	PtPdRh, 200-400 $\mu\text{m}$ , 4100	Ignition-extinction 4
MI-327	PtPdRh, 200-400 $\mu\text{m}$ , 4100	VTTAT 550-450 C water
MI-328	PtPdRh, 200-400 $\mu\text{m}$ , 4100	Ignition-extinction
MI-329	PtPdRh, 200-400 $\mu\text{m}$ , 4100	Ignition-extinction water
MI-330	Pt-Pd 150, 200-400 $\mu\text{m}$ , 4100	Ignition-extinction
MI-331	Pt-Pd 150, 200-400 $\mu\text{m}$ , 4100	VTHAT 550-450 C
MI-332	Pt-Pd 150, 200-400 $\mu\text{m}$ , 4100	Ignition-extinction
MI-333	Pt-Pd 150, 200-400 $\mu\text{m}$ , 4100	Ignition-extinction water
MI-334	Pt-Pd 150, 200-400 $\mu\text{m}$ , 4100	Ignition-extinction
MI-335 (600)	Pt-Pd 150, 200-400 $\mu\text{m}$ , 4100	Ignition-extinction
MI-336	Pt-Pd 150, 200-400 $\mu\text{m}$ , 4100	VTHAT 650-450 C
MI-337	Pt-Pd 150, 200-400 $\mu\text{m}$ , 4100	Ignition-extinction
MI-338	Pt-Pd 150, 200-400 $\mu\text{m}$ , 4100	Ignition-extinction water
MI-339	Pd 150, 200-400 $\mu\text{m}$ , 4100	Ignition-extinction 1
MI-340	Pd 150, 200-400 $\mu\text{m}$ , 4100	Ignition-extinction 2
MI-341	Pd 150, 200-400 $\mu\text{m}$ , 4100	VTTAT 550-350 C water
MI-342	Pd 150, 200-400 $\mu\text{m}$ , 4100	Ignition-extinction
MI-343	Pd 150, 200-400 $\mu\text{m}$ , 4100	Ignition-extinction water
MI-344	PdRh, 200-400 $\mu\text{m}$ , 4100	Ignition-extinction 1
MI-345	PdRh, 200-400 $\mu\text{m}$ , 4100	Ignition-extinction 2
MI-346	PdRh, 200-400 $\mu\text{m}$ , 4100	VTTAT 550-350 C water
MI-347	PdRh, 200-400 $\mu\text{m}$ , 4100	Ignition-extinction
MI-348	PdRh, 200-400 $\mu\text{m}$ , 4100	Ignition-extinction water
MI-349	PdRh, 200-400 $\mu\text{m}$ , 4100	Ignition-extinction
MI-350	PdRh, 200-400 $\mu\text{m}$ , 4100	VTTAT 550-450 C water
MI-351	PdRh, 200-400 $\mu\text{m}$ , 4100	Ignition-extinction
MI-352	PdRh, 200-400 $\mu\text{m}$ , 4100	Ignition-extinction water
MI-353	Cordierite, 200-400 $\mu\text{m}$ , 4100	Ignition-extinction
MI-354	Cordierite, 200-400 $\mu\text{m}$ , 4100	Ignition-extinction

MI-355	Cordierite, 200-400 $\mu\text{m}$ , 4100	Ignition-extinction
MI-356	Cordierite, 200-400 $\mu\text{m}$ , 4100	Ignition-extinction
MI-357	Pd 122, 200-400 $\mu\text{m}$ , 4100	Ignition-extinction
MI-358	Pd 122, 200-400 $\mu\text{m}$ , 4100	VHTAT 550-450 C
MI-359	Pd 122, 200-400 $\mu\text{m}$ , 4100	Ignition-extinction
MI-360	Pd 122, 200-400 $\mu\text{m}$ , 4100	Ignition-extinction water
MI-361	Pd 122, 200-400 $\mu\text{m}$ , 4100	Ignition-extinction
MI-362	Pd 122, 200-400 $\mu\text{m}$ , 4100	Ignition-extinction
MI-363	Pd 122, 200-400 $\mu\text{m}$ , 4100	VHTAT 550-450 C water
MI-364	Pd 122, 200-400 $\mu\text{m}$ , 4100	Ignition-extinction
MI-365	Pd 122, 200-400 $\mu\text{m}$ , 4100	Ignition-extinction water
MI-366	Cordierite, 200-400 $\mu\text{m}$ , 4100	Ignition-extinction
MI-367 (500)	Pt-Pd 150, 200-400 $\mu\text{m}$ , 4100	Ignition-extinction
MI-368	Pt-Pd 150, 200-400 $\mu\text{m}$ , 4100	VHTAT 500-450 C
MI-369	Pt-Pd 150, 200-400 $\mu\text{m}$ , 4100	Ignition-extinction
MI-370	Pd-Rh, 200-400 $\mu\text{m}$ , 4100	Ignition-extinction
MI-371	Pd-Rh, 200-400 $\mu\text{m}$ , 4100	VHTAT 550-450 C
MI-372	Pd-Rh, 200-400 $\mu\text{m}$ , 4100	Ignition-extinction
MI-373	Pd-Rh, 200-400 $\mu\text{m}$ , 4100	Ignition-extinction water
MI-374	Pd 150, 200-400 $\mu\text{m}$ , 4100	Ignition-extinction 1
MI-375	Pd 150, 200-400 $\mu\text{m}$ , 4100	VHTAT 550-350 C water
MI-376	Pd 150, 200-400 $\mu\text{m}$ , 4100	Ignition-extinction
MI-377	Pd 150, 200-400 $\mu\text{m}$ , 4100	Ignition-extinction water
MI-378	Pd 122, 200-400 $\mu\text{m}$ , 4100	Ignition-extinction
MI-379	Pd 122, 200-400 $\mu\text{m}$ , 4100	Ignition-extinction 1
MI-380	Pd 122, 200-400 $\mu\text{m}$ , 4100	Ignition-extinction 2
MI-381 red	Pd 122, 200-400 $\mu\text{m}$ , 4100	Ignition-extinction 3
MI-382	Pd 122, 200-400 $\mu\text{m}$ , 4100	Ignition-extinction 4
MI-383	Pd 122, 200-400 $\mu\text{m}$ , 4100	Ignition-extinction 1
MI-384	Pd 122, 200-400 $\mu\text{m}$ , 4100	Ignition-extinction 2